

AN ABSTRACT OF THE THESIS OF

Xiao Chen for the degree of Doctor of Philosophy in Chemistry
presented on June 14, 1990.

Title: A New General Method for the Optimization of HPLC
Ternary or Pseudo-quaternary Mobile Phases and the
Separation of Two New Metabolites of Nefopam from
Greyhound Urine.

Abstract approved: _____

Edward H. Piepmeier

A. Morrie Craig

A new general method is developed for the optimization of HPLC ternary or pseudo-quaternary mobile phases which are represented by the trilinear coordinate system. This method can predict the global optimum of the mobile phase composition. The global optimum composition along each edge of the triangle and the corresponding selectivity factor of the worst-separated peak pair(s) are used in this method. This method is named the weighted pattern comparison optimization method (WPCO) and is applicable for both known and unknown samples. The WPCO method is simpler than those currently in use. The WPCO method

was tested by using 68 literature data sets whose separation response surfaces are different. Results of the WPCO method agree with the results obtained by the minimum α plot method and by the grid search method, and do so with substantially fewer experimental measurements. Compared with the 5% (in eluent composition) step size grid-search procedure, the WPCO method using the same step size reduces the experimental work by 75%.

For further reducing the experimental work, the original WPCO method is simplified. In an ordinary HPLC separation, the separation factor and resolution are approximately proportional to the logarithm of the selectivity factor. Based on this, the separation factor replaces the logarithm of selectivity factor in the original WPCO method. This further reduces the experimental work and avoids the error introduced in the measurement of the column dead volume. The simplified WPCO method has been tested in the normal-phase and reversed-phase chromatography separation cases. The simplified WPCO method has been tested by using 27 literature data sets whose separation response surfaces are different. Results of the simplified and original WPCO methods are nearly identical when the capacity factors of the solutes of the worst-separated peak pairs are greater than 5. When the capacity factors are less than 5, the simplified WPCO method is satisfactory in less complex, less critical applications.

Two new metabolites of nefopam have been separated from greyhound urine. In the separation process, flash chromatography is used for cleaning up and preseparating the samples in a single step. Compared with other techniques, experimental work is reduced. The structure of one of the newly discovered metabolites is determined using MS and NMR. The most probable structure of the other metabolite is determined using MS. The main metabolic pathways at different doses in greyhounds are studied.

A NEW GENERAL METHOD FOR THE OPTIMIZATION OF HPLC TERNARY
OR PSEUDO-QUATERNARY MOBILE PHASES AND THE SEPARATION OF
TWO NEW METABOLITES OF NEFOPAM FROM GREYHOUND URINE

by

Xiao Chen

A THESIS

submitted to

Oregon State University

in partial fulfillment of the requirements
for the degree of
Doctor of Philosophy

Completed June 14, 1990

Commencement June, 1991

APPROVED:

Professor of Chemistry in Charge of Major

Professor of Veterinary Medicine in Charge of Major

Chairman of Department of Chemistry

Dean of the Graduate School

Date thesis is presented June 14, 1990

ACKNOWLEDGMENTS

I have many individuals to thank for contributions toward my achievement of this goal:

my wife, yongling, for her love and devotion. She has been supportive as I advanced and learned at Oregon State University.

my parents and family for their support.

Dr. Edward H. Piepmeier and Dr. A. Morrie Craig for their invaluable guidance and contributions as my research advisors. Without their help, this thesis cannot be completed.

Dr. Stephen J. Hawkes for his valuable suggestions and support during my research.

The chemistry faculty of Oregon State University for their advice.

TABLE OF CONTENTS

	Page
I INTRODUCTION	1
II HISTORICAL	5
1. Mobile Phase Selectivity and Solvent Selectivity Triangle	5
2. Methods for the Optimization of HPLC Mobile Phase Composition	19
2.1 Introduction	19
2.2 Window Diagrams	
2.2.1 Principles and Operations	21
2.2.2 Window diagram for HPLC	24
2.2.2.1 Retention Models for HPLC	26
2.2.2.1.1 One-parameter Models	27
2.2.2.1.2 Two-parameter Models	28
2.2.2.2 Operations in HPLC Separation	30
2.2.3 Applications	33
2.2.4 Summary	33
2.3 Overlapping Resolution Mapping	35
2.3.1 Principles and Operations	35
2.3.2 Applications	43
2.3.3 Summary	44
2.4 Iterative Mixture Design	46
2.4.1 Principles and Operations	46
2.4.2 Applications	55
2.4.3 Summary	57


2.5	Sequential Simplex Procedures	58
2.5.1	Principles and Operations	59
2.5.1.1	Ordinary Simplex	59
2.5.1.2	Modified Simplex	64
2.5.2	Applications	70
2.5.3	Summary	71
2.6	Step-search Design	72
2.6.1	Principles and Operations	72
2.6.2	Applications	74
2.6.3	Summary	75
2.7	Conclusion	76
	References	77
III	THE WEIGHTED PATTERN COMPARISON METHOD FOR OPTIMIZING THE MOBILE PHASE COMPOSITION IN LIQUID CHROMATOGRAPHY	87
	Abstract	88
	Introduction	89
	Theory	92
	Experimental	109
	Results and Discussion	116
	Conclusion	168
	References	169
IV	A SIMPLIFIED WEIGHTED PATTERN COMPARISON OPTIMIZATION METHOD	172
	Abstract	173
	Introduction	174

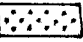
Theory	177
Experimental	184
Results and Discussion	191
Conclusion	227
References	228
V METABOLISM OF NEFOPAM IN GREYHOUND	230
Abstract	231
Introduction	232
Materials and Methods	235
Results	241
Discussion	262
References	270
BIBLIOGRAPHY	272

LIST OF FIGURES

<u>Figure</u>	<u>Page</u>
II.1 Selectivity grouping of solvents (ref. 23).	9
II.2 Selectivity triangles for the preferred solvent in reversed-phase (-----) and normal-phase (-----) chromatography (ref. 7).	13
II.3 A coordinate system used for the optimization of binary or pseudo-ternary mobile phase.	15
II.4 The trilinear coordinate system used for the optimization of a pseudo-ternary mobile phase consisting of components A, B and C. The composition at point O is determined by eqn.s 2, 3, and 4.	16
II.5 Two different ways for showing a separation response surface. (a) an isometric projection of a three dimensional figure, (b) contour lines (a from ref. 102).	18
II.6 Plots of capacity factor, k_R , against stationary phase composition (ϕ_A) for four hypothetical solutes (W, X, Y and Z) separated by GLC. The stationary phase consists of components A and S (ref. 32).	23
II.7 Window diagram for the solutes shown in Figure II.8. Optimum stationary phase composition is at $\phi_A=0.12$.	25
II.8 Minimum a plots (∇ , global optimum) for the separation of five sulphonamides using reversed-phase HPLC with water/methanol/THF mixtures. The	32

	complicated surface arises as a consequence of multiple peak cross-over (ref. 49).	
II.9	Simplex lattice design for reversed-phase HPLC optimization showing relative proportions of each solvent to be used (ref. 45).	38
II.10	Individual resolution maps for the five pairs of solutes with adjacent peaks in the six-solute test mixture. Shaded areas have resolutions, $R_s, < 1.5$, (ref. 17).	40
II.11	Overlapping resolution map (ORM) for the six-component test mixture. This map is constructed by overlapping the five individual resolution maps in Figure II.10. Unshaded area have adequate resolution, $R_s, > 1.5$ (ref. 17).	41
II.12	Experimental design for seven gradient runs to obtain basic data for separation optimization (ref. 44).	42
II.13	Plots of (a) $\ln k'$ and (b) minimum resolution against solvent composition. A is 60% MeOH/H ₂ O. B is 42% THF/H ₂ O (ref. 13).	50
II.14	Chromatogram obtained at the composition indicated as optimum in Figure II.13 (ref. 13).	52
II.15	Revised plots of (a) $\ln k'$ and (b) minimum resolution against composition now incorporating new data from Figure II.14 at Opt 1. Opt. 2 is the new optimum of R_s obtained from these new $\ln k'$ plots (ref. 13).	53
II.16	Chromatogram obtained using optimum composition from Figure II.3 (ref. 13).	54
II.17	Proposed possible fifteen-point initial design for the	56

	optimization of a pseudo-quaternary mobile phase for reversed-phase HPLC(ref. 102).	
II.18	Movements of the ordinary (fixed step size) simplex on a response surface. The initial simplex is 1, 2, 3 and the optimum region lies close to point 12 (ref. 13).	60
II.19	Example of showing several potential locations, T, U,R and S for the new point using the modified simplex method (ref. 1).	65
II.20a	Movements of the modified simplex procedure across the same response surface used in Figure II.18. The initial simplex is 1, 2, 3 and the last simplex is 9, 13 and 15 (ref.17).	68
II.20b	Illustration of a two-dimensional optimization using a modified simplex procedure. (ref. 28)	69
II.21	PESOS grid search process in a ternary or pseudo-quaternary solvent system (ref. 17).	73
III.1	Multisolubility parameter pattern of a mobile phase composition. The subscripts 1, 2, 3, 4, 5 and 6 refer to different interactions, the subscripts m and s refer to the mobile phase and the stationary phase, respectively, and δ is the solubility parameter.	98
III.2	Comparison of the patterns of two different mobile phase compositions. 1, 2, 3, 4, 5 and 6 refer to different interactions. () represents the magnitude of solubility parameters at one composition.	99

() represents the magnitude of solubility parameters at another composition.

a is the difference of a certain interaction between two compositions, $a = |(\delta_{f,m} - \delta_{f,s})_1 - (\delta_{f,m} - \delta_{f,s})_2|$, where the subscripts 1 and 2 refer to the two compositions.

- III.3 Pattern difference and distance. A, B and C refer to three isoeluotropic solvents, a and b refer to the distances between points L1 and O, and points L2 and O respectively, a is equal to b . 101
- III.4 The solvent composition triangle in the Gaussian coordinate system. L, M and N are the global optima on the edges. O is the global optimum of the solvent system ABC, x and y are coordinates of the points, a , b and c are the distances between corresponding points. 103
- III.5 Perpendicular projection of a peak of the hypothetical separation response surface onto the solvent composition triangle. a is the projection of the steepest slope of the peak. ABC is the solvent composition triangle. 120
- III.6 Search step size and the results. 123
 - (a) Best and worst situations for using 3 sampling points to locate a symmetrical peak.
 - (b) Best and worst situations for using 5 sampling points to locate a symmetrical peak.
 - (c) Best and worst situations for using the distance



of the projection of the steepest slope of an asymmetrical peak as the search step size.

(d) Best and worst situations for using half of the distance of the steepest slope of an asymmetrical peak as the search step size.

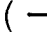




- III.7 Smallest symmetrical peak which can be located by a 10% in step size grid search. For area 1 the whole peak is in the triangle. For area 2 half of the peak is in the triangle. For area 3, 1/6 of a peak is in the triangle. 125
- III.8 Map of k' of solutes in eight different mobile phase. listed on the left. Each line represents one solute. 130
- III.9 Contours for the minimum separation response surface of case 30 in Table III.6. (\otimes) result of the WPCO method; (\diamond) global optimum of the edge.
- III.10 An analogue model of WPC. x_1 , x_2 and x_3 are strings that are tied to each other at one end and strung over frictionless pulleys located at the optima on each edge of the solvent triangle. The weights attached to the strings represent the value of $\ln \alpha$ of the worst-separated peak pair. 139
- III.11 Contours for the minimum separation response surface of 141 case 6 in Table III.7. (\otimes) result of the WPCO method; (\diamond) global optimum of the edge. 141
- III.12 Contours for the minimum separation response surface of case 13 in Table III.7. (\otimes) result of the WPCO method; (\diamond) global optimum of the edge. 142

III.13	Contours for the minimum separation response surface of case 24 in Table III.9. (⊗) result of the WPCO method; (◇) global optimum of the edge.	143
III.14	Contours for the minimum separation response surface of case 13 in Table III.9. (⊗) result of the WPCO method; (◇) global optimum of the edge.	144
III.15	Contours for the minimum separation response surface of case 23 in Table III.9. (⊗) result of the WPCO method; (◇) global optimum of the edge.	146
III.16	Contours for the minimum separation response surface of case 4 in Table III.9. (⊗) result of the WPCO method; (◇) global optimum of the edge.	147
III.17	Contours for the minimum separation response surface of case 5 in Table III.9. (⊗) result of the WPCO method; (◇) global optimum of the edge.	148
III.18	Comparison of window diagrams of cases 4 and 5 in Table III.9.	149
	(a1) Window diagram of Edge AB in case 4 of Table III.9.	
	(a2) Window diagram of Edge AB in case 5 of Table III.9.	
	(b1) Window diagram of Edge BC in case 4 of Table III.9.	
	(b2) Window diagram of Edge BC in case 5 of Table III.9.	
	(c1) Window diagram of Edge AC in case 4 of Table III.9.	
	(c2) Window diagram of Edge AB in case 5 of Table III.9.	
III.19	Contours for the minimum separation response surface of case 12 in Table III.6. (⊗) result of the WPCO method; (◇) global optimum of the edge.	150

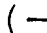



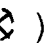
III.20	Two contours near the peak of the minimum separation response surface of the case in Table III.1.	159
	(\otimes) Prediction of the WPCO method;	
	(\diamond) global optimum of the edge.	
III.21	Contours for the minimum separation response surface of case 3 in table 12 or cases 7 and 8 of Table III.8. (\otimes) result of the WPCO method; (\diamond) global optimum of the edge.	160
III.22	Contours for the minimum separation response surface of case 5 in Table III.7. (\otimes) result of the WPCO method; (\diamond) global optimum of the edge.	161
III.23	Contours for the minimum separation response surface of case 36 in Table III.6. (\otimes) result of the WPCO method; (\diamond) global optimum of the edge.	163
III.24	Contours for the minimum separation response surface of case 35 in Table III.6. (\otimes) result of the WPCO method; (\diamond) global optimum of the edge.	164
IV.1a	The ratio of resolution to $\ln\alpha$ vs. selectivity factor (1 to 1.2), α , for different catracity factors, k' .	181
IV.1b	The ratio of resolution to $\ln\alpha$ vs. selectivity factor (1 to 2), α , for different catracity factors, k' .	181a
IV.2	(a) The results of the simplified and original WPCO methods appied to test case 10 of Table 6.	196
	(---) Global optimum area of the minimum $\ln\alpha$ surface. (---) Global optimum area of the minimum R_s surface. ($\text{---}\cdot\text{---}$) Valley of the minimum separation	

response surface ($\ln\alpha = 1, R_s = 0$). () result of the original WPCO method. () result of the simplified WPCO method. (b), (c) and (d) are the $\ln\alpha$ and R_s window diagrams along edges AB, BC and AC, respectively.

- IV.3 (a) The results of the simplified and original WPCO methods applied to test case 13 of Table IV.6. 198

() Global optimum area of the minimum $\ln\alpha$ surface. () Global optimum area of the minimum R_s surface. () Valley of the minimum separation response surface ($\ln\alpha = 1, R_s = 0$). () result of the original WPCO method. () result of the simplified WPCO method. (b), (c) and (d) are the $\ln\alpha$ and R_s window diagrams along edges AB, BC and AC, respectively.

- IV.4 (a) The results of the simplified and original WPCO methods applied to test case 12 of Table IV.6. 201

() Global optimum area of the minimum $\ln\alpha$ surface. () Global optimum area of the minimum R_s surface. () Valley of the minimum separation response surface ($\ln\alpha = 1, R_s = 0$). () result of the original WPCO method. () result of the simplified WPCO method. (b), (c) and (d) are the $\ln\alpha$ and R_s window diagrams along edges AB, BC and AC, respectively.

- IV.5 (a) The results of the simplified and original WPCO methods applied to test case 4 of Table IV.6. 203
- (———) Global optimum area of the minimum $\ln\alpha$ surface. (— — —) Global optimum area of the minimum R_s surface. (— · —) Valley of the minimum separation response surface ($\ln\alpha = 1$, $R_s = 0$). (\otimes) result of the original WPCO method. (\otimes) result of the simplified WPCO method. (b), (c) and (d) are the $\ln\alpha$ and R_s window diagrams along edges AB, BC and AC, respectively.
- IV.6 (a) The results of the simplified and original WPCO methods applied to test case 2 of Table IV.7. 209
- (———) Global optimum area of the minimum $\ln\alpha$ surface. (— — —) Global optimum area of the minimum R_s surface. (— · —) Valley of the minimum separation response surface ($\ln\alpha = 1$, $R_s = 0$). (\otimes) result of the original WPCO method. (\otimes) result of the simplified WPCO method. (b), (c) and (d) are the $\ln\alpha$ and R_s window diagrams along edges AB, BC and AC, respectively.
- IV.7 (a) The results of the simplified and original WPCO methods applied to test case 3 of Table IV.7. 211
- (———) Global optimum area of the minimum $\ln\alpha$ surface. (— — —) Global optimum area of the minimum R_s surface. (— · —) Valley of the minimum separation response surface ($\ln\alpha = 1$, $R_s = 0$). (\otimes) result of the

original WPCO method. (\otimes) result of the simplified WPCO method. (b), (c) and (d) are the $\ln\alpha$ and R_s window diagrams along edges AB, BC and AC, respectively.

IV.8 (a) The results of the simplified and original WPCO methods applied to test case 5 of Table IV.9. 215

(———) Global optimum area of the minimum $\ln\alpha$ surface. (— — —) Global optimum area of the minimum R_s surface. (— · —) Valley of the minimum separation response surface ($\ln\alpha = 1$, $R_s = 0$). (\otimes) result of the original WPCO method. (\otimes) result of the simplified WPCO method. (b), (c) and (d) are the $\ln\alpha$ and R_s window diagrams along edges AB, BC and AC, respectively.

IV.9 (a) The results of the simplified and original WPCO methods applied to test case 6 of Table IV.9. 219

(———) Global optimum area of the minimum $\ln\alpha$ surface. (— — —) Global optimum area of the minimum R_s surface. (— · —) Valley of the minimum separation response surface ($\ln\alpha = 1$, $R_s = 0$). (\otimes) result of the original WPCO method. (\otimes) result of the simplified WPCO method. (b), (c) and (d) are the $\ln\alpha$ and R_s window diagrams along edges AB, BC and AC, respectively.

IV.10 (a) The results of the simplified and original WPCO methods applied to test case 8 of Table IV.9. 221

(———) Global optimum area of the minimum $\ln\alpha$ surface. (— — —) Global optimum area of the minimum R_s surface. (— · —) Valley of the minimum separation response surface ($\ln\alpha = 1$, $R_s = 0$). (⊗) result of the original WPCO method. (⋈) result of the simplified WPCO method. (b), (c) and (d) are the $\ln\alpha$ and R_s window diagrams along edges AB, BC and AC, respectively.

IV.11 (a) The results of the simplified and original WPCO methods applied to test case of Table IV.3.	224
---	-----

(———) Global optimum area of the minimum $\ln\alpha$ surface. (— — —) Global optimum area of the minimum R_s surface. (— · —) Valley of the minimum separation response surface ($\ln\alpha = 1$, $R_s = 0$). (⊗) result of the original WPCO method. (⋈) result of the simplified WPCO method. (b), (c) and (d) are the $\ln\alpha$ and R_s window diagrams along edges AB, BC and AC, respectively.

V.1 Nefopam	233
V.2 TLC result of extract from enzyme hydrolyzed urine. (N) nefopam; (M3) nor-nefopam; (●) Dark color; (⊗) Medium color; (⋈) Light color.	242
V.3 MS spectra of M1 (upper) and M2 (lower).	243
V.4 GC peak height ratio of nor-nefopam to M1 vs. time.	245
V.5 HPLC profile of the subfraction of the flash chromatography process.	247

V.6a	Proton NMR of nefopam.	248
V.6b	COSY of nefopam.	249
V.7	Carbon NMR of nefopam.	252
V.8a	Proton NMR of M1.	254
V.8b	COSY of M1.	255
V.9	Carbon NMR (lower) and DEPT 45o of M1.	256
V.10	Structures of M1 and M2.	261
V.11	Proposed metabolic pathways of mefopam in greyhounds and humans.	263

LIST OF TABLES

<u>Table</u>	<u>Page</u>
II.1 Classification of solvent selectivities.	10
III.1 Separation parameters of four retinal isomers for seven solvents with a normal-phase column.	110
III.2 Capacity factors of thirteen substituted naphthalenes for seven solvents with a normal-phase column.	111
III.3 Capacity factors of six substituted aromatic compounds for seven solvents with a reversed-phase column.	112
III.4 Capacity factors of nine substituted naphthalenes for seven solvents with a reversed-phase column.	114
III.5 Capacity factors of ten polar adrenocortical steroids for seven solvents with a reversed-phase column.	115
III.6 Solute constituents of substituted naphthalenes for test cases with a normal-phase column.	127
III.7 Solute constituents of aromatic compounds for test cases with a reversed-phase column.	132
III.8 Solute constituents of substituted naphthalenes for test cases with a reversed-phase column.	133
III.9 Solute components of adrenocortical steroids for test cases with a reversed-phase column.	136
III.10 Comparison of the results of the WPCO and minimum α plot methods for the cases in Table III.6.	153

<u>Table</u>	<u>Page</u>
III.11 Comparison of the results of the WPCO and minimum α plot methods for the cases in Table III.7.	155
III.12 Comparison of the results of the WPCO and minimum α plot methods for the cases in Table III.8.	156
III.13 Comparison of the results of the WPCO and minimum α plot methods for the cases in Table III.9.	157
IV.1 Capacity factors of four substituted naphthalenes for seven solvents with a normal-phase column.	185
IV.2 Resolutions and selectivity factors of four retinal isomers for seven solvents with a normal-phase column.	186
IV.3 Capacity factors of ten polar adrenocortical steroids for seven solvents with a reversed-phase column.	187
IV.4 Capacity factors of six substituted aromatic compounds for seven solvents with a reversed-phase column.	189
IV.5 Capacity factors of nine substituted naphthalenes for seven solvents with a reversed-phase column.	190
IV.6 Test cases using constituents of polar adrenocortical steroids with a reversed-phase column.	194
IV.7 Test cases using constituents of substituted naphthalenes with a normal-phase column.	206
IV.8 Test cases using constituents of substituted aromatic compounds with a reversed-phase column.	207
IV.9 Capacity factors of peaks for the worst-separated	214

<u>Table</u>	<u>Page</u>
peak pairs at the global optimum of each edge of case 2 and 3 in Table IV.7.	
IV.10 Capacity factors of peaks for the worst-separated peak pairs at the global optimum of each edge of cases 5, 6 and 8 in Table IV.9.	217
IV.11 Capacity factors of peaks for the worst-separated peak pairs at the global optimum of each edge of the original case in Table IV.5.	226
V.1 Relative peak heights of nefopam and its metabolites in the GC chromatogram and ratios of these heights.	267

A NEW GENERAL METHOD FOR THE OPTIMIZATION OF HPLC TERNARY OR PSEUDO-QUATERNARY MOBILE PHASES AND THE SEPARATION OF TWO NEW METABOLITES OF NEFOPAM FROM GREYHOUND URINE

I. Introduction

The primary goal of liquid chromatography optimization is to achieve the desired separation with a minimum of time and effort. To achieve this goal, several variables, such as the stationary phase, flow rate, mobile phase solvent(s), solvent composition, and pH of the mobile phase must be optimized. Among these variables, mobile phase optimization has the greatest effect on selectivity^{1,2}.

The optimization of HPLC mobile phases actually has two major steps. The first is to choose solvents for the mobile phase that have characteristics that will lead to good separation. The other step is to find the composition of the mobile phase which provides the desired separation results. The optimization of mobile phases in liquid chromatography is very difficult¹. In many situations, a trial-and-error procedure is still used^{2,3}. This procedure usually takes a lot of time and effort.

In the method development process for the chromatographic separation of a sample, a chromatographer usually needs to do two

things. In the beginning of the development process, the chromatographer needs to choose the right solvents to form a mobile phase that is the most promising one to provide the desired separation. If the right choice is made, then the time spent later on in the experimental work will be minimized and good results can be obtained.

In the later stage, after a certain amount of time and effort, for example 2 to 3 weeks (even months), has been invested in the development of a chromatography system, and the desired separation has not been achieved, then, the chromatographer will be in a dilemma: should the work continue on this system, or should a new system be invested. Stated differently, the chromatographer has to be able to tell if the global optimal separation of this system has been achieved. The correctness of the answer is critical. A lot of time and effort could be saved or wasted. On the one hand, when the system can provide the desired separation, then the time and effort which has been invested will be wasted if the system is abandoned. On the other hand, when the system cannot provide the desired separation, the time and effort will be wasted if the chromatographer keeps working on the system. If a trial-and error method has been used in the method development process, it is very difficult to answer the question correctly, because only after all the possible compositions of this mobile phase are tried, can the question be answered correctly.

Therefore, a systematic approach for the optimization of HPLC mobile phases can help to answer these two questions correctly.

In recent years, several systematic approaches for optimizing HPLC mobile phases have been developed^{4,5,6,7,8,9,10,11,12,13,14}. These methods can be divided into two categories. One of these two categories includes the methods for known samples. The other category includes the methods for both known samples and unknown samples.

In chromatography, the term, known sample, refers to the samples whose chromatographic peaks can be recognized regardless of how their retention times change as the mobile phase is changed. It should be noted that, for the purpose of the optimization of HPLC mobile phases, it is not necessary to know the chemical structure of solute that produces the peak as long as the peak can be recognized. However, the way to recognize a peak usually is to run a chromatogram of a pure standard of each component, and then compare the retention times of the standard with the peaks in the chromatogram of the sample.

The term, unknown sample, refers to the samples whose components cannot be recognized.

The methods for known samples usually need fewer experiments than the trial-and-error method, and the performance of these methods usually are satisfactory. On the other hand, the performance of the methods for unknown samples are not as good

as the methods for known samples. One of the major methods used for unknown samples, the simplex procedures, usually will find a local optimum rather than the global optimum. The other major method, the step-search design method, usually requires more than two hundred experimental runs and several hundred working hours to find the global optimum of a ternary mobile phase¹⁵. Therefore, for the separation of unknown samples, it is necessary to develop a method which needs fewer experiments and still can locate the global optimum.

This thesis documents the development of a new method, the weighted pattern comparison optimization (WPCO) method, for the optimization of the liquid chromatography mobile phase. This method can be used for both known or unknown samples. It is simpler than the methods currently in use. Moreover, the global optimum can be located by this method with substantially fewer experimental measurements. The applications of the WPCO method in various forms of HPLC for the separation of various samples are also described in this thesis.

II. HISTORICAL

1. Mobile Phase Selectivity and the Solvent Selectivity Triangle

Selectivity is the ability of a stationary-mobile phase combination to separate a variety of components in a desired period of time. The goal of improving selectivity is to improve the resolution of all components of interest. Once a stationary phase has been chosen, further improvements must be obtained from optimization of the mobile phase composition; choosing the right solvents and the right compositions¹⁶.

The effect of the mobile phase selectivity on liquid chromatography separation can be seen from a well known equation:

$$R_s = 1/4 (N)^{1/2}(\alpha - 1)[k'/(1+k')] \quad (1)$$

where R_s is the resolution of the two peaks under consideration, N is the number of theoretical plates, k' is the average capacity factor of the peak pair, and α is the selectivity factor.

Since the mobile phase optimization process usually starts after a column has been chosen, N is a constant. Moreover, the

peaks are usually arranged in the capacity factor, k' , range of 1-10, so k' is also relatively constant. Thus, the selectivity factor, α , is the only parameter left that is subject to major adjustment. The main objective in the optimization of a separation is to make the selectivity factor as large as possible to improve the resolution. This goal is usually accomplished by changing the composition of the mobile phase because the composition is the factor which influences the selectivity factor strongly¹⁷.

Interactions exist between solutes and the mobile phase, and between solutes and the stationary phase. The interactions between solutes and the mobile phase carry the solutes through the column, whereas the interactions between the solutes and the stationary phase retain the solutes on the stationary phase. The interactions between the solutes and the mobile phase compete with those between the solutes and the stationary phase. Several different kinds of interactions constitute the interaction force between the mobile phase and the solutes. In general, the magnitude of the major interaction between a mobile phase and a solute will not be the same as the the magnitude of the same interaction between the mobile phase and another solute. These differences help to make some solutes elute out of the column earlier than others; that is, these differences are responsible for the separation effect of liquid chromatography. When the composition of the mobile phase changes, the magnitude of these interactions will also change; these changes, in turn, make the

selectivity of the mobile phase change. Stated differently, the different abilities of different solvents to interact with various solutes (sample components) which are to be separated is the major factor that will affect the value of the selectivity factor.

The major interactions between non-electrolytic solvents and solutes are hydrogen bonding, dipole orientation, dipole induction and dispersion^{18,19,20}.

Hydrogen bonding interaction exists between proton donor and proton acceptor molecules. That is, this type of interaction can occur only between a proton donor and a proton acceptor.

Dipole orientation refers to the interaction which occurs when the negative (positive) end of a polar molecule is surrounded by the positive (negative) ends of other polar molecules. This type of interaction only exists among polar molecules because a permanent dipole moment is required.

Dipole induction occurs when a polar molecule induces a temporary dipole in a neighboring molecule which could be polar or non-polar. The interaction between these dipoles is dipole induction.

Dispersion results from the mutual disturbance of the electron clouds of interacting molecules. This interaction exists between any molecules which are close enough to each other. Dispersion is weak and non-selective, hence it does not have much

significance on the selectivity of a liquid chromatography mobile phase²¹.

The major interactions between the mobile phase and solutes which have a significant effect on selectivity are hydrogen bonding and dipole interactions.

For the purpose of optimization of the mobile phase, hydrogen bonding is further categorized into two groups, proton donor and proton acceptor, based on the functionality of the corresponding molecule. The permanent and induced dipole related interactions will be called simply the dipole-dipole interaction. Therefore, three major interactions between the mobile phase and solutes which significantly affect the selectivity of the mobile phase are proton donor, proton acceptor and dipole-dipole²².

Snyder has proposed a scheme for categorizing common solvents based on their relative selectivities²³. A trilinear coordinate system is used to show the relative magnitudes of the proton donor, proton acceptor and dipole-dipole interactions of these solvents. Fig. II.1 shows these groups and the position of each solvent in the group. Each circle on the plot represents a group. The solvents in the same group have similar selectivity characteristics and generally the same functionality (see Table 1).

The greatest change in mobile-phase selectivity can be achieved when the relative importance of these various interactions between mobile phase and solutes is dramatically

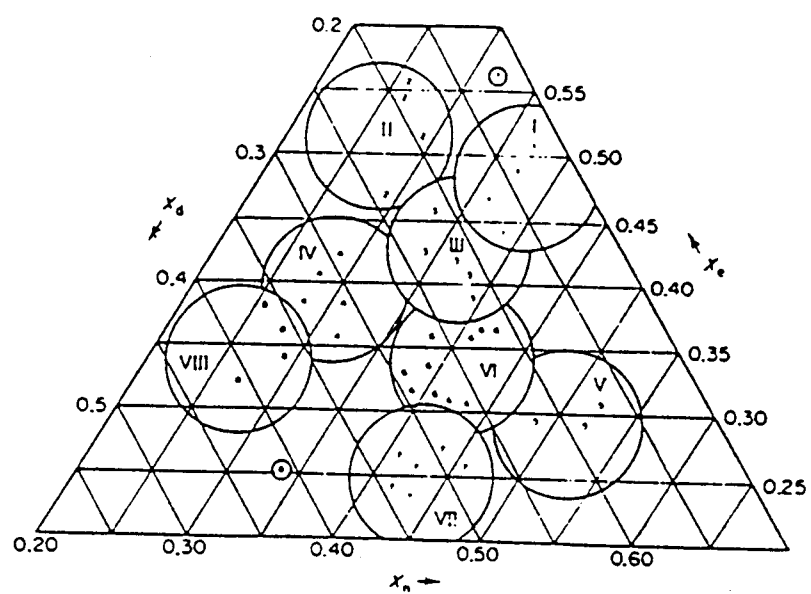


Fig. II.1 Selectivity grouping of solvents (ref. 23).

Table II.1 CLASSIFICATION OF SOLVENT SELECTIVITIES

Group	Solvents
I	Aliphatic ethers, tetramethylguanidine, hexamethylphosphoramide (trialkylamines)
II	Aliphatic alcohols
III	Pyridine derivatives, tetrahydrofuran, amides (except formamide), glycol ethers, sulphoxides
IV	Glycols, benzyl alcohol, acetic acid, formamide
V	Dichloromethane, dichloroethane
VI	(a) Tricresyl phosphate, aliphatic ketones and esters, polyethers, dioxane (b) Sulphones, nitriles, propylene carbonate
VII	Aromatic hydrocarbons, halogen-substituted aromatic hydrocarbons, nitro compounds, aromatic ethers
VIII	Fluoroalkanols, <i>m</i> -cresol, water (chloroform)

changed¹⁻³. For instance, a great change in selectivity will be expected if a proton donor solvent is replaced by a proton acceptor solvent. However, if a proton donor is replaced by another proton donor, selectivity would not be changed dramatically.

Based on these considerations, a common strategy for mobile phase optimization has been developed²⁴. First, solvents are chosen from the solvent groups as far apart as possible in the solvent selectivity map. For example, a solvent may be chosen from a proton donor group while another solvent may be chosen from a proton acceptor group. By mixing these solvents, a larger contrast in mobile phase selectivity can be achieved and this will, in turn, provide greater opportunity to produce the desired selectivity.

Since there are three major interactions, three solvents from different selectivity groups can be chosen to form a mobile phase: a solvent from a proton donor group; another one from a proton acceptor group; the third one from a dipole-dipole group. These solvents form the corner of a solvent selectivity triangle. By making this triangle as large as possible, the maximum contrast in solvent properties (interactions) will be achieved and the possibility of obtaining the desired selectivity in the solvent system is also maximized.

However, it is not practical to choose solvents from the groups at the extreme vertices of the classification shown in Fig.

II.1 when the cost, miscibility with other solvents and chromatographic suitability (e.g., the solvent may absorb UV light) are taken into consideration. The selection of the two practical sets of solvents are shown in Fig. II.2. One set is for reversed-phase chromatography; this set consists of methanol, acetonitrile and tetrahydrofuran. The other set is for normal-phase chromatography; it consists of diethyl ether (or methyl tertbutyl ether), dichloromethane and chloroform. However, it should be noted that this strategy is a general approach. It does not mean that these solvents are the only choices for mobile phases. It may be appropriate to select a different solvent to achieve a desired selectivity.

In addition, in practice, before these pure solvents are used as initial solvents to be mixed with each other, their solvent strengths should be adjusted first so that the capacity factors of the solutes will be in the range of 1-10. In order to adjust the solvent strength of each of these solvents, a carrier solvent which is assumed to have little of these major interactions, is usually used to mix with the solvent. For reversed-phase chromatography, water is usually used as the carrier. For normal-phase chromatography, hexane is usually used as the carrier.

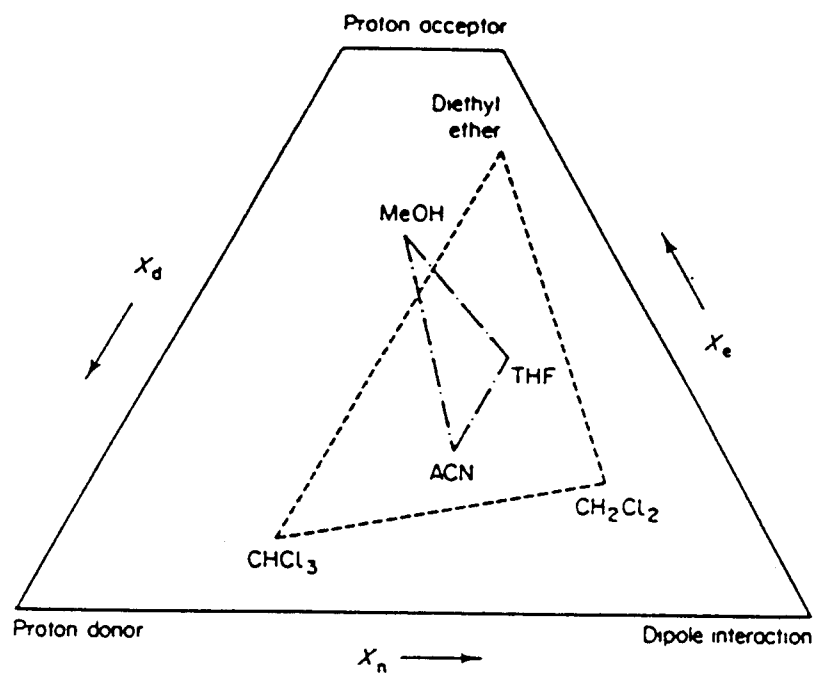


Fig. II.2 Selectivity triangles for the preferred solvent in reversed-phase (-----) and normal-phase (.....) chromatography (ref. 7).

Coordinate Systems for the Optimization of the Mobile Phase.

Since the coordinate systems used in the optimization of mobile phases are not the most common ones, two of these coordinate systems are described in this section.

One of the coordinate systems which are commonly used to represent mobile phase optimization results is shown in Fig. II.3. This coordinate system is used for a mobile phase with one solvent and one carrier (binary), or a two- solvents and one carrier (pseudo-ternary) mobile phase.

When the coordinate system is used for a mobile phase with one solvent and one carrier, one end of the x axis represents the pure solvent, or the blend in which the solvent has the highest proportion over the entire range; the other end of the x axis represents the carrier, or the blend in which the proportion of the carrier is highest. When the coordinate system is used for two solvents and one carrier, one of the x axis ends represents an initial binary mixture (a solvent and the carrier); the other end represents the other initial binary mixture (the other solvent and the carrier). In all these situations, the y axis is used for the selectivity function response, such as the selectivity factor or the resolution.

The trilinear coordinate system (see Fig. II.4) is commonly used for a three-solvent (pseudo-four-solvent) mobile phase. Each of the three vertices represents an initial solvent. For a mobile

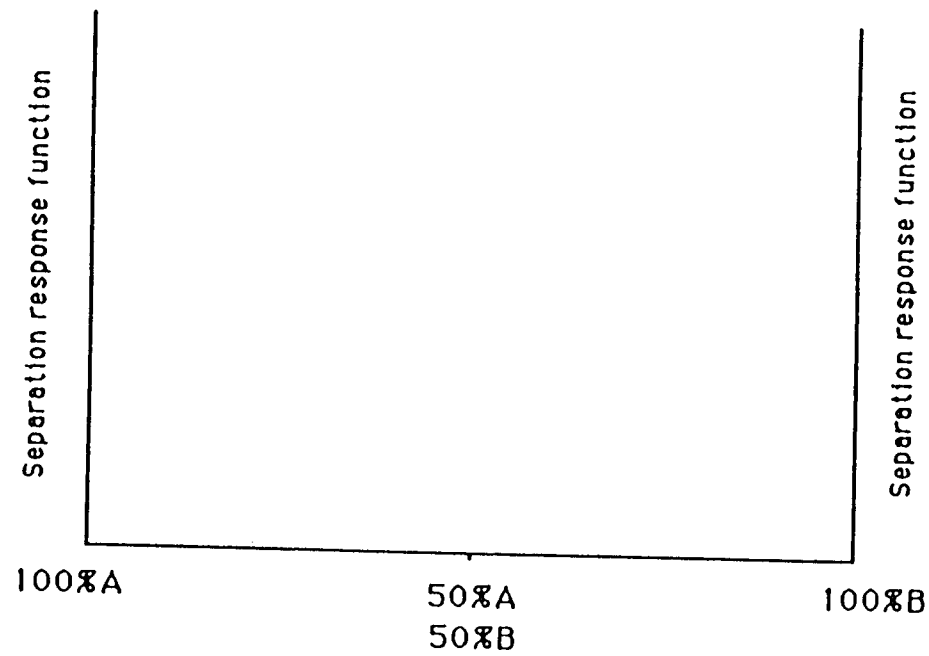


Fig. II.3 A coordinate system used for the optimization of binary or pseudo-ternary mobile phase.

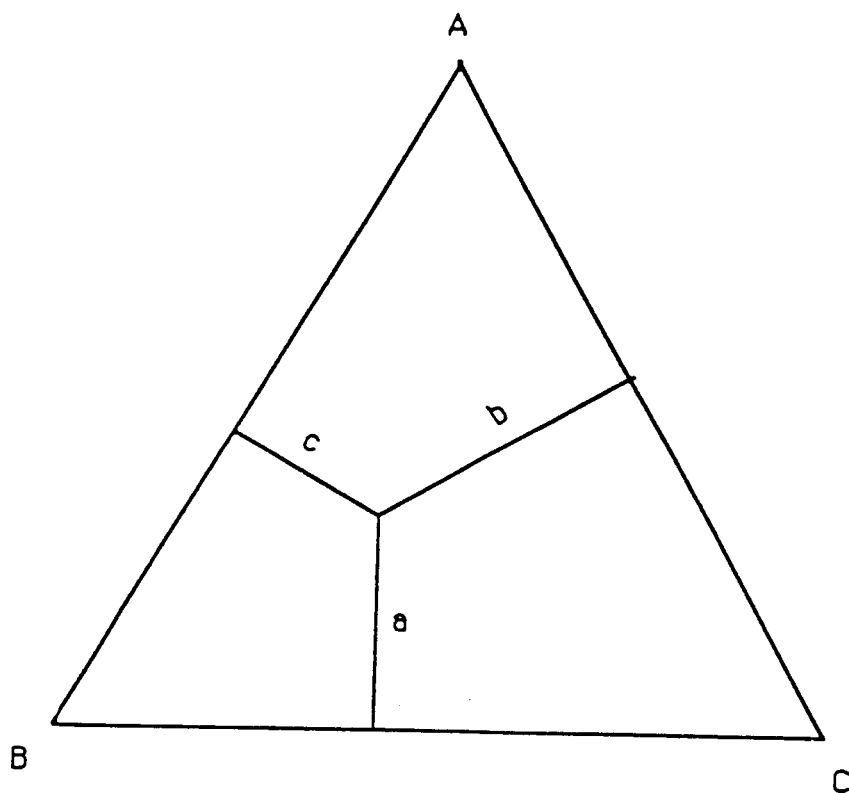


Fig. II.4 The trilinear coordinate system used for the optimization of a pseudo-ternary mobile phase consisting of components A, B and C. The composition at point O is determined by eqn.s 2, 3, and 4.

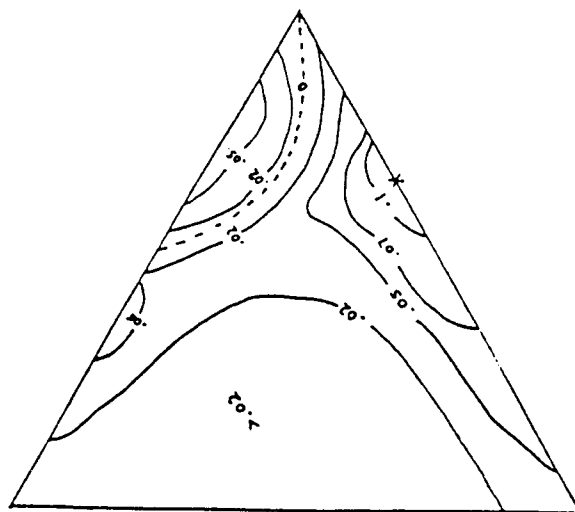
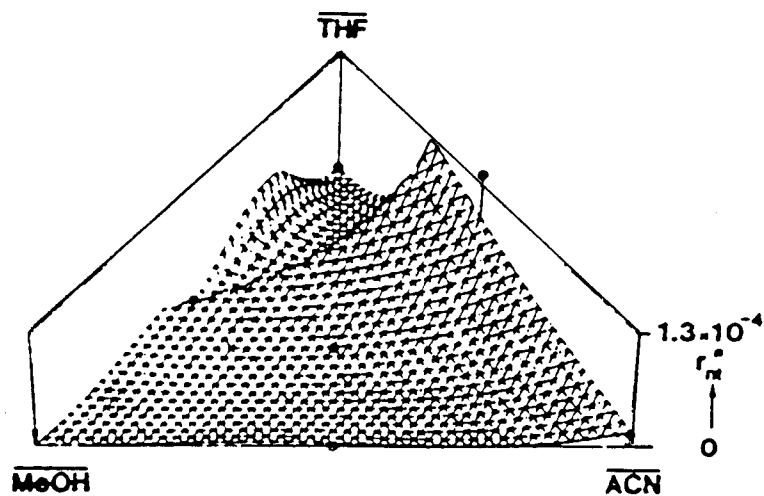
phase which has relatively constant solvent strength, the initial solvents are usually a binary mobile phase (a solvent and the carrier). The composition represented by each point of the triangle is determined as follows;

$$A\% = a/(a+b+c) \times 100 \quad (2)$$

$$B\% = b/(a+b+c) \times 100 \quad (3)$$

$$C\% = c/(a+b+c) \times 100 \quad (4)$$

The separation response is along the z axis perpendicular to the triangle, Fig. II.5a. The separation response surface is usually shown by its contour lines, Fig. II.5b. Fig II.5a shows an isometric projection at the same three-dimensional surface.



2. METHODS FOR THE OPTIMIZATION OF HPLC MOBILE PHASE COMPOSITION

2.1 Introduction

In recent years several methods for the optimization of liquid chromatography mobile phase compositions have been developed^{25,26,27,28}. These methods can be divided into two categories. One of these two category includes the methods which only can be used for known samples. The methods in this category usually require the recognition of peaks in chromatograms. Since the recognition process usually needs a pure standard for each of the sample components, these methods cannot be used for the separation of unknown samples. The window diagram, overlapping resolution mapping, and iterative mixture design methods are the major methods in this category.

The other category includes the methods which can be used for both known and unknown samples. These methods do not require the recognition of peaks in chromatograms. The sequential simplex procedures and step-search design are the major methods in this category.

The principles and development processes of these methods reflect the major considerations and approaches in the field of the optimization of HPLC mobile phases, and moreover, in the

developing process of the weighted pattern comparison method, these methods have been either used or compared. Therefore, these methods are reviewed in this section. The methods for known samples will be discussed first; then, the methods for both known and unknown samples will be discussed.

2.2 The Window Diagram Method

The window diagram method is a method which is used for liquid chromatography mobile phase optimization for known samples. For HPLC, originally, it was developed for binary mobile phase optimization. Later, it was further developed and used for ternary (or pseudo-quaternary) mobile phases. When several optimal points exist, the window diagram method can find the global optimum. Moreover this method allows chromatographers to select the best separation conditions simply by inspection because graphs are usually used to present the results in this method.

2.2.1 Principles and Operations

The window diagram method was initially introduced by Laub and Purnell^{29,30,31} in 1976 for the optimization of the selectivity of gas-liquid chromatography (GLC). Their original work is a very good example for demonstrating the basic principles of the window diagram method and transferring them to liquid chromatography. In GLC, the separation selectivity is basically controlled by the stationary phase. The composition of a two-component liquid stationary phase is adjusted in order to improve separation selectivity. The window diagram method is

used to find the composition of the blended packings which provides the best selectivity.

In Laub and Purnell's original work, first, a linear equation, which was found empirically³², was used to describe the relationship between capacity factors (k') and the composition of the binary mixed-bed stationary phase. Because of this linear relationship, if the capacity factor of a solute in each of the pure stationary phases is known, then, the capacity factor of this solute at any column composition can be predicted; straight lines result when the capacity factor is plotted against the composition of the binary stationary phase (see Fig. II.6). Then, the selectivity factors (α) can be calculated for all the possible peak pairs over the whole range of column compositions.

There are two points worth considering when using this method. First, the number of peak pairs which can be possibly formed for n peaks is calculated by the following equation:

$$\text{No. of peak pairs} = n!/2(n-2)! \quad (5)$$

The second point is that by its definition, α is always greater than 1. Therefore, in order to make the value of α greater than 1, when peak cross-over occurs, that is, a change in the order of elution of the two peaks, then α should be reversed accordingly. That is, the capacity factor of one solute which used to be the numerator should change to be the denominator; the capacity

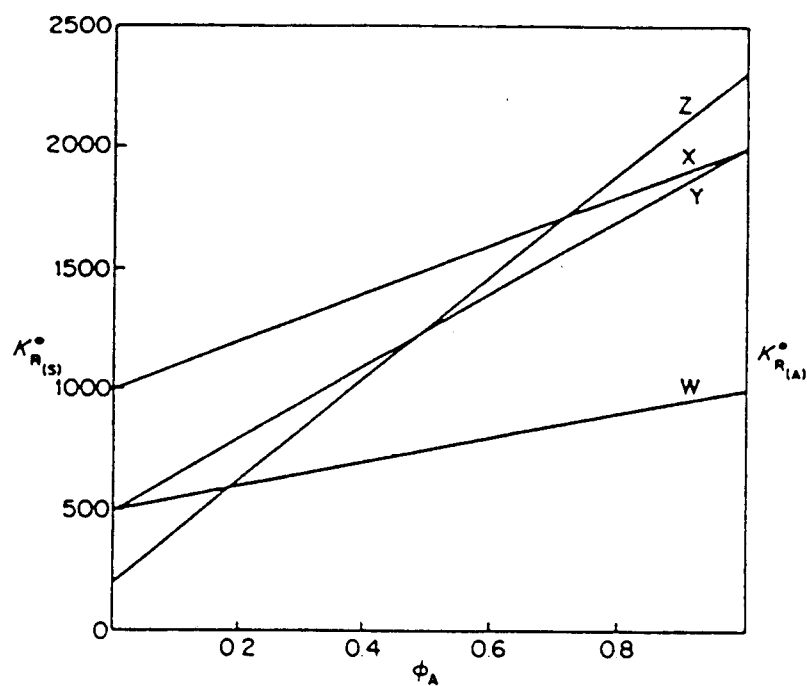


Fig. II.6 Plots of capacity factor, k_R , against stationary phase composition (ϕ_A) for four hypothetical solutes (W, X, Y and Z) separated by GLC. The stationary phase consists of components A and S (ref. 32).

factor of another solute which used to be the denominator should change to be the numerator.

The third step is to plot these α values against the composition of the stationary phase, and a window diagram is constructed by shading the area between the x axis and the lowest α curves in the manner shown in Fig. II.7. The shaded areas are the "windows". Since the α curves of all the other peak pairs are above the top of these windows, the top of the windows represents the α values of the worst separated peak pair(s). The composition corresponding to the highest peak in the window diagram is the global optimum of this mobile phase system.

Now, the composition of the stationary phase will be easily revealed by simply inspecting these windows. The composition corresponding to the highest peak of the windows gives the highest α value for the worst separated peak pair(s), and all other peak pairs have greater α values. Therefore, this composition is the global optimum, point A in Fig. II.6.

2.2.2. The window diagram method for HPLC

In 1978, the window diagram method was extended to optimize the column temperature in GLC, gas-solid chromatography and HPLC³³. Since then, the window diagram

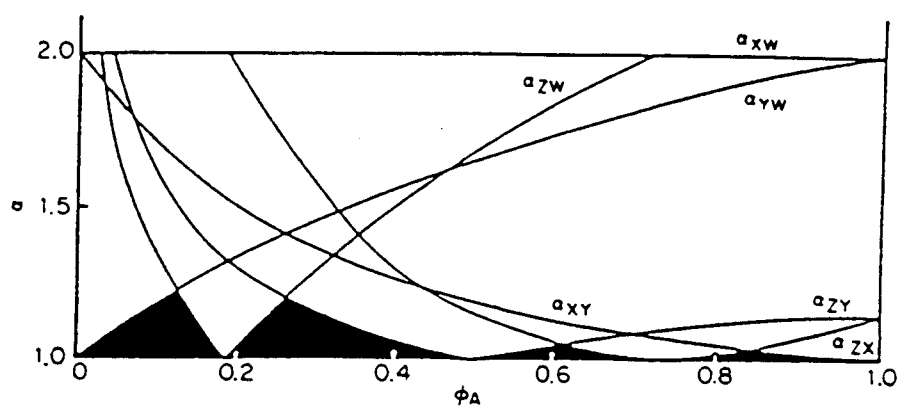


Fig. II.7 Window diagram for the solutes shown in Figure Fig. II.8.
 Optimum spationary phase composition is at $\phi_A=0.12$
 (ref.32).

method has become an important method for the optimization of HPLC mobile phases.

2.2.2.1 Retention models for HPLC

For applying the window diagram method to HPLC, it is necessary to have a model which describes the relationship between the separation response function, such as resolution, and the independent variables, such as the composition of mobile phase. Then, based on this model, the retention behavior of solutes between experiment points can be calculated.

Since this thesis is basically about liquid chromatography mobile phase optimization, and the window diagram method will be used, it will be helpful to discuss several models describing the relationship between the retention behavior of solutes and the composition of the mobile phase, and to consider applications of these models.

For the optimization of HPLC solvent composition, the establishment of a valid model is slightly more difficult than in gas-liquid chromatography³⁴. Up to date, several models have been established. However, one should note, in practice, a semi-empirical model is usually required, and the simplest model usually is the best one among all the models which can be used³⁵.

2.2.2.1.1. One-parameter models

For most mobile phases, a simple definitive linear relationship between solute capacity factors and mobile phase composition does not exist. However, for certain organic modifiers (10-80% methanol/water or acetonitrile/water), in reversed-phase separation and over a limited composition range for binary mobile phases, a linear relationship between the logarithm of the capacity factor, k' , and the mobile phase composition can be used as an approximation^{36,37};

$$\log k' = a + b\phi_B \quad (6)$$

where ϕ_B is the volume fraction of the solvent which effects the selectivity of the mobile phase most strongly, and a and b are the experimentally determined coefficients.

There is another linear model, eqn. 7, which is used for various binary mobile phase over the capacity factor range of 1-10^{38,39}.

$$\ln k' = \ln k_0 - S\phi \quad (7)$$

where k_0 is an imaginary extrapolated capacity factor in pure water, ϕ is the proportion of organic modifier and S is a coefficient determined by experiments.

Experiments have shown that, within the capacity factor range of 1-10, eqn. 7 is usually an adequate approximation.

Fortunately, this capacity factor range is the most useful one because capacity factors which are less than 1 usually result in insufficient resolution, while capacity factors which are great than 10 usually result in excessive retention times.

However, many solutes, including methanol/water and acetonitrile/water binary mobile phases exhibit markedly curved plots of the $\ln k'$ versus ϕ even within a limited composition range. A more complex model was then developed to describe these chromatographic retention behaviors by adding a quadratic term to eqn. 7 to give⁴⁰:

$$\log k' = a\phi^2 + b\phi + c \quad (8)$$

where a , b and c are experimentally determined coefficients, and ϕ is the volume proportion of an organic solvent.

2.2.2.1.2 Two-parameter Models

For the mobile phase optimization process which has two independent variables, such as ternary or pseud-quatarnary mobile phase, more complex models are necessary.

Eqn. 9 is the simplest model which can be used for a first approximation⁴¹.

$$\log k' = a + b\phi_B + c\phi_C \quad (9)$$

where C refers to the second modifier. This modifier can be a second organic solvent, a ligand, or a counter ion.

However, this simple model usually will fail because of non-linear retention behavior of solutes. To describe non-linear retention behaviors, second-order terms are added to eqn. 9 to give

$$\log k' = a_1\phi_1 + a_2\phi_2 + a_3\phi_3 + a_{12}\phi_1\phi_2 + a_{13}\phi_1\phi_3 + a_{23}\phi_2\phi_3 + a_{123}\phi_1\phi_2\phi_3 \quad (10)$$

where the subscripts ϕ_1 , ϕ_2 , and ϕ_3 refer to the concentrations of the three initial solvents (their sum must be unity), and a_1 - a_{123} are coefficients calculated by fitting eqn. 10 to experimental points.

In this equation, a_1 , a_2 and a_3 represent linear effects, and a_{12} , a_{13} and a_{23} indicate blending interactions between two solvents, and the term, $a_{123}\phi_1\phi_2\phi_3$ estimates ternary blending. Although this equation does not have a fundamental basis from the theories which describe physicochemical processes of liquid chromatography⁴², this equation has been found to be an adequate model for describing three-component mobile phases^{43,44}.

A well designed experimental plan is necessary to obtain the polynomial regression parameters in eqn. 10. A simplex lattice design is usually used for the optimization operation⁴⁵. To

describe the retention behavior of solutes, eqn. 10 is generally adequate⁴⁶. Equation 10 is the most commonly used model when the window diagram method is used for the optimization of a ternary (or pseudo-quaternary) mobile phase⁴⁷.

A better but more complex model has been developed for methanol, acetonitrile and tetrahydrofuran mixture with water⁴⁸:

$$\ln k' = c + a_M \phi_M^2 + b_M \phi_M + e_M \phi_M^{0.5} + a_A \phi_A^2 + b_A \phi_A + e_A \phi_A^{0.5} + a_T \phi_T^2 + b_T \phi_T + e_T \phi_T^{0.5} \quad (11)$$

where subscripts A, M and T denote acetonitrile, methanol and THF, respectively; a, b, c and e are coefficients determined by fitting eqn. 11 to experimental data.

This model can describe curvatures in log k' versus composition plot even at high water composition. However, many experiments are needed. In the original work, experiments were carried out with thirty-nine compositions for each solute. In fact, this equation has not been used to construct window diagrams for the optimization of a mobile phase in any published works.

2.2.2.2 Operations in HPLC Separation

After the retention behavior model has been chosen in the optimization of an HPLC binary (pseudo-ternary) mobile phase, the window diagram is constructed and used the same as in gas-liquid

chromatography. When the window diagram is used for the optimization of a ternary (or pseudo-quaternary) mobile phase, the principles and operations are the same as for a binary mobile phase. The only difference is the 3-dimensional nature of the retention behavior models. The two-dimensional window diagram in a binary mobile phase becomes three-dimensional in the ternary mobile phase. Similarly, the borders of the windows become surfaces. Fig. II.8 shows the windows of a ternary mobile phase separation case⁴⁹. The optima are the peaks of this surface.

When the effects of two (or more) variables are being studied, the term "window diagram" may be slightly misleading because the locus of the separation function of the worst-separated peak pair(s) is no longer a line which can be expressed by a two-dimensional window diagram. What is really being done is to examine multi-dimensional space to find a mobile phase composition which gives the maximum separation between the worst separated peak pair(s). An alternative term "minimum α plots" (MAPs), has been suggested for cases with two independent variables⁵⁰.

However, the term, MAPs, also has its own limitation. It gives the impression that the α value is the only factor that might be considered. In fact, the technique does not restrict itself to the use of α values only. Other parameters, such as resolution, also can be used as optimization criteria.

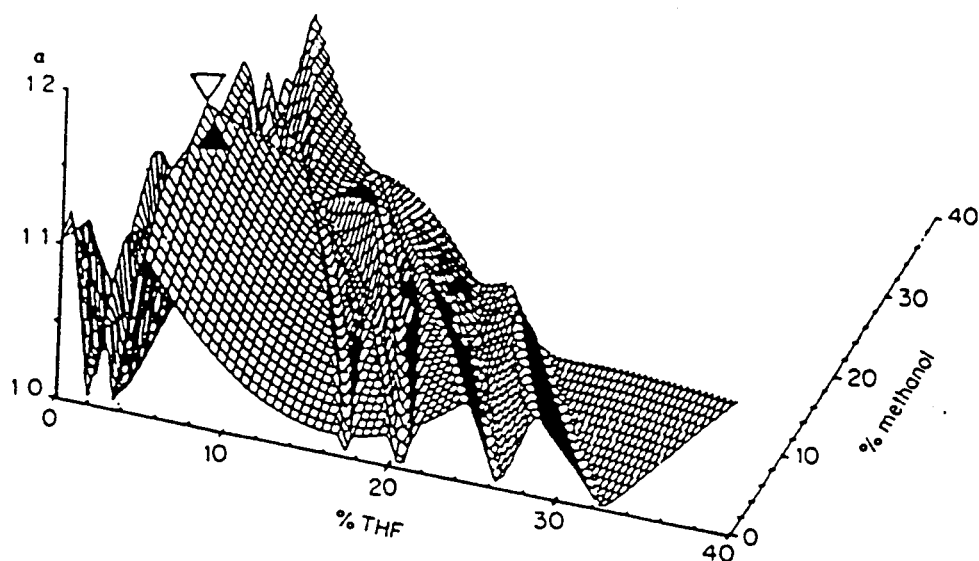


Fig. II.8 Minimum α plots (∇ , global optimum) for the separation of five sulphonamides using reversed-phase HPLC with water/methanol/THF mixtures. The complicated surface arises as a consequence of multiple peak cross-over (ref. 49).

2.2.3 Application

The window diagram method has been widely used to optimize HPLC mobile phases. This method has been applied to normal-phase⁵¹ and reversed-phase^{52,53,54,55,56,57,58,59,60,61,62} HPLC for various samples. Furthermore, the window diagram method has been applied to ion chromatography^{63,64}. This method also has been used for the optimization of pH^{65,66,67,68,69,70}, ionic strength^{71,72} and ion-pair concentration⁷³ of mobile phase. In addition, this method even has been used for the optimization of separation temperature. Recently, a commercially available software program, DRYLAB™, which is based on the principles of the window diagram method^{74,75,76,77} is becoming popular. This further promotes the wider application of the window diagram method.

2.2.4 Summary

The window diagram method is a method used for the optimization of the separation of known samples. This method is very useful for the optimization of HPLC binary, ternary and quaternary mobile phases. The window diagram method has also been used to optimize parameters (e.g. pH, ionic strength etc.) other than mobile phase composition. This method has several

advantages. First, the global optimum can be located. Second, this method shows the separation results over the entire composition range. This permits other factors to be taken into consideration, and allows a user to select the most suitable composition. However, the window diagram method also has some disadvantages. The major disadvantage is that this method requires the recognition of peaks, so it cannot be used for unknown samples. This really limits the application of this method. Second, the retention behavior of solutes has to be fit to a suitable model. A relatively simple model may not always be available, and complex models require many experiments.

2.3 The Overlapping Resolution Mapping Method(ORM)

The overlapping resolution mapping method (ORM) is another method used for liquid chromatography mobile phase optimization for known samples. This method has been developed for optimization of ternary (or pseudo-quaternary) mobile phases which are represented by a trilinear coordinate system. However, this model cannot be used for binary mobile phases. This method usually finds all the composition regions which provide the desired separation. However, when several optima exist, this technique usually can find the global optimum.

2.3.1 Principles and Operations

The overlapping resolution mapping method was introduced by Glajch et al.⁷⁸ for the optimization of a ternary (or pseudo-quaternary) mobile phase. The goal of this method is to find the compositions which provide an adequate separation or the best separation that the mobile phase system can provide, within a desired capacity factor range.

This goal is accomplished by manipulation of the selectivity of the mobile phase composition, and, at the same time, maintaining a relatively constant solvent strength. The

first step of this method is to choose three solvents according to Snyder's solvent selectivity triangle concept and other considerations about experimental constraints, such as solvent miscibility. Then, the solvent strength of each of these three solvents is adjusted by mixing with a carrier so that the capacity factors of the sample solutes will fall in a desired range. These three binary mobile phases which have about the same solvent strength are then used as the initial solvents of the ternary (or pseudo-quaternary) mobile phase. These three initial solvents are located at the three vertices of the trilinear coordinate system which represents the ternary mobile phase. All the other possible compositions of the ternary mobile phase system are mixtures of these three initial solvents.

A polynomial surface model, a special cubic equation, is used to describe the relationship between solute retention behavior and mobile phase compositions:

$$\ln k' = a_1\phi_1 + a_2\phi_2 + a_3\phi_3 + a_{12}\phi_1\phi_2 + a_{13}\phi_1\phi_3 + a_{23}\phi_2\phi_3 + a_{123}\phi_1\phi_2\phi_3 \quad (12)$$

where ϕ is the proportion of isoelutropic eluent, and k' is the capacity factor. The subscripts 1, 2 and 3 represent the three isoelutotropic eluents and a_1 - a_{123} are coefficients calculated from the seven experimental points needed to fit eqn. 12.

J. L. Glajch et al. have found that the most accurate result is achieved when the logarithm of the capacity factor is modelled⁷⁹. This chromatography retention model has been widely applied and satisfactory results have been obtained^{80,81}.

The chromatographic experiments are carried out by a pre-planned simplex lattice design (Fig. II.9), described by Snee⁸². According to this design, experiments are needed at ten composition points in the triangle to measure the retention times of solutes in order to calculate the coefficients in eqn. 12. However, later, it was found that seven experimental compositions (points 1-7 in Fig. II.9) are sufficient. Currently, this seven point design is usually used for the overlapping resolution mapping method.

After the coefficients of the model for each solute are calculated, retention behavior response surface of each solute over the entire trilinear coordinate system is built using eqn. 12. Then, a resolution response surface of every possible solute pair is built from the retention behavior response surfaces for those solutes. The total number of the possible peak pairs can be calculated by eqn. 5. For example, for a 4-solute sample, the total number of all the possible peak pairs is six. The possible peak pairs which contain solute 1 are solutes 1 and 2, 1 and 3, and 1 and 4, etc.

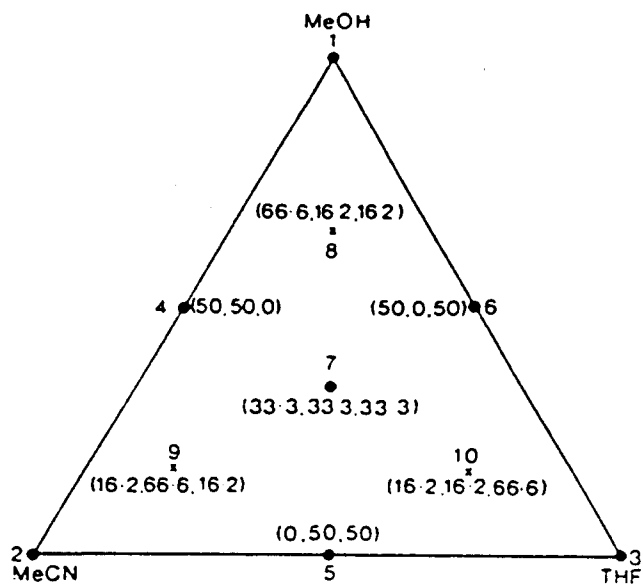


Fig. II.9 Simplex lattice design for reversed-phase HPLC optimization showing relative proportions of each solvent to be used (ref. 45).

A desired minimum resolution (e.g. 1.5) between two peaks is used as a criterion to eliminate the areas of each map which provide separations less than the minimum requirement. For example, Fig. II.10 shows the eliminated composition regions (shaded) for each of the adjacent peak pairs. Then, by overlapping the resolution maps of every peak pair, the region in which the resolution of every peak pair is equal to or greater than the required minimum resolution is located.

The working graphs of an overlapping resolution mapping optimization of a six-component mixture separation are shown in Fig. II.10 and Fig. II.11. Peak cross-over (reversal in the order of elution of two peaks) did not happen in this separation, so only the resolution maps (Fig. II.10) of adjacent peak pairs are needed. The blank areas in these maps represent the compositions which provide the desired separation (resolution 1.5 or greater). Within these five resolution maps, Fig. II.10, the resolution of the peak pair of solute 2 and 3 is always greater than 1.5, hence, this peak pair does not need to be considered anymore. The other four maps are overlapped, and two areas, A and B which produce satisfactory separation are found (Fig. II.11).

On the other hand, the final map of this example also shows a disadvantage of the overlapping resolution mapping method. The magnitude of R_s within the optimal area is not readily available as a logical consequence of the use of a threshold criterion (1.5 in this example). Hence, the exact optimum cannot be located.

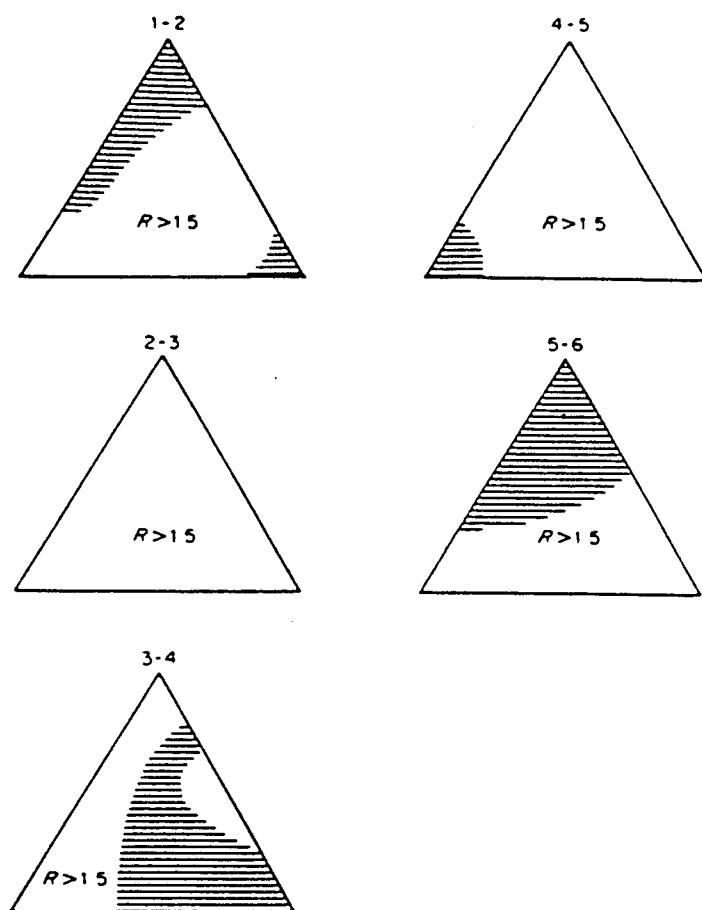


Fig. II.10 Individual resolution maps for the five pairs of solutes with adjacent peaks in the six-solute test mixture. Shaded areas have resolutions, R_s , < 1.5 , (ref. 17).

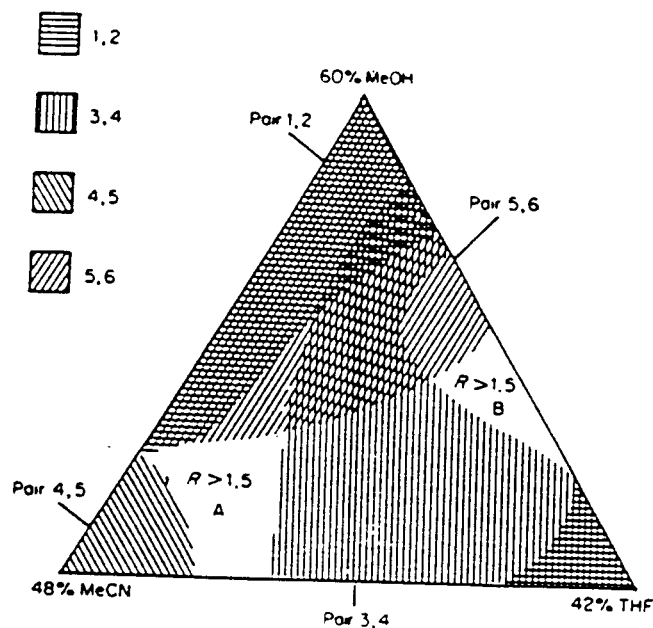


Fig. II.11 Overlapping resolution map (ORM) for the six-component test mixture. This map is constructed by overlapping the five individual resolution maps in Figure II.10. Unshaded area have adequate resolution, $R_s, > 1.5$ (ref. 17).

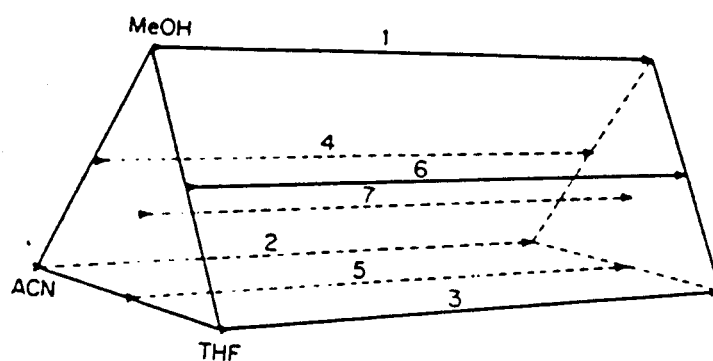


Fig. II.12 Experimental design for seven gradient runs to obtain basic data for separation optimization (ref. 44).

The overlapping resolution mapping method also can be used in gradient optimization⁸³. In the gradient experiment, a solvent selectivity prism, Fig. II.12, is considered instead of a planar triangle which is used for isocratic separations. The whole process is carried out in a way which is analogous to the overlapping resolution mapping method used for isocratic separations. The selectivity triangle is now replaced with a selectivity prism (Fig. II.12), and seven gradient experiments are conducted for each individual solute according to the design shown in Fig. II.12. During the separation, the proportion of carrier is reduced linearly, and the proportion of modifiers is increased linearly. Moreover, the rates of the carrier proportion change are the same at all seven experiment points. The same quadratic model, eqn. 12, is used to describe the response surface, and the values of the coefficients are calculated from the data acquired from the experiments at the seven experiment points. Then, just as in isocratic cases, resolution maps are built for all the possible peak pairs. Finally, these maps are overlaid so that the area(s) providing adequate separation can be found.

2.3.2 Applications

The overlapping resolution mapping method has been widely applied to the optimization of HPLC mobile phases^{84,85}. It has been reported that this method has been used to optimize

isocratic mobile phases in reverse-phase^{86,87,88,89,90}, normal phase silica^{91,92} and normal-bonded-phase⁹³ HPLC for various samples. Moreover, this method has also been used for the optimization of gradient elution^{94,95}. In addition, this method has been reportedly used for ion pair HPLC⁹⁶ and even used for optimization of a mixed stationary phase⁹⁷.

2.3.3 Summary

The overlapping resolution mapping method has been demonstrated to be applicable to major types of HPLC separation of known samples. It is one of the methods which is widely used for ternary or pseudo-quaternary mobile phases. It has several advantages. First, experiments only need to be carried out at seven composition points. This saves many experiments, compared with a trial-and-error method. Second, this method provides a comprehensive picture of the separation ability of a mobile phase system. This picture can help in choosing the most suitable separation composition with the consideration of other factors.

On the other hand, the overlapping resolution mapping method has its disadvantages. The major disadvantage is that this method requires the recognition of peaks. As a result, this method can not be used for unknown samples. Moreover, for known samples, many experiments are required for a sample

which contains many components, such as a ten-component sample. In addition, if the separation threshold criterion is too small, a single optimal area may not be necessarily identified; if the separation threshold is too high, no optimum may be found when all the desired areas of each peak pair are overlapped completely by undesired areas of the other peak pairs.

2.4 The Iterative Mixture design Method

The success of the window diagram and overlapping resolution mapping methods are largely dependent on the availability of a suitable model which describes the solute retention as a function of the variables (e.g., mobile phase composition) being adjusted. However, a suitable model is not always available. Consequently, a method that combines a model-dependent optimization method with a model-independent method was proposed^{98,99,100} in 1982. This method is named the iterative mixture design method or piecewise linear interpolation method. This method can only be used for known samples because this method needs to recognize peaks. The iterative mixture design method can be used for binary or ternary (pseudo-quaternary) mobile phase systems. One of the advantages of this method is that the global optimum can be found when several optima exist.

2.4.1 Principles and Operations

The basic philosophy of this approach is to approximate the retention response surface with a simple model and then explore the indicated optimum region with an iterative

procedure. The model is then refined according to the experience obtained.

The optimization process of this method for a binary (pseudo-ternary) mobile phase is used here to illustrate the basic principles and operations of this method. The optimization process is carried out by following steps.

First, two solvents are chosen based on the recommendation of the solvent selectivity triangle and the nature of the sample. For example, methanol may be selected from the proton donor solvent group, and acetonitrile may be selected from the proton acceptor group. Then, a carrier (e.g., water), is mixed with each of these two solvents to adjust the solvent strength. These two adjusted solvents, then, are used as the initial solvents of the binary (pseudo-ternary) mobile phase. All the other possible compositions of this mobile phase are mixtures of these two initial solvents.

Second, HPLC separations are carried out with these two initial solvents, and every peak in these two chromatograms is recognized. At this step, if the recognition is done by comparing with the retention time of a standard for each solute, then for a n -component sample, $n-1$ experiments are needed for each solvent, where n is the number of components. The first and second steps actually are the same as those used in the window diagram method.

Third, an assumption that a linear relationship exists between the logarithm of the capacity factor and mobile phase composition is made. Thus, for every solute, a linear plot of the logarithm of the capacity factor versus the composition is built over the entire composition range of the binary mobile phase.

Forth, the separation function (e.g., selectivity factor or resolution) of each possible peak pair is plotted against mobile phase composition, and a window diagram is built.

Fifth, the global optimum is found from the window diagram, and the sample is run at the composition corresponding to the global optimum. Since the linear model used for building the window diagram usually deviates to a large extent from the real solute retention behavior, the separation result at this composition will be different from the prediction, and this composition is not the real optimum. Therefore, the separation can still be improved. To do so, the peaks in this chromatogram need to be recognized. This means another $n-1$ experiments need to be conducted with this composition.

Then, using information obtained from these experiments, the previous model is modified by adding an additional point at this composition of the mobile phase to each $\ln k'$ plot. A adjacent points are again connected by straight lines. Next, a new window diagram is built and a new global optimum composition is located accordingly. Then, a separation is carried

out at the new global optimum composition. If the desired separation is achieved, then it is the end of this optimization process. If not, then all the peaks need to be recognized at this new composition, the retention model is modified again and a new global optimum is located. This procedure is repeated until the desired separation is achieved, or no further improvement can be done. An example of reversed-phase separation of a six-component mixture is used here to illustrate the procedure¹⁰¹.

First, methanol was chosen from the proton donor solvent group, and tetrahydrofuran (THF) was chosen from the dipole-dipole solvent group. Then, water, a carrier, was mixed with each of these two pure solvents in order to produce two initial binary mobile phases which had the desired solvent strength. Experimentally, it was found that methanol/water (60:40, v/v) and THF/water (42:58 v/v) were the proper compositions for the two initial binary mobile phase.

Second, experiments were carried out with both of these two initial binary mobile phase in order to recognize all the peaks.

Third, linear plots of the logarithms of the capacity factors versus the proportions of these two initial solvents were built (see Fig. II.13), and a window diagram was constructed. In this example, peak cross-over occurred between peaks 3 and 4, and as a result, there are two optimum compositions. One is

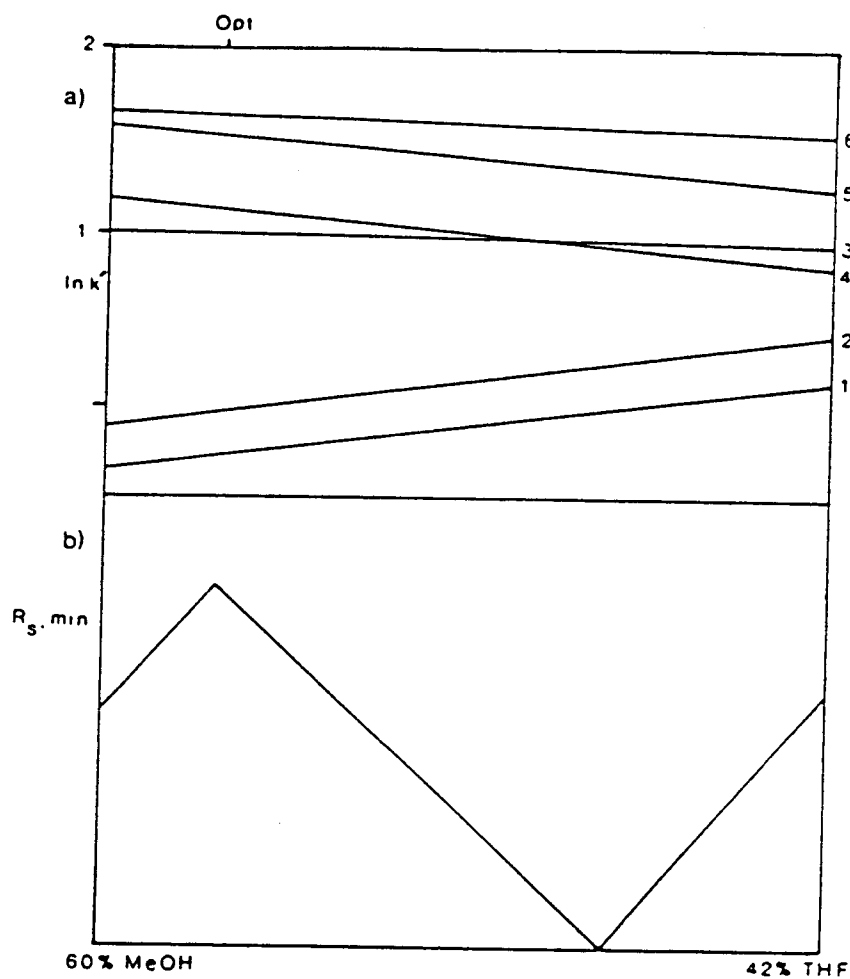


Fig. II.13 Plots of (a) $\ln k'$ and (b) minimum resolution against solvent composition. A is 60% MeOH/H₂O. B is 42% THF/H₂O (ref. 13).

100% of solvent B, and another one is about 84% of the solvent A and 16% of the solvent B blend. The later one is the global optimum.

Next, a chromatogram was run at the global optimum composition. However, the desired separation (Fig. II.14) was not achieved. Hence, more chromatograms were run at this composition to recognize all the peaks. The information obtained in these experiments were then used to modify the retention model by adding these points to the lines in Fig. II.13. Each plot now consists of two straight sections. Since the actual behavior of $\ln k'$ is a curve, these plots are still far from accurate.

A new optimum was found, Fig. II.15, and a separation was carried out with the new global optimum composition (the blend of 67% solvent A and 33% solvent B). Fig. II.16 shows the separation result. Since all the peaks are separated in the chromatogram, the optimization process could end at this point.

To sum up, the optimization of a binary or pseudo-ternary mobile phase is a single-parameter optimization. It is based on the assumption that the relationship between the logarithm of the capacity factor and mobile phase composition can be described by linear segments, and this assumption, in turn, allows a linear prediction of the capacity factor. As the iterative optimization process continues, the initial straight line model is segmented, and the modified model comes closer to the

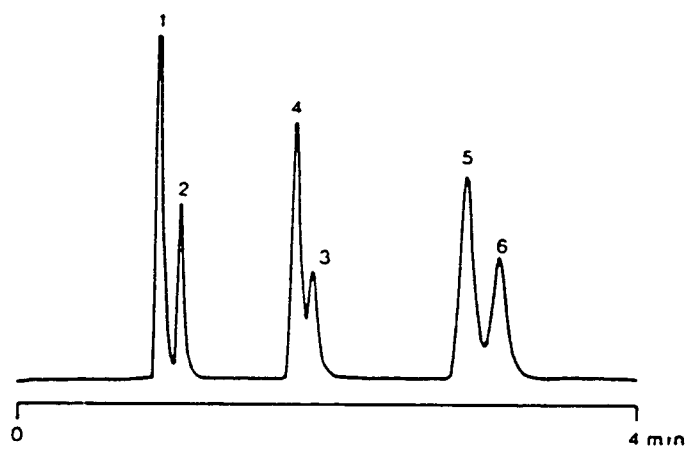


Fig. II.14 Chromatogram obtained at the composition indicated as optimum in Figure II.13 (ref. 13).

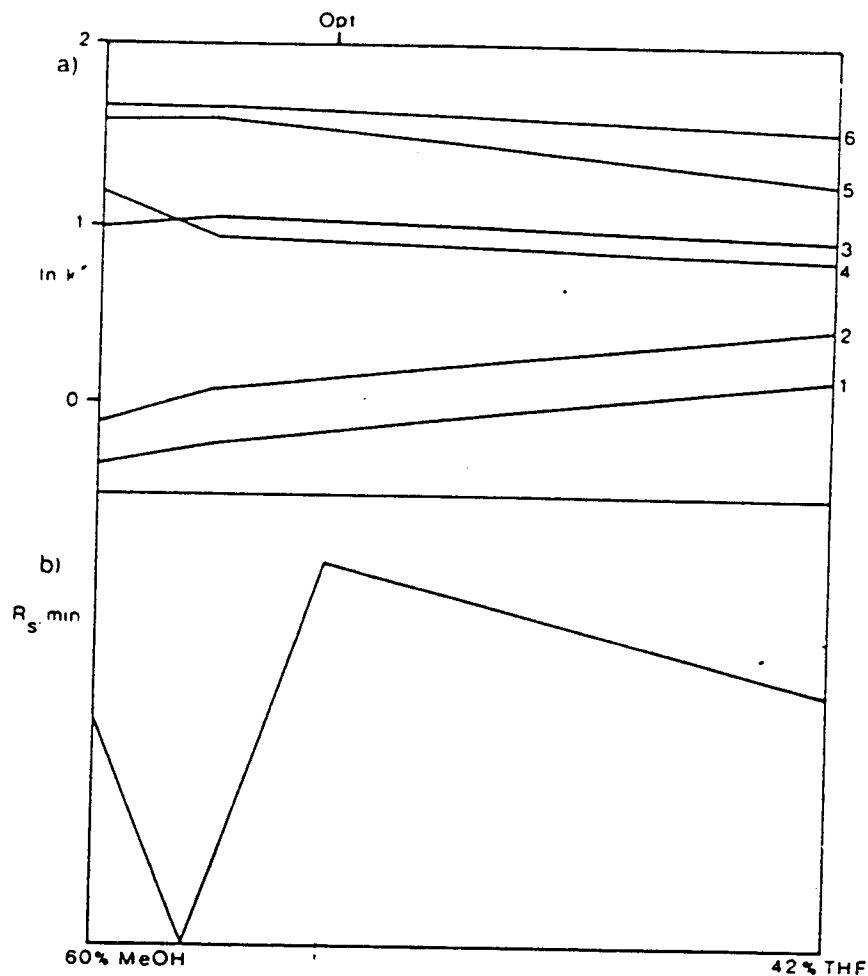


Fig. II.15 Revised plots of (a) $\ln k'$ and (b) minimum resolution against composition now incorporating new data from Figure II.14 at Opt 1. Opt. 2 is the new optimum of R_s obtained from these new $\ln k'$ plots (ref. 13).

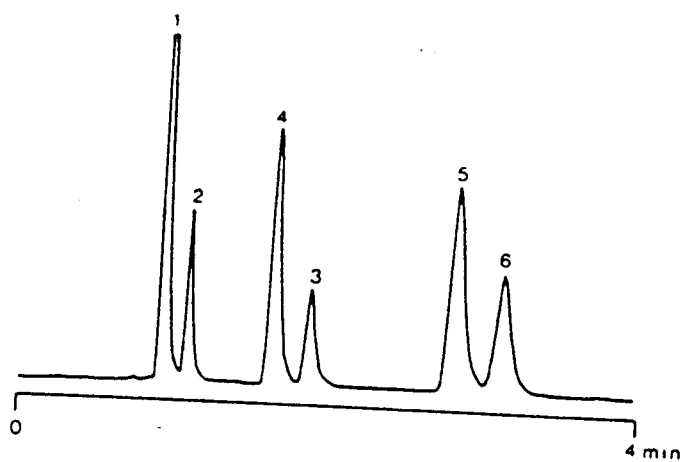


Fig. II.16 Chromatogram obtained using optimum composition from Figure It.3 (ref. 13).

actual curve. The process stops when a desired separation is achieved or the separation cannot be further improved.

This method can also be used for a multi-solvent mobile phase, such as a two-parameter (three-solvent) model. When the iterative method is used for two-parameter model cases, all the basic principles of the method are the same as those used for one parameter. However, in the two parameter model case, the retention behavior of a solute is represented by a plane which is fit through 3 composition points. As new experiments are carried out, the initial triangle is further divided into three smaller triangles. That is, in the second step, chromatograms need to be run with three new compositions instead of one new composition as in the one-parameter model case¹⁰². Fig. II.17 shows the experimental design for the initial step of the optimization. Compared with the overlapping resolution mapping method, the iterative method needs at least twice as many experiments as the overlapping resolution mapping method.

2.4.2 Applications

So far, most of the reported applications of the iterative mixture design method involve the separation of synthetic mixtures. These mixtures are designed to establish the feasibility of this method. This method has been used to optimize reversed-phase^{103,104,105,106} and normal-phase^{107,108}

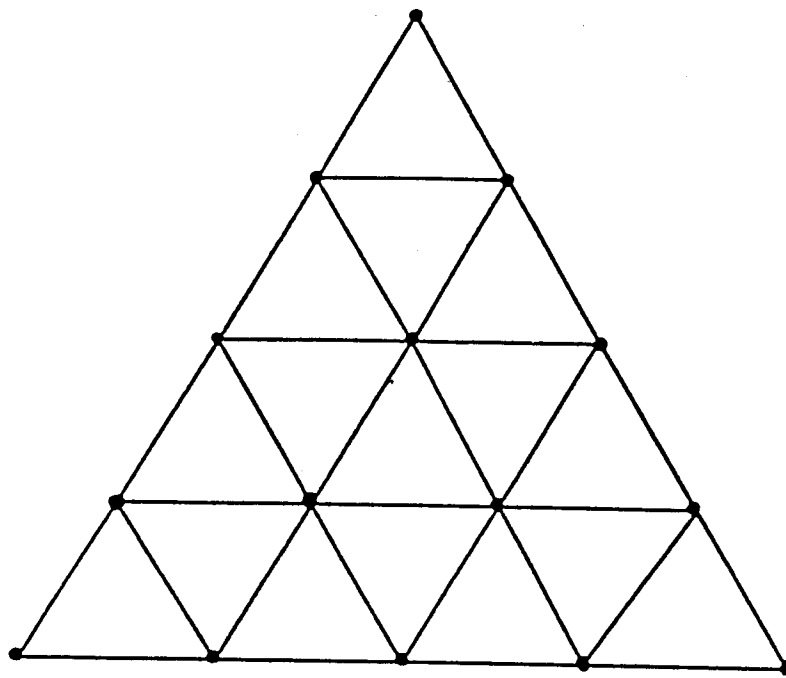


Fig. II.17 Proposed possible fifteen-point initial design for the optimization of a pseudo-quaternary mobile phase for reversed-phase HPLC (ref.102).

HPLC separations. Moreover, the application of this method to ion-pair reverse-phase^{109,110} separation has been reported. In addition, this method also has been used to optimize the pH of a mobile phase¹¹¹.

2.4.3 Summary

The iterative mixture design method has been demonstrated to be applicable to major types of HPLC separation of known samples. The advantages of this method include, (1) an ideal solute retention behavior is not assumed, (2) the global optimal area can be found, and (3) this method can achieve better separation¹¹² than the window diagram and the overlapping resolution mapping methods. However, this better result is obtained by doing more experiments. If a fine tuning procedure is followed for the window diagram or the overlapping resolution mapping methods, the same separation result may also be achieved, and the total number of experiments may still less than that needed by the iterative mixture design method.

2.5 The Simplex Search Procedures

In many situations, the pure standard of each component of a sample is not available. Then, the window diagram, ORM and iterative mixture design methods cannot be used for the optimization of mobile phases for these samples because all these three methods need to recognize peaks first before the retention behavior of solutes can be described. However, several methods which do not require the recognition of peaks have been developed, and these methods can be used for unknown samples. The simplex search procedure is one of these methods.

The simplex search procedure was introduced by Spendley et al.¹¹³ and modified by Nelder and Mead¹¹⁴. The simplex search is a general method that can be used in many fields. This technique has been widely used in analytical chemistry¹¹⁵. This method has been used for the optimization of binary, ternary and quaternary mobile phase systems. When the simplex method is used for the optimization of HPLC mobile phases, the simplex method literally does not need any knowledge of the behavior of the solutes. Therefore, peak recognition is not needed. As a result, this method can be used for both known and unknown samples.

2.5.1 Principles and Operations

A simplex is a geometric figure that has a number of vertices equal to one plus the number of parameters which are adjusted to obtain a desired result. For the purpose of HPLC mobile phase optimization, generally, only the simplex for one parameter or two parameters is needed. A simplex for a one-parameter model (binary mobile phase) is a line; a simplex for a two-parameter model (ternary mobile phase) is a triangle.

The rules of the simplex search procedure make the simplexes move away from a region of poor response and towards a region of good response until an optimum point is reached. Because the ordinary simplex introduced by Spendet et al. includes all the basic principles and most of the rules of simplex methods, their method will be described first. An example (Fig. II.18) will be used to illustrate the operation of this method.

2.5.1.1 Ordinary Simplex

Rule 1. An initial simplex is defined by choosing $n+1$ points as the vertices of the simplex in the n -dimensional factor space. For example, the case shown in Fig. II.18 has two independent variables, thus, three points, points 1, 2 and 3, are chosen to be the vertices of the initial simplex. In addition, in this ordinary simplex method, a constant step size is used. Therefore, these

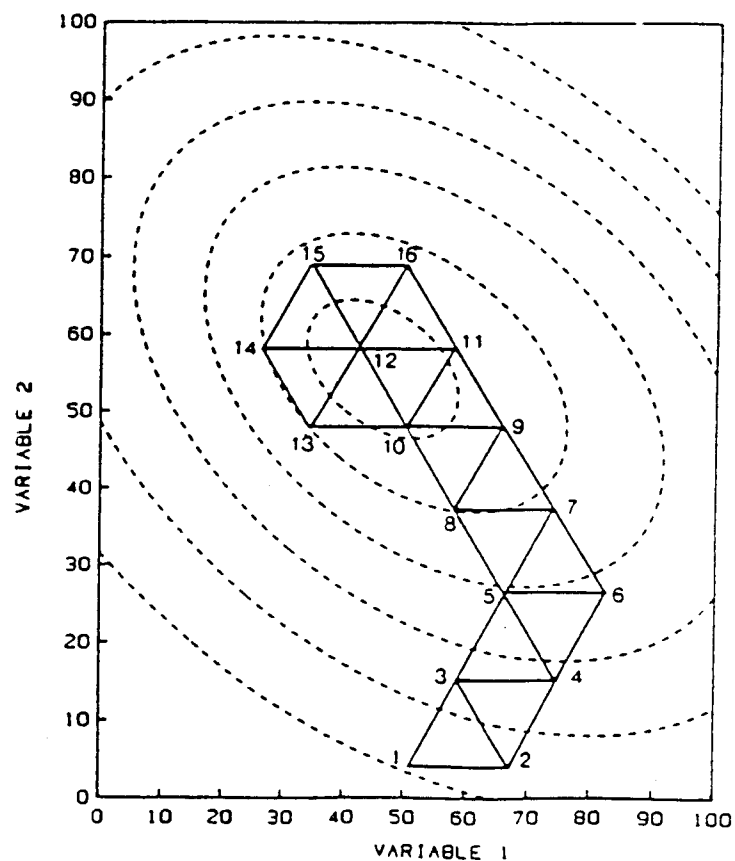


Fig. II.18 Movements of the ordinary (fixed step size) simplex on a response surface. The initial simplex is 1, 2, 3 and the optimum region lies close to point 12 (ref. 13).

three points are chosen in a way that the initial simplex is an equilateral triangle.

Rule 2. The point which has the worst response is dropped. A new experiment is carried out at the mirror image of the point dropped across the hyperplane of the remaining points. In this way, a new simplex is formed. In the example shown in Fig. II.18, point 1 has the worst response, so this point is dropped. Then, a new point, point 4, is added at the mirror image of point 1 across the hyperplane (a line in this case) of points 2 and 3. As a result, a new simplex is formed from points 2, 3 and 4. Then the responses of these three points are compared, and the one which has the worst response, point 2, is dropped. Next, a new point, point 5, is added at the mirror image of point 2, and a new simplex is formed. This process is repeated until the response of the new point is worse than that of the point which is just carried out before the new point. In Fig. II.18 consider the position at points 10, 11 and 12). The response of the new point, point 13, is the worst in its simplex (points 10, 12 and 13). If point 13 is dropped, then, by rule 2, point 11 needs to be added. However, point 11, has the worst response in its simplex. Then point 11 needs to be dropped again, and point 13 needs to be added again. The process goes into an oscillation. To break (prevent) this oscillation, Rule 3 is used.

Rule 3. If the reflected point has the worst response in the new simplex, then drop the second worst point and add the next

point to the mirror image of the second worst point. According to this rule, the second point, point 10 is dropped, and point 14 is added. As the simplex process continues, experiments at points 15 and 16 are carried out. Note that point 12 remains in the last three simplexes. The simplexes are circling around point 12. This means that the optimum has been reached, at least as close as simplexes of this size are able to determine. However, in the real world all experimentation is subject to errors and noise. Since the response of point 12 has only been measured once, it may be a false optimum, and this kind of false optimum actually will make simplexes stick to a non-optimal area instead of moving toward the real optimum region. To prevent this situation from happening, Rule 4 is introduced.

Rule 4. If a vertex has been retained in $n-1$ simplexes, before applying Rule 2, remeasure the response at the persistent vertex. If the vertex is actually near an optimum, it is likely that the result of the remeasurement will also be high. If the original result is in error then the result of the repeated measurement is assumed to have less error, the vertex will be dropped, and the simplex starts moving again. However, generally, the simplex method is not easily affected by mistakes, and Rules 2 and 3 usually can quickly correct a move in a wrong direction.

In addition, there is one more rule for dealing with the situation in which the procedure suggests that an experiment is

needed in the region which is inaccessible to an independent variable (e.g. a negative concentration).

Rule 5. If a new point suggested lies outside the boundaries of any of the independent variables, assign a very undesirable response to it instead of making an experimental observation. In this way Rules 2 and 3 can be applied, and the simplex will come back to the independent variable space allowed, and the process can continue.

When the simplexes completely circle around a vertex, the whole process reaches its end. The vertex will be close to the real optimum. For example in the case shown in Fig. II.18, point 12 is very close to the real optimum. At this point, if further improvement is still needed, a smaller step size simplex search can start from point 12.

Since this ordinary simplex method uses a fixed step size during the optimization process, it has limitations. First, there is no provision for changing the step size of search to accommodate different shapes of the response surface in the search process. This limit is usually overcome by carrying out a new optimization process with a smaller simplex when the previous process cannot locate a better response point anymore. The other limit is that the fixed step size simplex sometimes fails on a ridge in spite of using Rules 3 and 5. The simplex can straddle a ridge when the step size is too large and the orientation of the simplexes is just

right, and the only way to get off of this ridge is to change the orientation of the simplex slightly, and continue the process. However, there is no rule that refers to this orientation change in the ordinary simplex method. To overcome these limits, the modified simplex method can be used.

2.5.1.2 The Modified Simplex Procedure

The ordinary simplex method was modified by Nelder and Mead¹¹⁶. To a large extent, this modified method overcomes the limitations of the ordinary simplex method¹¹⁷. This modified simplex method accelerates the progress of the simplexes. It also actively changes the size and shape of the simplex, accommodating to the changing nature of the response surface.

The modified simplex method made several modifications on the ordinary simplex method. The example shown in Fig. II.19 is used to explain these modifications.

First, the modified simplex method does not require a fixed size step. Therefore, simplexes need not be equilateral (e.g., an equilateral triangle in a two dimensional case). Because of this modification, part of rule 2 also needs to be changed. After the point which has the worst response is dropped, the new point, instead of being added to the mirror image, is added to a location

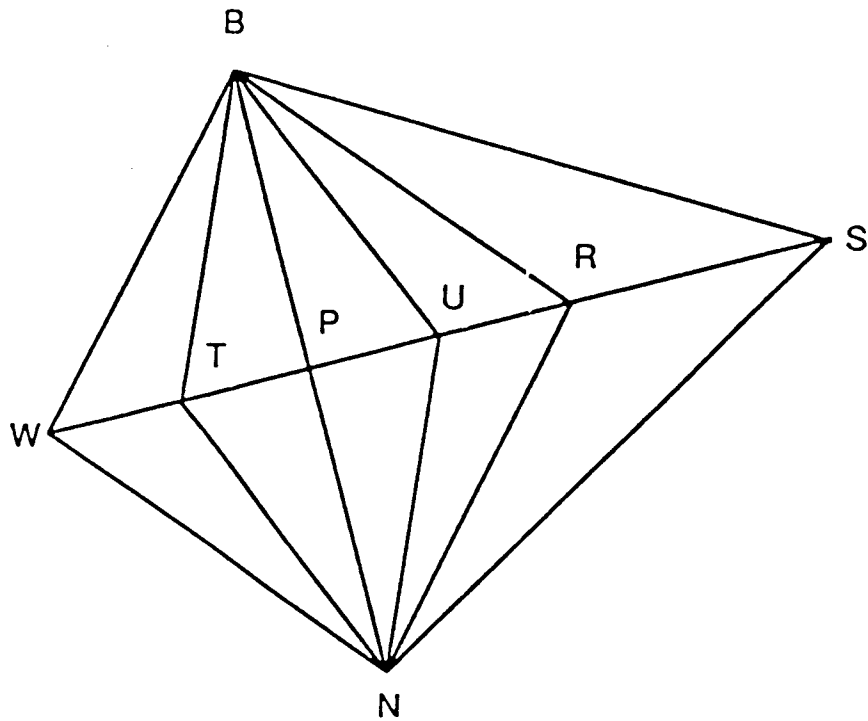


Fig. II.19 Example of showing several potential locations, T, U, R and S for the new point using the modified simplex method (ref. 1).

along the line connection points W and P according to following equation (in vector notation)

$$\vec{R} = \vec{P} + (\vec{P} - \vec{W}) \quad (13)$$

For instance, in the case shown in Fig. II.19, the initial simplex is BNW. Point B has the best response. Point N has the response next to that of point B. Point W has the worst response. Therefore, according to rule 2 of the ordinary simplex method, point W is dropped. According to eqn. 13 a new experiment is conducted at point R. WBSR is a parallelogram, and points W and R are opposite vertices.

There are three possibilities for the value of the response at point R. First, the response at point R is the best in the new simplex, BNR. This suggests that the simplex is moving in the right direction. Then an expansion to point S might be appropriate. Therefore, Rule 3 of the ordinary simplex method is replaced by a new rule, Rule 3 of the modified simplex method.

Rule 3a. If the response of the reflected image of the worst point of the initial simplex is the best in the new simplex, then, make an expansion to point S according to the following equation

$$\vec{S} = \vec{P} + b(\vec{P} - \vec{W}) \quad (14)$$

where P is the centroid of the hyperplane opposite W, b is an expansion coefficient that is greater than 1. If the response of point S is better than that of point R, then, the new simplex is

BNS; otherwise the new simplex is BNR. Then, rule 2 of the original simplex is applied for the next move.

Rule 3b. If the response of point R in the simplex BNR is the second best, then neither an expansion nor a contraction needs to be conducted. BNR is the new simplex.

Rule 3c. If the response of the point R is the worst one in the simplex BNR, this means that the simplex is moving in a wrong direction. A contraction needs to be conducted. There are two kinds of contraction operations depending on the response value of point R. If the response of R is greater than that of point W and less than that of point N, a positive contraction needs to be carried out. The value of b in eqn. 14 lies between 0 and 1 ($0 < b < 1$), and b is usually set to 0.5. This positive contraction results in point U.

$$\vec{U} = \vec{P} + 0.5(\vec{P} - \vec{W}) \quad (15)$$

If the response of R is worse than that of point W, then a negative contraction needs to be carried out, and b will be less than zero. It is usually set to -0.5¹¹⁸. This negative contraction results in point T.

Compared to the ordinary simplex method, the modified simplex method can locate the optimum faster, and the real optimum can actually be reached. Fig. II.20a shows the situation in which the modified simplex method is applied to find the

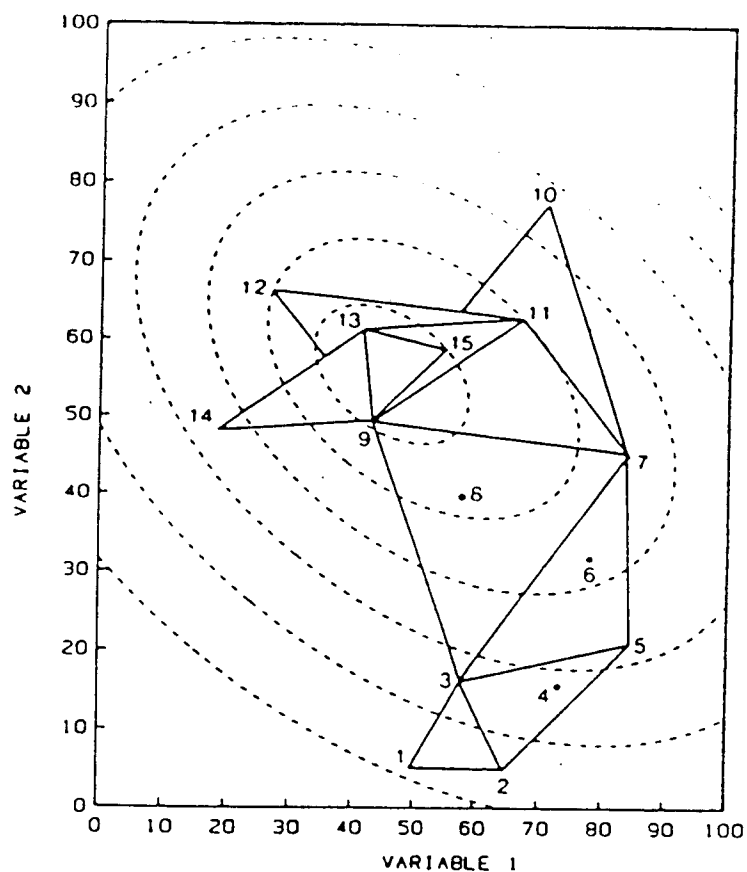


Fig. II.20a Movements of the modified simplex procedure across the same response surface used in Figure II.18. The initial simplex is 1, 2, 3 and the last simplex is 9, 13 and 15 (ref.17).

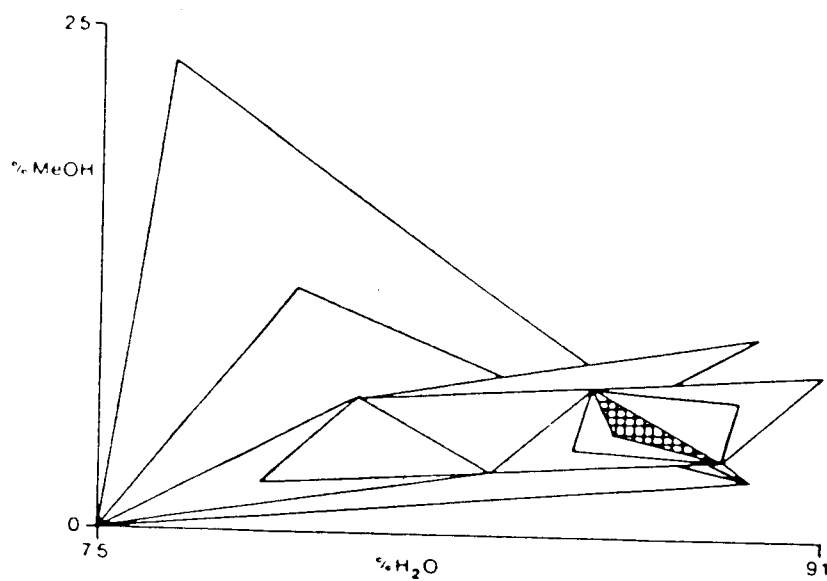


Fig. II.20b Illustration of a two-dimensional optimization using a modified simplex procedure. (ref. 28).

optimum of a case which is the same as the one in Fig. II.18. It takes the original simplex method 16 experiments to obtain the result which takes the modified simplex method 15 experiments. Moreover, the modified simplex method still can continue and eventually locate the real optimum. However, the ordinary simplex cannot continue any more; only a new search with a smaller step size can start from point 12 (Fig. II.18). Figure 20b shows another example in which the modified simplex procedure is used to find the optimum of a binary mobile phase.

The modified simplex also has its own limitations. If T or U is the worst point in the new simplex, then, the new point may eventually end up at point P, that is, the simplex will loss one degree of freedom and the simplex may become stranded. Several procedures have been suggested to overcome this problem^{119,120} including the reduction in size of the entire simplex. The details of these procedures are beyond the scope of this thesis.

2.5.2 Applications

As a general optimization method, sequential simplex search procedures eventually can be used to optimize all kinds of parameters. This method has been applied to the optimization of binary^{121,122,123,124}, ternary^{125,126,127,128,129} and quaternary mobile phases¹³⁰, and this method has also been applied to the optimization of gradient parameters¹³¹. Moreover, the simplex

method has also been used to optimize other parameters, such as, flow rate¹³², pH^{133,134}, buffer concentration¹³⁵ and temperature¹³⁶. Simplex procedures have also been built into several commercial HPLC systems^{137,138,139}. This further promotes the application of simplex methods.

2.5.3 Summary

As a general optimization method, the simplex method has very good versatility. This method has certain advantages. First, this method does not require peak recognition. Therefore, it can be used for unknown samples. Second, conceptually, it is simple, and readily understood by those not possessing a great theoretical knowledge of chromatographic principles. However, the simplex search procedures also have several disadvantages. First, the major disadvantage is that the simplex search procedures may only find one of the local optima when several optima exist. Moreover, the local optimum found by simplex search procedures may have very poor separation compared with the global optimum (see Fig. II.7). Second, it may explore regions which are of little interest to chromatographers. Third, it can be perturbed by a complex response surface. In short, the simplex search procedure can be used for unknown samples, but the chance of finding the global optimum is not large.

2.6 The Step-search Design Method

The step-search design method is another approach which does not require peak recognition. Therefore, this method can be used for unknown samples. Moreover, because of the design of this method, it generally can find the global optimum. This method can be used for binary, ternary and quaternary mobile phase systems.

2.6.1 Principles and Operations

This method starts with a composition point in the solvent composition space, and modifies the solvent composition slightly with each run until the global optimum is reached. The experiments are usually performed at points on a triangular grid with a fixed step size, and in such a sequence that column equilibration time between solvent changes is minimized. Fig. II.21 shows a part of the searching procedure. This method is basically a "brute force" procedure. As long as the step size is small enough (but within the range which is allowed by other experimental constraints), the global optimum usually can be found. However, since this procedure literally searches the whole variable space, it needs many experiments. For instance, if a 5% step size in eluent composition is used, it takes 231 experiments to search the whole solvent triangle. If the time needed for each

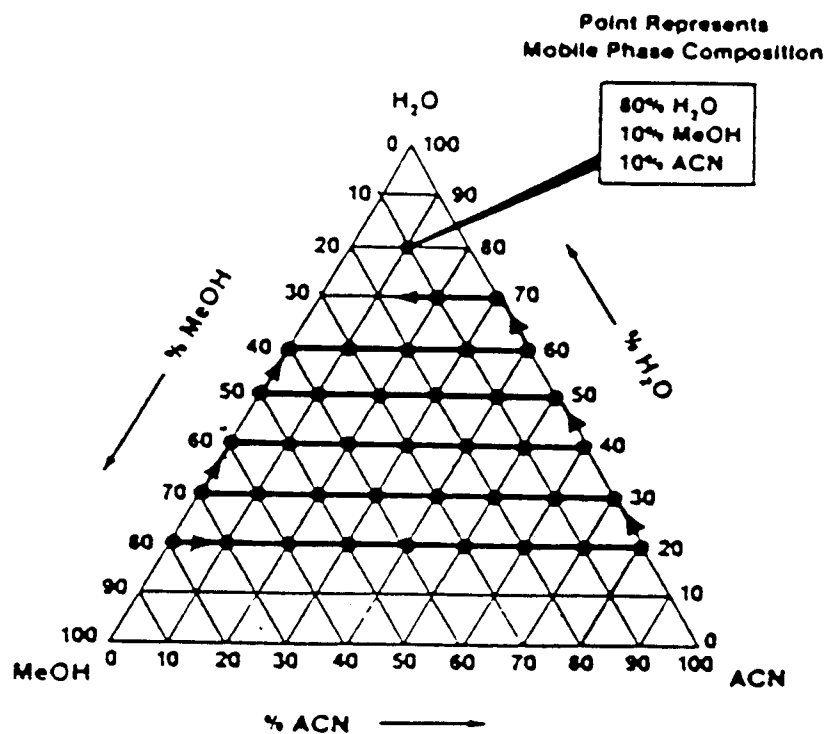


Fig. II.21 PESOS grid search process in a ternary or pseudo-quaternary solvent system (ref. 17).

experimental run and equilibration of the column is 1.5 hours, the whole search procedure will need about 347 hours.

Such a long experimental period causes another problem. During during many experiments, the degradation of the column could lead to large errors into the final result. Moreover, in some situations, the experimental period is even longer than the life-span of a column. If a column is changed during the search procedure, larger errors may occur in the final result. However, although the step-search design method has these disadvantages, for unknown samples, it is still the only published method which can find the global optimum when local optima exist.

2.6.2 Applications

This method was reported to be used in the optimization of a pseudo-quaternary mobile phase in a reversed-phase HPLC separation. The global optimum was found within several local optima¹⁴⁰. This step-search design method has been used in a computer-control HPLC system. This system is marketed as PESOS (Perkin-Elmer Solvent Optimization System)¹⁴¹.

2.6.3 Summary

The step-search design method can be used for all forms of HPLC. This method can be used for unknown samples, and, most important, can locate the global optimum. Moreover, this method is easy to understand. However, this method also has disadvantages. The major disadvantage is that this method need many experiments. In some cases, the number of the experiments required may be beyond the limits determined by other experimental constrains so that this method cannot be used.

2.7 Conclusion

After reviewing these methods, it is clear that the methods for unknown samples, the sequential simplex procedure and the step-search design method, have many limitations. For the separation of unknown samples, a new method needs to be developed for the optimization of the mobile phase composition. Ideally, this new method would be able to find the global optimum, and do so with substantially fewer experiments.

In the following chapters, the development of a new method which satisfies these requirements is described. In addition, applications of this new method, the weighted pattern comparison method, in normal-phase and reversed-phase HPLC for various samples are also described.

References

1. S. Ahuja, *Selectivity and Detectability Optimizations in HPLC*, Wiley, New York, 1989, p.461.
2. G. F. Poole and S. A. Schuette, *Contemporary Practice of Chromatography*, Elsevier, New York, 1984, p.262.
3. L. R. Snyder, *Practical HPLC Method Development*, Wiley, New York, 1988.
4. D. L. Massart, A. Dijkstra and L. Kaufman, *Evaluation and Optimization of Laboratory Methods and analytical Procedure*, Elsevier, Amsterdam, 1978.
5. G. S. G. Beveridge and R. S. Schechter, *Optimization: Theory and Practice*, McGraw-Hill, New York, 1970.
6. P. G. King and S. N. Deming, *Anal. Chem.*, 46(1974)1476.
7. J. L. Glajch, J. J. Kirkland, K. M. Squire and J. M. Minor, *J. Chromatogr.*, 199(1980)57.
8. R. J. Laub, *int. Lab.*, May/June(1981)16.
9. R. J. Laub and L. H. Purnell, *J. Chromatogr.*, 112(1975)71.
10. R. J. Laub and T. Kuqana (Ed), *Physical Methods in Modern Chemical Analysis*, Vol. 3, Academic Press, New York, 1983, Ch5.
11. M. Otto and W. Wegscheider, *J. Liq. Chromatogr.*, 6(1983)685.
12. M. P. T. Bradley and D. Gillen, *Spectra-Physics Chromatogr. Rev.*, 10(2)(1983)2.
13. P. J. Schoenmakers, A. C. J. H. Drouen, H. A. H. Billiet and L. de Galan, *Chromatographia*, 15(1982)688.

- 14 PESOS; Perkin-Elmer Solvent Optimisation System.
- 15 A. G. Wright, A. F. Fall and J. C. Berridge, *J. Chromatogr.*, 458(1988)335-353.
- 16 S. Ahuja, *Selectivity and Detectability Optimizations in HPLC*, Wiley, New York, 1989, p.v.
- 17 J. C. Berridge, *Techniques for the Automated Optimization of HPLC Separations*, Wiley, New York, 1985, p.56-57.
- 18 L. R. Snyder and J. J. Kirkland, *Introduction to Modern Liquid Chromatography*, 2nd Ed., Wiley, New York, 1979.
- 19 B. L. Karger, L. R. Snyder and C. Eon, *J. Chromatogr.*, 125(1976)71.
- 20 L. R. Snyder, *J. Chromatogr. Sci.*, 16(1978)223.
- 21 C. F. Poole and S. A. Schuette, *Contemporary Practice of Chromatography*, Elsevier, New York, 1984, p.258.
- 22 L. R. Snyder, *J. Chromatogr. Sci.*, 16(1978)223.
- 23 L. R. Snyder, *J. Chromatogr.*, 92(1974)223.
- 24 L. R. Snyder and J. J. Kirkland, *Introduction to Modern Liquid Chromatography*, 2nd Ed., Wiley, New York, 1979.)
- 25 S. Ahuja, *Selectivity and Detectability Optimizations in HPLC*, Wiley, New York, 1989.
- 26 L. R. Snyder, *Practical HPLC method Development*, Wiley, New York, 1988.
- 27 J. C. Berridge, *Techniques for the Automated Optimization of HPLC Separations*, Wiley, New York, 1985.

- 28 P. J. Schoenmaders, *Optimization of Chromatographic Selectivity*, Elsevier, New York, 1986.
- 29 R. J. Laub, *Int. Lab.*, May/June(1981)16.
- 30 R. J. Laub and J. H. Purnell, *J. Chromatogr.*, 112(1975)71.
- 31 R. J. Laub and T. Kuwana (Ed.), *Physical Methods in Modern Chemical Analysis*, Vol. 3, Academic Press, New York, 1983, Ch. 5.
- 32 R. J. Laub and J. H. Purnell, *J. Chromatogr.*, 112(1975)71.
- 33 R. J. Laub and J. H. Purnell, *J. Chromatogr.* 161(1978)49.
- 34 J. C. Berridge, *Techniques for the Automated Optimization of HPLC Separations*, Wiley, New York, 1985, p.102
- 35 J. C. Berridge, *Techniques for the Automated Optimization of HPLC Separations*, Wiley, New York, 1985, p.102.
- 36 L. R. Snyder, *Anal. Chem.*, 46(1974)1384.
- 37 P. J. Schoenmakers, H. A. H. Billiet and L. de Galan, *J. Chromatogr.*, 185(1979)179.
- 38 P. J. Schoenmakers, H. A. H. Billiet, and L. de Galan, *J. Chromatogr.*, 185(1979)179.
- 39 L. R. Snyder, J. W. Dolan and J. R. Gant, *J. Chromatogr.*, 165(1979)3.
- 40 P. J. Schoenmakers, H. A. H. Billiet and L. de Galan, *J. Chromatogr.*, 282(1983)107.
- 41 J. C. Berridge, *Techniques for the Automated Optimization of HPLC Separations*, Wiley, New York, 1985, p.105.

- 42 J. W. Weyland, C. H. P. Bruins and D. A. Doornbos, J. Chromatogr. Sci., 22(1984)31.
- 43 J. L. Glajch, J. J. Kirkland, J. Chromatogr., 218(1981)299.
- 44 J. L. Glajch, J. C. Gluckman, J. G. Charikofsky, J. M. Minor and J. J. Kirkland, J. Chromatogr., 318(1985)25.
- 45 R. D. Snee, Chemtech, 11(1979)702-710.
- 46 P. J. Schoenmakers, H. A. H. Billiet and L. de Galan, J. Chromatogr., 282(1983)107.
- 47 R. L. Snyder, Practical HPLC Method Development, Wiley, New York, 1989, p.210-216.
- 48 P. J. Schoenmakers, H. A. H. Billiet and L. de Galan, J. Chromatogr., 282(1983)107.
- 49 J. W. Weyland, C. H. P. Bruins and D. A. Doornbos, J. Chromatogr. Sci., 22(1984)31.
- 50 The same as Ref. 49.
- 51 J. P. Thomas, A. Brun and J. P. Bounine, J. Chromatogr., 172(1979)107.
- 52 H. J. Issaq, G. M. Muschik and G. M. Janini, J. Liq. Chromatogr., 6(1983)259.
- 53 H. J. Issaq, G. M. Muschik and G. M. Janini, J. Liq. Chromatogr., 6(1983)259.
- 54 B. Sachok, J. Stranahan and S. N. Deming, Anal. Chem., 53(1981)70.
- 55 L. A. Jones, R. W. Beaver and T. L. Schmoeger, Anal. Chem., 54(1982)182.

- 56 H. J. Issaq, G. M. Muschik and G. M. Janini, *J. Liq. Chromatogr.*, 6(1983)259.
- 57 H. J. Issaq, 'Statistical and Graphical Methods of Isocratic Solvent Selection for Optimal Separation in Liquid Chromatography' in J. C. Giddings, E. Grushka, J. Cazes and P. R. Brown (Eds), *Advances in Chromatography*, Vol. 24, Marcel Dekker. New York, 1984, Ch3.
- 58 C. M. Noyes, *J. Chromatogr.*, 266(1983)451.
- 59 J. W. Weyland, C. H. P. Bruins and D. A. Doornbos, *J. Chromatogr. Sci.*, 22(1984)31.
- 60 B. Patel, J. H. Purnell and C. A. Wellington. *J. High Resolut. Chromatogr. Commun.*, 7(1984)2674.
- 61 M. Otto and W. Wegscheider, *J. Chromatogr.*, 258(1983)11.
- 62 M. Otto, *Z. Chem.*, 23(1983)204.
- 63 D. R. Jenke, *Anal. Chem.*, 56(1984)2674.
- 64 D. R. Jenke and G. K. Pagenkopf, *Anal. Chem.*, 56(1984)85.
- 65 S. N. Deming and M. L. H. Turoff, *Anal. Chem.*, 50(1978)546.
- 66 J. H. Nickel and S. N. Deming, *Am. Lab. (Fairfield)*, 16(1984)69.
- 67 B. Sachok, R. C. Kong and S. N. Deming, *J. Chromatogr.*, 199(1980)317.
- 68 M. Otto and W. Wegscheider, *J. Chromatogr.*, 258(1983)11.
- 69 M. Otto, *Z. Chem.*, 23(1983)204.
- 70 B. Patel, J. H. Purnell and C. A. Wellington. *J. High Resolut. Chromatogr. Commun.*, 7(1984)2674.
- 71 D. R. Jenke, *Anal. Chem.*, 56(1984)2674.

- 72 D. R. Jenke and G. K. Pagenkopf, *Anal Chem.*, 56(1984)85.
- 73 B. Sachok, R. C. Kong and S. N. Deming, *J. Chromatogr.*, 199(1980)317.
- 74 L. R. Snyder, J. W. Dolan and M. P. Rigney, *LC-GC*, 4(1986)921.
- 75 M. A. Quarry, R. L. Grob, L. R. Snyder, J. W. Dolan and M. P. Riggney, *J. Chromatogr.*, 384(1987)163.
- 76 L. R. Snyder, M. A. Quarry and J. L. Glajch, *Chromatographia*, 24(1987)33.
- 77 L. R. Snyder, J. W. Dolan and M. A. Quarry, *TrAC Trends Anal. Chem.(Pers. Ed.)*, 6(1987)106.
- 78 J. L. Glajch, J. J. Kirkland, K. M. Squire and J. M. Minor, *J. Chromatogr.*, 199(1980)57.
- 79 J. L. Glajch, J. J. Kirkland and L. R. Snyder, *J. Chromatogr.*, 238(1982)269.
- 80 L. R. Snyder, J. L. Glajch and J. J. Kirkland, *J. Chromatogr.*, 218(1981)299.
- 81 P. E. Antle, *Chromatographia*, 15(1982)277.
- 82 R. D. Snee, *Chemtech*, 11(1979)702-710
- 83 J. J. kirkland and J. L. Glajch, *J. chromatogr.*, 255(1983)27.
- 84 L. R. Snyder, *Practical HPLC method Development*, Wiley, New York, 1988.
- 85 S. Ahuja, *Selectivity and Detectability Optimizations in HPLC*, Wiley, New York, 1989.
- 86 J. L. Glajch, J.J. Kirkland, K, M, Squire and J. M. Minor, *J. Chromatogr.*, 199(1980)57.

- 87 J. L. Glajch, J. C. Gluckman, J. G. Charikofsky, J, M, Minor and J. J. Kirkland, J. Chromatography, 318(1985)25.
- 88 G. D'Agostino, F. Mitchell, L. Castagnettes and M. J. O'Hare, J. Chromatogr. 305(1984)13.
- 89 S. J. Costanzo, J. Chromatogr. Sci., 24(1986)89.
- 90 T. Tsuneyoshi, A. Kawamoto and J. Koezuka, Clin. Chem., 30(1984)1889.
- 91 J. L. Glajch, J. J. Kirkland and L. R. Snyder, J. Chromatogr., 238(1982)269.
- 92 G. M. Landers and J. A. Olsen, J chromatogr., 291(1984)51.
- 93 P. E. Antle, Chromatographia, 15(1982)277.
- 94 J. L. Glajch and J. J. Kirkland, Anal. Chem., 54(1982)2593.
- 95 J. J. Kirkland and J. L. Glajch, J. Chromatogr., 255(1983)27.
- 96 A. P. Glodberg, E. L. Nowakowska, P. E. Antle and L. R. Snyder, J. Chromatogr., 316(1984)241.
- 97 J. L. Glajch, J. C. Gluckman, J. G. Charikofsky, J, M, Minor and J. J. Kirkland, J. Chromatography, 318(1985)25.
- 98 P. J. Schoenmakers, A. C. J. H. Drouen, H. A. H. Billiet and L. de Galan, Chromatographia, 15(1982)688.
- 99 A. C. J. H. Drouen, P. J. Schoenmakers, H. A. H. Billiet and L. de Galen, Chromatographia, 16(1982)48.
- 100 A. C. J. H. Drouen, H. A. H. Billiet and L. de Galan, J. Chromatogr., 352(1986)127.
- 101 J. C. Berridge, Techniques for the Automated Optimization of HPLC Separations, Wiley, New York, 1985, p.154-158.

- 102 P. J. Schoenmakers and T. Blaffert, *J. Chromatography*, 384(1987)117-133.
- 103 A. C. J. H. drouen, H. A. H. Billiet, P. J. Schoenmakers, and L. de Galan, *Chromatographia*, 16(1982)48.
- 104 A. C. J. H. Dronen, *Computerized Optimization and Solute Recognition in Liquid Chromatographic Separations*, Thesis TH, Delft, 1985.
- 105 A. C. J. H. drouen, H. A. H. Billiet, P. J. Schoenmakers, and L. de Galan, *J. Chromatogr.*, 352(1986)127.
- 106 H. A. Cooper and R. J. Hurtubise, *J. Chromatogr.*, 324(1985)1.
- 107 P. J. Schoenmakers, A. C. J. H. Drouen, H. A. H. Billiet and L. de Galan, *Chromatographia*, 15(1982)688.
- 108 S. H. Hansen and P. Helboe, *J. Chromatogr.*, 285(1984)53.
- 109 H. A. H. Billiet, A. C. J. H. Drouen and L. de Galan, *J. Chromatogr.*, 316(1984)231.
- 110 A. Bartha, H. A. H. Billiet and L. D. Galan, *J. Chromatogr.*, 458(1988)371.
- 111 P. R. Haddad, A. C. J. H. Drouen, H. A. H. Billiet and L. de Galan, *J. Chromatogr.*, 281(1983)71.
- 112 H. A. Cooper and R. J. Hurtubise, *J. Chromatogr.*, 328(1985)81.
- 113 W. Spendley, G. R. Hext and F. R. Hinsworth, *Technometrics*, 4(1962)441.
- 114 J. A. Nelder and R. Mead, *Comput. J.*, 7(1965)308.
- 115 H. J. G. Debet, *J. Liq. Chromatogr.*, 15(1985)2725.
- 116 J. A. Nelder and R. Mead, *Comput. J.*, 7(1965)308.

- 117 J. C. Berridge, Techniques for the Automated Optimization of HPLC Separations, Wiley, New York, 1985, p.129.
- 118 J. C. Berridge, Techniques for the Automated Optimization of HPLC Separations, Wiley, New York, 1985, p.130-131.
- 119 J. A. Nelder and R. Mead, Comput. J., 7(1965)308.
- 120 R. R. Ernst, Rev Sci. Instrum., 39(1968)998.
- 121 R. Smits, C. Vanroelen and D. L. Massart, Fresenius Z. Anal. Chem., 273(1975)1.
- 122 J. Rafel and J. Lema, Afinidad, 41(1984)30; Chem. Abstr., 100(1984)21614c.
- 123 J. Rafel, J. Chromatogr., 282(1983)287.
- 124 J. C. Berridge, Chromatographia, 16(1982)173.
- 125 J. C. Berridge, Analyst(London), 109(1984)291.
- 126 J. C. Berridge and E. G. Morrissey, J. Chromatogr., 316(1984)69.
- 127 J. C. Berridge, Proc. Anal. Div. Chem. Soc., 19(1982)472.
- 128 J. C. Berridge, Paper presented at Analyticon 83, London, 1983, Paper 505.
- 129 A. S. Kester and R. E. Thompson, J. Chromatogr., 310(1984)372.
- 130 D. L. Dunn and R. E. Thompson, J. Chromatogr., 264(1983)264.
- 131 M. W. Watson and P. W. Carr, Anal. Chem., 51(1979)1835.
- 132 G. Sabate, A. M. Diaz, X. M. Tomas and M. M. Gassiot, J. Chromatogr. Sci., 21(1983)439.
- 133 V. Svoboda, J. Chromatogr., 201(1980)241.

- 134 F. V. Warren and B. A. Bidlingmeyer, Paper presented at 188th Acs Meeting, Philadelphia, 1984, Paper 108.
- 135 V. Svoboda, J. Chromatogr., 201(1980)241.
- 136 D. M. Fast, P. H. Culbreth and E. J. Sampson, Clin. Chem., 28(1982)444.
- 137 SUMMIT Chromatographic System, Bruker Spectrospin, Coventry, UK.
- 138 TAMED Chromatographic System, LDC Milton Roy, Stone, UK.
- 139 OPTIMI Chromatographic System, Spectra Physics, USA.
- 140 A. G. Wright and A. F. Fell, J. Chromatogr., 458(1988)335.
- 141 M. W. Dong, R. D. Colon and A. F. Poile, Amer. Lab. Mag., May, 1988,p.48.

**III. The Weighted Pattern Comparison Optimization
Method for Optimizing the Mobile Phase Composition in
Liquid Chromatography**

by

Xiao Chen, Stephen J. Hawkes and Edward H. Piepmeier*

Department of Chemistry

Oregon State University

Corvallis, OR 97331

and

A. Morrie Craig

College of Veterinary Medicine

Oregon state University

Corvallis, OR 77331

For submission to the Journal of Chromatography

ABSTRACT

Based on the multicomponent solubility parameter theory, a new method is described for locating the global optimum composition of a liquid chromatography mobile phase system which is represented by the triangular coordinate system. The global optimum composition along each edge of the triangle and the corresponding functions which reflect the separation capability (e.g., selectivity factor) are used in this method to predict the global optimum of a three or four component mobile phase. This method is named the weighted pattern comparison optimization (WPCO) method and is applicable for both known and unknown samples. The WPCO method is simpler than those currently in use, and has the potential to be used for the four component mobile phase system represented by a tetrahedral coordinate system.

The WPCO method was tested by using 68 literature data sets whose separation response surfaces are different. Results demonstrate that the results of the WPCO method agree with the results obtained by the minimum α plot method and by the grid search method, and do so with substantially fewer experimental measurements.

INTRODUCTION

In recent years, several methods for the optimization of the liquid chromatography mobile phase composition have been developed^{1,2,3}.

For the separation of unknown samples, two major methods are available, the sequential⁴ and the grid-search⁵ methods.

Sequential methods use the information gathered during their optimization process to direct the further search process until an optimum is located. The sequential simplex⁶ and the modified simplex⁷ are the two principal sequential methods applied to HPLC separations.

The grid search method simply explores the whole of the composition space by some pre-defined pattern. Compared with the grid search method, the sequential methods need fewer experiments (e.g., 20-40)⁸. However, if several local optimum points exist, the sequential methods may not locate the global optimum. To locate the global optimum, the grid search method needs to be applied. However, the grid search method usually requires many experiments. For example, to search the whole triangular variable space of a ternary (or pseudo-quaternary) phase composition with 5% steps in eluent composition, 231 points will be involved.

For the separation of known samples, the major methods are the simultaneous and the hybrid (iterative regression analysis) methods. The sequential method can also be used.

For simultaneous methods, a certain experimental design which covers the whole variable space is planned first. The data then are collected by this design. These data are used to fit mathematical models that allow interpolation of the solute chromatographic behavior between the data collection points. Various procedures can then be used to predict the optimum composition for the separation. For a binary mobile phase, the major simultaneous method is the window diagram method^{9,10,11}. Several mathematical models are available to describe the solute chromatographic behavior^{1,2}. The overlapping resolution map (ORM)¹² and the minimum α plot¹³ are the major methods used for ternary and quaternary mobile phases. Among the mathematical models of chromatographic behavior used for these two methods, the simplex lattice mixture design¹⁴ is the one that is most widely used¹⁵.

The hybrid technique¹⁶ is an iterative mixture design. The model is refined in a sequential iterative process. This refining process stops at the point the optimum is located.

For known samples, both simultaneous and hybrid methods can locate the global optimum. The hybrid method is reported to be more accurate¹⁷.

In this work, based upon the multisolubility solubility parameter theory, a method to predict the global optimum composition of a mobile phase represented by a triangular coordinate system is proposed. This method can be used on both known and unknown samples. The results of this method are compared with the results of the simplex lattice mixture design minimum α plot method and the grid search method.

Theory

In this section, a mathematic model is proposed for locating the global optimum of the tertiary mobile phase. Based on solubility parameter theory, first, the relationship between the logarithm of the selectivity factor and the composition of the mobile phase is discussed. Second, two concepts, the multisolubility parameter pattern and the pattern difference, are defined, and two assumptions about the relationships among the multisolubility parameters of different mobile phase compositions are proposed. Then, based on this background, a mathematical function is formulated.

Interactions exist between solutes and the mobile phase, and between solutes and the stationary phase. The interactions between solutes and the mobile phase carry the solutes through the column, whereas the interactions between the solutes and the stationary phase retain the solutes on the stationary phase. The interactions between solutes and the mobile phase compete with those between solutes and the stationary phase. Several different kinds of interactions constitute the total interaction force between the mobile phase and the solutes. When the composition of the mobile phase changes, the magnitude of these interactions will also change; these changes, in turn, change the selectivity of the mobile phase. The magnitude of the interaction can be expressed in terms of the solubility parameter, δ . Since several kinds of interactions exist, to describe these interactions, the

multisolubility parameter model is used, in which a separate solubility parameter is assigned to each kind of interaction. For example the product of $\delta_{a,m}$ and $\delta_{b,i}$ represents the energy of an acid-base interaction between the mobile phase, m, as the acid, a, and the solute i as the base, b.

The relationship between the selectivity factor α and the solubility parameters may be derived from their definitions.

The square of the solubility parameter δ for a solute is defined by

$$\delta^2 = \Delta E/v \quad (1)$$

where E is the molar energy of partition and v is the molar volume of the solute. Thus for two solutes

$$\delta_j^2 - \delta_i^2 = \Delta \Delta E/v \quad (2)$$

The selectivity factor is given by

$$\begin{aligned} \alpha_{j,i} &= k'_j/k'_i = \exp(\Delta G^0_j/RT)/\exp(\Delta G^0_i/RT) \\ &= (\exp (\Delta \Delta G^0_{j,i}/RT)) \end{aligned} \quad (3)$$

where the subscripts i and j represent the two solutes, k'_j and k'_i are the partition coefficients for those solutes between the mobile and stationary phases, ΔG is the standard free energy of partition, $\Delta \Delta G^0$ is the difference between their standard free

energies of partition, R is the gas constant, and T is the absolute temperature.

It is assumed that both solutes have about the same molar volume, which will usually be true of two substances that are difficult to resolve. Following the usual custom in "regular solution" theory¹⁸, we further assume that entropy effects will cancel. It then follows that

$$\Delta\Delta E = \Delta\Delta G \quad (4)$$

Taking the logarithm of both sides of eqn. 1 and combining with eqn's. 3 and 4 gives

$$\ln\alpha = (v/RT) (\delta_j^2 - \delta_i^2) \quad (5)$$

The logarithm of the selectivity factor ($\ln\alpha$) of two solutes, i and j , with equal molar volumes, v , is related to the various interaction solubility parameters of the two phases by the equation¹⁹:

$$\begin{aligned}
\ln \alpha_{j,i} = & 2v/RT \{ (\delta_{d,i} - \delta_{d,j}) (\delta_{d,m} - \delta_{d,s}) \\
& + (\delta_{o,i} - \delta_{o,j}) (\delta_{o,m} - \delta_{o,s}) \\
& + (\delta_{d,i} - \delta_{d,j}) (\delta_{ind,m} - \delta_{ind,s}) \\
& + (\delta_{ind,i} - \delta_{ind,j}) (\delta_{d,m} - \delta_{d,s}) \\
& + (\delta_{a,i} - \delta_{a,j}) (\delta_{b,m} - \delta_{b,s}) \\
& + (\delta_{b,i} - \delta_{b,j}) (\delta_{a,m} - \delta_{a,s}) \}
\end{aligned} \tag{6}$$

where the subscripts m and s refer to the mobile phase and stationary phase, respectively; the subscripts d, o, ind, a and b refer to the dispersion, dipole orientation, dipole induction and acid-base (a for an acidic and b for a basic molecule moiety) interactions respectively; and the subscripts i and j refer to the two solutes.

For a mixed solvent mobile phase, m, the solubility parameter of a mobile phase can be approximated as:

$$\delta_m = \sum \phi_p \delta_p \tag{7}$$

where ϕ is the volume fraction of the solvent of the mobile phase m, and p is a particular solvent. The multisolubility solubility parameter model assumes that the different types of interactions are independent. For each interaction, the following assumption may be made:

$$\delta_{m,f} = \sum \phi_p \delta_{p,f} \tag{8}$$

where the subscript, f , refers to a particular interaction.

Substituting eqn. 8 into eqn. 6 and assigning interaction identities to f gives:

$$\begin{aligned}
 \ln \alpha_{j,i} = & 2v/RT \{ (\delta_{d,i} - \delta_{d,j}) (\Sigma \phi_p \delta_{p,d,m} - \delta_{d,s}) \\
 & + (\delta_{o,i} - \delta_{o,j}) (\Sigma \phi_p \delta_{p,o,m} + \delta_{o,s}) \\
 & + (\delta_{d,i} - \delta_{d,j}) (\Sigma \phi_p \delta_{p,ind,m} + \delta_{ind,s}) \\
 & + (\delta_{ind,i} - \delta_{ind,j}) (\Sigma \phi_p \delta_{p,d,m} + \delta_{d,s}) \\
 & + (\delta_{a,i} - \delta_{a,j}) (\Sigma \phi_p \delta_{p,b,m} + \delta_{b,s}) \\
 & + (\delta_{b,i} - \delta_{b,j}) (\Sigma \phi_p \delta_{p,a,m} + \delta_{a,s}) \}
 \end{aligned} \tag{9}$$

We assume the solubility parameters of the solutes and the stationary phase are independent of any change in mobile phase composition²⁰. Then the terms, $\Sigma \phi_p \delta_{p,f} - \delta_{f,s}$, in eqn. 9 have a linear relationship with the volume fractions of the mobile phase. The value of this term will be changed by changing the composition of the mobile phase. This change will, in turn, change the separation capability of the mobile phase. In conclusion, the logarithm of the selectivity factor for a two component mixture is a linear function of the mobile phase composition.

Now this conclusion will be extended into a complicated separation case, such as a multi-component mixture. When the minimum logarithm-of-the-selectivity-factor surface is

constructed from the logarithm of the selectivity factor of the worst separated peak pairs, then each facet of the surface corresponds to a particular worst peak pair. Therefore, within a very small area which is centered about the global optimum composition, we may assume that the logarithm of the selectivity factor is a linear function of the mobile phase composition. This assumption will be used later to construct a mathematical function.

Now, we will define the concept of a multisolubility parameter pattern. For a particular liquid chromatography system, at any given composition of the mobile phase, the set of the multisolubility solubility parameters and their corresponding magnitudes can be viewed as a pattern. We call this pattern the multisolubility parameter pattern. Fig. III.1 is used to express this concept visually.

The second concept we need to define is the pattern difference (PD), which is used as a measure of the difference between two multisolubility parameter patterns. In Fig. III.2, two patterns are overlapped for comparison and their differences, a , are indicated. It is helpful to use a single value to show the difference between two patterns. To obtain such a value the multisolubility parameter values of two different mobile phase compositions are subtracted and the absolute values of the differences, a , are summed to produce a value which is called the

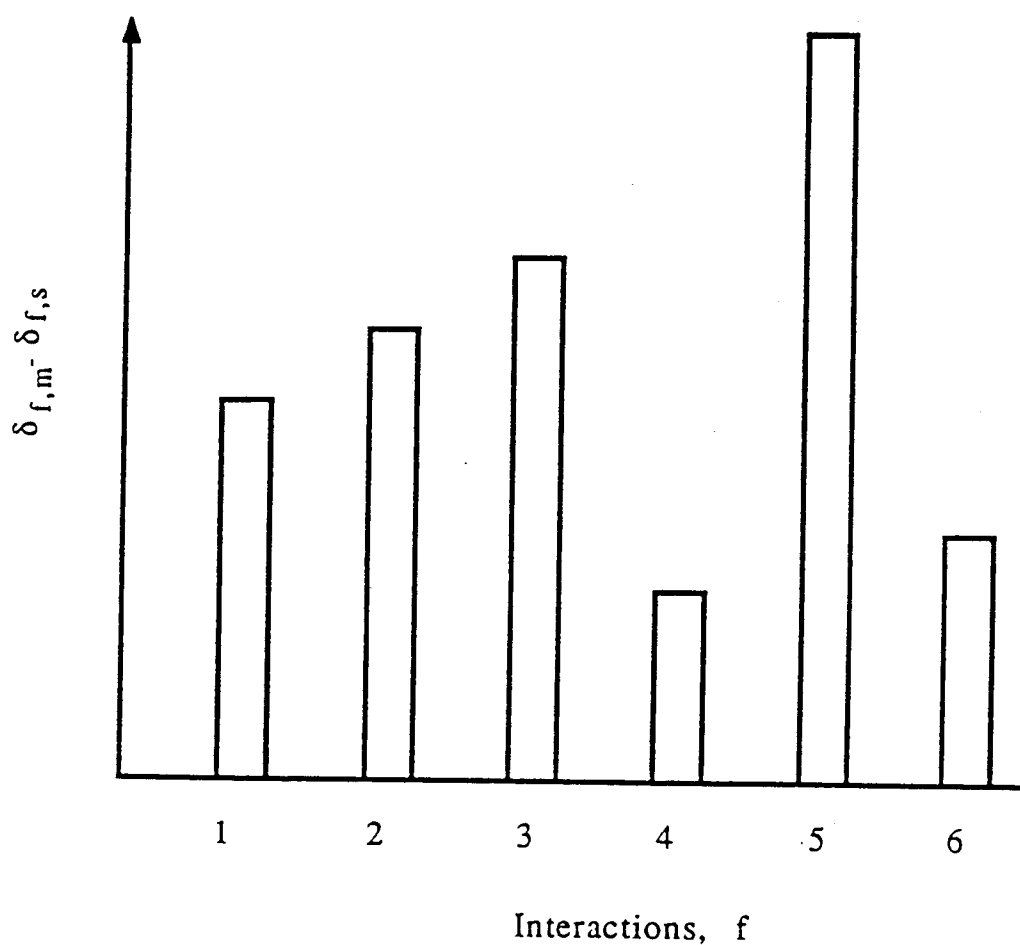


Fig. III.1 Multisolubility parameter pattern of a mobile phase composition. The subscripts 1, 2, 3, 4, 5 and 6 refer to different interactions, the subscripts m and s refer to the mobile phase and the stationary phase, respectively, and δ is the solubility parameter.

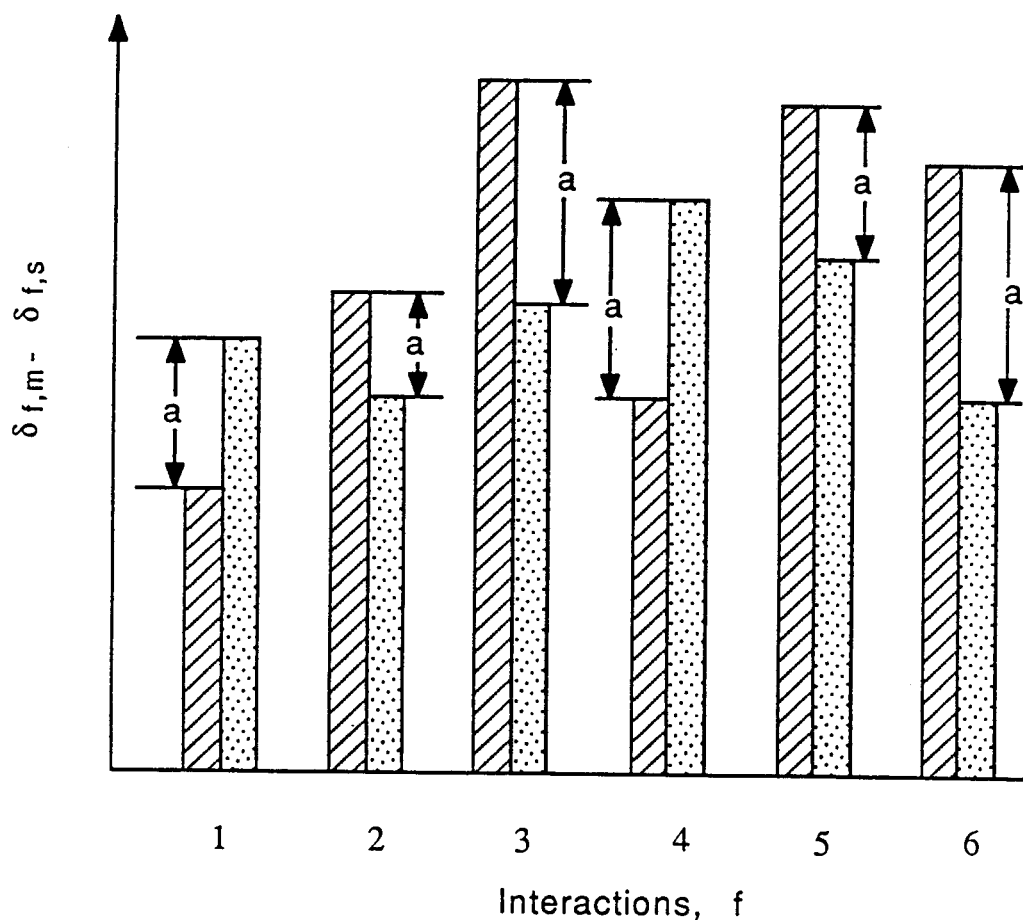




Fig. III.2 Comparison of the patterns of two different mobile phase compositions.

1, 2, 3, 4, 5 and 6 refer to different interactions.

() represents the magnitude of solubility parameters at one composition.

() represents the magnitude of solubility parameters at another composition.

a is the difference of a certain interaction between two compositions, $a = |(\delta_{f,m} - \delta_{f,s})_1 - (\delta_{f,m} - \delta_{f,s})_2|$, where the subscripts 1 and 2 refer to the two compositions.

pattern difference (PD):

$$PD = \sum |(\delta_{f,m} - \delta_{f,s})_1 - (\delta_{f,m} - \delta_{f,s})_2| = \sum a \quad (10)$$

where the subscripts 1 and 2 refer to the two mobile phase compositions. Clearly, the higher the similarity of the two patterns, the smaller the pattern difference will be.

These two concepts, the multisolubility parameter pattern and the pattern difference, can also be applied to a ternary (or pseudo-quaternary) mobile phase (Fig. III.3). According to eqn. 8, the pattern change has a linear relationship with the change in the mobile phase composition. Since a change in mobile phase composition is proportional to the distance between the two composition points in the linear coordinate system, the change in pattern difference is proportional to the distance between two compositions. For example, in Fig. III.3, the distance between points L₂ and O is twice as long as the distance between L₁ and O. Therefore, the pattern difference between L₂ and O is twice as large as the pattern difference between L₁ and O; the distance between L₁ and L₂ is equal to that between L₁ and O, so the pattern difference between L₂ and L₁ will be the same as the one between L₁ and O. These two concepts, the multisolubility parameter pattern and the pattern difference, are used in the following discussion about the interrelationship between the global optimum composition of a mobile phase composition represented by a trilinear coordinate system and the global

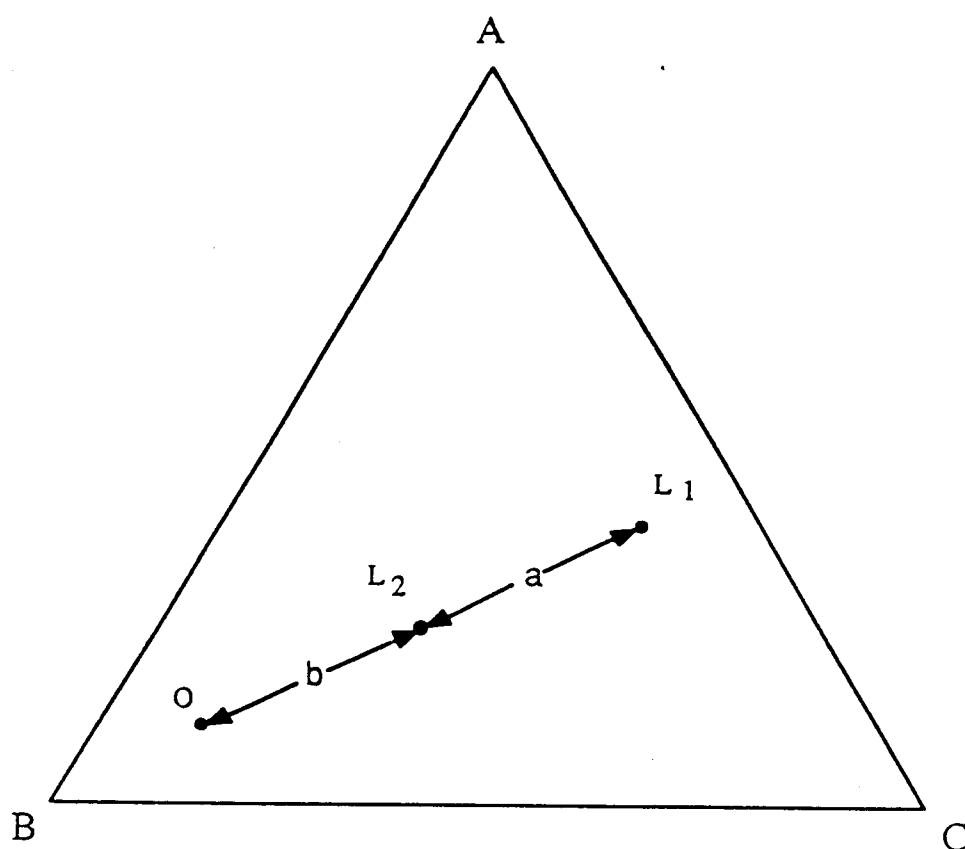


Fig. III.3 Pattern difference and distance. A, B and C refer to three isoeluotropic solvents, a and b refer to the distances between points L₁ and O, and points L₂ and O respectively, a is equal to b.

optimum composition of the mobile phases represented by the three edges of the trilinear coordinate system.

In Fig. III.4, point L represents the mobile phase composition which has the best separation capability on edge AB. Similarly, point M is the global optimum composition on edge BC, and point N is the global optimum composition on edge AC. In this figure, corner A represents a proton donor interaction dominant solvent; corner B represents a proton acceptor interaction dominant solvent; and corner C represents a dipole-dipole interaction dominant interaction solvent. For convenience of the discussion, assume that in a solvent represented by a corner, all of the other interactions, except the dominant interaction, are so small that they can be neglected. Therefore, the proton donor and proton acceptor interactions are the dominant interactions in the mobile phase at point L. In the same way, the proton acceptor and dipole-dipole interactions are the dominant interactions in the mobile phase at point M, and the proton donor and dipole-dipole interactions are the dominant interactions in the mobile phase at point N. Each of these interactions, proton donor, proton acceptor and dipole-dipole, exists along two edges, but is absent along the third edge of the triangle. Then, the mobile phase of the global optimum of the entire triangle can be viewed as a mixture of these three mobile phases represented by points L, M and N. Therefore, the solubility parameter pattern of the global optimum of the entire solvent system has

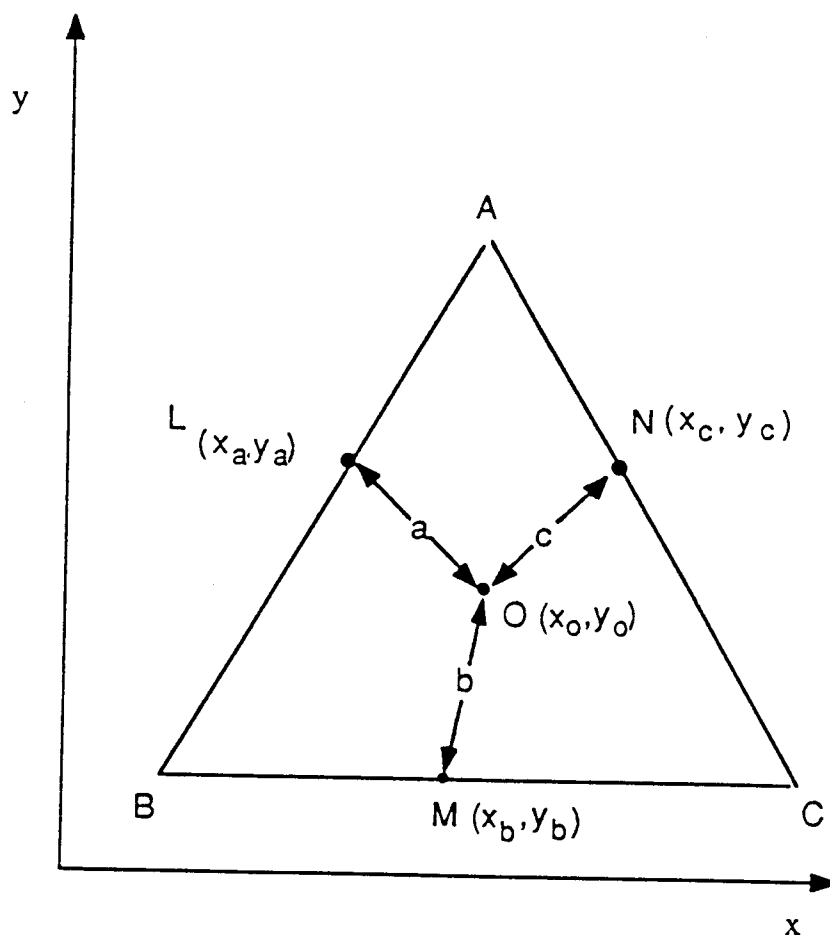


Fig. III.4 The solvent composition triangle in the Gaussian coordinate system. L, M and N are the global optima on the edges. O is the global optimum of the solvent system ABC, x and y are coordinates of the points, a, b and c are the distances between corresponding points.

the elements of the solubility pattern of the composition at point L, the elements of the solubility parameter pattern of the composition at point M, and the elements of the solubility parameter pattern of the composition at point N. That is, the solubility parameter pattern of the global optimum of the entire triangle has similarities to the patterns at points L, M, and N, simultaneously.

However, when the separation capabilities and therefore the patterns at points L, M and N are all different, then the similarities of the solubility parameter pattern of the global optimum composition to the patterns at points L, M and N are not all equal. More weight should be given to the pattern of the edge optimum which has a better separation capability. Therefore, a weighting parameter is needed to reflect the relative importance of the solubility parameter patterns of the optima of each edge.

Using the principles discussed above we propose, an optimization object function (eqn. 11) to find the global optimum composition of the entire triangle. This function will be called the separation pattern difference function (SPDF) and is

$$SPDF = \ln \alpha_L PD_{L,O} + \ln \alpha_M PD_{M,O} + \ln \alpha_N PD_{N,O} \quad (11)$$

where α is the selectivity of the worst separated peak pair at the point indicated by its subscript. The subscripts L, M, N, and O refer to the points L, M, N, and O respectively in Fig. III.4. $PD_{L,O}$ refers to the pattern difference between the points L and O; $PD_{M,O}$

refers to the pattern difference between the points M and O; $PD_{N,O}$ refers to the pattern difference between the points N and O, where O represents the global optimum.

First, because the solubility parameter pattern of the global optimum of the solvent triangle is similar to each of the three solubility parameter patterns of the optima along each edge, three corresponding pattern differences between the pattern of the global optimum of the triangle and the pattern of the optimum of each edge, respectively, are used in eqn. 11 to represent the similarities (or differences) between the corresponding patterns. Second, because all the relationships in the system are linear, and the logarithm of selectivity is a linear function of the solubility parameter pattern, the logarithm of the selectivity, $\ln \alpha$, of the worst separated peak pair(s) at the global optimum of each edge is used as a weighting parameter in eqn. 11 to reflect the separation capability of the solubility parameter pattern at this optimum.

Because the pattern at point L represents the combination of proton donor and proton acceptor interactions that has the best separation capability among all the possible combinations of these two interactions, and the pattern at point M represents the best combination of proton acceptor and dipole-dipole interactions that has the best separation capability among all the possible combination of proton acceptor and dipole-dipole interactions, and the pattern at point N represents the combination of proton donor and dipole-dipole interactions which

has the best separations capability among all the possible combinations of proton donor and dipole-dipole interactions, the mobile phase composition that has a pattern that is most similar to the patterns of points L, M and N should be the global optimum of the entire triangle. That is, the composition that has the minimum SPDF is the global optimum of the entire triangle.

For the calculation of SPDF, the relationship that the pattern difference is proportional to the distance, d , between two composition points is used, or

$$PD = R d \quad (12)$$

where R is a proportionality factor, d refers to distances a , b , or c in Fig. III.4, between the corresponding points will now be used to replace PD in eqn. 11. The distances, a , b , and c in Fig. III.4, can be expressed as the following:

$$a = [(x_a - x_o)^2 + (y_a - y_o)^2]^{1/2} \quad (13)$$

$$b = [(x_b - x_o)^2 + (y_b - y_o)^2]^{1/2} \quad (14)$$

$$c = [(x_c - x_o)^2 + (y_c - y_o)^2]^{1/2} \quad (15)$$

where x and y refer to the rectangular coordinates of the composition point, and the subscripts a , b , c and o refer to the composition points L, M, N, and O (Fig. III.4), respectively.

Substituting eqn's. 12-15 into eqn. 11 gives:

$$\begin{aligned}
 \text{SPDF} = & \ln\alpha_L R[(x_a - x_o)^2 + (y_a - y_o)^2]^{1/2} \\
 & + \ln\alpha_M R[(x_b - x_o)^2 + (y_b - y_o)^2]^{1/2} \\
 & + \ln\alpha_N R[(x_c - x_o)^2 + (y_c - y_o)^2]^{1/2}
 \end{aligned} \tag{16}$$

The optimization of ternary or pseodu-quaternary mobile phases is usually carried out under an isoelutropic condition; that is, the solvent strength at any composition of the mobile phase system is approximately a constant. As a result, the proportionality factor, R , is also approximately a constant. Dividing both sides of eqn. 16 by R , gives

$$\begin{aligned}
 \text{SPDF}/R = & \ln\alpha_L [(x_a - x_o)^2 + (y_a - y_o)^2]^{1/2} \\
 & + \ln\alpha_M [(x_b - x_o)^2 + (y_b - y_o)^2]^{1/2} \\
 & + \ln\alpha_N [(x_c - x_o)^2 + (y_c - y_o)^2]^{1/2}
 \end{aligned} \tag{17}$$

Since R is a constant, to find the global optimum in the solvent triangle, the right hand side of eqn. 17 is solved for the values of x_o and y_o which give the minimum SPDF. These values can be found by any computer program capable of finding the global minimum of a nonlinear function within the bounds of the solvent triangle. This study used a grid search routine with a grid size equal to 1% in eluent composition.

This method of locating the global optimum of the ternary or pseudo-quaternary mobile phase is called the weighted pattern comparison optimization method to emphasize the two key points of the method: the comparison of the multisolubility parameter patterns between corresponding composition points, and the use of the parameter, $\ln\alpha$, as a weighting factor to express the separation capability.

Experimental

The data for the normal phase HPLC separation experiments used in this work are from two published works^{21, 22}. The data listed in Table 1 are from G.M.Landers et al.²¹ who used a uPorasil silica 30x0.39 cm column, and a mobile phase consisting of chloroform, methylene chloride, isopropyl ether and hexane. The sample consisted of four retinol isomers. All the experiments were carried out at a flow rate of 3 ml/min.

The data listed in Table 2 are from J. L. Glajch et al.²² who used three Zorbax-SIL 15x0.46 cm columns from the same production lot. Methylene chloride, acetonitrile, methyl tertbutyl ether and hexane were used as the components of the mobile phase. Mobile phase solvents were 50% water saturated. The sample consisted of 13 substituted naphthalenes. All experiments were carried out with a flow rate of 2.0 ml/min at 35°C.

The data for the reverse phase HPLC separation experiments are from²³⁻²⁵. The data listed in Table 3 are from S. J. Costanzo²³ who used a Partisil-10, C8, 25x0.46cm column. Methanol, acetonitrile, tetrahydrofuran and water were used as the components of the mobile phase. In addition, all mobile phase compositions contained 1% acetic acid. The sample consisted of six substituted aromatic compounds.

TABLE III.1

SEPARATION PARAMETERS OF FOUR RETINAL ISOMERS FOR SEVEN SOLVENTS WITH A NORMAL-PHASE COLUMN

 μ Porasil Si 30 x 039 cm column; 3.0 ml/min.

Solvent	Separation parameter			
	11/13**		9/all***	
	R_s	α	R_s	α
A	0.096	1.0038	0.67	1.027
B	0.43	1.017	0.051	1.002
C	0.084	1.0034	0.35	1.014
A/B (1:1)	0.43	1.017	0.26	1.011
A/C (1:1)	0.13	1.0052	0.36	1.014
B/C (1:1)	0.68	1.027	0.20	1.0080
A/B/C (1:1:1)	0.47	1.019	0.37	1.015

* resolution data are from reference 21. The selectivity factors, α , calculated from resolution data.

** 11-*cis* retinaldehyde/13-*cis* retinaldehyde

*** 9-*cis* retinaldehyde/all-*trans* retinaldehyde

A- isopropyl ether/hexane (21.3:78.7 v/v)

B- methylene chloride/hexane (75:25 v/v)

C- chloroform/hexane (25:75 v/v)

TABLE III.2

THE CAPACITY FACTORS* OF THIRTEEN SUBSTITUTED NAPHTHALENES
FOR SEVEN SOLVENTS WITH A NORMAL-PHASE COLUMN

Zorbax-SIL 15 x 0.46 cm column; 35°C; 2.0 ml/min.

Compound** Number		<i>k'</i>						
		Solvent:						
		A	B	C	A:B (1:1)	B:C (1:1)	A:C (1:1)	A:B:C (1:1:1)
1	2-OCH ₃	0.58	0.57	0.59	0.65	0.67	0.54	0.67
2	1-NO ₂	0.86	1.20	1.62	1.10	1.36	0.90	1.30
3	1,2-(NO ₂)	1.15	0.82	1.00	1.02	0.95	0.91	1.02
4	1,5-(NO ₂) ₂	2.37	3.27	3.70	2.98	3.62	2.63	3.63
5	1-CHO	2.75	1.69	2.45	2.22	2.11	2.27	2.33
6	2-CO ₂ CH ₃	3.29	2.49	2.83	3.00	2.99	2.78	3.25
7	1-CO ₂ CH ₃	3.31	2.71	3.07	3.13	3.33	2.85	3.57
8	2-CHO	3.97	2.22	3.25	3.19	2.83	3.12	3.17
9	1-CH ₂ CN	4.06	4.73	7.23	4.86	6.09	4.83	6.30
10	1-OH	4.44	8.17	6.65	6.77	7.14	6.27	8.00
11	1-COCH ₃	5.17	2.58	3.54	3.71	3.25	3.72	3.72
12	2-COCH ₃	7.33	3.33	4.76	5.14	4.39	5.16	5.10
13	2-OH	7.98	11.86	11.35	10.69	11.58	11.57	13.42

* Data are from reference 22.

** Compounds are substituted naphthalenes.

A- methylene chloride/hexane (57.8:42.2 v/v/v).

B- methylene chloride/acetonitrile/hexane (10:3:87 v/v/v).

C- methyl *tert* butyl ether/hexane (4.2:95.8 v/v).

TABLE III.3

CAPACITY FACTORS* OF SIX SUBSTITUTED AROMATIC COMPOUNDS FOR SEVEN SOLVENTS WITH A REVERSED-PHASE COLUMN

μPartisil-10 C₈ 25 x 0.46 cm column.

Compound Number**	<i>k'</i>						
	Solvent :						
	A	B	C	A/B (1:1)	B/C (1:1)	A/C (1:1)	A/B/C (1:1:1)
1	1.41	1.66	2.96	1.63	2.00	1.88	1.76
2	2.68	2.45	4.19	2.94	3.07	3.04	2.97
3	3.27	4.54	6.44	4.01	4.92	4.07	4.10
4	3.40	3.13	9.68	3.73	5.23	5.52	4.70
5	3.84	3.96	18.67	4.66	7.50	8.87	6.52
6	6.88	7.73	8.13	8.62	7.05	6.10	7.03

* Data are from reference 23.

** Compounds 1 through 6 represent, respectively: 4-aminobenzoic acid; 3,4-dimethoxybenzoic acid; benzaldehyde; benzoic acid; 4-nitrobenzoic acid; and 3,4,5-trimethoxymethylbenzoate.

A- methanol/water/acetic acid (45:54:1 v/v/v).

B- acetonitrile/water/acetic acid (30:69:1 v/v/v).

C- tetrahydrofuran/water/acetic acid (20:79:1 v/v/v).

The data listed in Table 4 are from J. L. Glajch et al.²⁴ who used a Zorbax-C8 15x0.46cm column. Methanol, acetonitrile, tetrahydrofuran and water were used as the components of the mobile phase. The sample consisted of nine substituted naphthalenes. All experiments were carried out with a flow rate of 2ml/min at 40°C.

The data listed in Table 5 are from G. D'agostino et al.²⁵. In their work, a ODS-Hypersil, C18, 15X0.5cm column was used. Methanol, acetonitrile, tetrahydrofuran and water were used as the components of the mobile phase. The sample consisted of ten polar adrenocortical steroids. All experiments were carried out with a flow rate of 1ml/min at 45°C.

TABLE III.4

CAPACITY FACTORS* OF NINE SUBSTITUTED NAPHTHALENES FOR SEVEN SOLVENTS WITH A REVERSED-PHASE COLUMN

Zorbax-C₈ 15 x 0.46 cm column; 40°C; 2 ml/min.

Comp. No. **	Group	<i>k'</i>						
		Solvent:						
		A	B	C	A/B (1:1)	B/C (1:1)	A/C (1:1)	A/B/C (1:1:1)
1	N-1	0.65	0.69	0.57	0.52	0.69	0.74	0.73
2	2-SO ₂ CH ₃	0.78	1.28	0.98	0.88	1.08	0.88	1.01
3	2-OH	1.22	1.35	2.46	1.13	2.02	2.55	2.07
4	1-COCH ₃	2.26	2.79	2.46	2.25	2.53	2.55	2.61
5	1-NO ₂	3.02	3.79	3.85	3.14	3.84	4.60	4.16
6	2-OCH ₃	4.04	4.56	4.63	3.87	4.62	5.56	5.44
7	Naph	4.04	4.72	5.20	3.87	5.08	6.00	5.44
8	1-SCH ₃	6.67	6.93	6.73	6.40	7.05	9.16	8.32
9	1-C1	7.77	7.88	6.73	7.32	8.09	10.36	9.71

* Data are from reference 24.

** Compounds are the substituted naphthalenes.

A- methanol/water (63:37 v/v).

B- acetonitrile/water (52:48 v/v)

C- tetrahydrofuran/water (52:48 v/v)

TABLE III.5

CAPACITY FACTORS* OF TEN POLAR ADRENOCORTICAL STEROIDS
FOR SEVEN SOLVENTS WITH A REVERSED-PHASE COLUMN

ODS-Hyptrsil C₁₈ 15 x 0.5 cm column; 45°C; 1 ml/min.

Compound Number**	<i>k'</i>						
	Solvent:						
	A	B	C	A:B (1:1)	B:C (1:1)	A:C (1:1)	A:B:C (1:1:1)
1	9.4	10.8	8.0	11.8	7.8	7.5	8.0
2	10.8	12.5	8.3	13.7	8.3	7.9	8.4
3	13.5	15.3	8.8	17.2	9.1	8.2	9.8
4	14.3	13.6	10.3	16.9	9.3	9.3	9.9
5	15.6	12.0	12.9	16.7	10.3	11.7	11.0
6	18.1	17.1	11.7	20.8	10.8	10.7	11.6
7	19.1	13.2	13.0	18.0	10.7	12.4	12.3
8	19.1	24.3	19.1	24.0	15.4	14.0	15.4
9	22.6	15.8	17.1	22.3	12.7	14.9	14.3
10	22.6	23.2	27.0	26.0	18.6	19.4	19.3

* Data are from reference 25.

** The chemical names of these compounds are listed in Table 3b.

A- methanol/water (35:65).

B- acetonitrile/water (20:80).

C- tetrahydrofuran/water (12:88).

Results and Discussion

In this work, the optimization performance of the weighted pattern comparison method was studied under both known and unknown sample separation situations. The data in Tables 1, 2, 3, 4 and 5 were used to form test cases.

For the known sample separation situation, the global optimum mobile phase composition was located by the WPCO method and compared with that located by the minimum α plot method. For the cases in which peak cross-over occurs, the separation response surface will consist of several optimum areas. For comparison of these two methods, if the result of the WPCO method is close to the result of the minimum α plot and these two results are in the same optimum area, then the WPCO method has essentially the same capability as does the minimum α plot method under those particular experimental conditions.

In this work, for building the separation response surface of the test samples in the minimum α plot method, the special cubic function^{26,27,28} (eqn. 13) was used for each solute to describe the retention behavior for every point on the entire solvent triangle response surface. This function is as follows:

$$\begin{aligned} \ln k' = & a_1X_1 + a_2X_2 + a_3X_3 + a_{12}X_1X_2 \\ & + a_{13}X_1X_3 + a_{23}X_2X_3 + a_{123}X_1X_2X_3 \end{aligned} \quad (13)$$

where X is the proportion of the isoeluotropic eluent, and k is the capacity factor. The subscripts 1, 2 and 3 represent the three isoeluotropic eluents. The coefficients a_1 - a_{123} are calculated from the minimum of seven experimental points needed to fit eqn. 13.

J. L. Glajch et al.²⁹ found that the most accurate result was achieved when the logarithm of the capacity factor was modeled. This chromatography behavior model (eqn. 13) has been widely applied and satisfactory results have been achieved^{4,30,31,32,33}. Additionally, the data used in this work are readily fit to the special cubic function.

For the weighted pattern comparison method, the global optimum of each edge of the solvent triangle has to be located first. In this work, the window diagram method was chosen to accomplish this task. eqn. 14 was used as the retention behavior model along the edges of the solvent triangle.

$$\ln k' = a_1X_1 + a_2X_2 + a_{12}X_1X_2 \quad (14)$$

where X_1 and X_2 are the volume fractions of two isoeluotropic eluents, and a_1 - a_{12} are the coefficients calculated from the experimental points needed to fit eqn. 14. Equation 14 is a quadratic equation because the sum of X_1 and X_2 is a constant corresponding to unity. Equation 14 is used for two reasons. First, eqn. 14 results when eqn. 13 is applied along an edge of the

solvent triangle. Because eqn. 13 is used for the minimum α plot and its special form, eqn. 14, is used along the triangle edge for the weighted pattern comparison method, no difference is produced in describing the retention behavior along the edge of the solvent triangle for these two methods. Second, the data pattern used in this work easily fits eqn. 14.

Although, the window diagram method was the best choice for locating the global optimum along the triangle edge in these studies, this does not mean that the window diagram method will be the most suitable method under all situations. For instance, the grid search method may be the only choice to find the global optimum along an edge for an unknown sample.

For the minimum α plot method and the window diagram method, the logarithm of the selectivity factor of the worst separated peak pair was used as the optimization criterion^{34,35}. In this work, the only consideration is the adequate separation of all peaks. All the other peak pairs would be better separated than the worst separated peak pair. Additionally, the results obtained from a window diagram can be used directly in the WPCO method (eqn. 15).

The data needed for the WPCO method, eqn. 15, are the global optimum composition on each edge of the solvent triangle and the corresponding selectivity factor of the worst separated peak pair at each of these three compositions. It is not necessary

to identify the substance causing these peaks. Hence, the WPCO method may be used for unknown samples.

For the unknown sample separations, the "unknown" sample test cases were the same as those in the study of the known samples. The minimum α response surfaces of the known sample test cases were used for the "unknown" sample cases. Then, the WPCO method and the grid search method were compared.

Because the choice of the search step size for the grid search method and the choice of the solute chromatographic behavior model for the simultaneous method depend on the shape (complexity) of the minimum separation response surface, it is necessary to use some features of the minimum separation response surface to describe the complexity of the surface.

In this work, two features of the minimum separation response surface are used as measures of the complexity of the minimum separation response surface. One is the number of local optima on the entire separation response surface; the other is the width of the peak or similarly the size of the area of the peak's perpendicular projection onto the plane of the solvent triangle (see Fig. III.5). Generally, the surface becomes more complex as the number of optima increases. A small optimum area will also make the response surface more complicated, because a denser grid search is needed to locate a small peak for unknown samples,

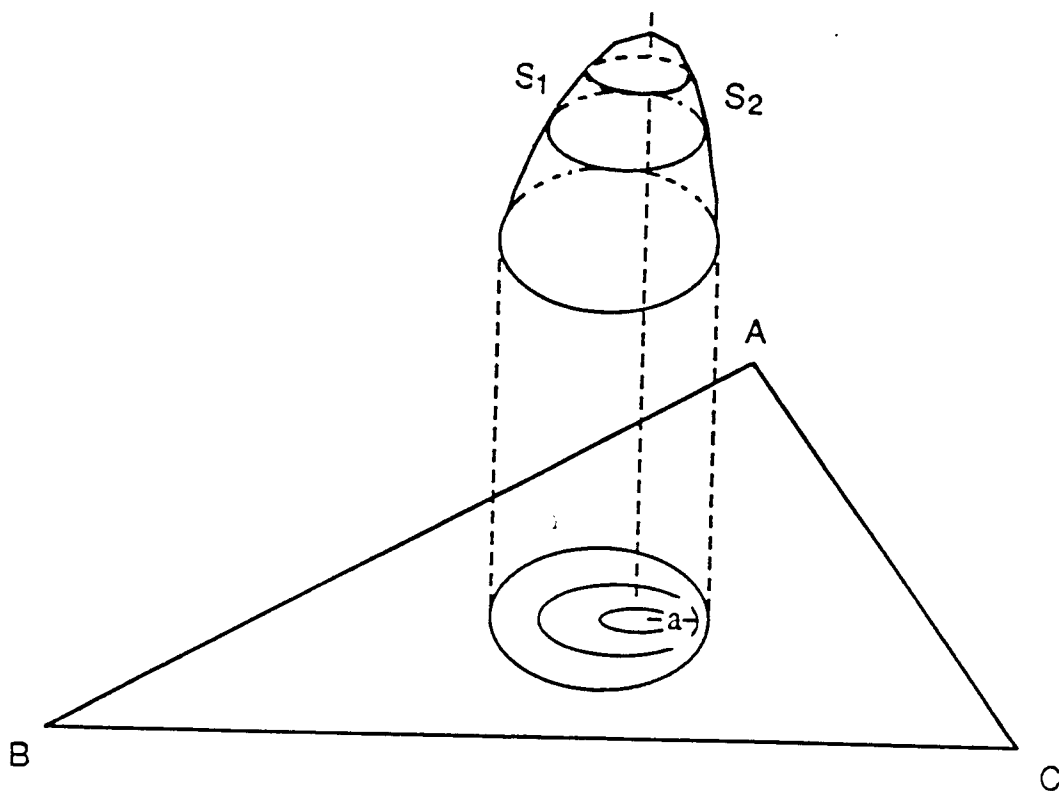


Fig. III.5 Perpendicular projection of a peak of the hypothetical separation response surface onto the solvent composition triangle. a is the projection of the steepest slope of the peak. ABC is the solvent composition triangle.

or a more accurate chromatographic behavior model might be needed for known samples.

When applying the grid search method to an unknown sample, the step size of the search is determined by the smallest optimum area (peak projection) on the solvent triangle plane. The global optimum cannot be located with certainty unless all the optima (peaks) have been located.

For locating a peak maximum correctly, the peak's shape and width (or size of its projection area) have to be considered. Since there may be more than one worst separated peak pair which comprises a peak of a separation response surface, the peak may be asymmetrical. However, first consider a symmetrical peak. When the solvent triangle lies on the xy plane, the altitude of the response surface is in the direction of the z axis. Because a peak's projection on the xy plane is two dimensional, to find a composition which corresponds to the best separation result in this projection, this composition has to be located in the search along both the x and y axes. Since the considerations for choosing the search step size are the same along both directions, a search in one direction will be discussed. When a response surface peak is intersected by a plane which is in the z -axis direction and perpendicular to the xy plane, a vertical cross sectional view of this peak is produced. Fig. III.6 shows several of these cross sectional views for peaks that have flat or planar surfaces.

When a response surface peak is symmetrical, its vertical cross section will also be symmetrical, Fig. III.6a,b. For determining the presence of a peak, a minimum of two sampling points will be necessary within a spacing of the projection of each side of a peak. A larger spacing may miss the peak completely. Fig. III.6 shows the results under both best and worst sampling conditions. To locate a peak, at least two points are needed on each side of the peak so that lines can be drawn through the points and the peak location can be determined by their intersection. That is, practically, at least four to five sampling points are necessary to locate a symmetrical peak without serious distortion for the purpose of the mobile phase composition optimization. This means at least 4 to 5 sampling points (experiment compositions) are needed within the projection of the peak on the xy plane in the search along x-axis direction, and in the search along y-axis direction. Therefore, for a grid search with step size of 5% in eluent composition, the smallest projection area of a symmetrical peak that can be located has the diameter of 20% in eluent composition. Fig. III.7 shows the situation when 10% step size is used. Under this situation, the smallest projection area of a symmetrical peak that can be located has a diameter of 40% in eluent composition.

For an asymmetrical peak, the step size is determined by the length of the projection (in the plane of the solvent triangle) of the side of the peak with the steepest slope (see Fig. III.5c, d).

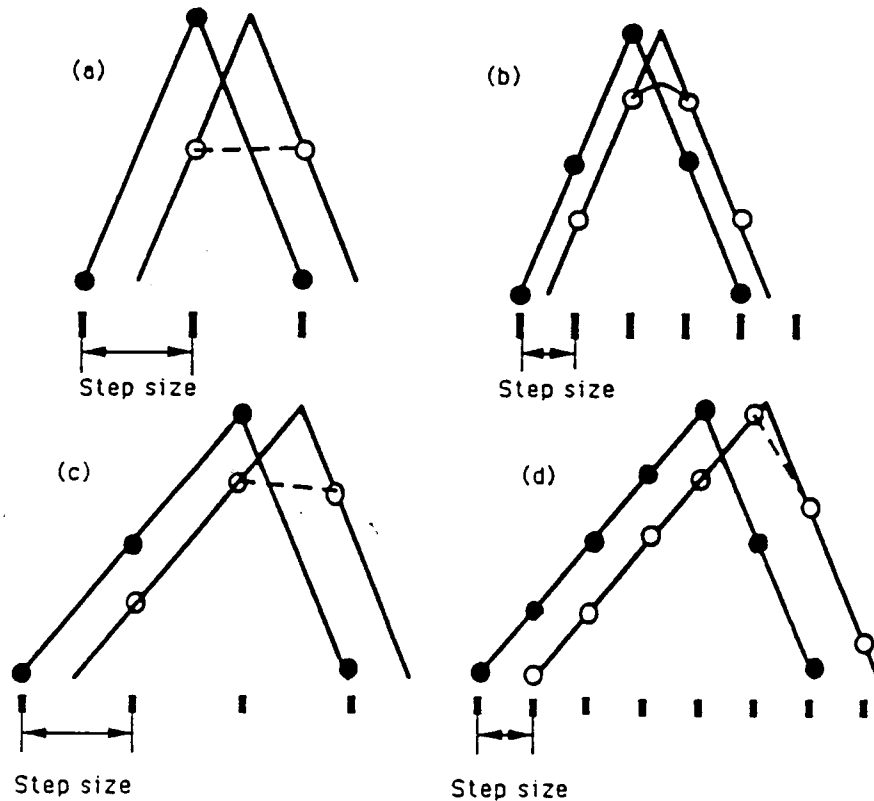


Fig. III.6 Search step size and the results.

- (a) Best and worst situations for using 3 sampling points to locate a symmetrical peak.
- (b) Best and worst situations for using 5 sampling points to locate a symmetrical peak.
- (c) Best and worst situations for using the distance of the projection of the steepest slope of an asymmetrical peak as the search step size.
- (d) Best and worst situations for using half of the distance of the steepest slope of an asymmetrical peak as the search step size.

Therefore, for a non-symmetrical peak, the search step size must be smaller. The best way to choose the step size for a surface that contains asymmetrical peaks is to use half of the distance of the projection (in the plane of the solvent triangle) of the steepest slope. In this way, every peak will be located.

For testing the WPCO method, first, five original cases from five published works were tested. Then more test cases were formed by using subsets of the data in four of these published works. The other published work, Table III.1, only has two peak pairs for which data were reported. So no more cases could be formed.

Thirty-seven test cases were constituted from the data in Table III.2. The constituents for these cases are listed in Table III.6. These cases represent three different levels of complexity. Component 13 was removed from the original sample to save computer time, because this component was always well separated from the other components, and it usually was not a constituent of a worst separated peak pair. There were thirteen test cases at the most complex level. One of the cases was the original sample (Table III.6, case 1). The other twelve cases were formed by removing one component from the twelve components in turn. In this way, all the eleven-component cases which could possibly be formed in this original sample were formed. The separation response surface of case 2 (Table 6) was the same as that of case 3 (Table 6). The surface of case 4 (Table 6) was the

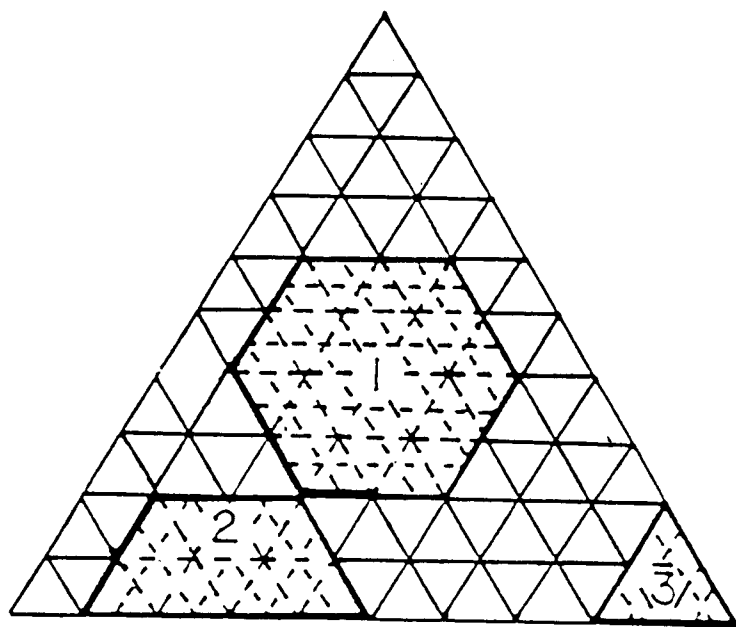


Fig. III.7 Smallest symmetrical peak which can be located by a 10% in step size grid search. For area 1 the whole peak is in the triangle. For area 2 half of the peak is in the triangle. For area 3, $1/6$ of a peak is in the triangle.

same as that of case 5 (Table 6). Therefore, there were eleven different separation response surfaces in these thirteen cases. Peak cross-over occurred extensively in these test cases. The number of optima (global and local) in each of these cases was in the range of 13 to 32. The surfaces for these cases were different from each other at various levels.

The medium complexity test samples consisted of one six-component case and six five-component cases. Components 4, 5, 6, 7, 8, 11, in Table III.6 were used to constitute the six- and five-component cases. There were several considerations for choosing these six components. First, the number of possible combinations for the six- and five-component cases that could be formed from the original twelve-component sample is very large, so the simpler cases were omitted. We presumed that if the WPCO method could work on the most complex six- and five-component cases that could be formed in this sample, then, the WPCO method would also work on the rest of the six- and five-component cases.

In Fig. III.8, the area surrounded by the dashed line is the most crowded area, and peak cross-over occurs most frequently here. Therefore, the six- and five-component cases formed from the components in this area would be more complex than the other five-component test cases. Seven six- and five-component cases were chosen for their complexity. The separation response

TABLE III.6

SOLUTE CONSTITUENTS OF SUBSTITUTED NAPHTHALENES FOR TEST CASES*WITH A NORMAL-PHASE COLUMN.

<i>Case</i>		<i>Component**</i>											
1	1	2	3	4	5	6	7	8	9	10	11	12	13
2	1	2	3	4	5	6	7	8	9	10	11	12	
3		2	3	4	5	6	7	8	9	10	11	12	
4	1		3	4	5	6	7	8	9	10	11	12	
5	1	2		4	5	6	7	8	9	10	11	12	
6	1	2	3		5	6	7	8	9	10	11	12	
7	1	2	3	4		6	7	8	9	10	11	12	
8	1	2	3	4	5		7	8	9	10	11	12	
9	1	2	3	4	5	6		8	9	10	11	12	
10	1	2	3	4	5	6	7		9	10	11	12	
11	1	2	3	4	5	6	7	8		10	11	12	
12	1	2	3	4	5	6	7	8	9		11	12	
13	1	2	3	4	5	6	7	8	9	10		12	
14	1	2	3	4	5	6	7	8	9	10	11		
15				4	5	6	7	8			11		
16					5	6	7	8			11		
17				4		6	7	8			11		
18				4	5		7	8			11		
19				4	5	6		8			11		
20				4	5	6	7				11		
21				4	5	6	7	8					

(continue to next page)

(Table III.6 continued)

22	1	2	3	4															
23		2	3	4															
24	1		3	4															
25	1	2		4															
26	1	2	3																
27					5	6	7	8											
28						6	7	8											
29					5		7	8											
30					5	6		8											
31					5	6	7												
32									9	10	11	12							
33										10	11	12							
34									9		11	12							
35									9	10		12							
36									9	10	11								

* Capacity factors are in Table 2.

** The compound number is the same as that in Table 2.

surfaces for these seven cases were different from each other, and the number of optima that each case had ranged from 7 to 23.

The least complex test case group consisted of three four-component cases and twelve three-component cases. It was presumed that the most complex cases in this group should be formed from the components whose retention times were close to each other. Furthermore, two different types of test cases were formed. One of the subgroups was formed from the components that (most of them) were not used to form the medium complexity cases. The other subgroup was formed from the components that were also used for the medium complexity cases. In this way, the performance of the WPCO method can be observed more thoroughly. The separation response surfaces of these cases were different from each other. The number of optima that each case had was about four. Overall thirty-three different cases from this original sample were used to test the WPCO method.

Third, eleven test cases were constituted from the data in Table III.3. The constituents of these cases are listed in Table. III.7. Since there are only 6 components in the original sample, two kinds of test cases were formed. One group consisted of one six-component case and six five-component cases. These cases were the most complicated cases in this sample. The number of optima that each case had was about six. In this group, the separation response surfaces of cases 1, 2 and 3, were the same,

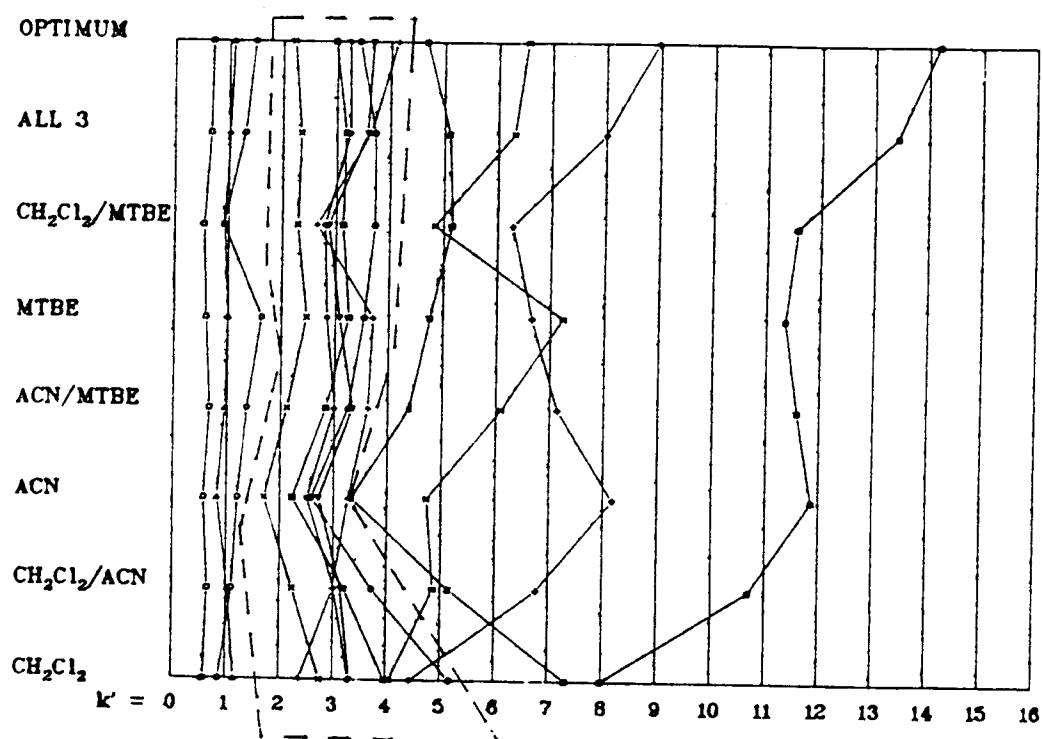


Fig. III.8 Map of k' of solutes in eight different mobile phase. listed on the left. Each line represents one solute. (ref. 22).

so four different cases in this group were used to test the WPCO method.

The other group consisted of five four-component cases. For this group, component 4 was removed from the original sample first, and then another component was removed in turn from the five components left. In forming this group, component four was removed first because it was found by accident that in the resulting group the global optima of some cases were located inside of the triangle. In this group, there were two cases (cases 8 and 12 in Table III.7) that had common separation surfaces, so four cases in this group were used. Overall, eight test cases were formed from the original sample.

Twelve test cases were constituted from the data in Table III.4. The constituents of these cases are listed in Table III.8. These cases included one nine-component case, nine eight-component cases and several seven-component cases. However, peak cross-over only happened once in the original sample, so most of the surfaces for these cases were very simple and very similar to each other. Consequently, there were only three cases which were significantly different from each other, and they were the ones studied. Overall, three cases were used from this original sample.

The next original sample used for testing the WPCO method was a complex reverse phase separation case (Table III.5).

TABLE III.7

SOLUTE CONSTITUENTS OF AROMATIC COMPOUNDS FOR TEST
CASES WITH A REVERSED-PHASE COLUMN*

<i>Case</i>		<i>Component**</i>					
1	1	2	3	4	5	6	
2		2	3	4	5	6	
3	1		3	4	5	6	
4	1	2		4	5	6	
5	1	2	3		5	6	
6	1	2	3	4		6	
7	1	2	3	4	5		
8	1	2	3		5		
9	1	2	3			6	
10	1	2			5	6	
11	1		3		5	6	
12		2	3		5	6	

* capacity factors are in Table 3.

** The component number is the same as that in Table 3.

TABLE 8

SOLUTE CONSTITUENTS OF SUBSTITUTED NAPHTHALENES FOR TEST CASES WITH A REVERSED-PHASE COLUMN*

<i>Case</i>	<i>Component**</i>								
1	1	2	3	4	5	6	7	8	9
2		2	3	4	5	6	7	8	9
3	1		3	4	5	6	7	8	9
4	1	2		4	5	6	7	8	9
5	1	2	3		5	6	7	8	9
6	1	2	3		5	6	7	8	9
7	1	2	3	4		6	7	8	9
8	1	2	3	4	5		7	8	9
10	1	2	3	4	5	6		8	9
11	1	2	3	4	5	6	7		9
12	1	2	3	4	5	6	7	8	

* Capacity factors are in Table 4.

**The component number is the same as in Table 4.

Twenty-six cases were formed. The constituents of these cases are listed in Table III.9. The most complicated group consisted of eleven cases. One of these cases was the original case. The other ten cases were formed by removing one component from the original components in turn. These eleven cases covered all the ten- and nine-component cases which could be formed in this sample. The number of optima that each case had was in the range of eight to eleven. In this group, the separation surfaces of cases 2 and 3 (Table III.9) were the same, so ten different cases were used to test the WPCO method. In addition, fifteen seven-components cases were formed. First, component 1 was removed from the original sample, because this component was always well separated from the other components, and it was never a constituent of a worst-separated peak pair. Second, component 3 was removed from the nine components left. Then, one of the components left was removed in turn. In this way, eight eight-component case were formed. In these eight cases, the separation surfaces of two cases were the same, so that seven of these eight cases were used. The other seven eight-component cases were formed in a similar way. First, component 1 was removed from the original sample. Second, component 7 was removed. Then, one of the components left was removed in turn. Among these eight cases, the separation surfaces of two cases were the same, leaving seven cases to be studied. In addition, subtracting these two cases left thirteen of these eight- or seven-component cases

to test the WPCO method. The number of optima that each case had was about 8. Overall, 23 cases were formed.

In summary, 68 cases have been used to test the WPCO method. These cases can be divided into two groups. In one group, the separation response surfaces of one subgroup are similar to each other; that is, the major features (the general location of the global optimum, shape and location of the projection of the base of the peaks on a solvent triangle plane) of these surfaces are similar, but the heights and locations of the tops of some peaks are different from the others. These cases were used to test the ruggedness of the WPCO method. If the WPCO method was not confused by the difference between these surfaces and located the global optimum area in these cases, then the WPCO method would be considered rugged.

In the other group, every separation response surface is completely different from the others; their global optimum areas and other features are different. These cases were used to test the versatility of the WPCO method.

Now, the performance of the WPCO method under these different situations is discussed.

First, consider the case where the global optimum is at a corner of solvent triangle. The pattern difference concept makes no distinction between a PD caused by a set of interactions having

TABLE 9

SOLUTE COMPONENTS OF ADRENOCORTICAL STEROIDS FOR
TEST CASES WITH A REVERSED-PHASE COLUMN*

<i>Case</i>		<i>Component**</i>								
1	1	2	3	4	5	6	7	8	9	10
2		2	3	4	5	6	7	8	9	10
3	1		3	4	5	6	7	8	9	10
4	1	2		4	5	6	7	8	9	10
5	1	2	3		5	6	7	8	9	10
6	1	2	3	4		6	7	8	9	10
7	1	2	3	4	5		7	8	9	10
8	1	2	3	4	5	6		8	9	10
9	1	2	3	4	5	6	7		9	10
10	1	2	3	4	5	6	7	8		10
11	1	2	3	4	5	6	7	8	9	
12		2		4	5	6	7	8	9	10
13		2			5	6	7	8	9	10
14		2		4		6	7	8	9	10
15		2		4	5		7	8	9	10
16		2		4	5	6		8	9	10
17		2		4	5	6	7		9	10
18		2		4	5	6	7	8		10
19		2		4	5	6	7	8	9	
20				4	5	6	7	8	9	10
21		2	3	4	5	6		8	9	10
22		2	3	4	5	6		8	9	
23		2		4	5	6		8	9	10
24		2	3		5	6		8	9	10
25		2	3	4		6		8	9	10
26		2	3	4	5			8	9	10
27		2	3	4	5	6			9	10
28		2	3	4	5	6		8		10
29			3	4	5	6		8	9	10

* Capacity factors are in Table 5

** The component number is the same as in Table 5.

small differences and an equal PD produced by a single dramatic difference for one interaction. If a dramatic difference represents a kind of interaction that causes separation of a particularly difficult pair, then the two pattern differences could have dramatically different effects even though their PD values are the same.

However, when one interaction dominates the process, the solvent that shows it most powerfully will be the only solvent of interest and the global optimum will be at a corner of the triangle. Our results show that whenever this is the case, the WPCO method finds the global optimum. The method therefore works for cases where one interaction dominates the separation. Fig. III.9 shows the result of one of these cases

Now, consider the situation where the global optimum is on an edge. Fig. III.10 shows a physical analogue model for solving eqn. 10³⁶. Three frictionless pulleys are in a horizontal plane. (For the WPCO method, the locations of these three pulleys are the global optima of the three edges, and the plane is the solvent composition triangle.) Take three strings and tie them together at one end with each of other ends strung over a pulley. Then, tie a weight to each string. For the WPCO method, these weights are proportional to the corresponding $\ln\alpha$ of the worst-separated peak pair(s). The resting place of the joint point of the strings is the global optimum of the entire triangle. This model shows that

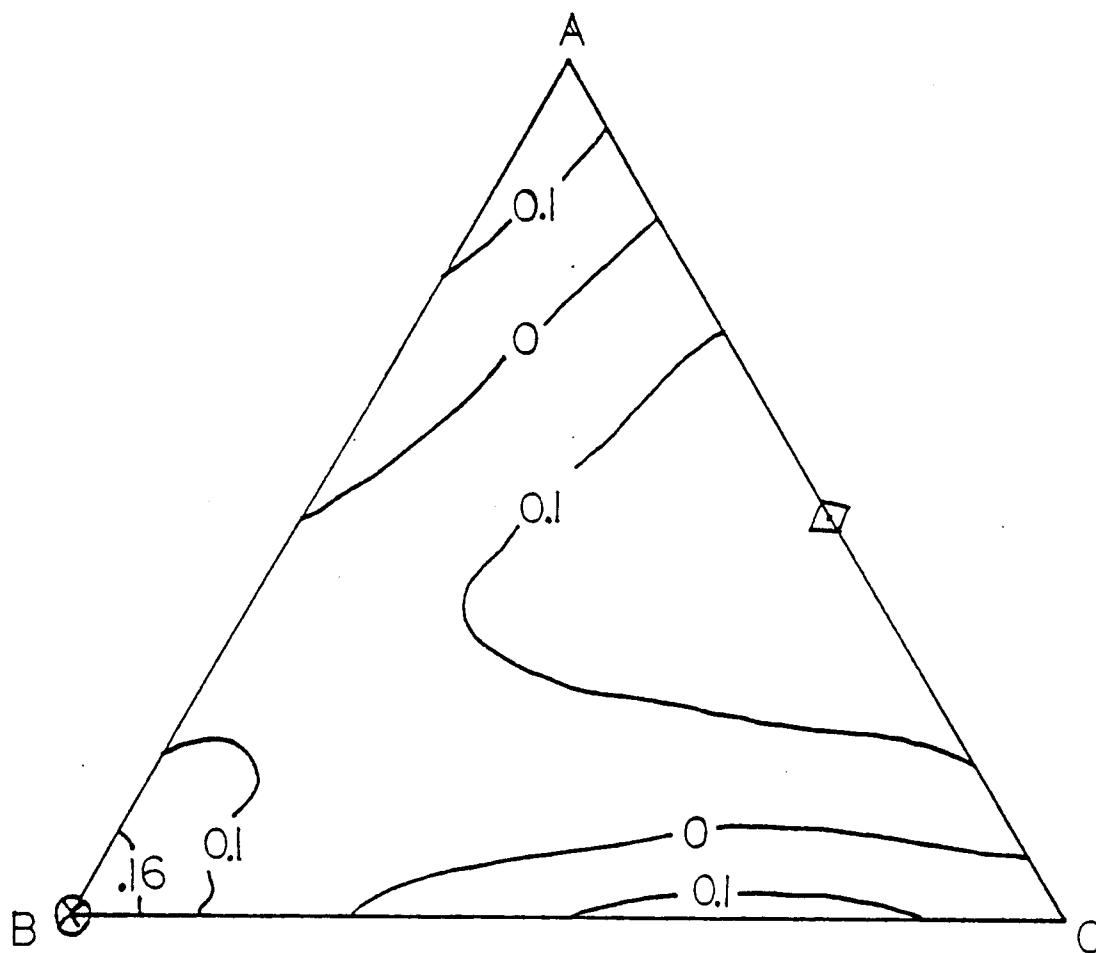


Fig. III.9 Contours for the minimum separation response surface of case 30 in Table 6. (X) result of the WPCO method; (◇) global optimum of the edge.

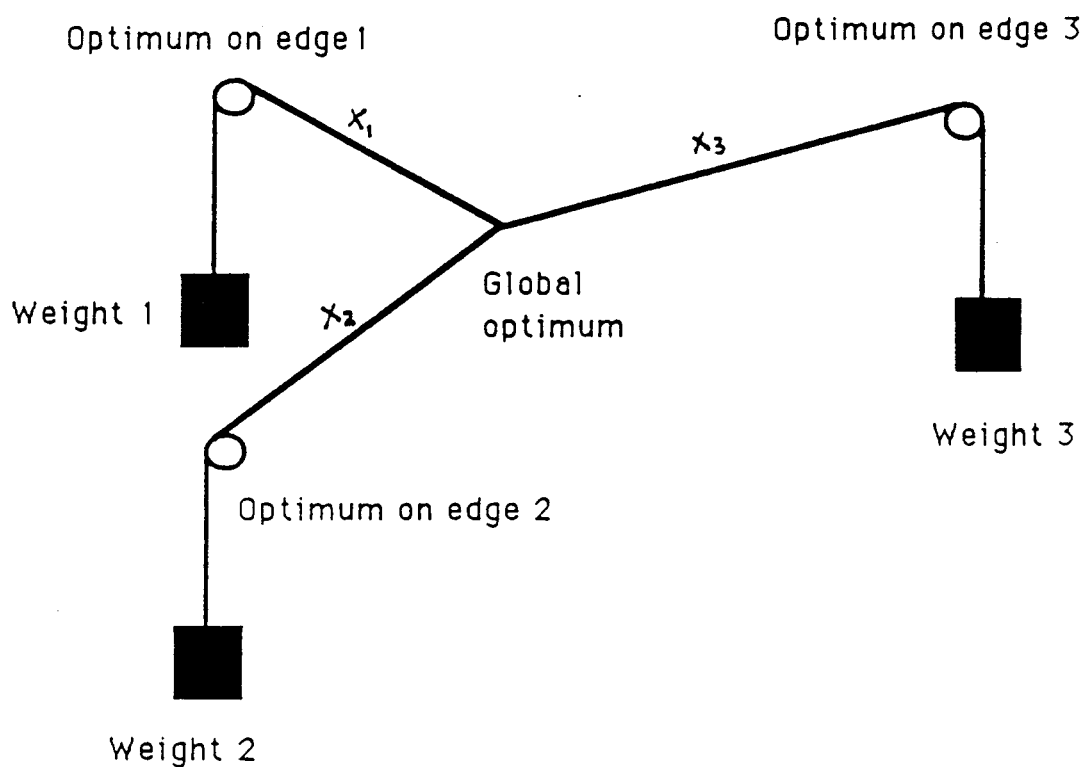


Fig. III.10 An analogue model of WPC. x_1 , x_2 and x_3 are strings that are tied to each other at one end and strung over frictionless pulleys located at the optima on each edge of the solvent triangle. The weights attached to the strings represent the value of $\ln \alpha$ of the worst-separated peak pair.

when the differences among the three weights are not very large, the global optimum of the triangle will settle somewhere in the central area of the triangle rather than along one edge. Therefore, the cases in which the global optimum is on an edge provides a good test of the WPCO method. In all cases that we have tried where the global optimum is on an edge, the WPCO method finds it, and the optima found on the other edges have not confused the issue, even when the optima on those edges are nearly as good as the global optimum. Three of these cases are shown in Fig. III.11 and 12. Therefore, the WPCO method works for cases where the global optimum is on an edge.

Even when the global optimum of the triangle is close to two edges whose optima are individually the second and third best among the optima of three edges, and far from the edge whose optimum is the best among the optima of the three edges, the WPCO method is still not confused and locates the global optimum. Two such cases are shown in Fig. III.13 and 14. In Fig. III.13, the global optimum of the triangle is close to the optima of edges AC and AB. The weight ($\ln \alpha$) of the optimum on AB is 0.063. The weight ($\ln \alpha$) of the optimum on AC is 0.069. In contrast, the weight of the optimum on edge BC is far from the global optimum of the triangle, even though it has the highest weight ($\ln \alpha$), 0.081. The WPCO method is not confused by this situation and locates the global optimum area (0.085)

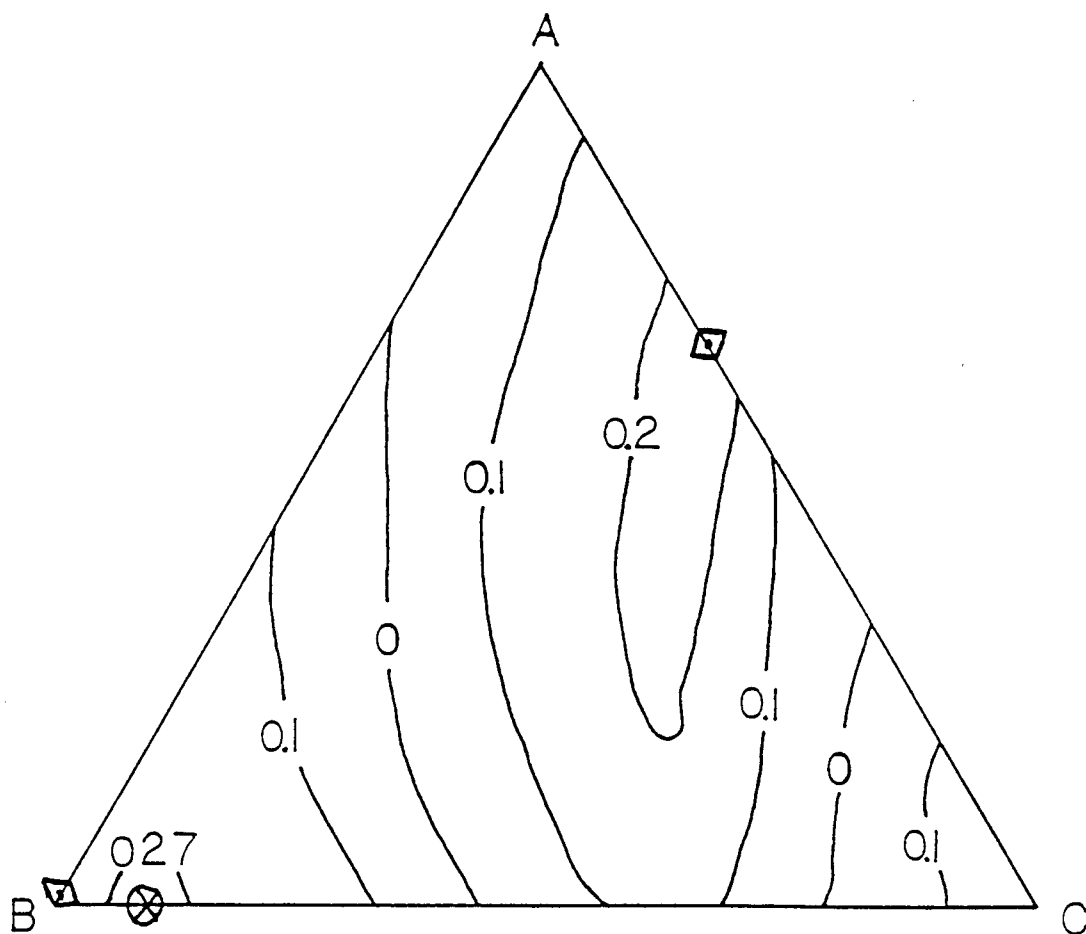


Fig. III.11 Contours for the minimum separation response surface of case 6 in Table 7. (\otimes) result of the WPCO method; (\diamond) global optimum of the edge.

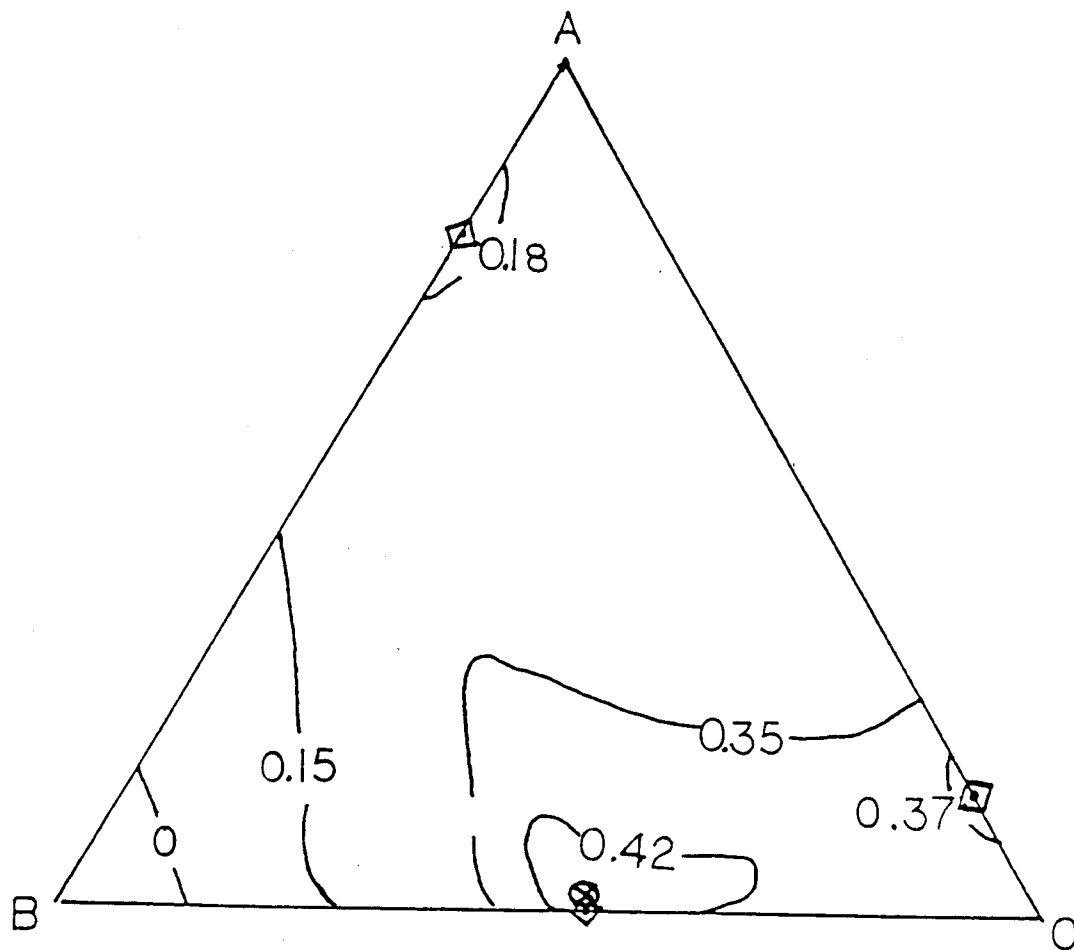


Fig. III.12 Contours for the minimum separation response surface of case 8 in Table 7. (⊗) result of the WPCO method; (◇) global optimum of the edge.

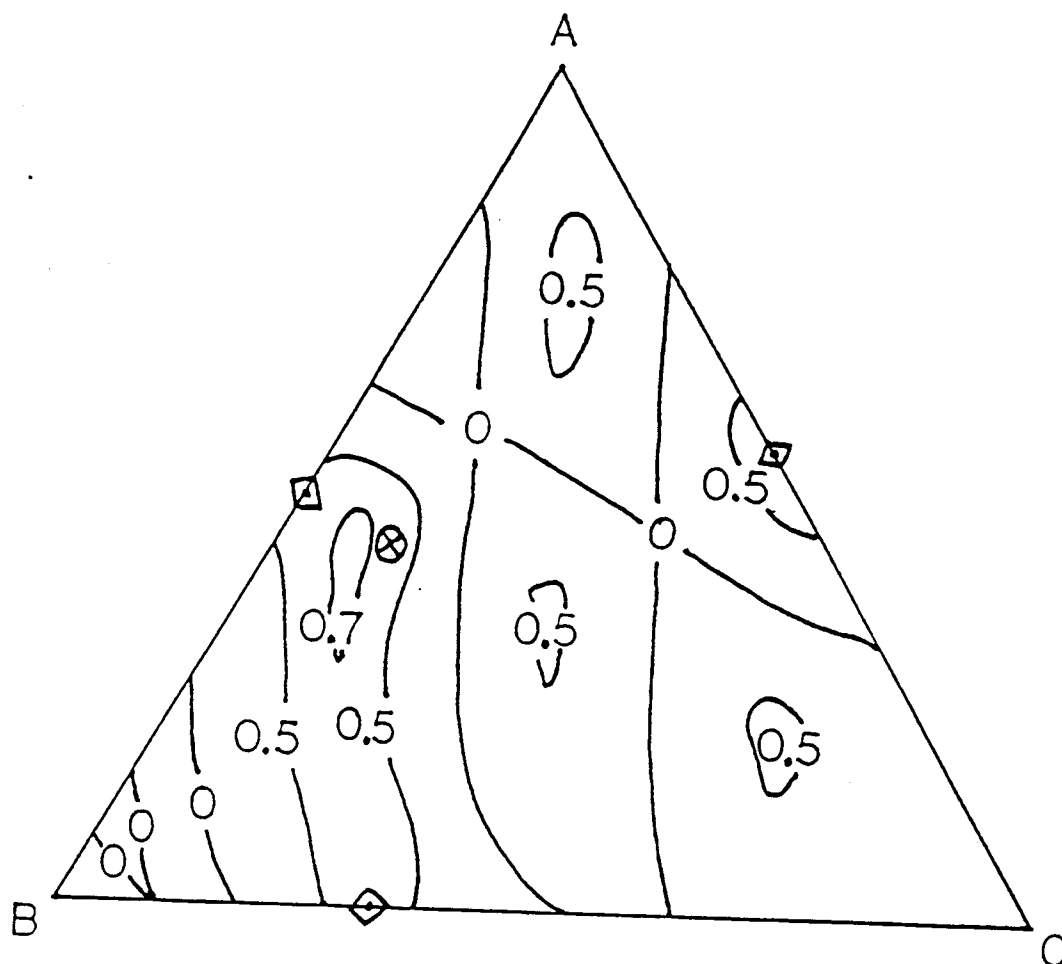


Fig. III.13 Contours for the minimum separation response surface of case in Table 9. (⊗) result of the WPCO method; (◈) global optimum of the edge.

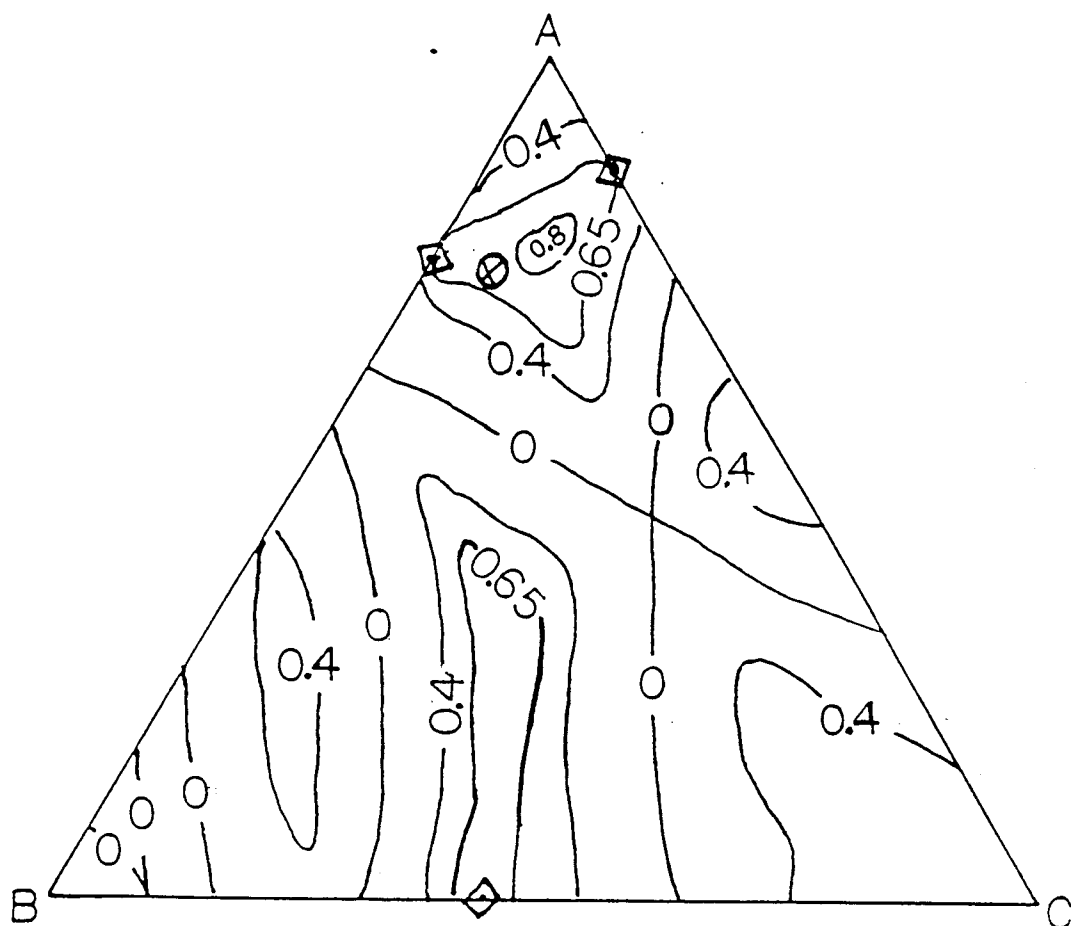


Fig. III.14 Contours for the minimum separation response surface of case 13 in Table 9. (⊗) result of the WPCO method; (◈) global optimum of the edge.

When the overall shapes of two separation response surfaces for two cases are slightly different, but the global optima are at very different locations of the triangle, the WPCO method adjusts accordingly and locates correctly the global optimum in both cases, Fig. III.13 and 15. The surfaces of these two cases are similar because there is only one different solute in these two seven-component cases. However, the global optimum of the case in Fig. III.13 is near corner A, but the global optimum of the case in Fig. III.15 is at corner C in another optimum area. The WPCO method finds the global optimum in these two cases.

Figs. III.16 and III.17 show another example. These two nine-solute cases have only one different solute, and there is only a slight difference between the overall shapes of these two surfaces (see Fig. III.16, Fig. III.17 and Fig. III.18). In Fig. III.18, the window diagrams that are the side views of these two surfaces along the three edges of the solvent triangle are shown. The difference between the corresponding side views along the AB edges and along the BC edges are not noticeable. Along the AC edges, the difference is also small. However, the global optima are in different areas. In Fig. III.17, the global optimum is on an edge, while in Fig. III.16, the global optimum is within the triangle. The WPCO method finds the global optimum area in both cases.

In Fig. III.16, the results of the WPCO method and minimum α plot are in somewhat different locations. This may suggest that although the WPCO method will find the global optimum area, in

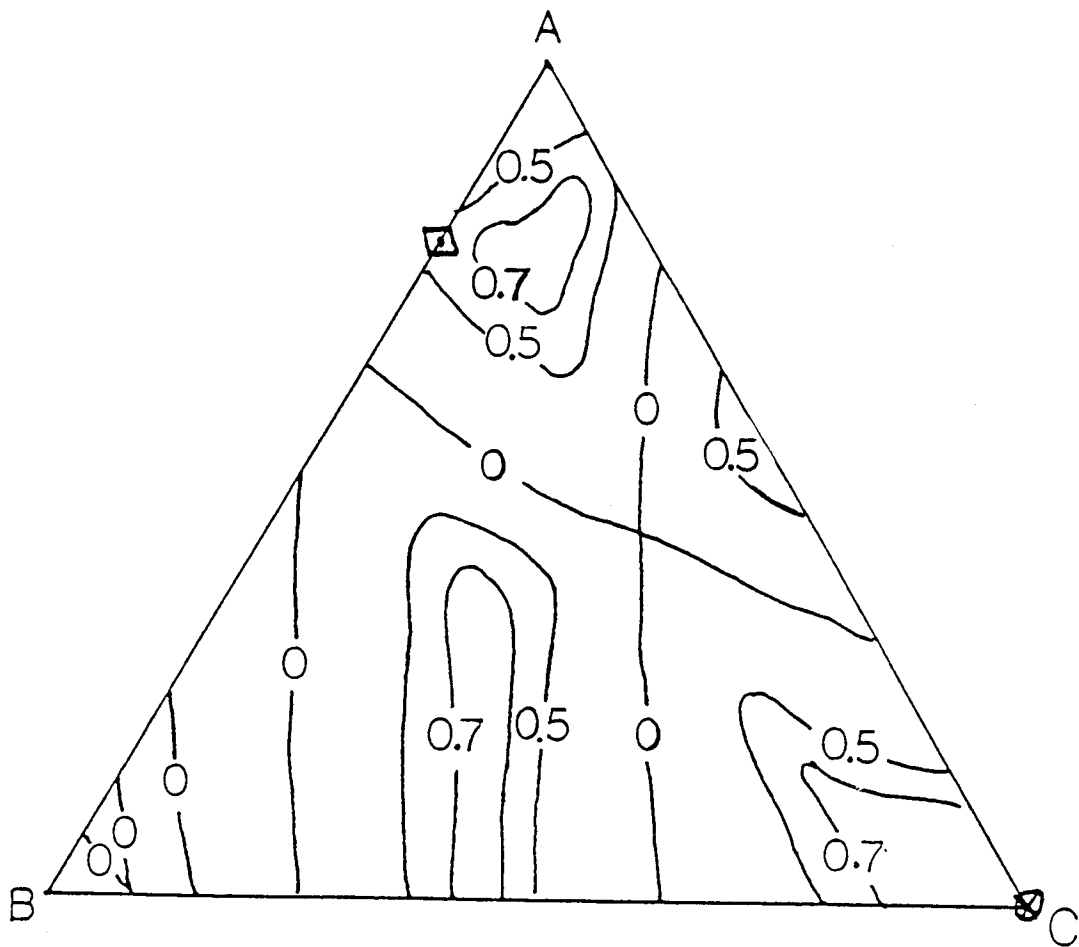


Fig. III.15 Contours for the minimum separation response surface of case 23 in Table 9. (\otimes) result of the WPCO method; (\diamond) global optimum of the edge.

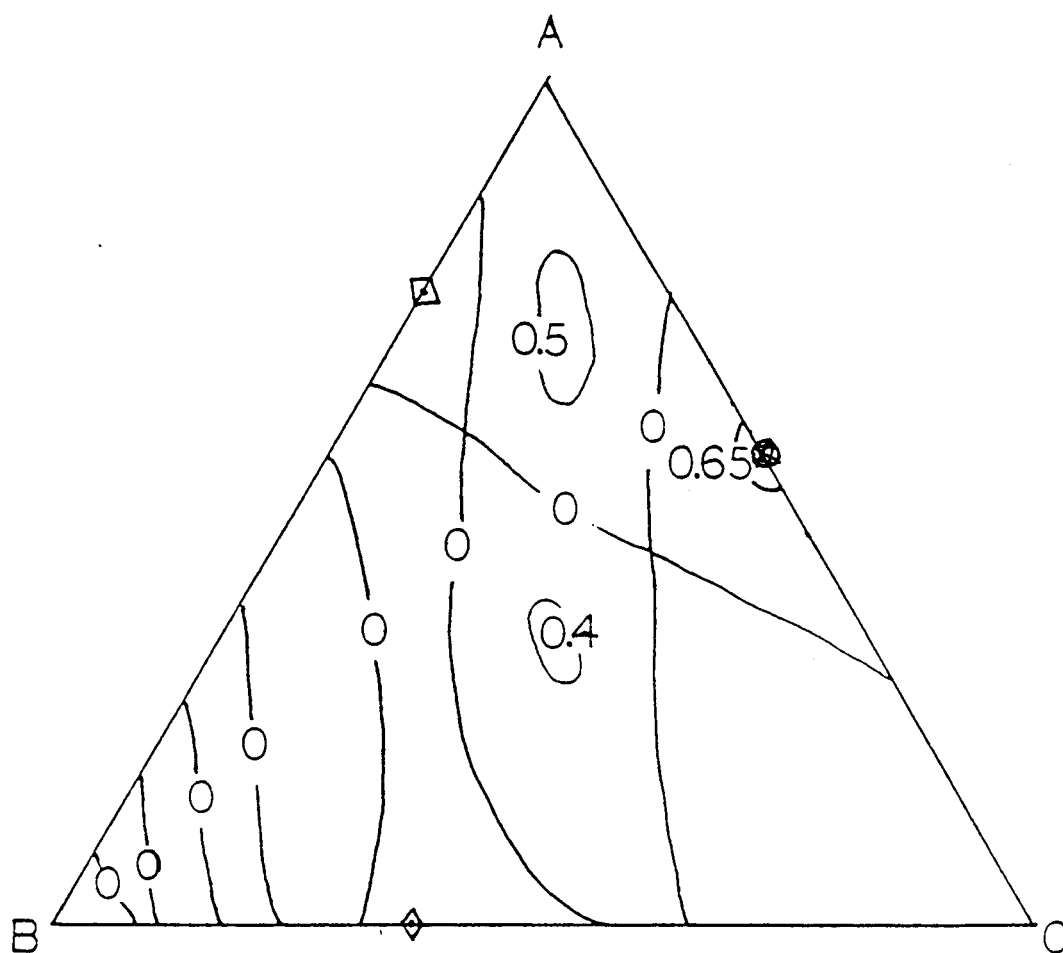


Fig. III.16 Contours for the minimum separation response surface of case 4 in Table 9. (⊗) result of the WPCO method; (◇) global optimum of the edge.

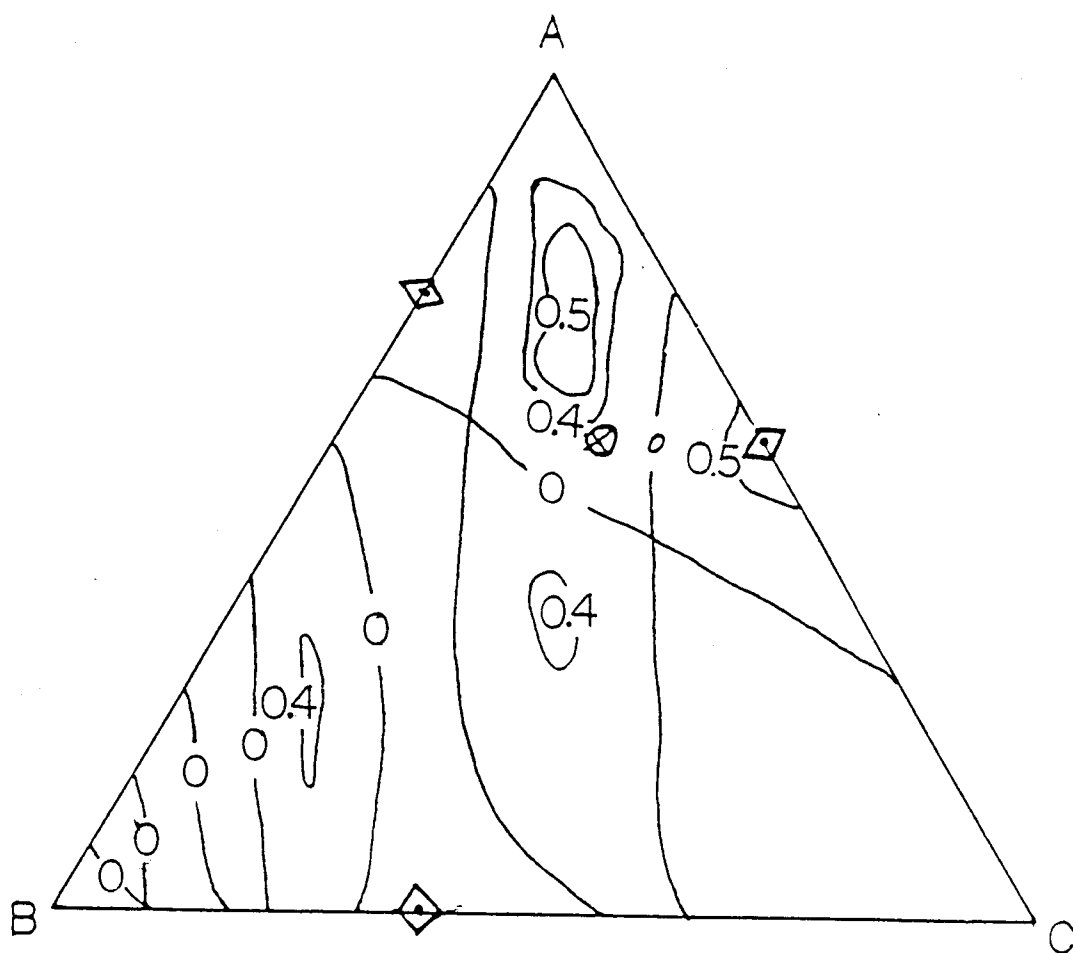


Fig. III.17 Contours for the minimum separation response surface of case 5 in Table 9. (⊗) result of the WPCO method; (◈) global optimum of the edge.

Fig. III.18 Comparison of window diagrams of cases 4 and 5 in Table 9.

(a1) Window diagram of Edge AB in case 4 of Table 9.

(a2) Window diagram of Edge AB in case 5 of Table 9.

(b1) Window diagram of Edge BC in case 4 of Table 9.

(b2) Window diagram of Edge BC in case 5 of Table 9.

(c1) Window diagram of Edge AC in case 4 of Table 9.

(c2) Window diagram of Edge AC in case 5 of Table 9.

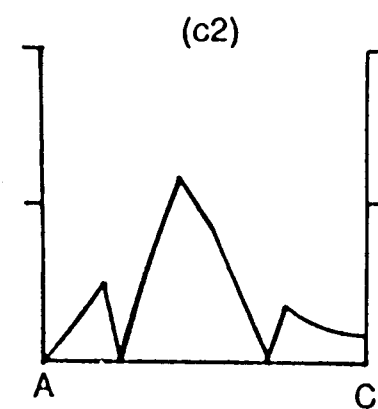
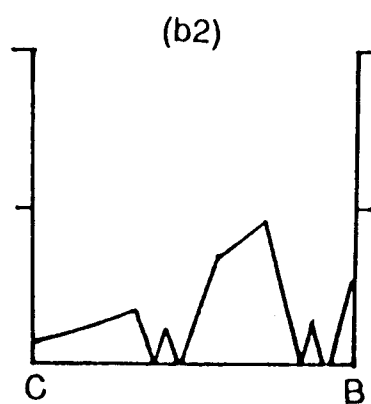
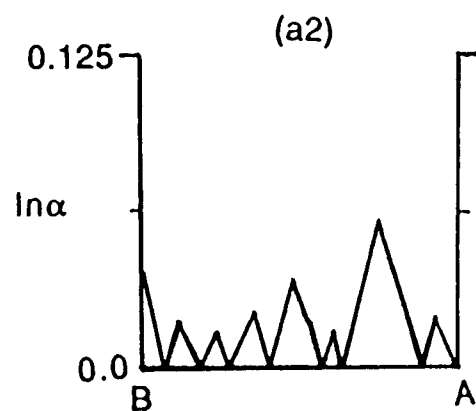
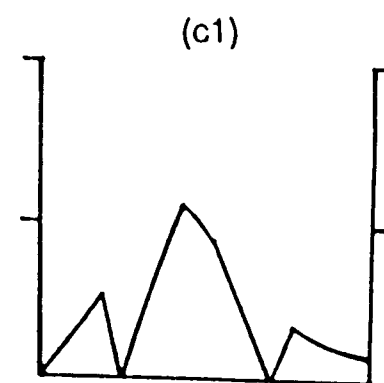
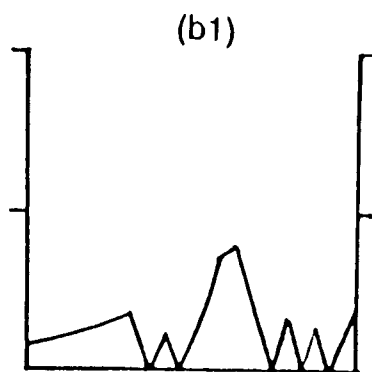
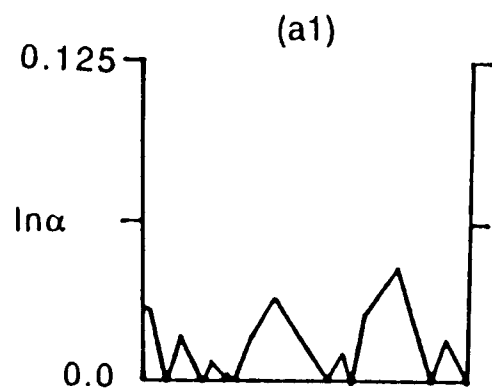


Fig. III.18

some instances there may be a relative large difference between the result of the WPCO method and the real maximum of this optimum area. However, since a fine tuning usually follows an initial optimization method, such as the WPCO and minimum α plots methods, as long as the general area of global optimum is found, the real maximum can be located. A further discussion about fine tuning will appear later in this section.

Since the WPCO method can locate only one composition in the triangle, its performance was tested under the situation in which the heights of several local optima peaks are close to each other. Two such cases are shown in Figs. III.13 and III.14. Under this situation, the WPCO method finds the highest one. Since there may be errors in the capacity factor data, the location of the highest peak in the separation response surface that was built may be in error. However, the WPCO method will locate one of the highest peaks when several high peaks exist in a response surface.

Now, consider the performance of the WPCO method on the most complex cases. Fig. III.19 shows one of the twelve most complex cases that was used to test the WPCO method. The WPCO method predicts an optimum close to the global optimum for all of these twelve cases. Because peak cross-over happens extensively, the optimum areas are so narrow that even using a 2-3% step size in a grid search, it is still possible to miss some optimum areas. In addition, errors in solvent composition and minor differences in the stationary phases of different columns even from the same lot

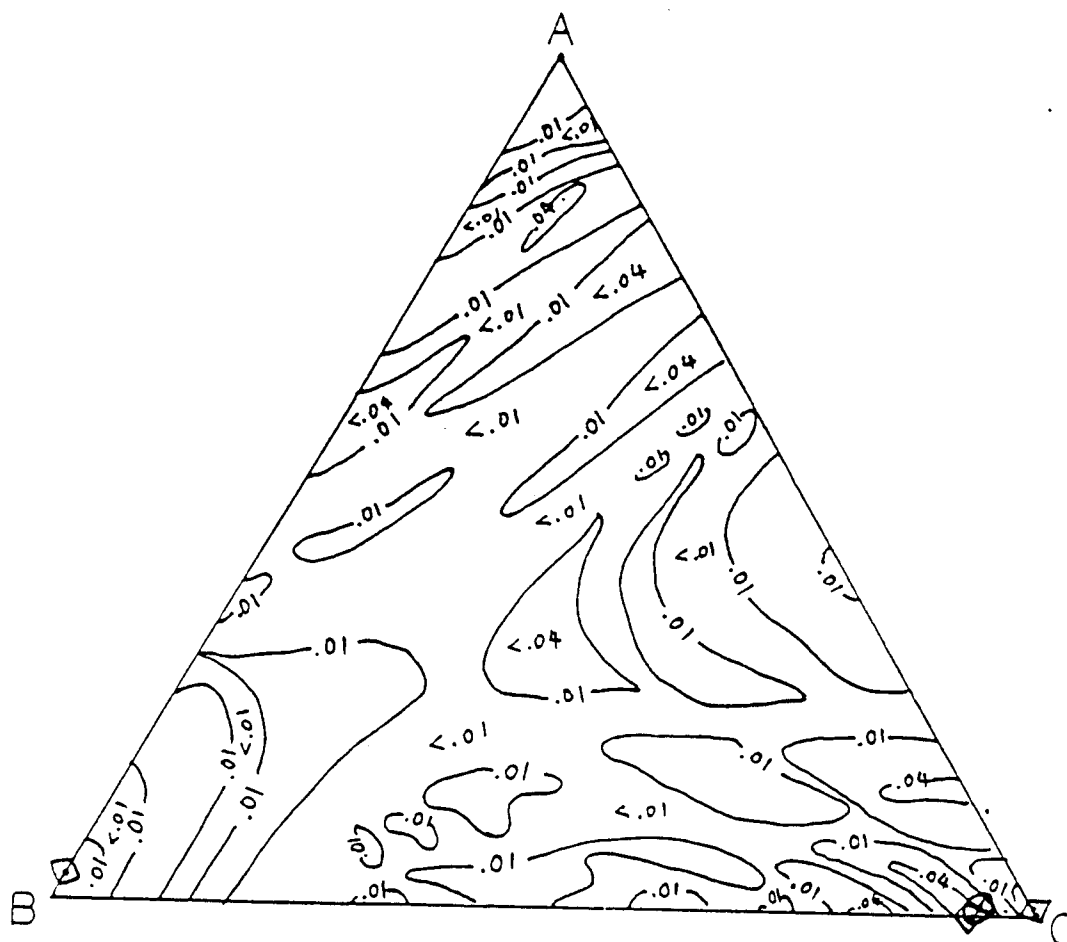


Fig. III.19 Contours for the minimum separation response surface of case 2 in Table 6 (⊗) result of the WPCO method; (◊) global optimum of the edge.

will also affect the separation results to a large extent. In such cases great care is needed in preparing the different mobile phases for a grid search, and in obtaining reproducible separations during routine analyses, once an optimum has been found for a particular column. Whether or not it is practical to optimize the mobile phase in such cases depends upon the needs and resources of the user.

The results of all the test cases are listed in Tables III.10 to 13. In most of these cases, the results of the WPCO and minimum α plot methods are close to each other. Fig. III.20 shows the result of one of these cases. However, there are several cases in which the differences between the results of the two methods are relatively large. Among these cases, case 3 of Table III.12 and cases 4, 5, 9 and 10 in Table III.11 have the largest differences in eluent composition between the results of two methods. However, the difference between the separation capabilities of two results is small (within 5%), because the minimum separation response surfaces of these cases are relatively simple, and the global optimum areas are broad. In all these cases, the results of the WPCO and the minimum α plot methods are near the top of the global optimum peak. Two case which have the largest differences in eluent composition between the results of the two methods are shown in Fig. III.20 and III.21. In Fig. III.20 the results of the two methods are on the crest of the peak. Although,

TABLE III.10

COMPARISON OF THE RESULTS OF THE WPCO AND MINIMUM α PLOT
METHODS FOR THE CASES IN TABLE 6

	Composition (%)*						Difference (%)**
	WPCO			Minimum α plot			
Case***	A	B	C	A	B	C	
1	0.0	0.0	100	0.0	0.0	100	0.0
2	0.0	0.0	100	0.0	0.0	100	0.0
3	0.0	0.0	100	0.0	0.0	100	0.0
4	0.0	0.0	100	0.0	0.0	100	0.0
5	0.0	0.0	100	0.0	0.0	100	0.0
6	0.0	97.6	2.4	0.0	97.6	2.4	0.0
7	0.0	0.0	100	0.0	0.0	2.4	0.0
8	97.6	0.0	2.4	97.6	0.0	2.4	0.0
9	10.1	88.1	1.8	6.0	89.9	4.1	0.6
10	2.2	0.0	97.8	2.2	0.0	97.8	0.0
11	0.0	0.0	100	0.0	0.0	100	0.0
12	0.0	0.0	100	0.0	0.0	100	0.0
13	0.0	6	94	0.0	6	94	0.0
14	0.0	0.0	100	0.0	0.0	100	0.0
15	1.2	14.2	84.6	2.7	9.2	88.1	1.2
16	0.0	4.3	95.7	0.0	4.3	95.7	0.0
17	2.3	6.4	91.3	2.9	5.6	91.5	1.2
18	100	0.0	0.0	100	0.0	0.0	0.0
19	100	0.0	0.0	100	0.0	0.0	0.0
20	5.0	3.2	91.8	7	0.0	93	3.7

(continue to next page)

(Table III.10 continued)

21	0.0	100	0.0	0.0	100	0.0	0.0
22	3.9	0.0	96.1	3.9	0.0	96.1	0.0
23	12.6	0.0	87.4	12.6	0.0	87.4	0.0
24	100	0.0	0.0	100	0.0	0.0	0.0
25	8.5	0.0	81.5	8.5	0.0	81.5	0.0
26	3.9	0.0	96.1	3.9	0.0	96.1	0.0
27	0.0	100.0	0.0	0.0	100.0	0.0	0.0
28	0.0	100.0	0.0	0.0	100.0	0.0	0.0
29	0.0	100.0	0.0	0.0	100.0	0.0	0.0
30	97.6	2.4	0.0	97.6	2.4	0.0	0.0
31	35.2	0.0	64.8	35.2	0.0	64.8	0.0
32	7.8	90.4	1.8	4.6	92.8	2.6	3.7
33	41.0	46.6	12.4	44.9	41.4	13.8	5.5
34	31.2	14.2	54.6	33.1	15.4	51.5	3.2
35	0.0	100.0	0.0	0.0	100.0	0.0	0.0
36	0.0	100.0	0.0	0.0	100.0	0.0	0.0

* A, B, and C are the same as in Table 2.

** Difference is the distance in eluent composition between the results of the two methods.

* * * Case number is the same as in Table 6.

TABLE III.11

COMPARISON OF THE RESULTS OF THE WPCO AND MINIMUM α PLOT METHODS FOR THE CASES IN TABLE 7

Case***	Composition (%)*						Difference (%)**
	WPCO			Minimum α plot			
	A	B	C	A	B	C	
1	31.2	72.8	59.8	31.2	0.0	59.8	0.0
2	31.2	72.8	59.8	31.2	0.0	59.8	0.0
3	31.2	72.8	59.8	31.2	0.0	59.8	0.0
4	16.1	69.2	14.7	12.8	63.8	23.7	9.1
5	30.3	18.3	67.7	20.2	17	62.8	11
6	0.0	91.3	8.7	0.0	91.3	8.7	0.0
7	14.9	0.0	85.1	14.9	0.0	85.1	0.0
8	2.8	0.0	85.1	14.9	0.0	85.1	0.0
9	4.6	74.3	25.7	12.4	72	15.6	10.1
10	18.3	73.5	8.25	25.7	67.9	6.4	7.8
11	4.8	0.0	51.2	48.8	0.0	51.2	0.0
12	2.8	0.0	85.1	14.9	0.0	85.1	0.0

* A, B, and C are the same as in Table 3.

** Difference is the distance in eluent composition between the results of the two methods.

*** Case number is the same as in Table 7.

TABLE III.12

COMPARISON OF THE RESULTS OF THE WPCO AND MINIMUM α PLOT METHODS FOR THE CASES IN TABLE 8

Case***	Composition (%)*						Difference (%)**
	WPCO			Minimum α plot			
	A	B	C	A	B	C	
1	0.0	33	67	0.0	33	67	0.0
2	0.0	34	66	0.0	34	66	0.0
3	0.0	93.7	6.3	37.6	24.8	37.6	59.6****

* A, B, and C are the same as in Table 4.

** Difference is the distance in eluent composition between the results of the two methods.

*** Case number is the same as in Table 8. Case 1 represents cases 1, 2, 3, 6, 8 and 9 of Table 8; Case 2 represents cases 4 and 5 of Table 8; Case 3 represents cases 6 and 7 of Table 8.

**** The results of the two methods are on a crest, the relative difference between $\ln \alpha$ of these two results is 1.9%.

TABLE III.13

COMPARISON OF THE RESULTS OF THE WPCO AND MINIMUM α PLOT METHODS FOR THE CASES IN TABLE 9

Case***	Composition (%)*						Difference (%)**
	WPCO			Minimum α plot			
	A	B	C	A	B	C	
1	56.3	0.0	43.7	56.3	0.0	43.7	0.0
2	56.3	0.0	43.7	56.3	0.0	43.7	0.0
3	56.3	0.0	43.7	56.3	0.0	43.7	0.0
4	57.5	0.0	42.5	57.5	0.0	42.5	0.0
5	56.9	15.6	27.5	76.2	9.1	17	14.7
6	64.6	0.0	35.4	63.8	2.7	33.5	2.7
7	64.8	2.8	30.3	67.9	5.5	26.6	4.1
8	85.4	1.8	12.8	83.6	3.6	12.8	2.7
9	85.4	1.8	12.8	83.6	3.6	12.8	2.7
10	59.1	0.0	40.9	59.1	0.0	40.9	0.0
11	59.5	0.0	40.5	53.7	1.8	44.5	3.6
12	55.1	2.7	42.2	56.7	0.0	43.4	2.7
13	47.7	39.5	12.8	49.5	41.3	9.2	6.4
14	44.5	45.9	9.6	42.2	50.0	7.8	2.7
15	64.2	0.0	35.8	84.2	0.0	35.8	0.0

(continue to the next page)

(Table III.13 continued)

16	0.0	0.0	100.0	0.0	0.0	100.0	0.0
17	56.0	2.7	41.3	56.7	0.0	43.3	2.7
18	57.9	2.7	39.4	58.3	0.0	41.7	2.7
19	57.5	0.0	42.5	57.5	0.0	42.5	0.0
20	55.1	2.7	42.2	56.7	0.0	43.4	2.7
21	85.4	1.8	12.8	83.6	3.6	12.8	2.7
22	0.0	0.0	100.0	0.0	0.0	100.0	0.0
23	74.4	19.2	6.4	77.2	12.8	10.0	6.4
24	71.3	0.0	28.7	71.3	0.0	28.7	0.0
25	65.1	5.5	29.4	69.3	1.8	28.9	4.5
26	88.2	0.0	11.8	88.2	0.0	11.8	0.0
27	89.0	0.0	11.0	89.0	0.0	11.0	0.0
28	89.0	0.0	11.0	89.0	0.0	11.0	0.0

* A, B, and C are the same as in Table 5.

** Difference is the distance in eluent composition between the results of the two methods.

* * * Case number is the same as in Table 9.

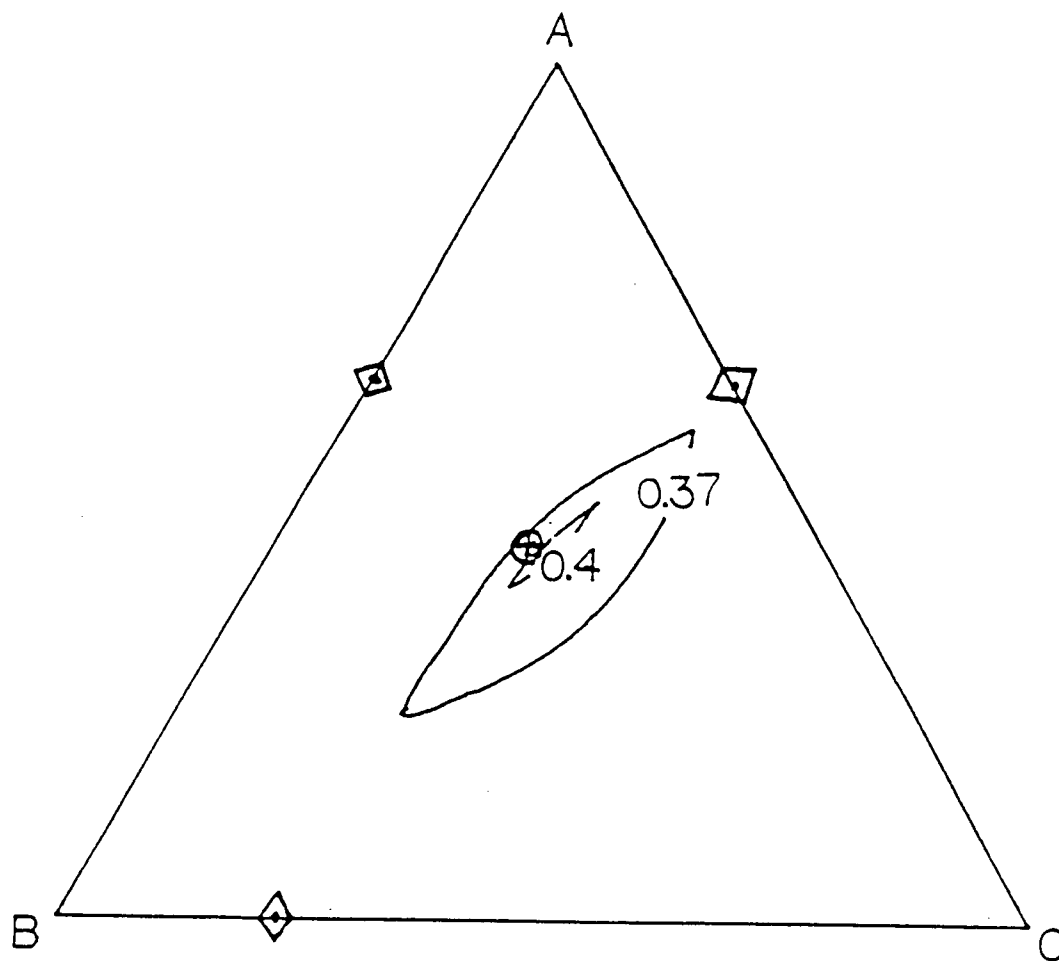


Fig. III.20 Two contours near the peak of the minimum separation response surface of the case in Table 1. (⊗) Prediction of the WPCO method; (◇) global optimum of the edge.

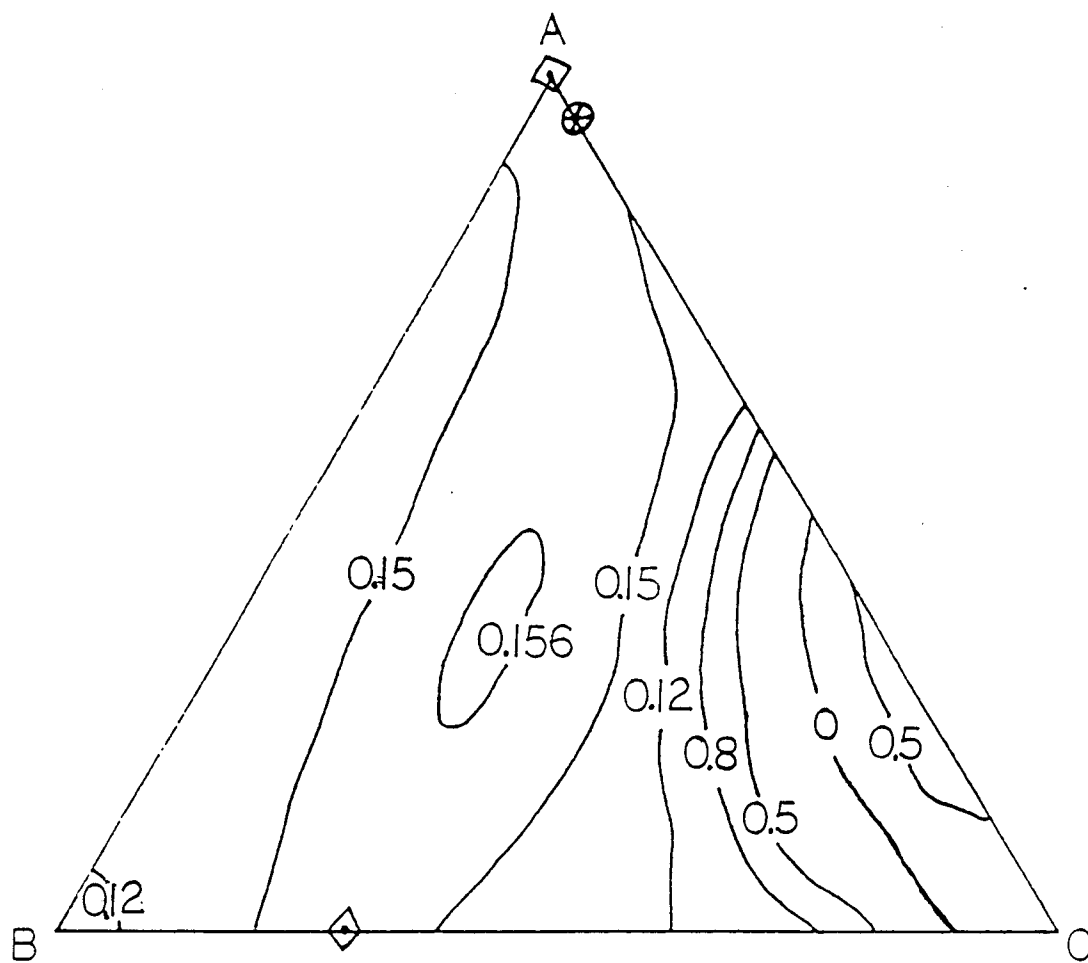


Fig. III.21 Contours for the minimum separation response surface of case in table or cases 7 and 8 of Table 8. (\otimes) result of the WPCO method; (\diamond) global optimum of the edge.

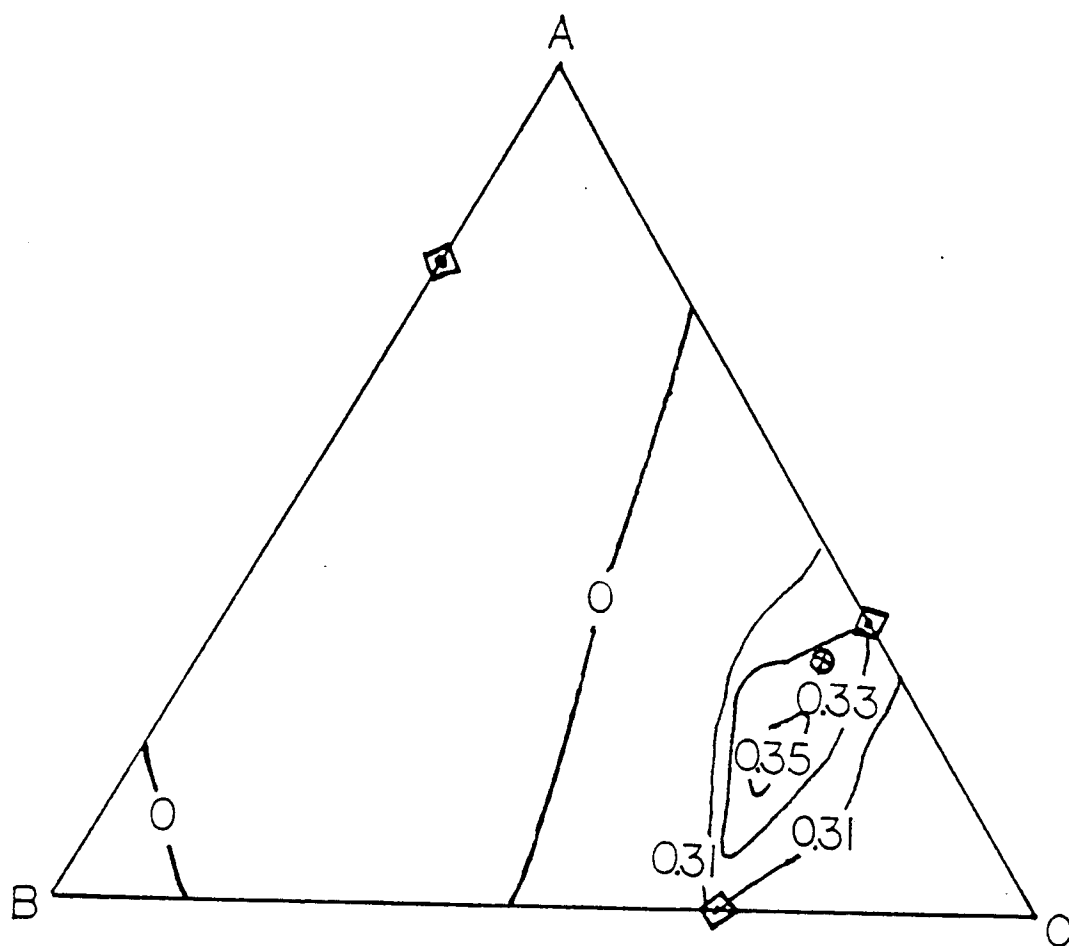


Fig. III.22 Contours for the minimum separation response surface of case 5 in Table 7. (⊗) result of the WPCO method; (◈) global optimum of the edge.

the difference between these two results is 49% in eluent composition, the relative difference of $\ln\alpha$ between these two compositions is only 1.9%. In Fig. III.21 the shape of the top of the global optimum peak is round and flat. The relative difference between the $\ln\alpha$ values is only 5.7%.

The advantage of using the WPCO method can be seen in the large reduction in the number of experiments that occurs compared to a grid search. For the simplest cases which are shown in Figs. 9, 11, 12, 23 and 24, a 10% step size is necessary for a grid search to locate all the optima in a response surface. After all the optima are located, then the global optimum can be determined. This takes 66 experiments to search the entire triangle to ensure that the global optimum is located. On the other hand, the WPCO method only needs to search the three edges to find the optimum composition on each edge and the selectivity factor of the worst separated peak pair(s) at this composition. With a 10% step size, it takes only 30 experiments to search three edges. If we assume that the number of experiments needed for fine tuning following the WPCO or the grid search methods is the same, then the WPCO method saves 36 experiments.

For more complex cases, such as the cases in Figs. III.13 to 18, a 5% step size is necessary for the grid search method to find the global optimum of the triangle. This takes 231 experiments to search the entire triangle. For the WPCO method, it takes 60 experiments to search three edges, saving 171 experiments.

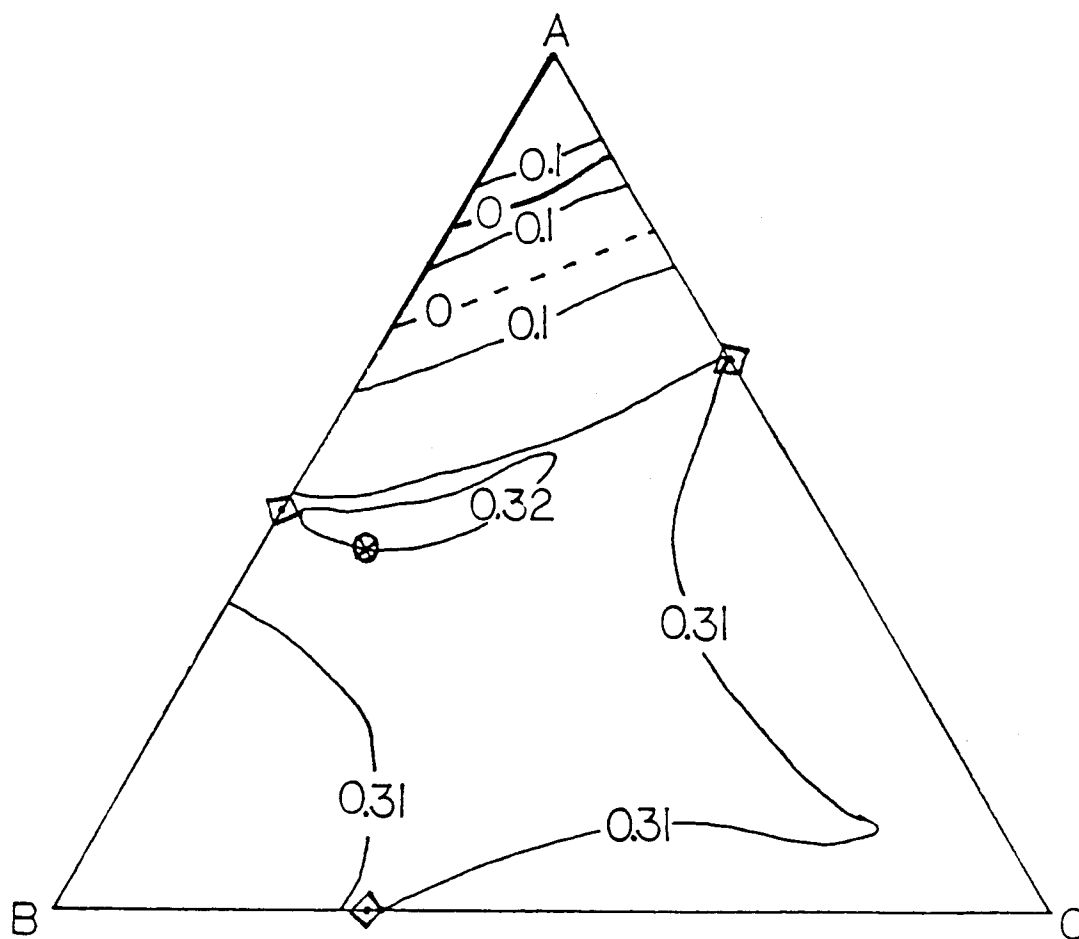


Fig. III.23 Contours for the minimum separation response surface of case 33 in Table 6. (\otimes) result of the WPCO method; (\diamond) global optimum of the edge.

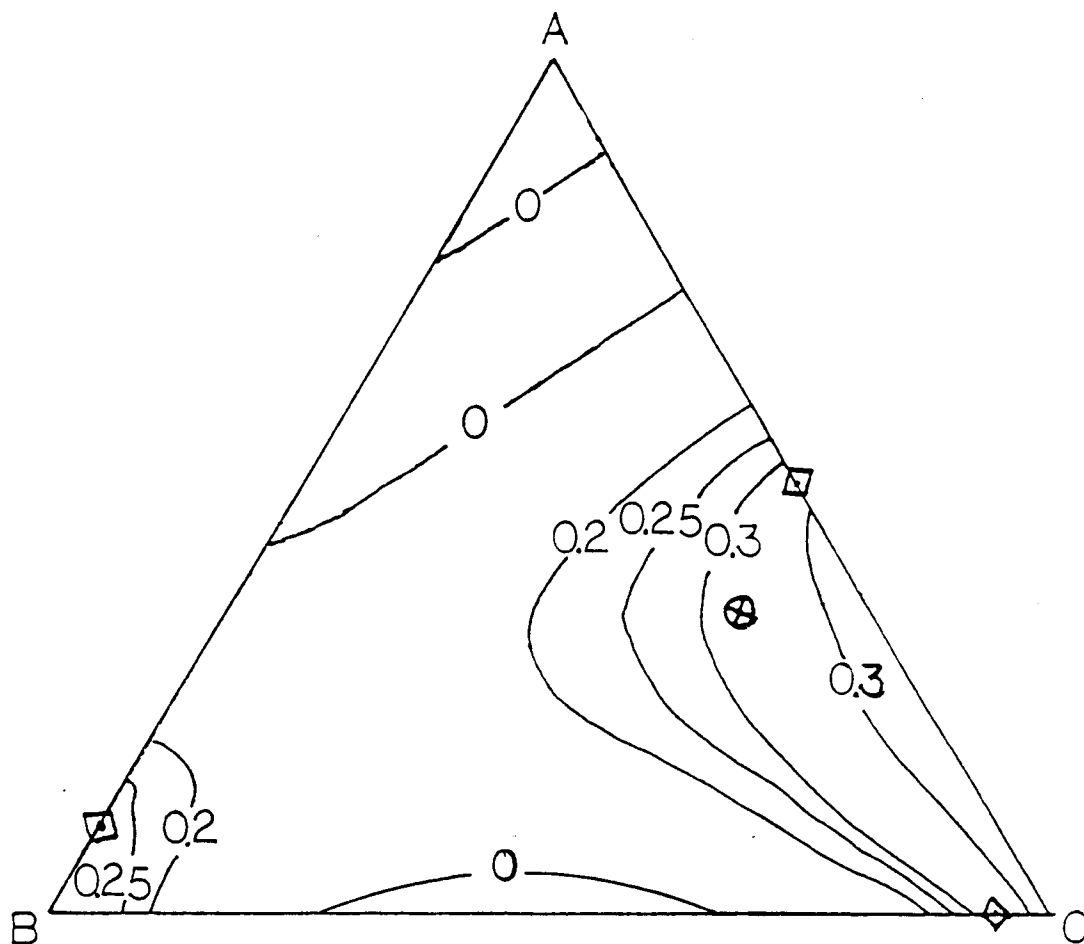


Fig. III.24 Contours for the minimum separation response surface of case 34 in Table 6. (⊗) result of the WPCO method; (◈) global optimum of the edge.

However, the WPCO method may need more fine tuning experiments than the grid search method. When a 5% step size is used for the grid search method, the largest possible error is 2.9% in composition because the real global optimum may be located at the middle of the triangle formed by three adjacent points on the grid. For the grid search method, a few experiments (about two to five) may be needed for fine tuning. For the WPCO method, in some cases, the difference between the composition located by the WPCO method and the real global optimum may be larger than 2.9%. It is assumed that WPCO's fine tuning process takes 10 more experiments than that of the grid search, then the WPCO method saves 161 experiments when a 5% step size is used.

Our cases show that a 10% step size search is only suitable for simple cases. For a medium level case in which separation response surface consists of about six optimum areas, a 5% step size is necessary. This means that the WPCO method usually can save 161 experiments compared to the grid search method. It is obvious that when a global optimum is within a triangle, the WPCO method saves 161 experiments. However, when the global optimum is on an edge or corner, the WPCO method still saves 161 experiments because for the grid search method, only after the entire triangle has been searched, can the global optimum be determined.

Although, with a known sample, the minimum α plots method requires experiments with 7 different compositions (one

at each corner, each edge and one in the center of the triangle), the WPCO method needs experiments at only 6 compositions because the composition in the center of the solvent triangle is omitted. However, when the fine tuning process following the WPCO method needs more experiments than that of the minimum α plot method, the WPCO method may have little advantage over the minimum α plot method for a known sample. On the other hand, for an unknown sample, the WPCO method usually can save over 150 experiments.

For mobile phase optimization, one experiment (including the time needed for equilibration of the column) usually takes about 1.5 hours when a 25x0.46cm column is used. This means the WPCO method can save over 225 working hours by eliminating over 150 experiments. Stated differently, the WPCO method reduces the experimental work by 75%. In addition, the column will degrade gradually during the optimization experiments. Since the grid search method needs many experiments, at the end of a grid search the column may have degraded significantly and even reached the end of its useful life. Since the properties of a column are different at the beginning of the grid search and at the end of the grid search, the result of the grid search may be less reliable than the WPCO method. Moreover, a new column may be needed to replace the old column near the end of a grid search, or soon after the grid search, to carry out the routine separation work. This means that more fine tuning experiments need to be

carried out for the grid search. Overall, the WPCO method has a big advantage over the grid search for the optimization of the mobile phase composition for unknown samples.

Conclusion

The WPCO method can be used for optimizing normal-phase and reversed-phase LC compositions. This method is suitable for both known and unknown samples. Results show that this method can accommodate peak cross-over and locate the global optimum of the mobile phase composition. This method is especially useful for unknown samples. Compared with the grid-search method, experimental work can be reduced substantially.

References

- 1 J. C. Berridge, Techniques for Automated Optimization of HPLC Separations, Wiley, New York, 1985.
- 2 P. J. Schoenmakers, Optimization of Chromatographic Selectivity, Elsevier, Amsterdam, 1986.
- 3 L. R. Snyder, J. L. Glajch and J. J. Kirkland, Practical HPLC Method Development, Wiley, New York, 1988.
- 4 A.G. Wright, A.F. Fell and J.C. Berridge, Chromatographia, 24(1987)533.
- 5 PESOS: Perkin-Elmer Solvent Optimisation System.
- 6 Wspendley, G.R.Hext and F.R. Himsworth, Technometrics,
- 7 J. A. Nelder and R.Mead, Comput. J. , 7(1965)308.
- 8 J. C. Berridge, J. Chromatogr., 244(1982)1.
- 9 R. J. Laub, J. H. Purnell, and P. S. Williams, J. Chromatogr., 134(1977)246.
- 10 R. J. Laub, and J. H. Purnell, Anal. Chem. 48(1976)1720.
- 11 R. J. Laub, and J. H. Purnell, D. M. Summers and P. S. Williams, J. Chromatogr., 199(1980)57.
- 12 J. L. Glajch, J. J. Kirkland, K. M. Squire and J. M. Minor J. Chromatogr., 199(1980)57.
- 13 J. W. Weyland, C. H. P. Bruins and D. A. Doornbos, J. Chromatogr. Sci., 22(1984)31.
- 14 R. D. Snee, Chemtech, 9(1979)702.
- 15 L. R. Snyder, J. L. Glajch and J. J. Kirkland, Practical HPLC Method Development, Wiley, New York, 1988.

- 16 P. J. Schoenmakers, A. C. J. H. Drouen, H. A. H. Billiet and L. de Galan, *Chromatographia*, 15(1982)48.
- 17 P. J. Schoenmakers and T. Blaffert, *J. Chromatogr.*, 384(1987)117.
- 18 J. H. Hildetrand, J.M. Prausnitz and R.L. Scott, *Regular and Related Solutions*, Van Nostrand Reinhold Company, (1977)3-4
- 19 P.J. Schoenmakers, H.A.H. Billiet and L. de Galan, *Chromatographia*, 15(1982)205-214.
- 20 P.J. Schoenmakers, H.A.H. Billiet and L. de Galan, *Chromatographia*,15(1982)205.
- 21 G. M. Landers and J. A. Olson, *J. Chromatogr.*, 291(1984)51.
- 22 J. L. Glajch, J. J. Kirkland and L. R. Snyder, *J. Chromatogr.*, 238(1982)269.
- 23 S. J. Costanzo, *J. Chromatogr. Sci.*, 24(1986).
- 24 J. L. Glajch, J. J. Kirkland, K. M. Squire and J. M. Minor, *J. Chromatogr.*, 199(1980)57.
- 25 G. D'agostino, F. Mitchell, L.Castagnetta, and M. J. O'hare, *J. Chromatogr.*, 305(1984)13-26.
- 26 H. Scheffe, *J. Royal Stat. Soc. B*, 20(1958)344.
- 27 J. W. Gorman and J. E. Hinman, *Technometrics*, 4(1962)463.
- 28 R. D. Snee, *Chemtech*, 9(1979)702.
- 29 J. L. Glajch, J. J. Kirkland and L. R. Snyder, *J Chromatogr.*, 238(1982)269.

- 30 L. R. Snyder, J. L. Glajch, and J. J. Kirkland, *J. Chromatogr.*, 218(1981)299.
- 31 P. E. Antle, *Chromatographia*, 15(1982)277.
- 32 J. L. Glajch, J. C. Gluckman, J. G. Charikofsky, J. M. Minor, and J. J. Kirkland, *J. Chromatogr.*, 318(1985)25.
- 33 A. G. Wright, A. F. Fell and J. C. Berridge, *J. Chromatogr.*, 458(1988)335.
- 34 R.J. Laub and J. H. Purnell. *J. Chromatogr.*, 161(1978)49.
- 35 J. W. Weyland, C. H. P. Bruins and D. A. Doornbos, *J. Chromatogr. Sci.*, 22(1984)31.
- 36 D.J. White. *Operational Research*, Wiley, New York, 1985, p.85.

IV. A Simplified Weighted Pattern Comparison Optimization Method for HPLC

by

Xiao Chen and Edward H. Piepmeier*

Department of Chemistry

Oregon State University

Corvallis, OR 97331

and

A. Morrie Craig

College of Veterinary Medicine

Oregon State University

Corvallis, OR 97331

For submission to Journal of Chromatography

Abstract

The separation factor and resolution are approximately proportional to the logarithm of the selectivity factor in the capacity factor range normally used. Based on this, the logarithm of the selectivity factors in the original WPCO method are replaced by the separation factor or the resolution to further reduce the experimental work and avoid the error introduced in the measurement of the dead column volume. The simplified WPCO method has been tested in the optimization of normal-phase and reversed-phase chromatography separations. Results demonstrate that the simplified and original WPCO methods are nearly identical when the capacity factors of the solutes of the worst-separated peak pairs are greater than 5. When the capacity factors are less than 5, the simplified WPCO method is satisfactory in less complex or less critical applications.

Introduction

The weighted pattern comparison optimization (WPCO) method¹ is a recently developed general method for the optimization of HPLC mobile phases. The WPCO method can obtain a result which is similar to those obtained by the minimum α plots², overlapping resolution mapping³ and step-search design⁴ methods, and do so with substantially less experimental work. For the optimization of unknown samples, the WPCO method can reduce the experimental work by about 75% and find the global rather than just a local optimal mobile phase composition. In this work, a simplified WPCO method is proposed. In certain situations, the experimental work can be further reduced by using the simplified WPCO method.

The logarithm of the selectivity factor is used in the WPCO method. The selectivity factor is simply the ratio of the two capacity factors of the two peaks under consideration. To obtain the precise value of the capacity factor, it is necessary to measure the column void volume (or column dead time, t_0) and the retention volume (or retention time, t_r) of the solute. However, the precise column void volume is difficult to obtain^{5,6}.

To measure the column dead time, a solute which is not sorbed by the column is used. However, a solute which is completely not retained by the column may not exist. Moreover, if

this kind of solute exists, it may not be able to be used because of the experimental constraints. For example, the solutes may not desolve in the mobile phase, or the solutes may not be compatible with the detector.

Several kinds of interactions between a solute and a column exist. These interactions are the interaction between the solute and the sorbed mobile phase solvents, underivatized surface silanol groups of the stationary phase, and the surface of the stationary phase^{7,8,9,10}. Because of these interactions, a solute is likely to have at least some minor retention on the column. Therefore, a column void volume calculated from chromatographic measurements will be larger than the true value. Consequently, if other parameters which reflect the separation results can be used in the WPCO method to replace the selectivity factor, the experimental work can be further reduced. Moreover, the error caused by the inaccurate column dead volume can also be avoided.

The resolution is a parameter which reflects the separation result. Moreover, the resolution can be calculated without knowing the column void volume. In practice, the resolution is usually calculated from the distance between two peaks, and the peak base line widths or half-height widths. However, when the separation of a sample is not good enough, the peak base line and even the half-height width will be hard to measure.

A alternative parameter, the separation factor, has been proposed by Jones and Wellington¹¹ to overcome the difficulties

discussed above. The separation factor reflects the separation condition of two solutes. Moreover, the separation factor is proportional to the resolution. On the other hand, the only measurement required for the calculation of the separation factor is the measurement of the retention volumes of the two solutes.

In this work, the WPCO method is simplified by replacing the logarithm of the selectivity factor with the separation factor or the resolution in order to further reduce the experimental work. This method will be called the simplified WPCO method. In this work, the limitations of the simplified WPCO method are also discussed.

Theory

This section considers replacing the logarithm of the selectivity factor with other parameters which reflect the separation results. A simplified WPCO method is proposed, and its limitations are discussed.

The original WPCO method uses eqn. 1 to find the global optimum of the entire ternary or pseudo-quaternary mobile phase system¹²

$$\text{SPDF} = \ln\alpha_L D_{L,O} + \ln\alpha_M D_{M,O} + \ln\alpha_N D_{N,O} \quad (1)$$

where α is the selectivity factor of the worst separated peak pair(s) of the global optimum of the corresponding triangle edge, D is the distance between the global optimum of an edge and the global optimum of the entire solvent system. The subscripts, L, M and N refer to the global optimal composition points of the edges. The subscript, O, refers to the global optimal composition point of the entire solvent system. SPDF is the separation pattern difference function.

One of the methods of solving eqn. 1 for the coordinates of the global optimum of the entire solvent system is simply calculating the values of SPDF of all the possible compositions of the entire solvent system (scan the whole triangle). The

composition which has the smallest SPDF is the global optimum.

Multiplying both sides of eqn. 1 by a constant, A, gives

$$A(\text{SPDF}) = A(\ln\alpha_L)D_{L,O} + A(\ln\alpha_M)D_{M,O} + A(\ln\alpha_N)D_{N,O} \quad (2)$$

The composition point which has the smallest value of $A(\text{SPDF})$ will be the same point which has the smallest value of SPDF in eqn. 1. Therefore, for the purpose of locating the point of optimal composition, any other parameters which reflect separation results and are proportional to the logarithm of the selectivity factor can be used to replace the logarithm of the selectivity factor in eqn. 1.

The resolution, R_s , and the separation parameter¹, S , are two parameters that reflect the separation result. In chromatography, the resolution, R_s , is used to define the separation of two solutes A and B with elution volumes V_A and V_B ¹³

$$R_s = (V_B - V_A)/(w_A + w_B) \quad (3)$$

where w is the base line width of the peak of a solute.

The separation factor is derived from R_s . Accordingly to plate theory¹⁴.

$$w = 2N^{1/2}(v_m + K_A v_s) \quad (4)$$

where N is the number of theoretical plates v_m and v_s are the volumes per plate of the mobile and stationary phase respectively, and K_A and K_B are the partition coefficients.

Since

$$V_A = N(v_m + K_A v_s) \quad (5)$$

$$V_B = N(v_m + K_B v_s) \quad (6)$$

Therefore, eqn. 3 can be rewritten as

$$R_s = N^{1/2}(V_B - V_A) / 2(V_A + V_B) \quad (7)$$

Rearranging eqn. 7 gives

$$2R_s/N^{1/2} = (V_B - V_A)/(V_A + V_B) \quad (8)$$

The right hand side of eqn. 8 is defined as the separation parameter, S . It can be seen that the separation parameter is directly proportional to the resolution, R_s . The proportional factor is $2/N^{1/2}$. That is, if the value of the separation parameter is used as the criterion for the optimization of chromatographic separation, the largest S corresponds to the best separation result.

For the purpose of expressing the result of the chromatographic separation, the resolution is better than the selectivity factor because resolution involves the peak width; whereas the selectivity factor does not. Since the separation parameter is proportional to the resolution, the separation parameter can be viewed as involving the peak width. Therefore, the separation parameter is a better separation criterion than the selectivity factor.

The separation parameter can be evaluated most easily because it requires only the measurement of the retention volume (or retention time) of peaks only. On the other hand, the resolution requires the measurement of retention volumes and peak widths (or half peak widths). The peak width and half peak width cannot always be measured accurately. The selectivity factor requires the measurement of the retention volume and the column dead time. As discussed in the introduction, the measurement of the dead volume is not a simple matter. Consequently, if the separation parameter can be used in eqn. 1 instead of the logarithm of the selectivity factor, the experimental work can be further reduced.

In Fig. IV.1, the ratio of the resolution to $\ln\alpha$ for various capacity factors, k' are plotted against the selectivity factor.

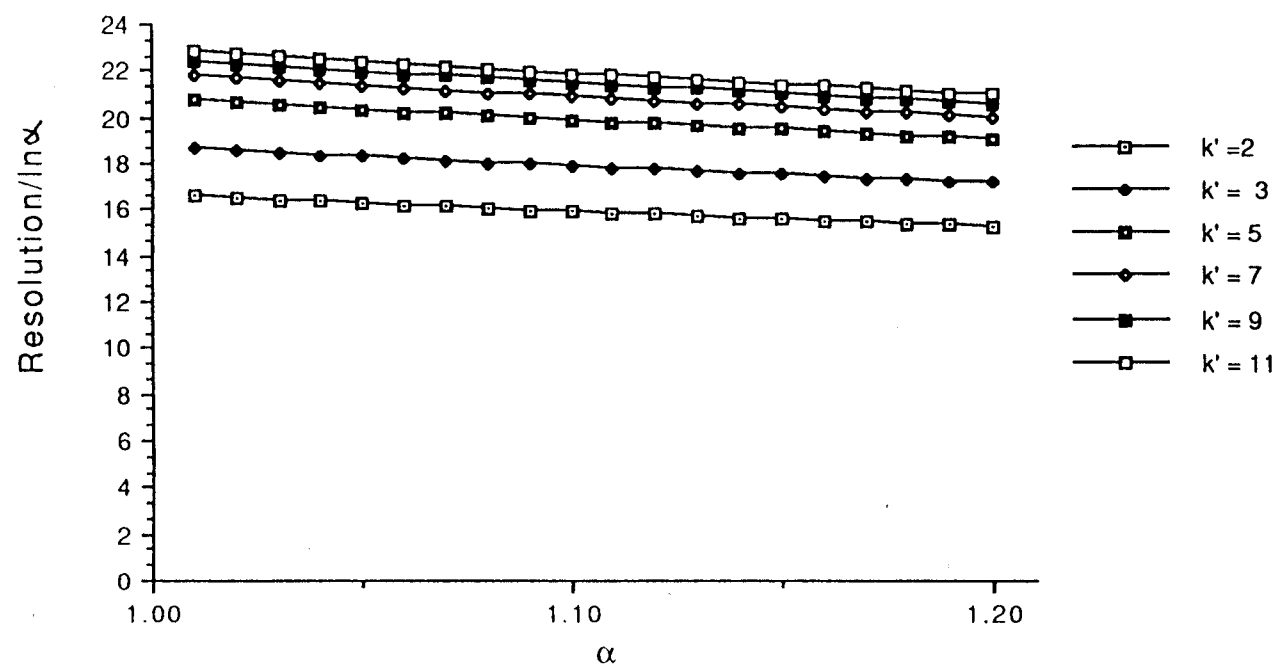


Figure IV.1a The ratio of resolution to $\ln\alpha$ vs. selectivity factor (1 to 1.2), α , for different catalytic factors, k' .

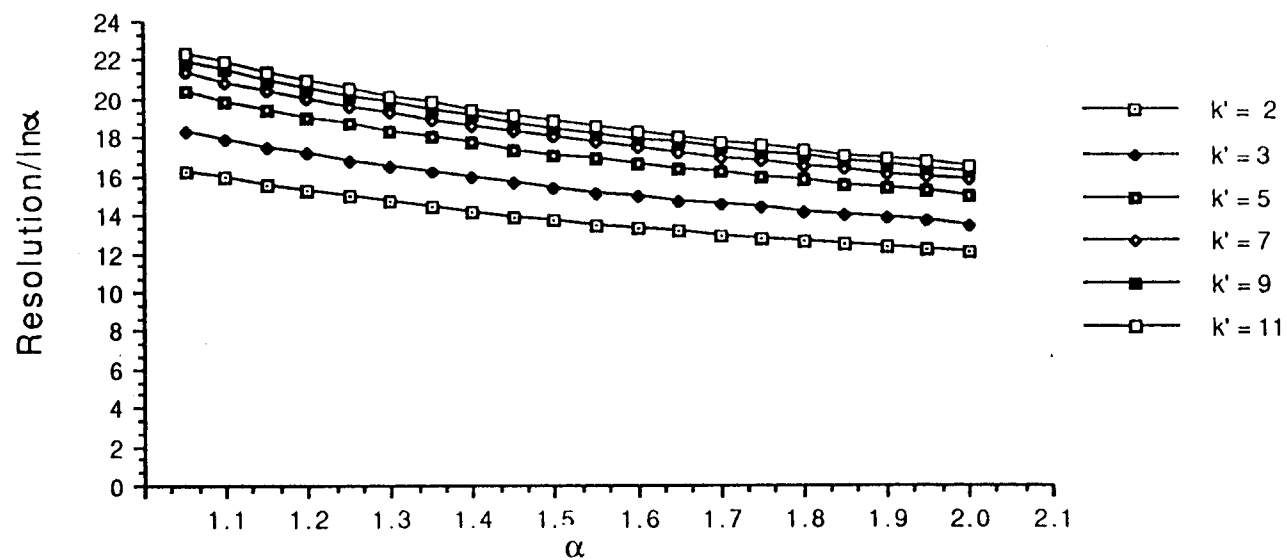


Figure IV.1b The ratio of resolution to $\ln\alpha$ vs. selectivity factor (1 to 2), α , for different capacity factors, k' .

Since the separation factor is proportional to the resolution, in the following discussion, the separation factor curve will be treated as equivalent to the resolution curves.

For a column with 10,000 theoretical plates, a selectivity factor of 1.2 is equivalent to resolution of 2.7 for $k' = 2$ and 3.8 for $k' = 11$. Since these are larger (better) than a resolution of 1.5 that is considered a good separation, a selectivity factor of 1.2 is a reasonable upper limit for this study. Ideally, if the curves in Fig. IV.1 were perfectly horizontal and superimposed upon each other, then this would indicate that resolution was directly proportional to $\ln\alpha$ and eqn. 1 would predict the same optimal composition regardless of whether resolution or $\ln\alpha$ were used in this equation. Since the curves are not quite horizontal, and are not superimposed, the predictions will be somewhat different. When the capacity factor is greater than 5, the curves of the ratio of the resolution to $\ln\alpha$ vs. selectivity factor are close to each other. This suggests that using the resolution in eqn. 1 instead of $\ln\alpha$ for separation cases in which the capacity factors of solutes are greater than 5 will not change the result of the WPCO method a lot.

When the capacity factors of the solutes are below 5, larger deviations are expected. However, in those cases where the capacity factors of solutes are close to each other, resolution may still be used, and satisfactory results can still be obtained.

Moreover, because the separation factor, S , is proportional to the resolution, the separation factor can also be used in eqn.1 with

similarly satisfactory results. In this way, the measurement of the dead volume or the peak width is not necessary, and the experimental work is reduced.

We call the WPCO method which uses the logarithm of the selectivity factor the original WPCO method and the WPCO method which uses the separation parameter (or resolution) the simplified WPCO method.

Experimental

The data of the normal phase HPLC separation experiments used in this work are from two published works. The data listed in Table IV.1 are from J. L. Glajch et al.¹⁵. They used three Zorbax-SIL 15x0.46cm columns, which were from the same lot. Methylene chloride, acetonitrile, methyl tert-butyl ether and hexane were used as the components of the mobile phase. Mobile phase solvents were 50% water saturated. The sample consisted of 13 substituted naphthalenes. All experiments were carried out with a flow rate of 2.0 ml/min at 35°C.

The data listed in Table IV.2 are from G.M.Landers et al.¹⁶. They used a μ Porasil silica 30x0.39cm column. Chloroform, methylene chloride, isopropyl ether and hexane were used as the components of the mobile phase. The sample consisted of four retinol isomers. All the experiments were carried out at a flow rate of 3ml/min.

The data of reverse phase HPLC separation experiments used in this work are from three published works. The data listed in Table IV.3 are from G. D'agostino et al.¹⁷. They used a ODS-Hypersil, C₁₈, 15x0.5cm column. Methanol, acetonitrile, tetrahydrofuran and water were used as the components of the mobile phase. The sample consisted of ten polar adrenocortical

TABLE IV.1

THE CAPACITY FACTORS* OF FOUR SUBSTITUTED NAPHTHALENES FOR SEVEN SOLVENTS WITH A NORMAL-PHASE COLUMN (ZORBAX-SIL)

Compound** Number		k'						
		Solvent						
		A	B	C	A:B (1:1)	B:C (1:1)	A:C (1:1)	
1	1-CH ₂ CN	4.06	4.73	7.23	4.86	6.09	4.83	6.30
2	1-OH	4.44	8.17	6.65	6.77	7.14	6.27	8.00
3	1-COCH ₃	5.17	2.58	3.54	3.71	3.25	3.72	3.72
4	2-COCH ₃	7.33	3.33	4.76	5.14	4.39	5.16	5.10

* Data are from reference 15.

** Compounds are substituted naphthalenes.

A- methylene chloride/hexane (57.8:42.2 v/v/v).

B- methylene chloride/acetonitrile/hexane (10:3:87 v/v/v).

C- methyl *tert* -butyl ether/hexane (4.2:95.8 v/v).

TABLE IV.2

RESOLUTIONS AND SELECTIVITY FACTORS OF FOUR RETINAL ISOMERS FOR SEVEN SOLVENTS WITH A NORMAL-PHASE COLUMN(mPorasil Si)

Solvent	Separation parameter			
	11/13**		9/all***	
	R _s	a	R _s	a
A	0.096	1.0038	0.67	1.027
B	0.43	1.017	0.051	1.002
C	0.084	1.0034	0.35	1.014
A/B (1:1)	0.43	1.017	0.26	1.011
A/C (1:1)	0.13	1.0052	0.36	1.014
B/C (1:1)	0.68	1.027	0.20	1.0080
A/B/C (1:1:1)	0.47	1.019	0.37	1.015

* Resolution data are from reference 16. The selectivity factors are calculated from the resolution data.

** 11/13 11-*cis* retinaldehyde/13-*cis* retinaldehyde

*** 9/all 9-*cis* retinaldehyde/all-*trans* retinaldehyde

A- isopropyl ether/hexane (21.3:78.7 v/v)

B- methylene chloride/hexane (75:25 v/v)

C- chloroform/hexane (25:75 v/v)

TABLE IV.3

CAPACITY FACTORS* OF TEN POLAR ADRENOCORTICAL STEROIDS FOR SEVEN SOLVENTS WITH A REVERSED-PHASE COLUMN (ODS-Hyptrsil C₁₈).

Compound Number**	k'						
	<i>Solvent</i>						
	A	B	C	A:B (1:1)	B:C (1:1)	A:C (1:1)	A:B:C (1:1:1)
1	9.4	10.8	8.0	11.8	7.8	7.5	8.0
2	10.8	12.5	8.3	13.7	8.3	7.9	8.4
3	13.5	15.3	8.8	17.2	9.1	8.2	9.8
4	14.3	13.6	10.3	16.9	9.3	9.3	9.9
5	15.6	12.0	12.9	16.7	10.3	11.7	11.0
6	18.1	17.1	11.7	20.8	10.8	10.7	11.6
7	19.1	13.2	13.0	18.0	10.7	12.4	12.3
8	19.1	24.3	19.1	24.0	15.4	14.0	15.4
9	22.6	15.8	17.1	22.3	12.7	14.9	14.3
10	22.6	23.2	27.0	26.0	18.6	19.4	19.3

* Data are from reference 17.

** For the chemical names of these compounds, see reference 17.

A- methanol/water (35:65).

B- acetonitrile/water (20:80).

C- tetrahydrofuran/water (12:88).

steroids. All experiments were carried out with a eluet flow-rate of 1ml/min at 45°C.

The data listed in Table IV.4 are from S. J. Costanzo¹⁸. He used a Partisil-10, C₈, 25x0.46cm column. Methanol, acetonitrile, tetrahydrofuran and water were used as the components of the mobile phase. In addition, the mobile phase of all compositions also contained 1% acetic acid. The sample consisted of six substituted aromatic compounds.

The data listed in Table IV.5 are from J. L. Glajch et al.¹⁹. They used a Zorbax-C8 15x0.46cm column. Methanol, acetonitrile, tetrahydrofuran and water were used as the components of the mobile phase. The sample consisted of nine substituted naphthalenes. All experiments were carried out with the flow rate of 2ml/min at 40°C.

TABLE IV.4

CAPACITY FACTORS* OF SIX SUBSTITUTED AROMATIC COMPOUNDS FOR SEVEN SOLVENTS WITH A REVERSED-PHASE COLUMN (Partisil-10 C₈).

Compound Number**	k'						
	<i>Solvent</i>						
	A	B	C	A/B (1:1)	B/C (1:1)	A/C (1:1)	A/B/C (1:1:1)
1	1.41	1.66	2.96	1.63	2.00	1.88	1.76
2	2.68	2.45	4.19	2.94	3.07	3.04	2.97
3	3.27	4.54	6.44	4.01	4.92	4.07	4.10
4	3.40	3.13	9.68	3.73	5.23	5.52	4.70
5	3.84	3.96	18.67	4.66	7.50	8.87	6.52
6	6.88	7.73	8.13	8.62	7.05	6.10	7.03

* Data are from reference 18.

** Compounds 1 through 6 represent, respectively: 4-aminobenzoic acid; 3,4-dimethoxybenzoic acid; benzaldehyde; benzoic acid; 4-nitrobenzoic acid; and 3,4,5-trimethoxymethylbenzoate.

A- methanol/water/acetic acid (45:54:1 v/v/v).

B- acetonitrile/water/acetic acid (30:69:1 v/v/v).

C- tetrahydrofuran/water/acetic acid (20:79:1 v/v/v).

TABLE IV.5

CAPACITY FACTORS* OF NIN SUBSTITUTED NAPHTHALENES FOR SEVEN SOLVENTS WITH A REVERSED-PHASE COLUMN (Zorbax-C₈)

Comp. No.**	Group	k'						
		<i>Solvent</i>						
		A	B	C	A/B (1:1)	B/C (1:1)	A/C (1:1)	A/B/C (1:1:1)
1	N-1	0.65	0.69	0.57	0.52	0.69	0.74	0.73
2	2-SO ₂ CH ₃	0.78	1.28	0.98	0.88	1.08	0.88	1.01
3	2-OH	1.22	1.35	2.46	1.13	2.02	2.55	2.07
4	1-COCH ₃	2.26	2.79	2.46	2.25	2.53	2.55	2.61
5	1-NO ₂	3.02	3.79	3.85	3.14	3.84	4.60	4.16
6	2-OCH ₃	4.04	4.56	4.63	3.87	4.62	5.56	5.44
7	Naph	4.04	4.72	5.20	3.87	5.08	6.00	5.44
8	1-SCH ₃	6.67	6.93	6.73	6.40	7.05	9.16	8.32
9	1-C1	7.77	7.88	6.73	7.32	8.09	10.36	9.71

* Data are from reference 19.

** Compounds are the substituted naphthalenes.

A- methanol/water (63:37 v/v).

B- acetonitrile/water (52:48 v/v)

C- tetrahydrofuran/water (52:48 v/v)

Results and Discussion

In this work, the test cases were formed by using the data in Table IV.1-5. The simplified and original WPCO methods are applied to each of the test cases and the results are compared. It is assumed that the errors in the capacity factor data are very small so that they can be neglected, and if these errors are not small enough to be neglected, then, at least, these errors occur in the same direction, and their effects will be cancelled out in the mathematical operation of the WPCO methods.

Two test categories are used. In one category, the capacity factors of all the solutes of each case are greater than 6. In the other category, the capacity factors of some solutes of each case are in the range of 2 to 6.

For each test case, the minimum a plots method was used to build the minimum separation response surface. Two versions of the minimum separation response surfaces were built and compared first. One of these two versions was the minimum $\ln a$ response surface. The other one was the minimum resolution response surface. To build these two response surfaces, the special cubic function^{20,21} was used to describe the retention behavior for every point of the response surface of the entire solvent triangle

$$\ln k' = a_1x_1 + a_2x_2 + a_3x_3 + a_{12}x_{12} + a_{13}x_{13} + a_{23}x_{23} + a_{123}x_{123} \quad (1)$$

where x is the proportion of the isoeluotropic eluent, and k' is the capacity factor. The subscripts 1, 2 and 3 represent three isoeluotropic eluents. The coefficients a_1 - a_{123} are calculated from the seven experimental points needed to fit Eq. 1. The validity of the model has been discussed in reference 1.

Then, the minimum $\ln a$ response surface, and the minimum resolution response surface were built by using the data provided by Eq. 1. The following equation²² was used to calculate the resolution for building the minimum resolution response surface

$$R_s = 1/4 N^{1/2} (a - 1) (k'/k' - 1) \quad (2)$$

where N is the number of the theoretical plates, a is the selectivity factor and k' is the capacity factor of the peak which leaves the column first.

To build the window diagrams along the triangle edges, the following equation was used to describe the retention behavior of the solutes

$$\ln k' = a_1x_1 + a_2x_2 + a_{12}x_{12} \quad (3)$$

where x_1 and x_2 are the two isocratic eluents, the coefficients a_1 - a_{12} are calculated from the experimental points needed to fit Eq. 3. The reasons for using this equation are discussed in reference 1.

The 13 cases in which the capacity factors of all the solutes are greater than 6 were formed by using the data in Table IV.3. The components of these cases are listed in Table IV.6. In these twelve cases, the minimum resolution response surface is almost equivalent to the corresponding minimum $\ln a$ response surface. The results of the simplified and original WPCO methods are also almost identical. The results of four test cases are shown in Figures 2, 3, 4 and 5.

The solvent triangle contour plots in these figures and later figures have been simplified by omitting all contour lines except for the contour lines of $\ln a$ and R_s near the global optimum, and the contour lines for $\ln a = 0$. The contour lines for $\ln a$ and $R_s = 0$ and the other corresponding contour lines for $\ln a$ and R_s are very close to each other (within 3% in eluent composition). The $\ln a$ and R_s window diagrams of the three edges are shown, because they are cross sections of the corresponding response surfaces, and the whole profile of these cross sections can be seen from the window diagram, which makes it easier observe the similarity of these cross sections. In this way, the most interested area, the global optimum can be compared, and the shape and size of the corresponding optimum area (the area surrounded by zero contours) can also be compared.

TABLE IV.6.

TEST CASES USING CONSTITUTES OF POLAR ADRENOCORTICAL
STERIODS WITH A REVERSED-PHASE COLUMN

Case		Components*								
1	1	2	3	4	5	6	7	8	9	10
2		2	3	4	5	6	7	8	9	10
3	1		3	4	5	6	7	8	9	10
4	1	2		4	5	6	7	8	9	10
5	1	2	3		5	6	7	8	9	10
6	1	2	3	4		6	7	8	9	10
7	1	2	3	4	5		7	8	9	10
8	1	2	3	4	5	6		8	9	10
9	1	2	3	4	5	6	7		9	10
10	1	2	3	4	5	6	7	8		10
11	1	2	3	4	5	6	7	8	9	
12		2			5	6	7	8	9	10
13		2	3		5	6		8	9	10

* The compound number is the same as that in Table 3.

For the first case Fig. IV.2a (case 10 of Table IV.6), the shape of the minimum I_{na} response surface was found to be almost equivalent to that of the minimum resolution (and separation parameter) surface. In the window diagrams, Fig. IV.2b-d, show that along each edge, the shape of the I_{na} vs. composition window diagram is almost equivalent to the corresponding R_s vs. composition window diagram (Since resolution is proportional to the separation parameter, the separation parameter vs. composition window diagrams will be also equivalent to the I_{na} vs. composition window diagrams). In these window diagrams, the difference between the locations of the corresponding peaks and valleys are also very small. These differences are within 1% of the eluent composition. Similarly, the top views of these two response surfaces are also similar. In Fig. IV.2a the positions of these valleys and optimal areas of the I_{na} and R_s response surfaces are almost the same. Both the simplified and original WPCO methods find the global optimum of the entire mobile phase system, and the difference between the results of these two methods is within 1% in eluent composition.

In Fig. IV.3a, the minimum I_{na} response surface is very similar to the minimum resolution (and separation parameter) response surface. The I_{na} and R_s window diagrams along corresponding edges (Fig. IV.3b-d) are very similar. The differences between the locations of the corresponding peaks and valleys are within 1% of the eluent composition. The top views of

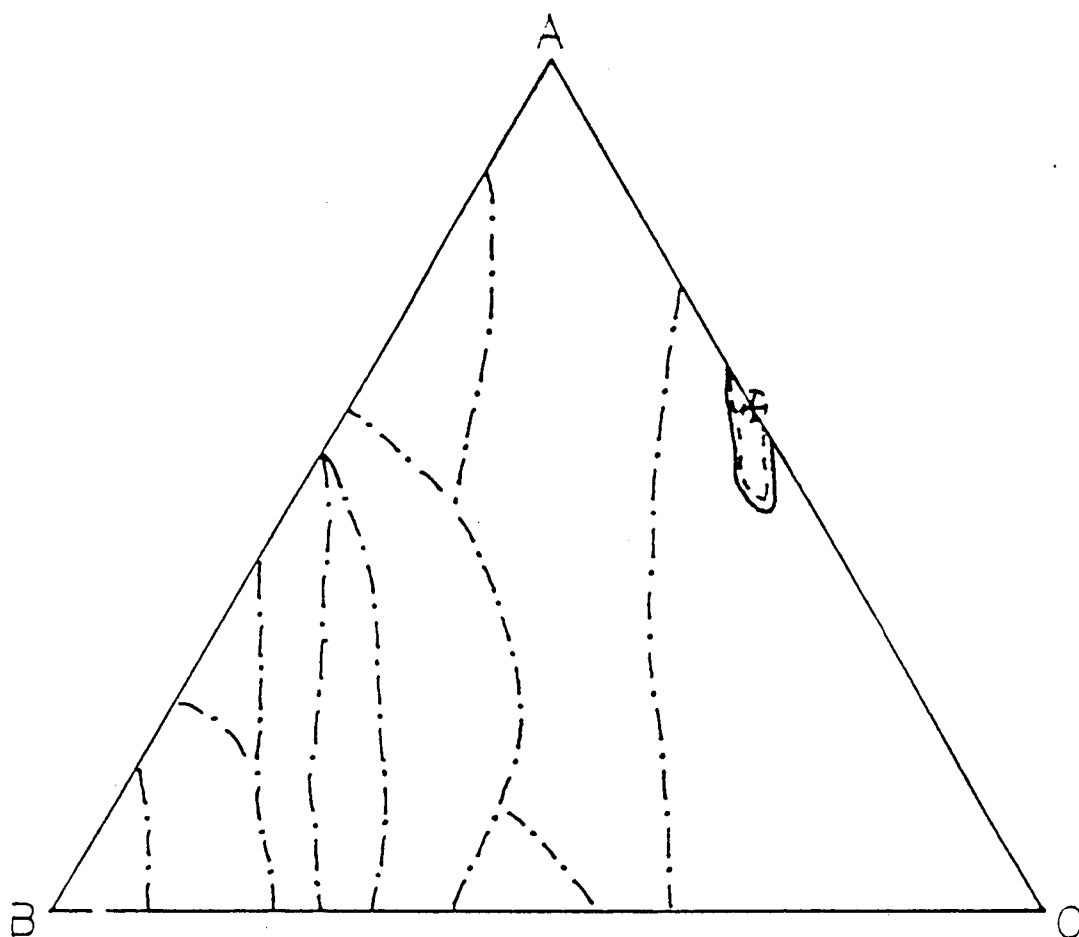
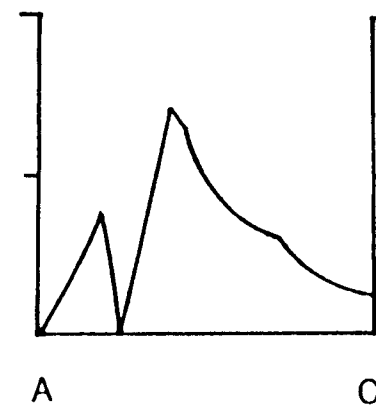
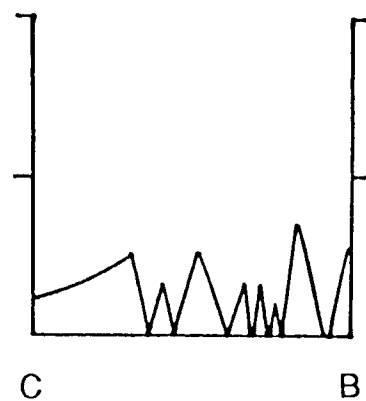
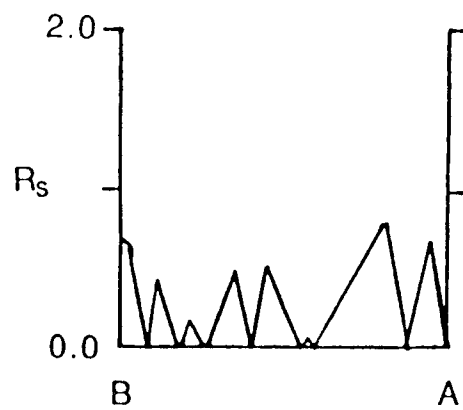
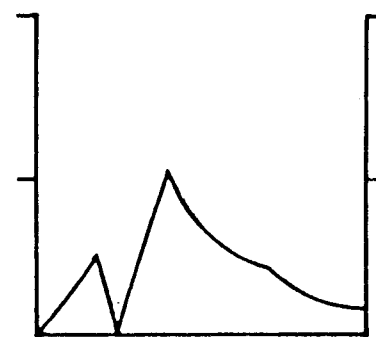
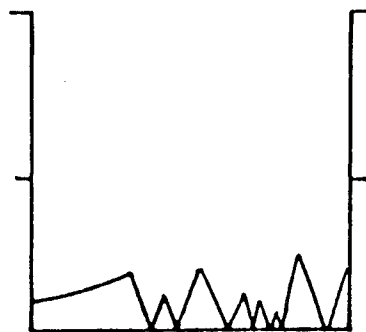
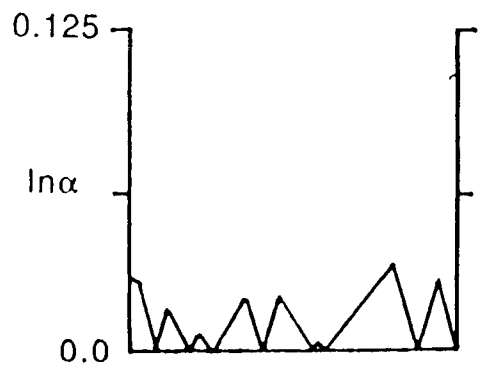


Fig. IV.2 (a) The results of the simplified and original WPCO methods applied to test case 10 of Table 6. (—) Global optimum area of the minimum $\ln\alpha$ surface. (- - -) Global optimum area of the minimum R_s surface. (- · - ·) Valley of the minimum separation response surface ($\ln\alpha = 0$, $R_s = 0$). (⊗) result of the original WPCO method. (⊕) result of the simplified WPCO method. (b), (c) and (d) are the $\ln\alpha$ and R_s window diagrams along edges AB, BC and AC, respectively.



(b)

(c)

(d)

Figure IV.2 continued

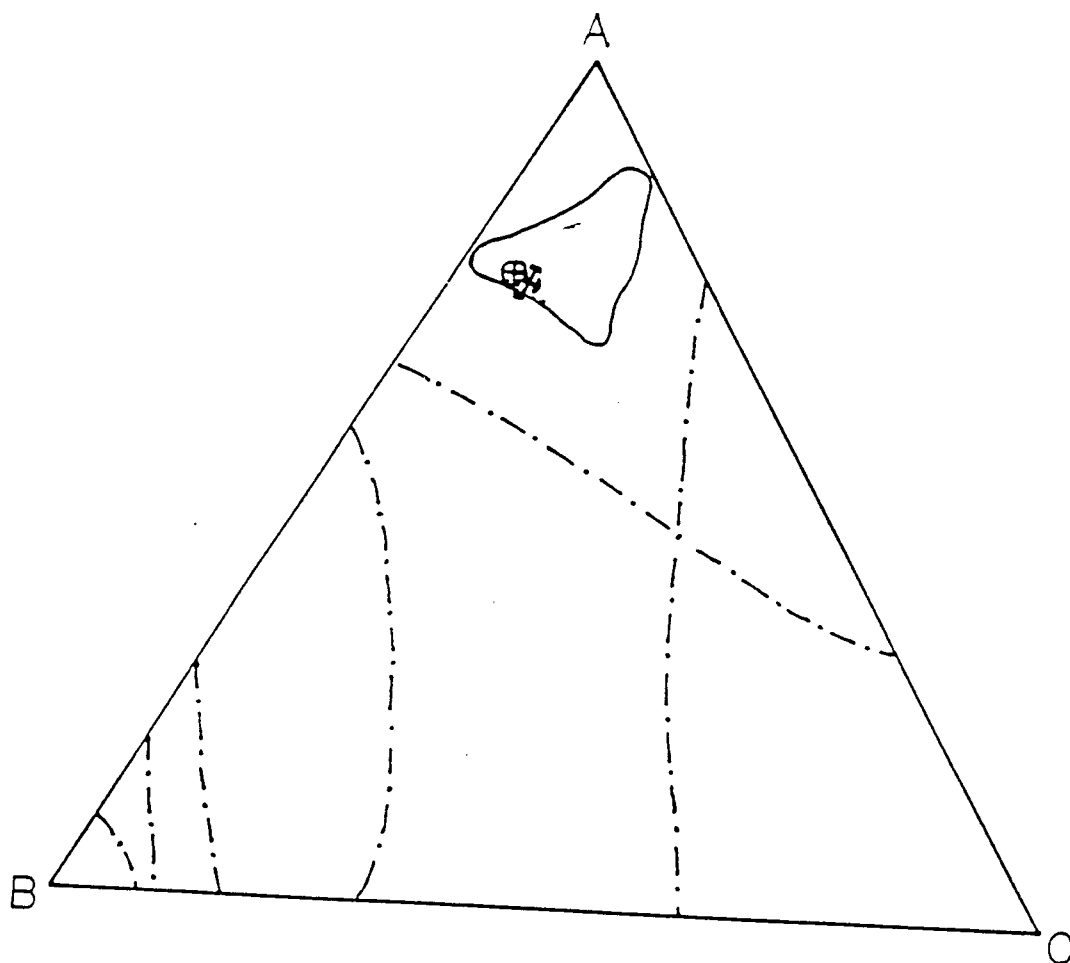


Fig. IV.3 (a) The results of the simplified and original WPCO methods applied to test case 13 of Table 6. (—) Global optimum area of the minimum $\ln\alpha$ surface. (---) Global optimum area of the minimum R_s surface. (-.-) Valley of the minimum separation response surface ($\ln\alpha = 0$, $R_s = 0$). (\otimes) result of the original WPCO method. (\oplus) result of the simplified WPCO method. (b), (c) and (d) are the $\ln\alpha$ and R_s window diagrams along edges AB, BC and AC, respectively.

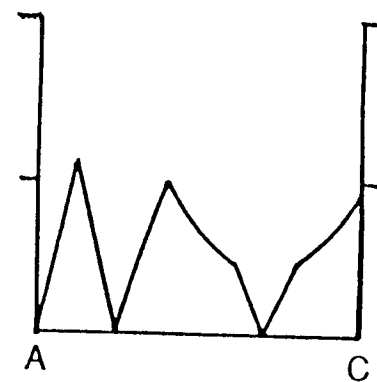
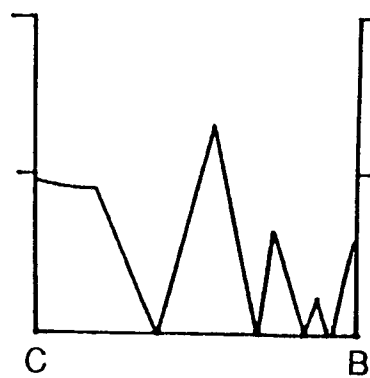
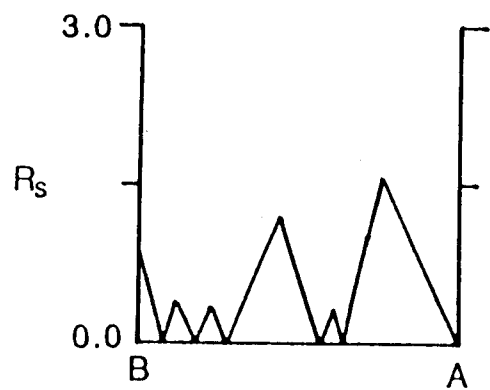
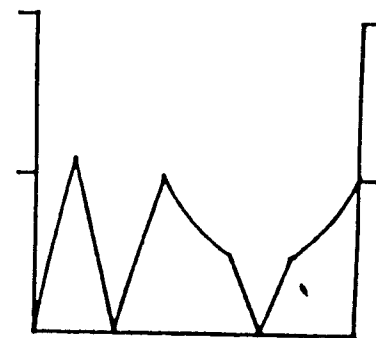
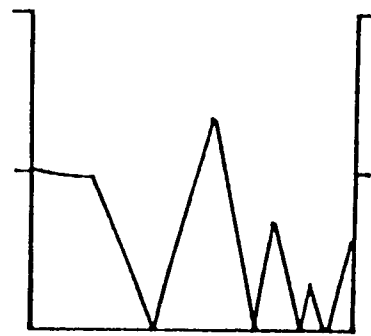
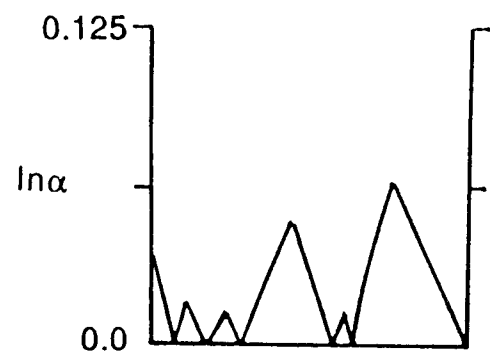


Figure IV.3 continued

these two minimum response surfaces are also similar. In this case, the global optimum of the entire solvent system is inside the triangle, and this global optimum is close to the global optima of the second and third edges. The simplified and original WPCO methods find the global optimum, and the difference between these two methods is within 1% of eluent composition.

Fig. IV.4 shows another case in which the global optimum of the triangle is inside the triangle and close to two edges whose optima are individually the second and third best among the optima of the three edges, and far from the edge whose optimum is the best among the optima of the three edges. Again the $\ln a$ and R_s minimum separation response surfaces are similar, and the results of the simplified and original WPCO methods agree.

In these thirteen cases, there is only one case in which the difference between the results of the simplified and original methods is noticeably larger than those of the other cases. This case is case 4 in Table IV.6 and is shown in Fig. IV.5. The overall shape of the minimum resolution response surface is still very similar to the corresponding minimum $\ln a$ response surface. However, the difference between the results of the simplified and original WPCO methods is about 8% in eluent composition, and the result of the original WPCO method is close to the global optimum located by the minimum a plots method. This may suggest that the original WPCO method, in some situations, has better accuracy.

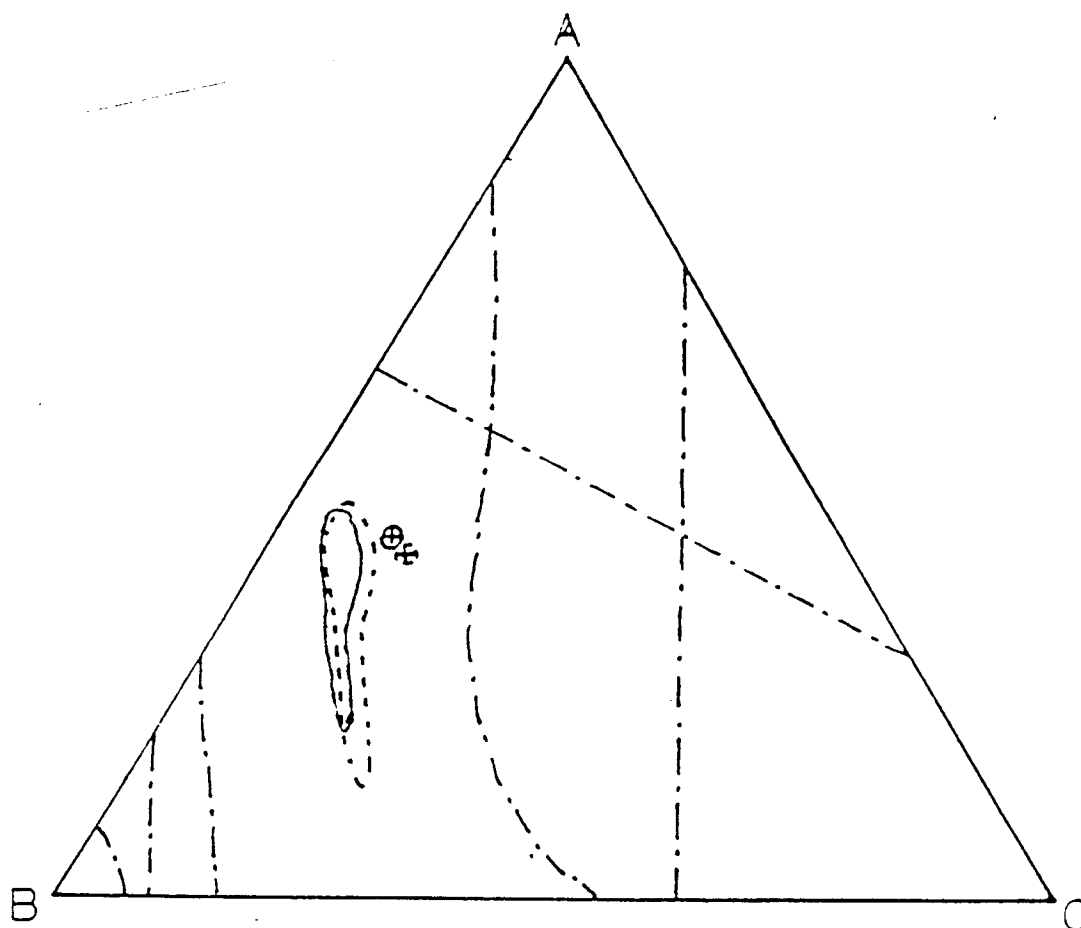
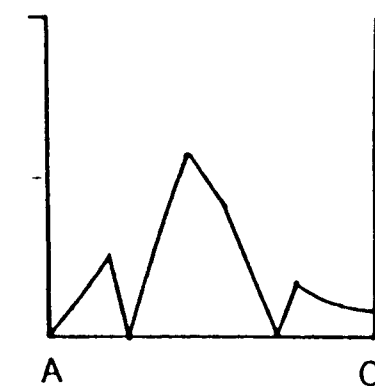
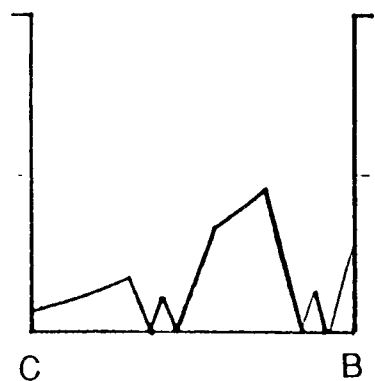
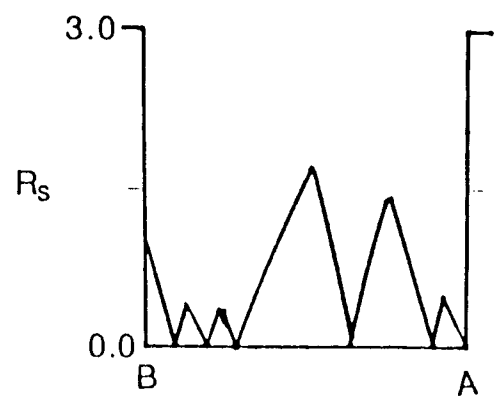
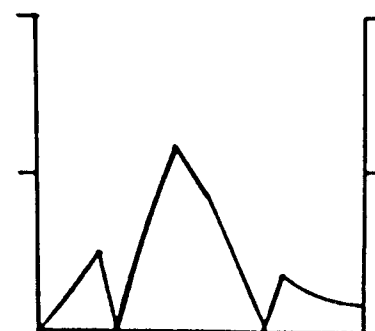
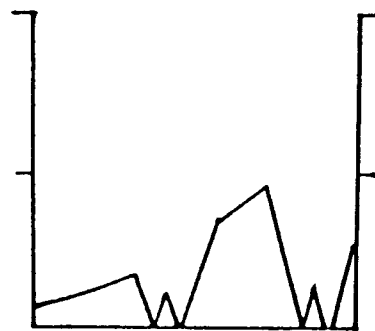
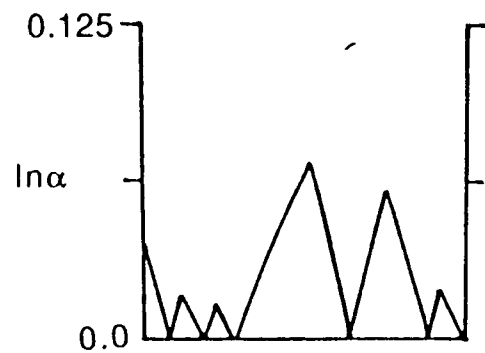


Fig. IV.4 (a) The results of the simplified and original WPCO methods applied to test case 12 of Table 6. (—) Global optimum area of the minimum $\ln\alpha$ surface. (---) Global optimum area of the minimum R_s surface. (-·-) Valley of the minimum separation response surface ($\ln\alpha = 0$, $R_s = 0$). (\oplus) result of the original WPCO method. (\oplus) result of the simplified WPCO method. (b), (c) and (d) are the $\ln\alpha$ and R_s window diagrams along edges AB, BC and AC, respectively.



(b)

(c)

(d)

Figure IV.4 continued

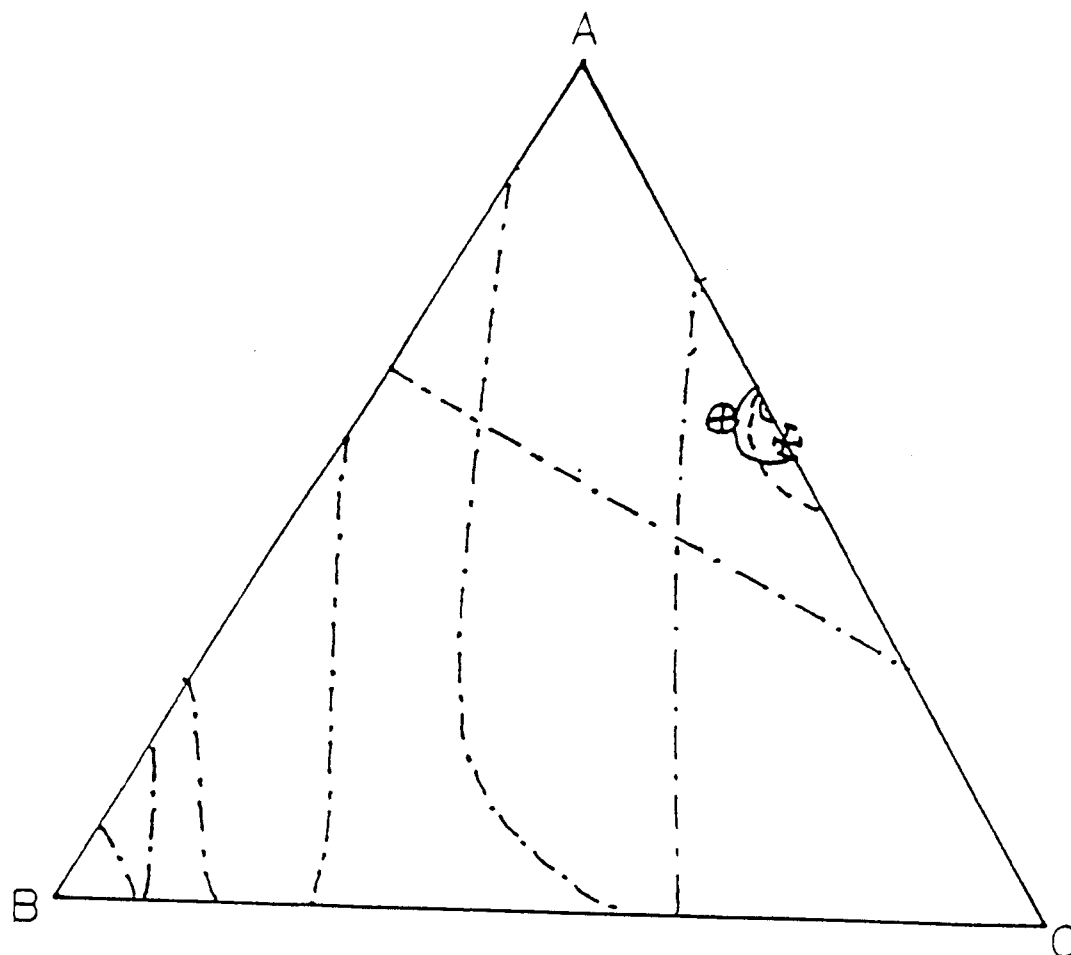
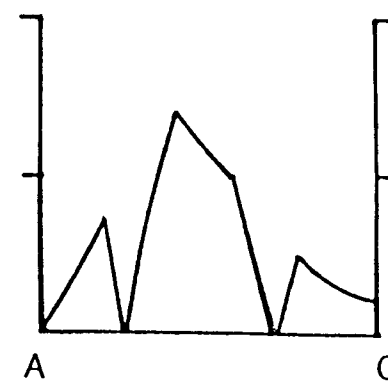
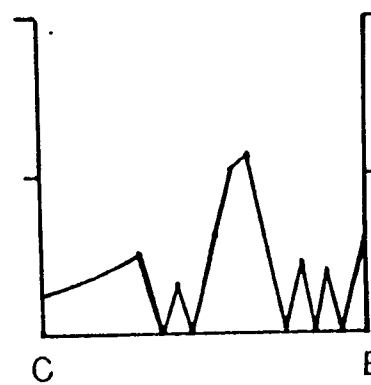
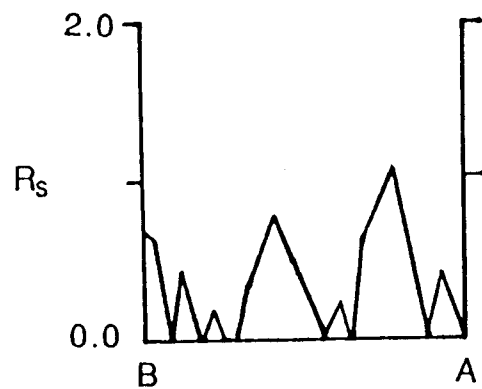
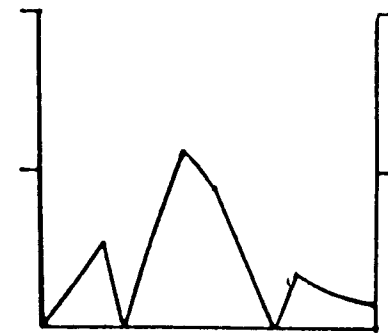
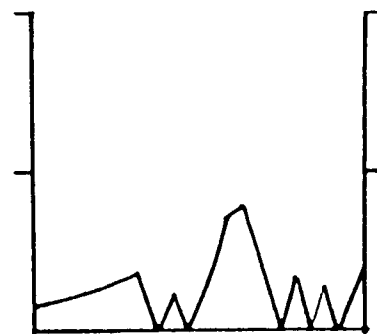
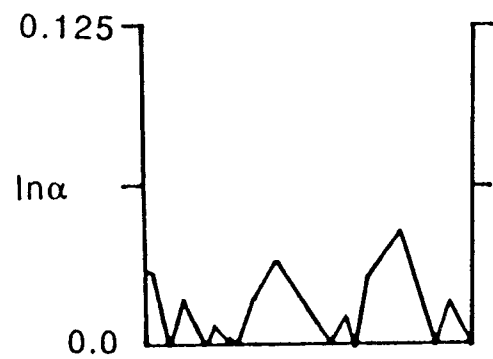


Fig. IV.5 (a) The results of the simplified and original WPCO methods applied to test case 4 of Table 6. (—) Global optimum area of the minimum $\ln\alpha$ surface. (---) Global optimum area of the minimum R_s surface. (-·-) Valley of the minimum separation response surface ($\ln\alpha = 0$, $R_s = 0$). (⊕) result of the original WPCO method. (⊗) result of the simplified WPCO method. (b), (c) and (d) are the $\ln\alpha$ and R_s window diagrams along edges AB, BC and AC, respectively.



(b)

(c)

(d)

Figure IV.5 continued

However, since a fine-tuning procedure usually follows the initial optimization process, the difference is relatively minor.

Overall, the results of these 13 cases show that when the capacity factors of all the solutes are greater than 5, the simplified WPCO method usually produces the same result as the original WPCO method. The differences among the resolution vs. selectivity factor curves is relatively small. Since the simplified WPCO method does not require the measurement of the column dead time, experimental and data processing work can be further reduced.

Now, consider the separation cases in which the capacity factors of some solutes are in the range of 2 to 6, and the difference between the capacity factors of the solutes which are members of the different worst separated peak pair(s) are large. Because the curves in Fig. IV.1 for $k=2$, 3 and 5 are relatively far from each other, large deviations in the results for the simplified WPCO method are expected. However, for the cases which have simple separation response surfaces, the differences between the capacity factors may not cause large deviations, and the simplified WPCO method may still be used.

The test cases in which the capacity factors of some solutes are in the range of 2 to 6 are formed by using the data in Table IV.1 and Table IV.4. The components of these test cases are listed in Table IV.7 and Table IV.8. The cases in Table IV.7 are

TABLE IV.7.

TEST CASES USING CONSTITUENTS OF SUBSTITUTED NAPHTHALENES
WITH A NORMAL-PHASE COLUMN

CASE		Component*			
1	1	2	3	4	
2		2	3	4	
3	1		3	4	
4	1	2		4	
5	1	2	3		

* The compound number is the same as that in Table IV.1.

TABLE IV.8.

TEST CASES USING CONSTITUENTS OF SUBSTITUTED AROMATIC
COMPOUNDS WITH A REVERSED-PHASE COLUMN

CASE		Component*				
1	1	2	3	4	5	6
2		2	3	4	5	6
3	1		3	4	5	6
4	1	2		4	5	6
5	1	2	3		5	6
6	1	2	3	4		6
7	1	2	3	4	5	
8	1	2	3		5	

* The compound number is the same as that in Table 4.

discussed first. In these 5 cases, the capacity factors of the solutes are in the range of 4 to 12 (see Table IV.1), and all of these solutes belong to the worst separated peak pairs. However, the deviations of the results of these cases are not as large as expected. In all these cases, there is only one case in which the difference between $\ln a$ and R_s minimum separation response surfaces is relatively visible, Fig. IV.6. The results of the simplified and original WPCO methods still agree with those of the minimum a plots method.

Now consider two of these 5 cases. In Fig. IV.7, at the global optimal compositions of the three edges, the capacity factors of the members of the worst separated peak pairs are in the range of 3.25 to 7, Table IV.9. The minimum separation surfaces of both versions (Fig. 7a) are similar to each other. Along the edges of the solvent triangle, the side views of these response surfaces (i.e., the window diagrams in Fig. 7b-d) are similar to each other. The window diagrams of both versions are similar at each edge. In these window diagrams, the differences between the corresponding peaks and valleys are within 2% in eluent composition. The results of both the simplified and original WPCO methods still agree with that of the corresponding minimum a plots method.

In Fig. IV.6 (case 2 of Table IV.7), at the global optimal compositions of three edges, the capacity factors of three solutes

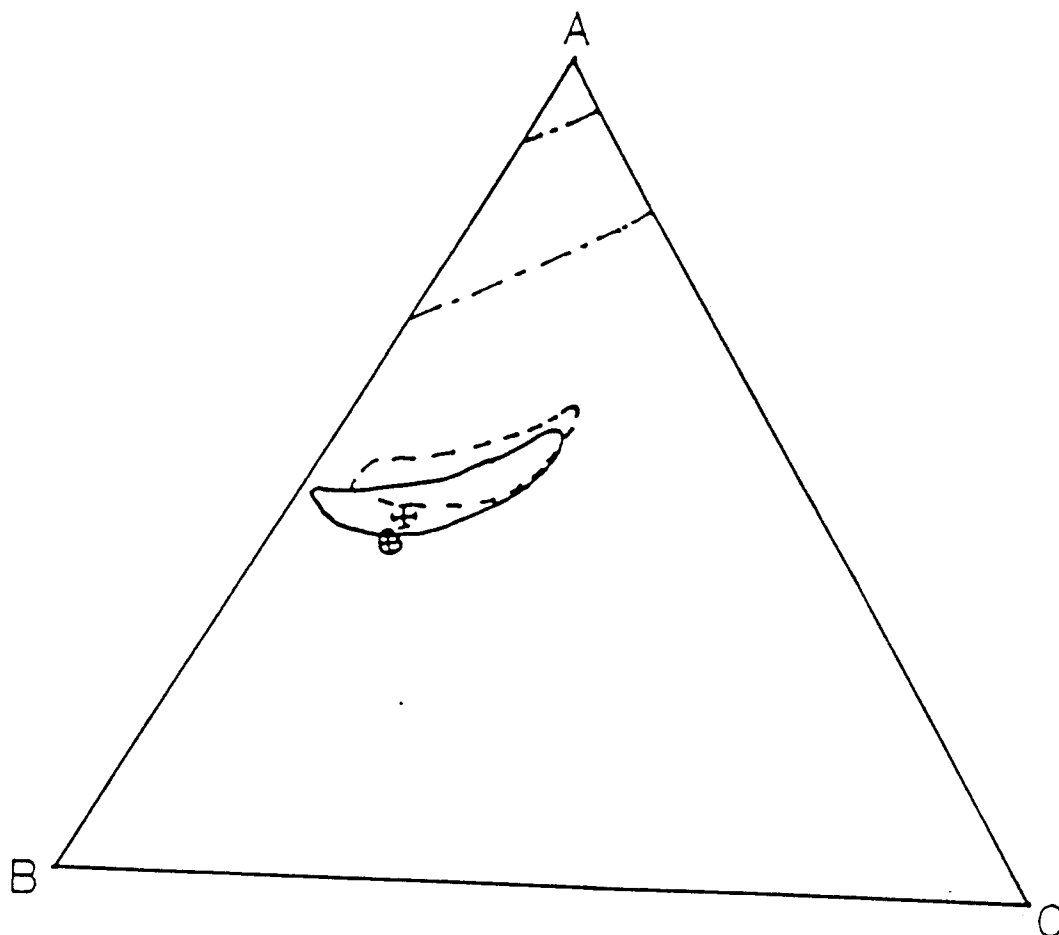
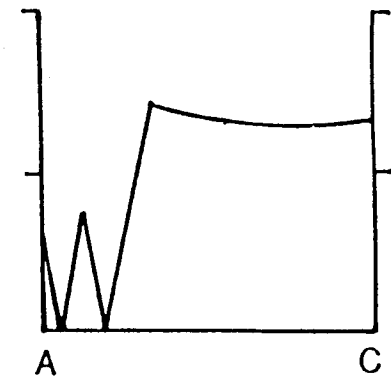
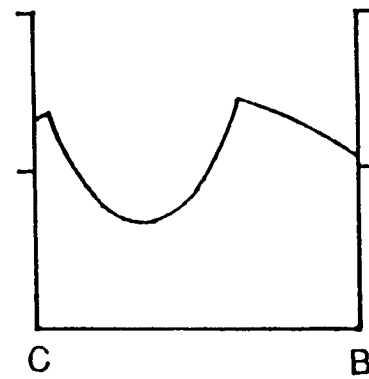
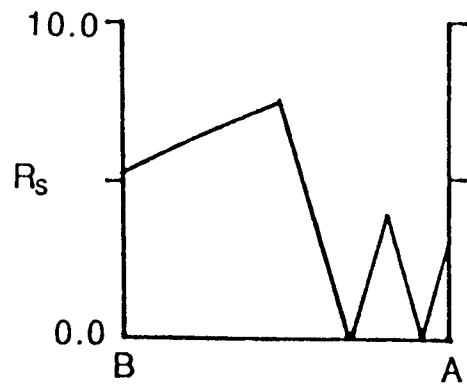
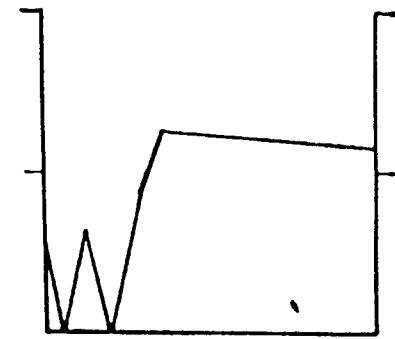
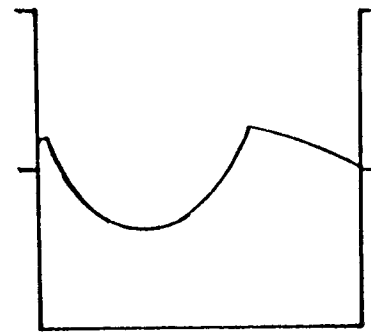
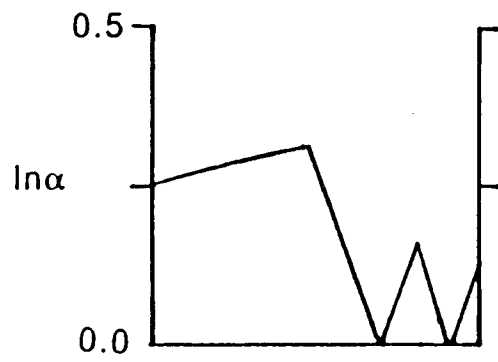


Fig. IV.6 (a) The results of the simplified and original WPCO methods applied to test case 2 of Table 7. (—) Global optimum area of the minimum $\ln\alpha$ surface. (---) Global optimum area of the minimum R_s surface. (-·-) Valley of the minimum separation response surface ($\ln\alpha = 1$, $R_s = 0$). (\oplus) result of the original WPCO method. (\otimes) result of the simplified WPCO method. (b), (c) and (d) are the $\ln\alpha$ and R_s window diagrams along edges AB, BC and AC, respectively.



(b)

(c)

(d)

Figure IV.6 continued

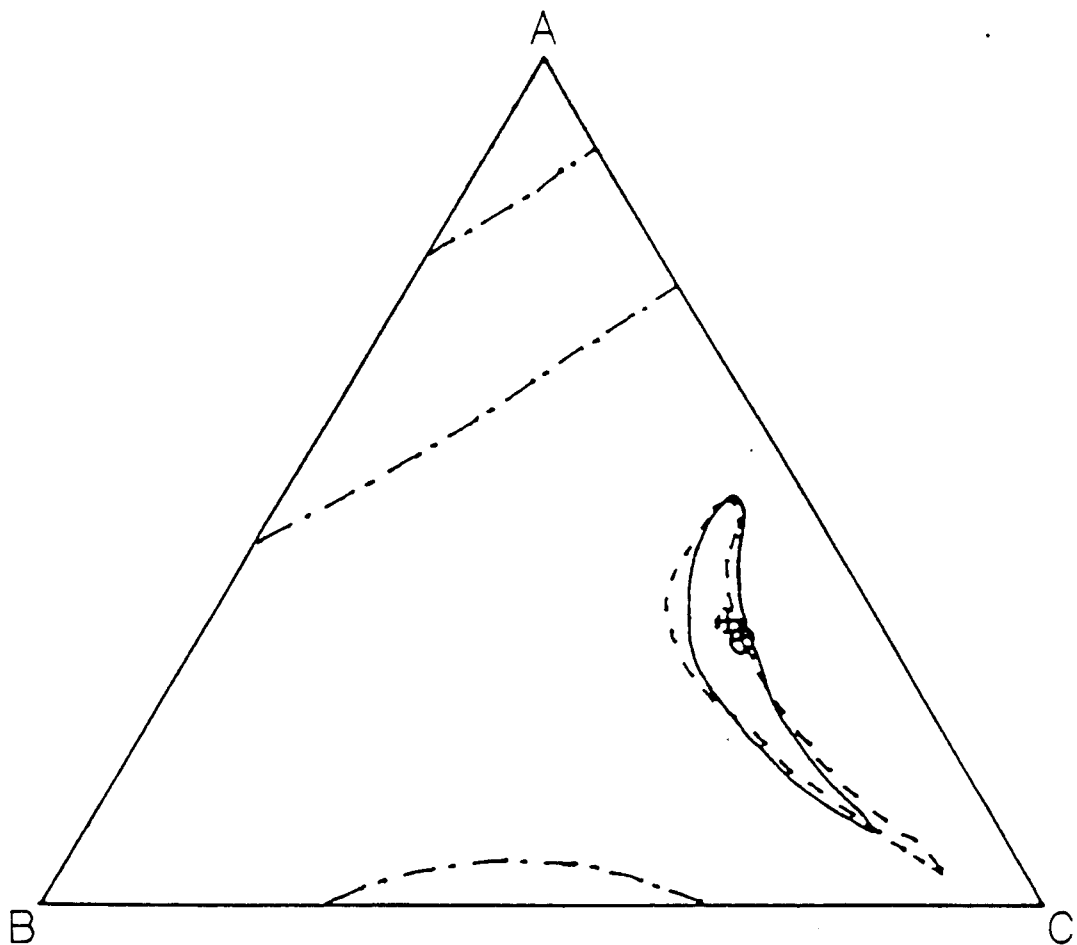
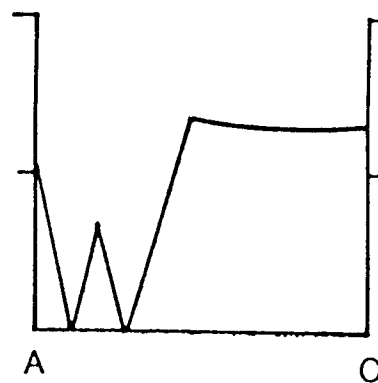
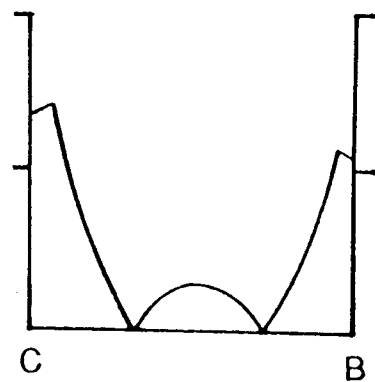
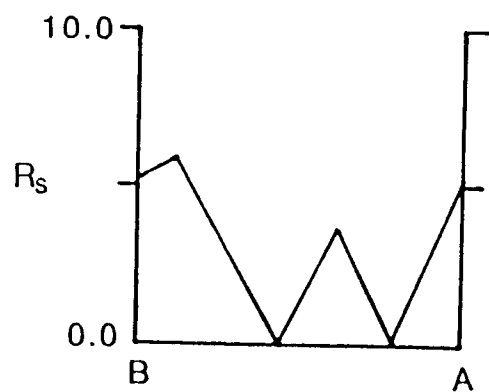
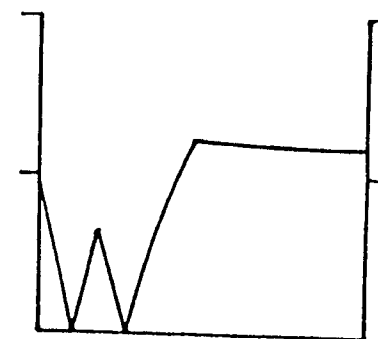
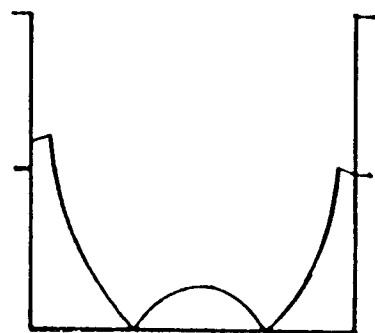
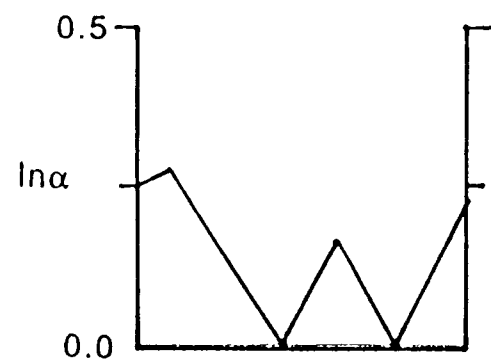


Fig. IV.7 (a) The results of the simplified and original WPCO methods applied to test case 3 of Table 7. (—) Global optimum area of the minimum $\ln\alpha$ surface. (---) Global optimum of the minimum R_s surface. (- · -) Valley of the minimum separation response surface ($\ln\alpha = 1$, $R_s = 0$). (\oplus) result of the original WPCO method. (\oplus) result of the simplified WPCO method. (b), (c) and (d) are the $\ln\alpha$ and R_s window diagrams along edges AB, BC and AC, respectively.



(b)

(c)

(d)

Figure IV.7 continued

are in the range from 3.5 to 6.5, Table IV.9. In Fig.6b-d, the I_{na} and R_s window diagram of each edge is similar, and the difference between the corresponding peaks and valleys are within 2% in eluent composition. On the whole, the I_{na} and R_s minimum separation response surface (Fig. IV.6a) are similar. However, it can be seen that, compared with the location of the global optimal area of the minimum I_{na} response surface, the global optimal area of the minimum resolution response surface is shifted toward the middle of the triangle to a small extent. It is interesting that the result of the simplified WPCO method also shifts towards the same direction.

For the cases in Table IV.8, the results of the simplified WPCO method also agree with those of the minimum a plots method. Three cases of particular interest are shown in Figures IV.8, 9 and 10.

For the case in Fig. IV.8, at the global optima of the three edges, the capacity factors of the solutes which are the worst separated peak pairs are in the range from 3.5 to 10 (Table IV.10). The I_{na} and R_s window diagrams are similar (Fig. IV.8b-d). The difference between the locations of the corresponding peaks and valleys are within 3%. Similarly, the I_{na} and R_s minimum separation surfaces (Fig. IV.8a) are also similar. Both the simplified and original WPCO methods find the region of the global optimum.

TABLE IV.9.

CAPACITY FACTORS OF PEAKS FOR THE WORST-SEPARATED PEAK PAIRS AT THE GLOBAL OPTIMUM OF EACH EDGE OF CASES 2 AND 3 IN TABLE 7.

CASE**		EDGE*								
		AB			BC			AC		
2	Peak No.	1	3	4	1	3	4	1	3	4
	k'	4.25	4.75	7	6.7	3.7	5	5.7	3.25	4.5
3	Peak No.	2	3	4	2	3	4	2	3	4
	k'	6.5	3.7	5.2	6.5	3.5	4.5	6.5	3.7	5

* See the footnotes of Table 2 for the notation of A, B and C.

** The case number is the same as in Table 7.

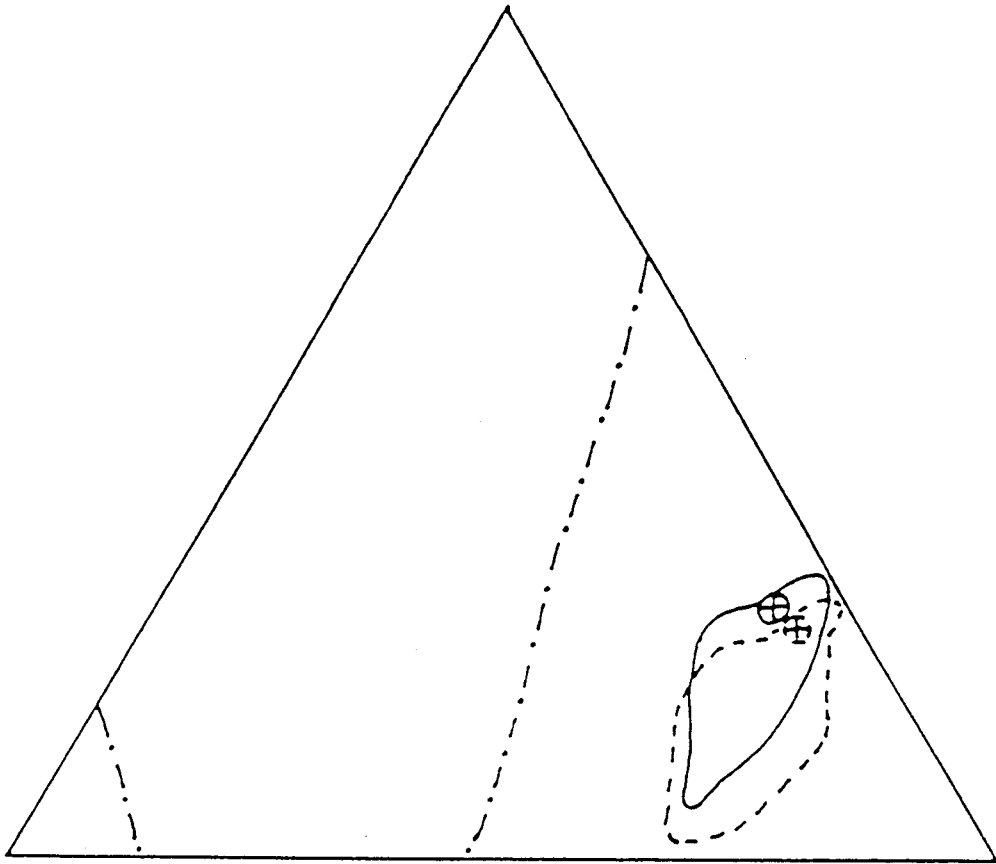
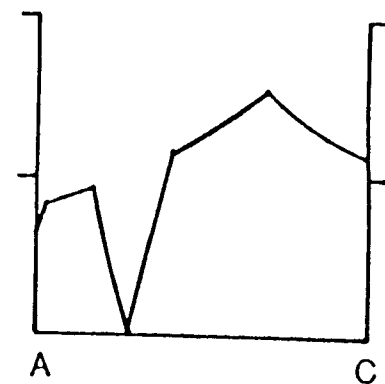
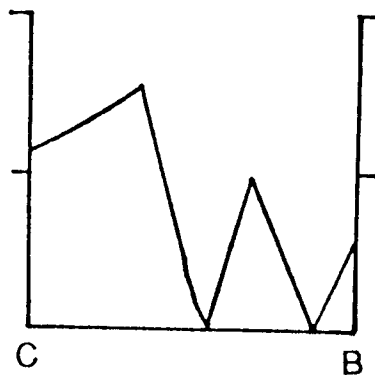
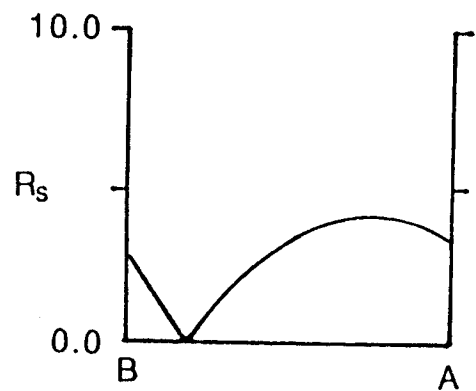
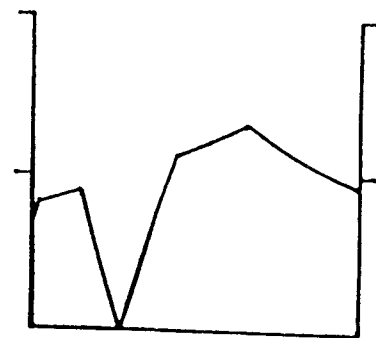
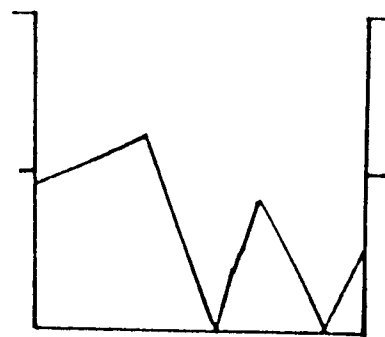
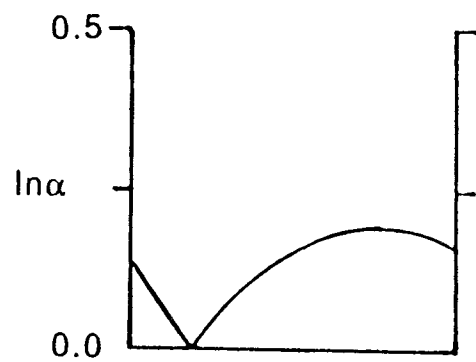


Fig. IV.8 (a) The results of the simplified and original WPCO methods applied to test case 5 of Table 9. (—) Global optimum area of the minimum $\ln\alpha$ surface. (---) Global optimum area of the minimum R_s surface. (-·-) Valley of the minimum separation response surface ($\ln\alpha = 1$, $R_s = 0$). (⊗) result of the original WPCO method. (⊕) result of the simplified WPCO method. (b), (c) and (d) are the $\ln\alpha$ and R_s window diagrams along edges AB, BC and AC, respectively



(b)

(c)

(d)

Figure IV.8 continued

Table IV.10.

CAPACITY FACTORS OF PEAKS FOR THE WORST-SEPARATED PEAK PAIRS AT THE GLOBAL OPTIMUM OF EACH EDGE OF CASES 5, 6 AND 8 IN TABLE 9.

CASE**		EDGE*								
		AB		BC			AC			
5	Peak No.	3	5	3	5	6	2	3	6	
	k'	4.0	4.5	3.25	10	6.3	3.3	5	6.5	
6	Peak No	2	4	3	4	6	2	3	4	
	k'	2.5	13.1	5.25	6.25	7.2	3.8	5.8	8.7	
8	Peak No.	3	5	1		2	1	2	3	
	k'	3.5	4.2	2		3	2	3.6	5.3	

* See the footnotes of Table 4 for the notation of A, B and C.

** The number is the same as that in Table 10

For the case in Fig. IV.9, the capacity factors of the solutes which are the worst separated peak pairs are in the range of 2.5 to 8.7 (case 6 of Table IV.10). The $\ln a$ and R_s window diagrams and the minimum separation response surfaces are similar. The differences of the corresponding peaks and valleys are within 3% in eluent composition. In this case, the global optimum of the entire solvent triangle is along one of the edges, and the optima ($\ln a = 0.24$) of the other two edges are nearly as good as the global optimum ($\ln a = 0.28$) of the entire solvent triangle. However, the simplified WPCO method is not confused by this situation and finds the global optimum of the triangle.

In this group, there is only one case, shown in Fig. IV.10, in which the differences in the $\ln a$ and R_s window diagrams and the minimum separation response surface are relatively large. In this case, the capacity factors of the solutes which are the members of the worst separated peak pairs are in the range of 2 to 5.2. On the whole the profiles of the window diagrams are still similar. However, the differences of the corresponding peaks are about 5% in eluent composition. These differences are a factor of 1.7 greater than those in other cases of this group. In the minimum resolution response surface, the global optimal area also shifts towards inside of the triangle. However, the result of the simplified WPCO method also moves accordingly. The capacity factors of the solutes are in the range of 2 to 5.2, and in this range, the differences of the resolution vs. composition curves at

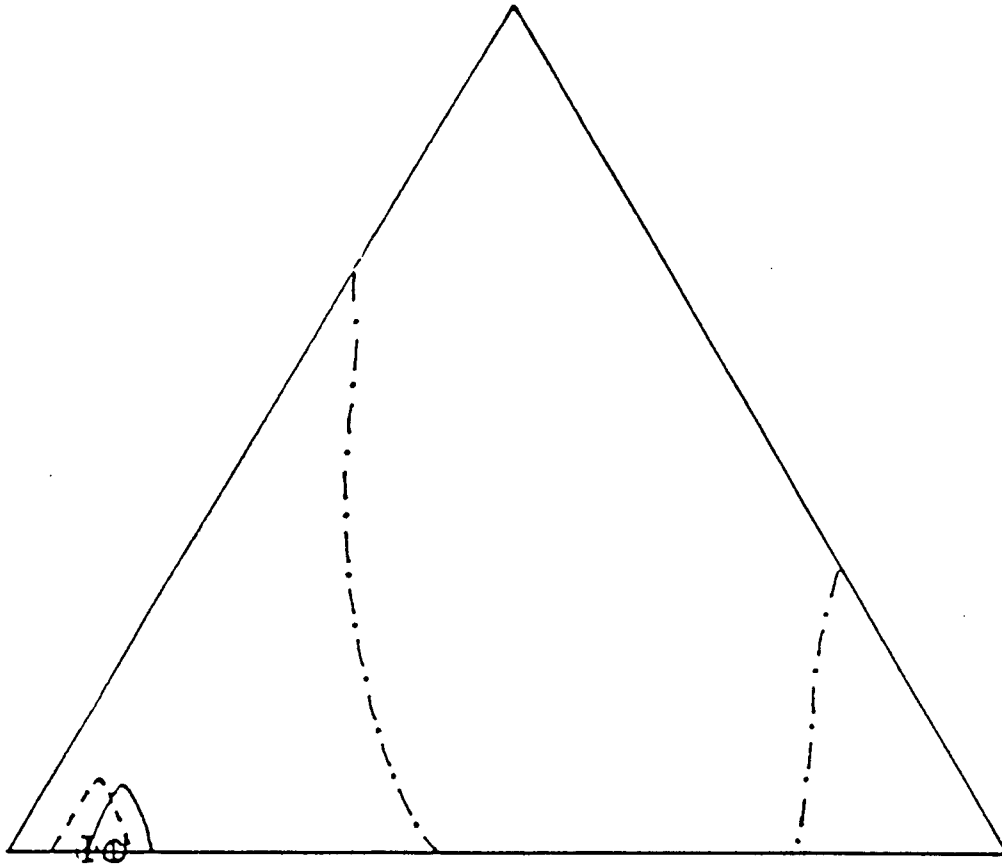
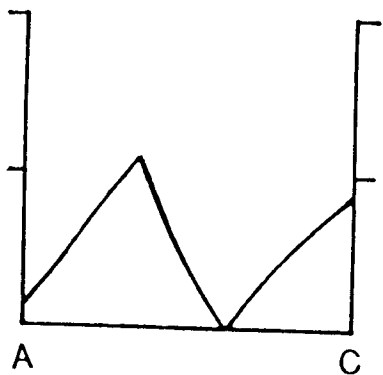
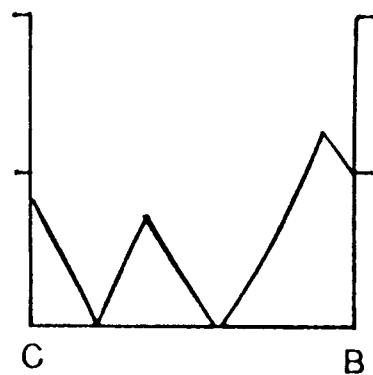
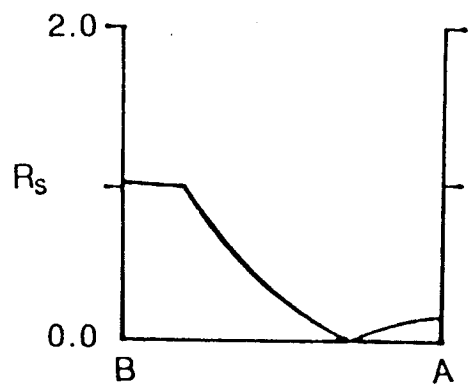
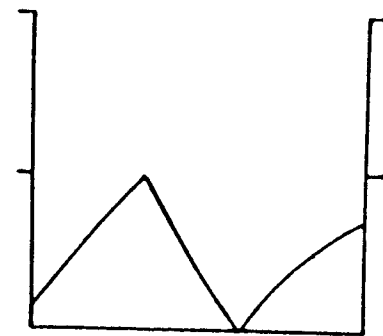
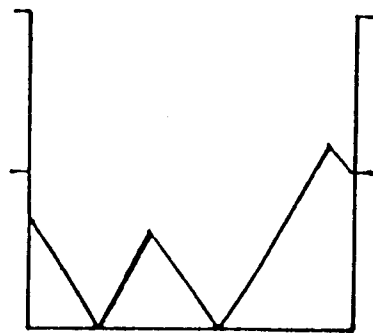
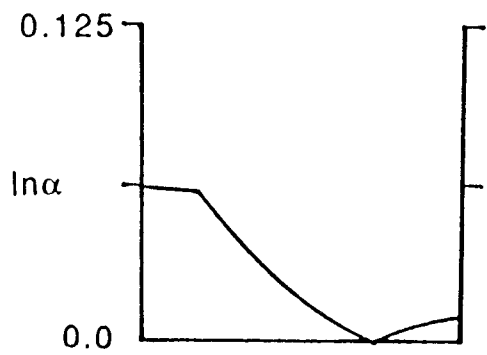


Fig. IV.9 (a) The results of the simplified and original WPCO methods applied to test case 6 of Table 9. (—) Global optimum area of the minimum $\ln\alpha$ surface. (---) Global optimum area of the minimum R_s surface. (-·-) Valley of the minimum separation response surface ($\ln\alpha = 1$, $R_s = 0$). (⊕) result of the original WPCO method. (⊗) result of the simplified WPCO method. (b), (c) and (d) are the $\ln\alpha$ and R_s window diagrams along edges AB, BC and AC, respectively.



(b)

(c)

(d)

Figure IV.9 continued

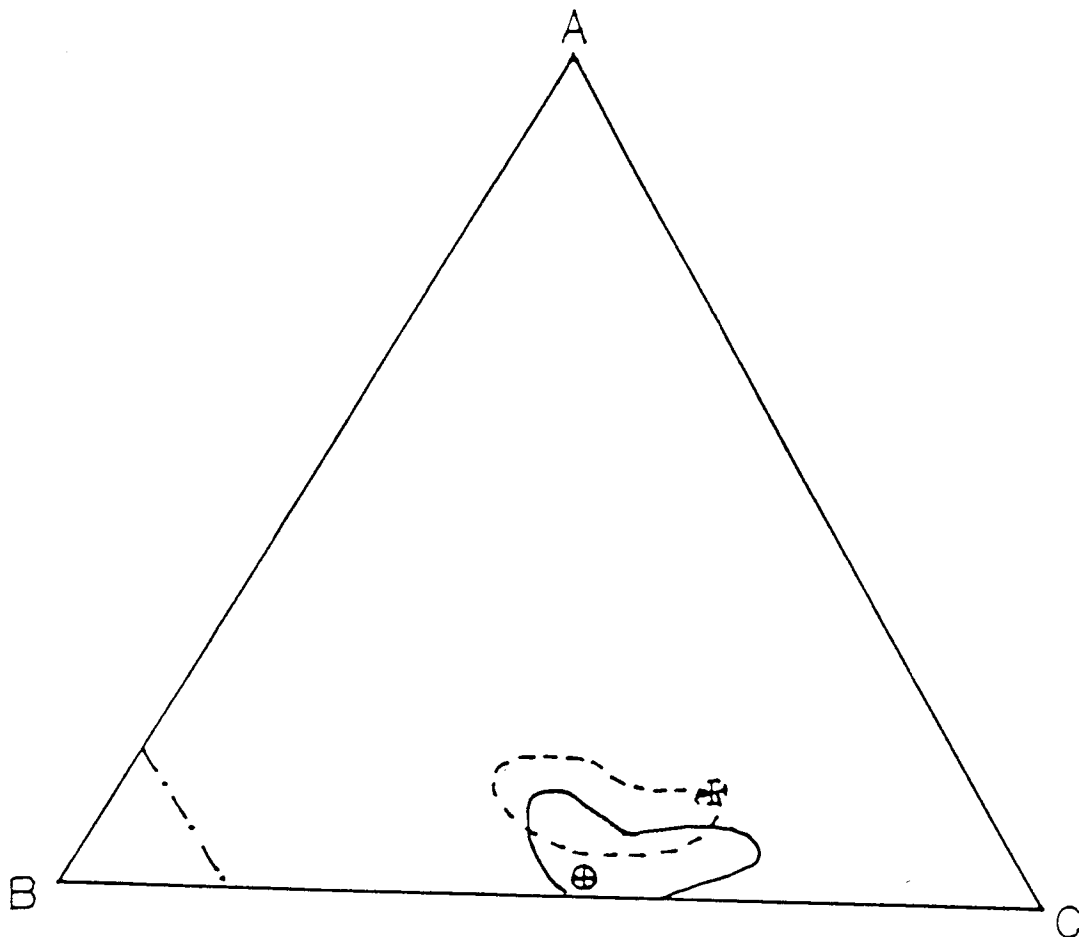
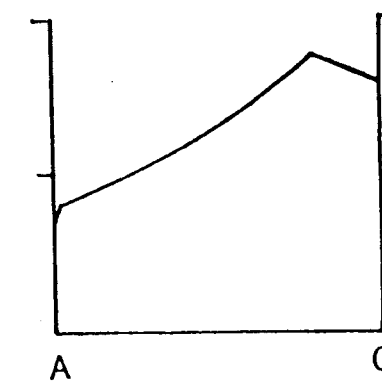
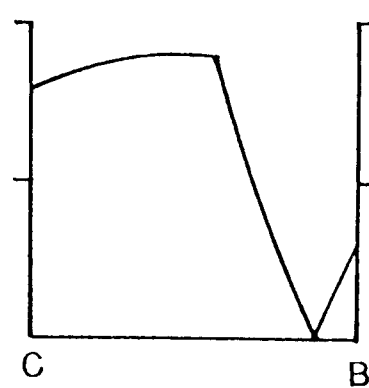
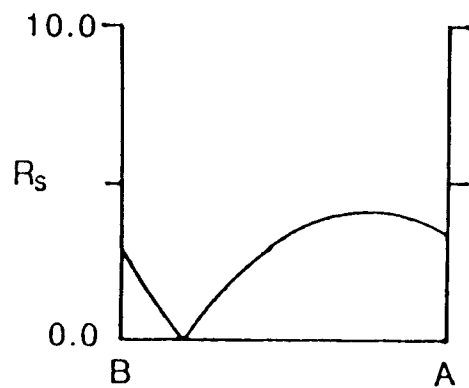
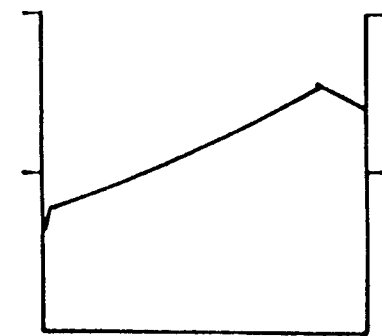
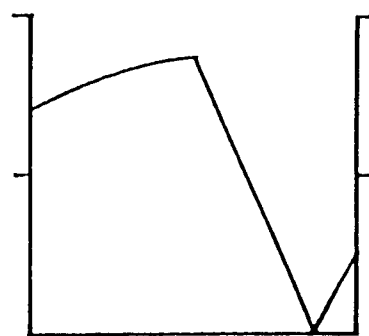
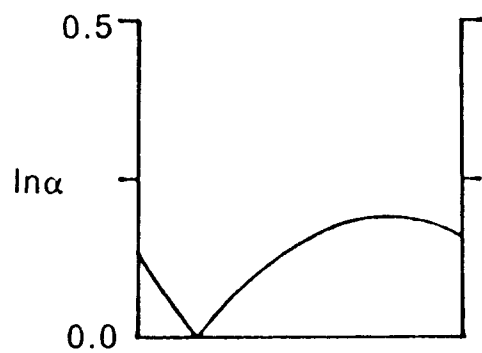


Fig. IV.10 (a) The results of the simplified and original WPCO methods applied to test case 8 of Table 9. (—) Global optimum area of the minimum $\ln\alpha$ surface. (---) Global optimum area of the minimum R_s surface. (— · —) Valley of the minimum separation response surface ($\ln\alpha = 1$, $R_s = 0$). (\oplus) result of the original WPCO method. (\otimes) result of the simplified WPCO method. (b), (c) and (d) are the $\ln\alpha$ and R_s window diagrams along edges AB, BC and AC, respectively.



(b)

(c)

(d)

Figure IV.10 continued

different capacity factors are large. This may be the cause for the large difference between the results of the simplified and original WPCO methods. However, the results still are acceptable as good starting points for a fine tuning process to more accurately locate the global optimum.

Finally, the original case of Table IV.5 is used as a test case, Fig. IV.11. In this case, the capacity factors of the solutes which are the worst separated peak pairs are in the range of 2 to 9 (Table IV.11). However, the $\ln a$ and R_s window diagrams and the minimum response surfaces are still similar (Fig. IV.11). The differences of the corresponding peaks and valleys are within 3% in eluent composition. The difference between the results of the simplified and original WPCO methods is within 2% in eluent composition.

Overall, in the separation of simple samples in which the capacity factors of some solutes of a sample are below 3 (even 2 in some cases), the differences between the results of the simplified and original WPCO methods are small and acceptable in most of the cases. However, when using the simplified WPCO method instead of the original WPCO method, consideration should be given to insure that the advantage of fewer experimental measurements outweighs the potentially reduced accuracy in predicting the location of the region of the global optimum.

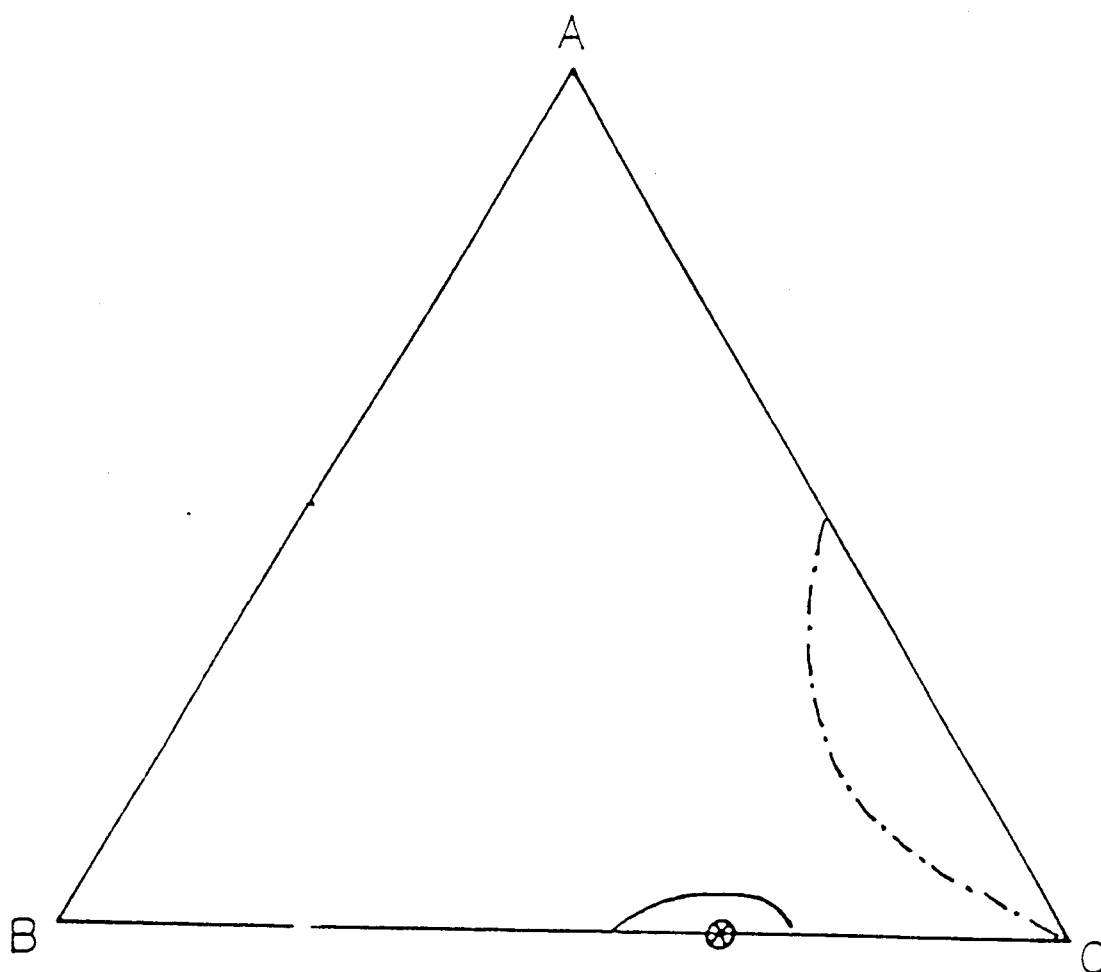
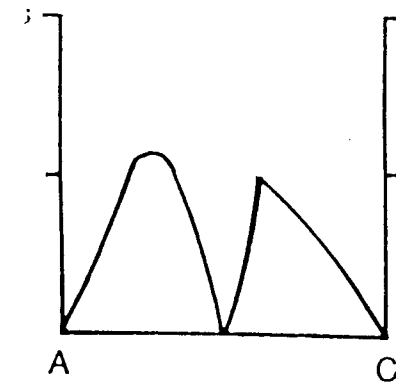
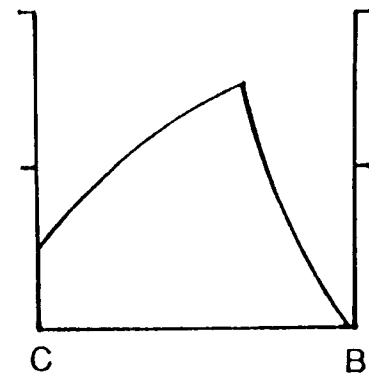
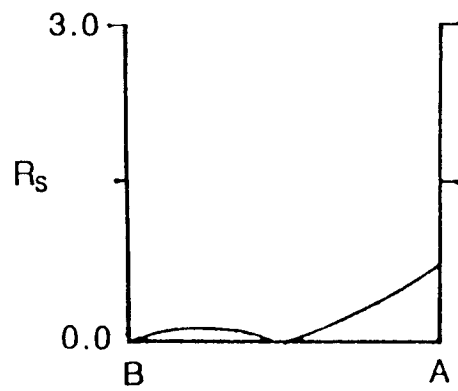
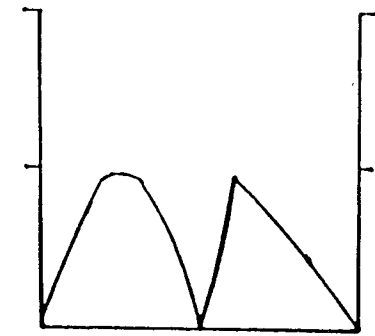
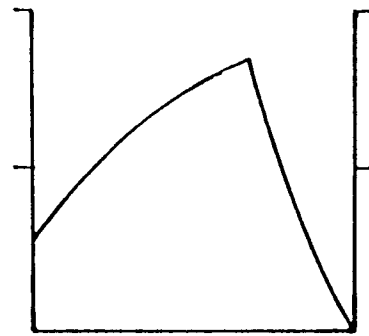
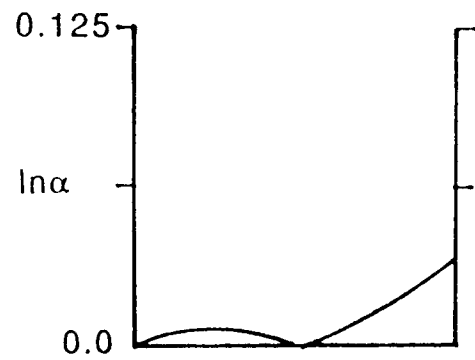


Fig. IV.11 (a) The results of the simplified and original WPCO methods applied to test case of Table 3. (—) Global optimum area of the minimum $\ln\alpha$ surface. (---) Global optimum area of the minimum R_s surface. (-·-) Valley of the minimum separation response surface ($\ln\alpha = 0$, $R_s = 0$). (⊗) result of the original WPCO method. (⊕) result of the simplified WPCO method. (b), (c) and (d) are the $\ln\alpha$ and R_s window diagrams along edges AB, BC and AC, respectively.



(b)

(c)

(d)

Figure IV.11 continued

TABLE IV.11.

CAPACITY FACTORS OF PEAKS FOR THE WORST-SEPARATED PEAK PAIRS AT THE GLOBAL OPTIMUM OF EACH EDGE OF THE ORIGINAL CASE IN TABLE 5.

	EDGE*									
	AB		BC				AC			
Peak No.**	6	7	3	4	6	7	6	7	8	9
k'	4.6	4.7	2.2	2.5	4.6	5.2	5.4	6.0	8.5	9.1

* See the footnotes of Table 5 for the notation of A, B and C.

** The number is the same as thst in Table 5.

Conclusion

Compared with the original WPCO method, the simplified WPCO method needs fewer experimental measurements and avoids the error produced in the measurement of the column dead volume. When the capacity factors of all the solutes are greater than 6, the results of the simplified and original methods are nearly identical. In the separation in which the capacity factors of solutes are less than 6, the simplified WPCO method is satisfactory in less complex, less critical applications.

References

1. The first paper of this thesis.
2. J. W. Weyland, C. H. P. Bruins and D. A. Doornbos, *J. Chromatogr. Sci.*, 22(1984)31.
3. J. L. Glajch, J. J. Kirkland, K. M. Squire and J. M. Minor, *J. Chromatogr.*, 199(1980)57.
4. PESOS: Perkin-Elmer Solvent Optimization System.
5. H. Colin, A. Krstulovic, G. Guiochon and J. P. Bounine, *Chromatographia*, 17(1983)209.
6. R. J. Laub and S. J. Madden, *J. Liq. Chromatogr.*, 8(1985).
7. R. E. Boehm and D. E. Martire, *J. Phys. Chem.*, 84(1980)3620.
8. D. E. Martire and R. E. Boehm, *J. Phys. Chem.*, 87(1983)1045.
9. H. A. H. Billiet, J. P. J. Van Dalen, P. J. Schoenmaker and L. De Galan, *Aanl. Chem.*, 55(1983)847.
10. A. J. Hsu, R. J. Laub and S. J. Madden, *J. Liq. Chromatogr.*, 7(1984)615.
11. P. Jones and C. A. Wellington, *J. Chromatogr.*, 213(1981)357.
12. The first paper in this thesis.
13. P. Jones and C. A. Wellington, *J. Chromatogr.*, 213(1981)375.
14. R. P. W. Scott, *Techniques of Chemistry, Vol. XI, Contemporary Liquid Chromatography*, Wiley, New York, 1976, p.25.
15. J. L. Glajch, J. J. Kirkland and L. R. Snyder, *J. Chromatogr.*, 238(1982)269.
16. G. M. Landers and J. A. Olson, *J. Chromatogr.*, 291(1984)51-57.

17. G. D'agostino, F. Mitchell, L.Castagnetta, and M. J. O'hare, J. Chromatogr., 305(1984)13-26.
18. S. J. Costanzo, J. Chromatogr. Sci., 24(1986)89-93.
19. J. L. Glajch, J. J. Kirkland, K. M. Squire and J. M. Minor, J. Chromatogr., 199(1980)57.
20. R. D Snee, Chemtech, 11(1979)702.
21. J. L. Glajch, J. J. Kirkland, J. Chromatogr., 218(1981)299.
22. L. R. Snyder, J. J. Kirkland, Introduction to Modern Liquid Chromatography, 2nd., Wiley, New York, 1979, p.36.

V. Metabolism of Nefopam in Greyhound

by

Xiao Chen and Edward H. Piepmeier*

Department of Chemistry

Oregon State University

Corvallis, OR 97331

and

A. Morrie Craig

College of Veterinary Medicine

Oregon State University

Corvallis, OR 97331

For submission to the Drug Metabolism and Deposition.

Abstract

Two new metabolites of nefopam as well as two previously discovered metabolites have been isolated from the urine of greyhounds given nefopam. The metabolites were extracted from urine by a one step liquid-liquid extraction. The residues were cleaned up and pre-separated by normal phase flash chromatography using methanol/chloroform (1:20, v/v) as the eluent for cleaning up and methanol/chloroform (1:4, v/v) as the eluent for pre-separation. Then, metabolites were separated by HPLC on a normal phase column (Ultrasphere) using isopropane/chloroform/hexane (5:45:1, v/v/v) as a mobile phase. The structure of the first new metabolite was determined by MS and NMR spectrometric analysis as 3,4,5,6,-tetrahydro-5-methyl-1-(16-methoxyl-17-hydroxyl)phenyl-1H-2,5-benzoxazocine. The second metabolite's structure was determined by MS. There is one more methoxyl group in the 1-phenyl ring than in the first metabolite. In greyhounds, at a dose of 2 mg/kg, the main metabolic pathway is aromatic hydroxylation followed by O-methylation, but, at a dose of 30 mg/kg, the main metabolic pathway is oxidation in the non-aromatic ring.

Introduction

Nefopam (Acupan), 3,4,5,6-tetrahydro-5-methyl-1-phenyl-1H-2,5-benzoxazocine hydrochloride (Fig. VI.1), is a member of non-narcotic analgesic¹ with an unique heterocyclic structure. It was originally synthesized by Klohe et al². In 1975, nefopam was first introduced as an analgesic drug in 1975 in Mexico³. Nefopam is a centrally acting non-narcotic analgesic with both supraspinal and spinal sites of reaction. Currently, it is used for relieving postoperative or musculoskeletal pain in clinical settings. The drug has been used nefariously as a doping substance in thoroughbred horse racing⁴ as well as in greyhound racing.

In humans, seventy-five percent of nefopam binds with protein. Most of the nefopam is transformed into metabolites, and more than 95% of nefopam is excreted in the urine in metabolic forms. For healthy subjects, the elimination half-life is 3 to 8 hours (mean 4 hours) after an oral or intravenous dose⁵. The metabolites of nefopam have been studied in humans, and 11 metabolites have been found^{6,7}. However, the study of the metabolism of nefopam in greyhounds has not been published. In this article, we describe the identification as well as extraction, isolation and purification of metabolites of nefopam from greyhound urine. Four metabolites have been identified in urine. Two of these four metabolites have not been found elsewhere.

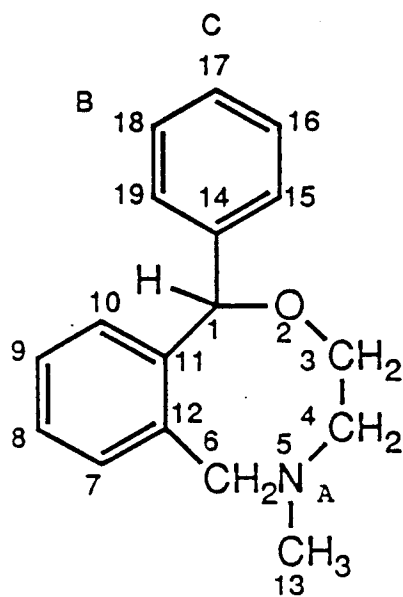


Fig. V.1 Nefopam

The structure of one of the newly discovered metabolites was determined by the mass spectroscopy (MS) and NMR. The structure of the other metabolite was determined by MS.

Materials and Methods

Chemicals. Nefopam and β -glucuronidase were obtained from the Sigma Chemical Company. All the organic solvents were HPLC grade. The inorganic chemicals were reagent grade. Deuterated Aceton and Chloroform were obtained from the Cambridge Isotope Laboratories.

Administration and Urine Collection. For the purpose of studying the metabolic pathways in greyhounds at a dose of 2 mg/kg, six healthy male and female greyhounds, weighing 25 kg to 31 kg, were used. Urine samples were collected at 2, 4, 6, 8, 10, 12 and 24 hours after the oral administration. The urine samples were stored at -20°C until analyzed.

For the purpose of studying the effect of the high nefopam dose on the metabolic pathways, The same six greyhounds were used. A single oral dose of 30 mg/kg of nefopam was given. The urine was collected in the 12-hour period immediately after the administration. The urine sample was stored at -20°C until analyzed.

For the purpose of NMR analysis of the new metabolites, a large amount of metabolites need to be separated from urine. The same six greyhounds were given a single oral dose of 2 mg/kg of nefopam each day for three successive days. A complete collection of urine was obtained during the 4 days following the

first oral administration. Pooled urine samples were stored at -20°C until analyzed.

Sample Preparations for TLC and GC/MS Analysis. For the extraction of basic organic compounds from the urine sample, 12 ml of urine was adjusted to pH 9.0 with an addition of 3.0 M NH_4OH . The sample was mixed with 6 ml of dichloromethane. Then, the aqueous phase was discarded, and the organic phase was mixed with 2 ml of 0.2 N sulfuric acid. The organic layer was discarded, and the aqueous phase was mixed with 2 ml of 0.6 N NH_4OH . The aqueous solution was mixed with 6 ml of dichloromethane. The organic phase was separated from the aqueous phase and evaporated to dryness under gentle nitrogen flow at 35°C. The residue was subjected to TLC and GC/MS.

For hydrolysis of conjugates, 5 ml of the urine was mixed with 2 ml of 0.1M sodium acetate buffer (pH 5.0) and 1 ml of β -glucuronidase (5000 units/ml), and the mixture was incubated at 65°C for 3 hours. Then, the enzyme treated sample was adjusted to pH 9.0 by adding 3.0 M NH_4OH . The sample was mixed with 5 ml of dichloromethane. The aqueous phase was discarded, and the organic layer was mixed with 2 ml of 0.2 N sulfuric acid solution. The organic phase was discarded. The aqueous layer was mixed with 2ml of 0.6 N NH_4OH , and mixed with 5 ml of dichloromethane. The organic layer was separated from the aqueous phase and evaporated to dryness under gentle nitrogen flow at 35°C. The residue was subject to TLC and GC/MS.

Isolation and Detection of Metabolites by TLC and

GC/MS. The residue resulted from the above procedure was dissolved in a small amount dichloromethane to make a saturated solution. The sample was subjected to TLC and GC/MS. TLC was carried out on silica gel 60 F254 plates (Merck precoated) with the solvent: propionic acid/methanol/chloroform 10:18:72 (v/v/v). A spray of Dragendorff's reagent revealed the metabolites to be alkaloidal bases. Each metabolite spot was also scraped off of the TLC plate and soaked in about 1 ml of pH 9.0 NH₄OH solution. The free metabolites in the aqueous solution were extracted by Dichloromethane. The organic phase was separated from the aqueous phase and evaporated to dryness under gentle nitrogen flow at 35°C. The residues were kept at 4°C until GC/MS analysis.

Hydrolysis and Extraction Metabolites for NMR Analysis.

500 ml of a pooled urine sample was mixed with 200 ml of 0.1M sodium acetate buffer (pH 5.0) and 100 ml of β -glucuronidase(2500 units/ml), and the mixture was incubated at 37°C for 8 hours.

After the incubation, the hydrolyzed urine sample was adjusted to pH 8.5 with an addition of 8.0 M NH₄OH solution. Then, the sample was extracted 5 times with 200 ml of dichloromethane. Organic phases were removed and rotorvaporated to dryness at

40°C. A total of 13.5 liters of urine had been processed by this procedure. The residue was stored at 4°C until chromatographed.

Fractionation and purification of Metabolites for NMR

Analysis. Flash chromatography columns (0.9 x 10in., silica gel for flash chromatography) were used to fractionize the residue. For each run, about 20 mg of residue was dissolved in a small amount of 5:95 (v/v) methanol/chloroform solvent to make a saturated solution; the sample solution was loaded onto the column. The eluent, 5:95 (v/v) methanol/chloroform, was used to elute most yellow none-metabolite substances. After most of these yellow none-metabolite substances were eluted, 20:80 (v/v) methanol/chloroform was used to fractionize the sample left in the column. Through the cleaning up and fractionizing process, compressed nitrogen was used to drive the eluent through the column. The pressure of the nitrogen was adjusted until the eluent head above the stationary phase dropped at the rate of 2.0 in./min. The TLC method which is described above was used to check for the presence of the metabolites in the subfractions. The subfractions which contained the new metabolite were evaporated to dryness under gentle nitrogen flow at 35°C. The residues were kept at -60°C until further separation by HPLC.

HPLC. A liquid chromatograph (ALTEX) equipped with a model 110A pump, and a model 420 UV detector set at 254nm was used. An ALTEX ULTRASPHERE 4.6 x 250mm Si 5u column was used for

the separation of the new metabolite. The mobile phase composition was 5:45:1 (v/v/v) isopropanol/chloroform/hexane, and the flow rate was 1 ml/min. The new metabolite peaks (R_T 8.7min and R_T 11.7min) were collected separately. The collections were evaporated to dryness at 40°C under gentle nitrogen flow. The dry metabolites were kept at -60°C until analyzed by NMR or GC/MS.

Mass Spectrometry. Electron impact spectra were obtained with a Finnigan-5100 quadrupole mass spectrometer. Samples were introduced into the MS by gas chromatography. A DB5 (30m x 0.32mm ID x 0.25 μ m df) capillary column was used. The temperature program used for the residues extracted from urine was: initial temperature 100°C, then, increase to 260°C at the rate of 5°C/min, and constant at 260°C for 30 minutes. The temperature program used for the samples after flash chromatography was: initial temperature 230°C, then, increase to 260°C at the rate of 10°C/min. and constant at 260°C for 10 minutes.

The chemical ionization spectrum was obtained with a Finnigan-4023 quadrupole mass spectrometer. Methane was used as a reactant gas. The samples were introduced into the MS by gas chromatography. A DB5 (30m x 0.32mm ID x 0.25 μ m) capillary column was used. The temperature program was the same as the second program described in above paragraph.

The high resolution mass spectrometer data were obtained with a Kratos MS50TC. The sample was directly introduced into the mass spectrometer by a probe.

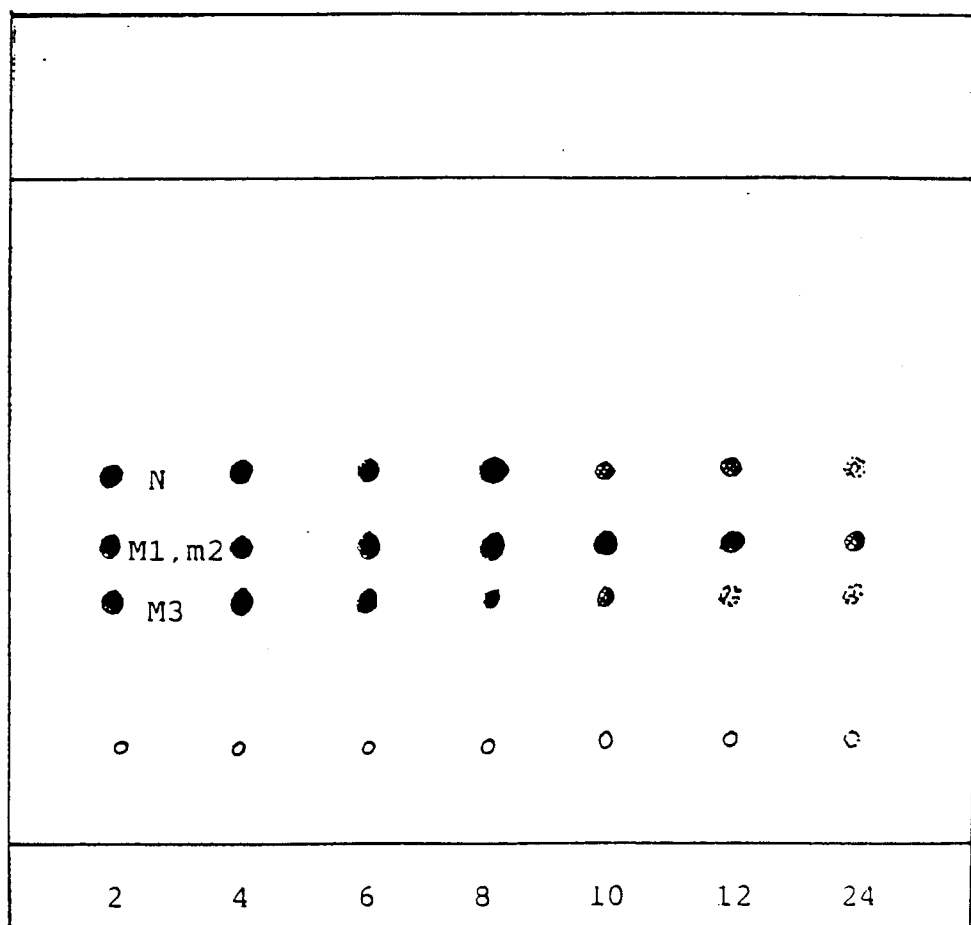
NMR Spectroscopy. NMR spectra were obtained with a Bruker AM400 (400MHz) fourier transform NMR spectrometer. To obtain the spectra of nefopam, about 0.3g of nefopam was dissolved in 50 ml of water, then the solution was adjusted to pH 8.5 with 3.0 M NH_4OH solution. Nefopam (not combined with hydrochloride) was extracted twice from the basic solution with 50 ml of dichloromethane. The organic layer was removed and evaporated at 40°C under gentle nitrogen flow. The residue was 3,4,5,6-tetrahydro-5-methyl-1-phenyl-1H-2,5-benzoxazocine (nefopam). The nefopam was dissolved in deuterated acetone ($\text{C}_3\text{D}_6\text{O}$) or chloroform (CDCl_3) for NMR analysis.

Results

Urinary Metabolites. By the procedure described above, the 2, 4, 6, 8, 10, 12 and 24 hour urine samples were analyzed by TLC and GC/MS for identification of metabolites. TLC results indicated the presence of at least two main metabolites (Fig. VI.2) in the enzyme hydrolyzed urine. For the extract of basic urine (not hydrolyzed), the TLC result showed the presence of two metabolites. A spot which we will call M1 (R_F 0.45) was observed only faintly.

Metabolites M1 and M2. GC/MS result showed that there were two metabolites in the same TLC area. These two metabolites have not been reported found in humans. In the electron ionization (EI) mass spectra, Fig. VI.3, one metabolite exhibited a molecular ion peak at m/z 299, and the other one exhibited a molecular ion peak at m/z 329. These results were confirmed by the chemical ionization (CI) mass spectra of these two metabolites. The structure elucidation of these two metabolites will be discussed in the later part of this section.

Metabolite M3. GC./MS results showed that there was one metabolite in the corresponding TLC spot. The MS of the metabolite was identical with that of nor-nefopam⁷. This metabolite has been found in humans and has not been reported in greyhounds.



Urine collection time (hour)
after drug administration

Fig. V.2 TLC result of extract from enzyme hydrolyzed urine.

(N) nefopam; (M3) nor-nefopam; (●) Dark color;

(⊗) Medium color; (⊗) Light color.

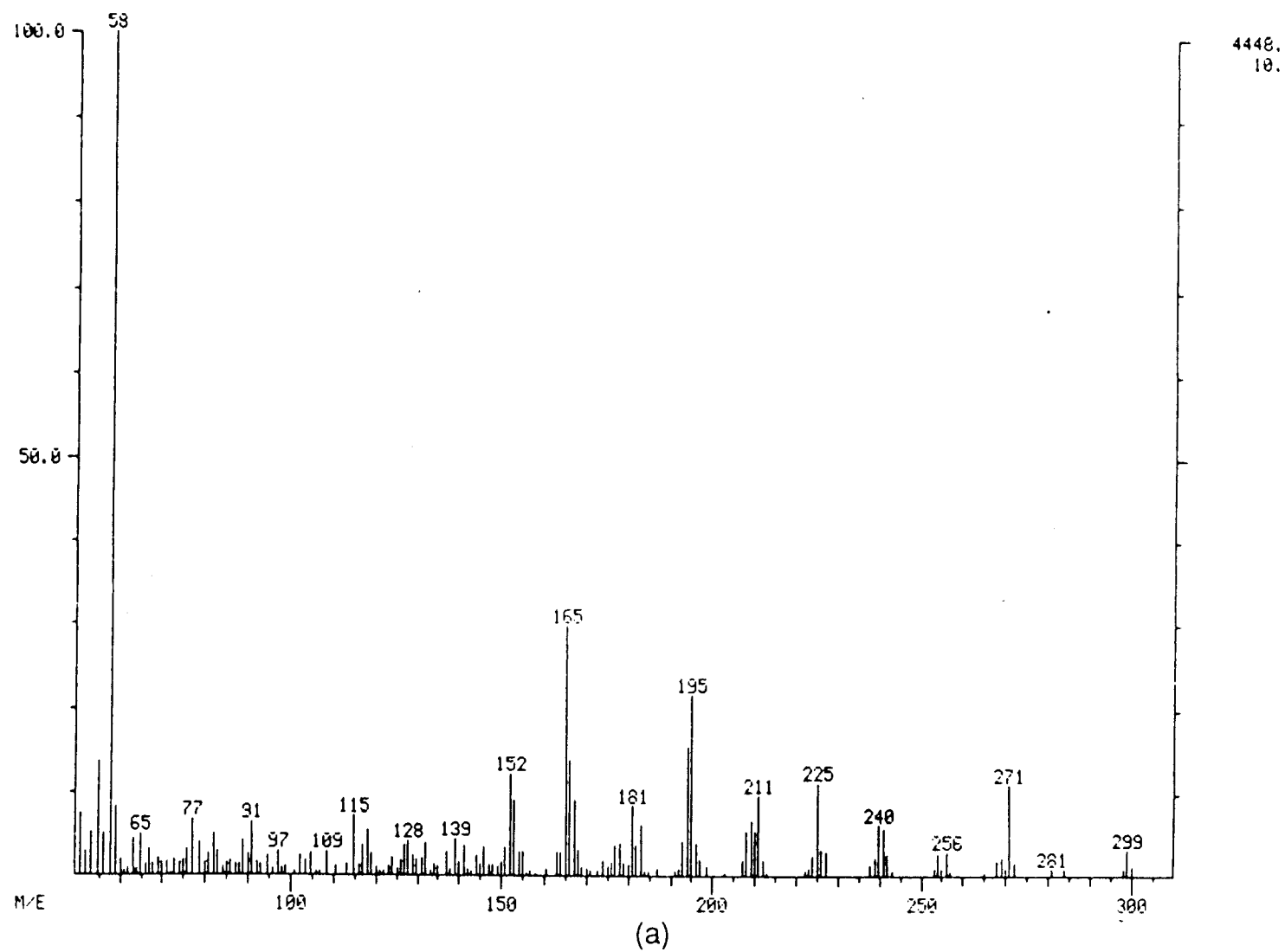
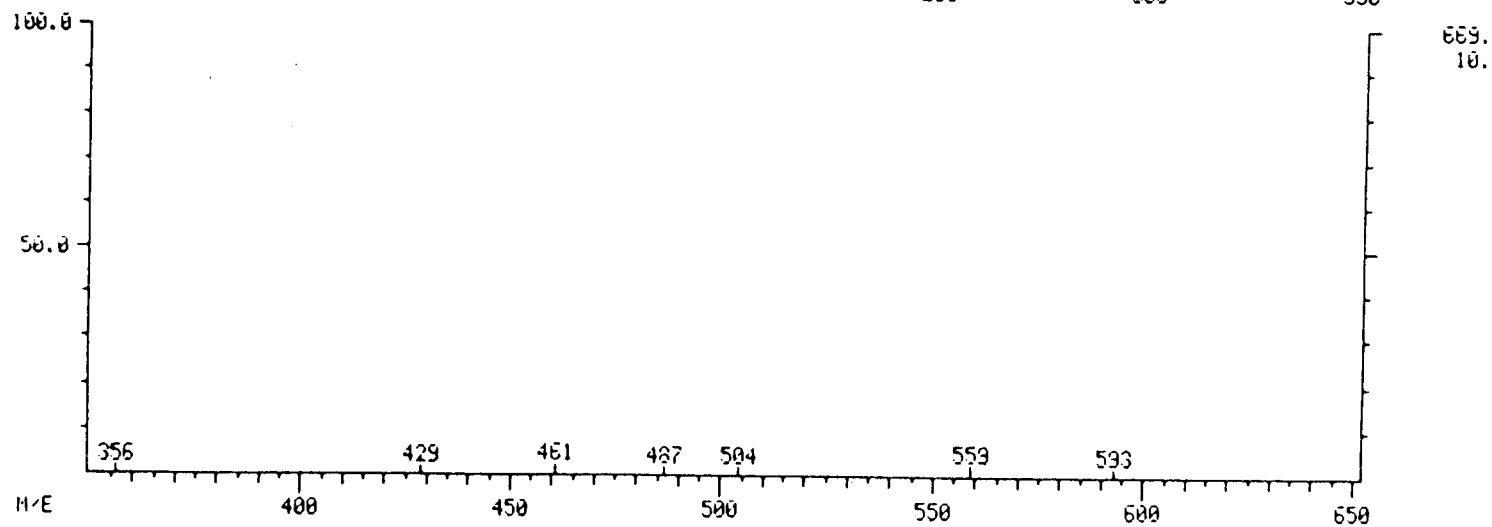
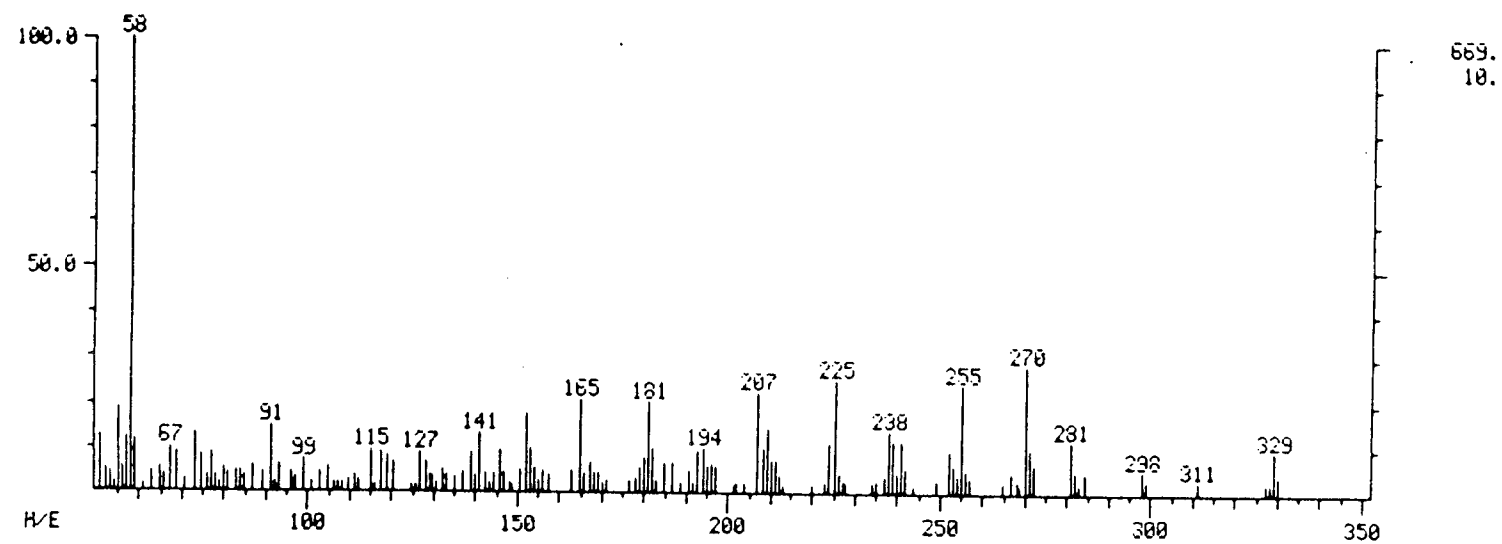


Fig. V.3 (a) EI MS spectrum of M1. (b) EI MS spectrum of M2.



(b)

Figure V.3 continue

Metabolite M4: nefopam-N-oxide. GC/MS of the extract from the enzyme hydroxylized urine showed the presence of the nefopam-N-oxide. However, in the TLC test, the spot which corresponded to nefopam-N-oxide was only sometimes observed in different samples and was always a faint spot at a dose of 2 mg/kg.

GC peak height Ratio of nor-nefopam to M1. In order to identify major metabolic pathways at a dose of 2 mg/kg, the 2, 6, 10, 12 and 24 hour urine samples were used. The peak height ratios of nor-nefopam to M1 are plotted in Fig. VI.4 In the first 24-hour period, the largest ratio is 0.67 at 10 hours. The tendency of the ratio shows that it will become even smaller after the first 24 hours.

Identification of the Major Metabolite at a dose of 30 mg/kg. In order to investigate the effect of different doses on the nefopam metabolism in greyhounds. TLC and GC/MS were used to analyze urine sample collected at a dose of 30 mg/kg. TLC of the enzyme hydrolyzed urine sample showed the spot corresponding to nor-nefopam. However, the spot corresponding to M1 and M2 was barely observed. GC/MS also confirmed that the nor-nefopam was the major metabolite at a dose of 30 mg/kg.

Separation of M1 and M2 for Structure Elucidation. By the isolation procedure described, about 5.5 mg M1 and less than

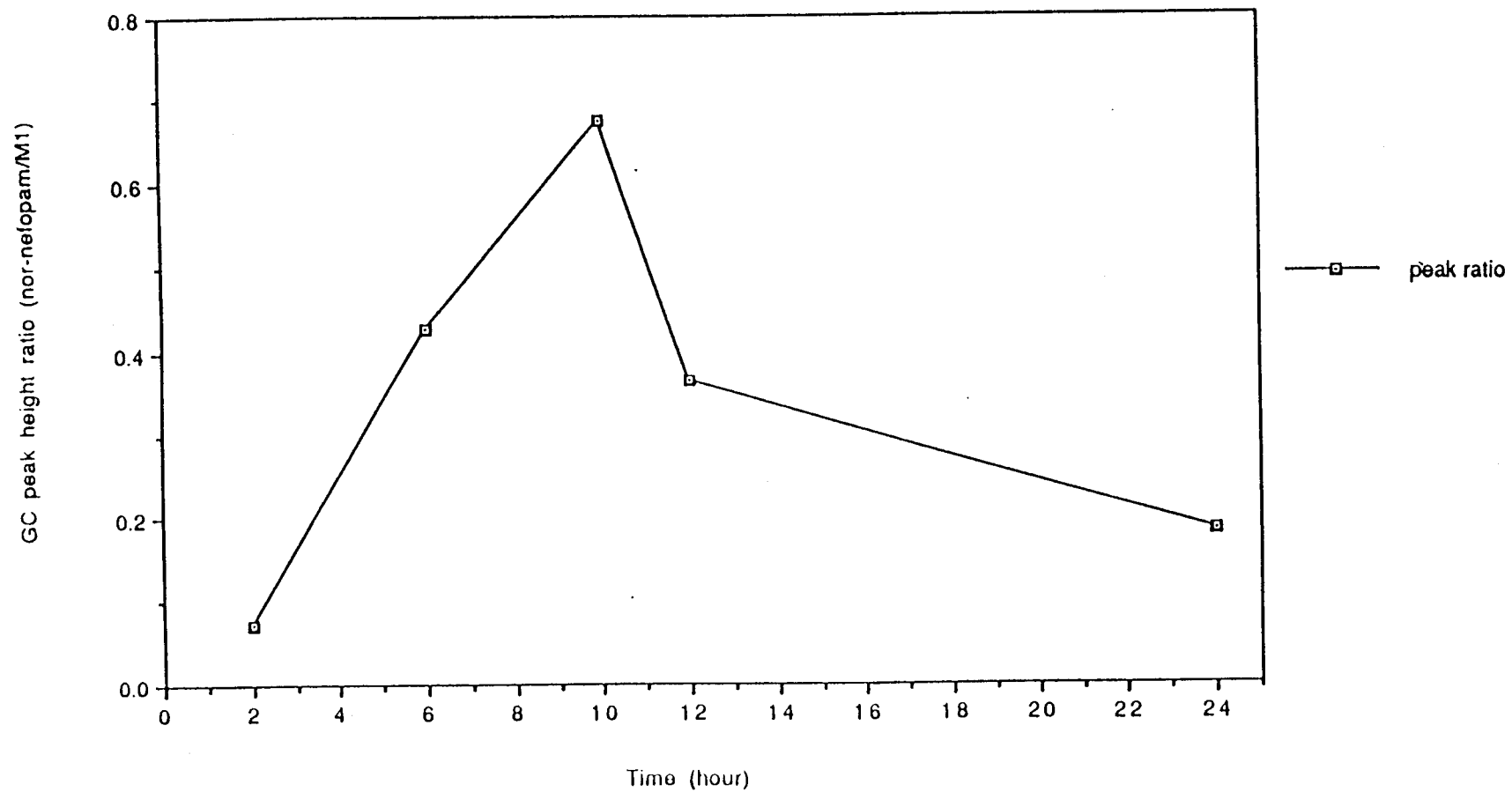


Fig. V.4 GC peak height ratio of nor-nefopam to M1 vs. time.

0.1 mg M2 were separated from the urine collected in four days (13.5 L). Fig. VI.5 shows an HPLC chromatogram of the subfraction from the flash chromatography process. the retention time of M1 was 8.7min, and the retention time of M2 was 11.7min. M1 and M2 gave positive results for silver nitrate reagent⁸ and aqueous ferric chloride reagent for containing phenol groups, and both metabolites showed positive results for Dragendorff's reagent test for amines.

Metabolites M1 and M2 structure Elucidation

Nefopam NMR Spectra Analysis. The appearance of the NMR spectrum of Nefopam is similar to the corresponding spectrum of M1. Therefore the structure of M1 can be determined from NMR analysis by comparison with the spectra of nefopam. Because an extensive analysis of nefopam NMR spectra has not been published, the nefopam NMR spectra are analyzed before the structure elucidation of M1.

From the ¹H NMR (Fig. VI.6a) and COSY (Fig. VI.6b) spectra of nefopam, a number of initial assignments can be made. H1 can be assigned to the downfield singlet signal at 5.8ppm (see H-NMR spectrum in Fig. VI.6a). This assignment is made for two reasons. First, the area of this singlet signal is the only one corresponding to one proton in the chemical shift range below 6ppm. Second, C1 is attached to two aromatic rings and one

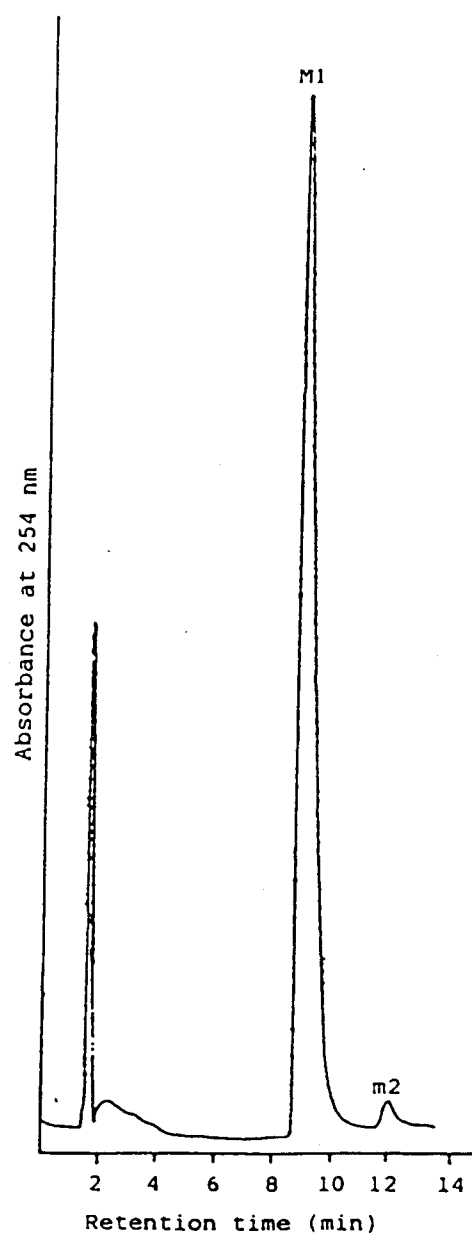


Fig. V.5 HPLC profile of the subfraction of the flash chromatography process.

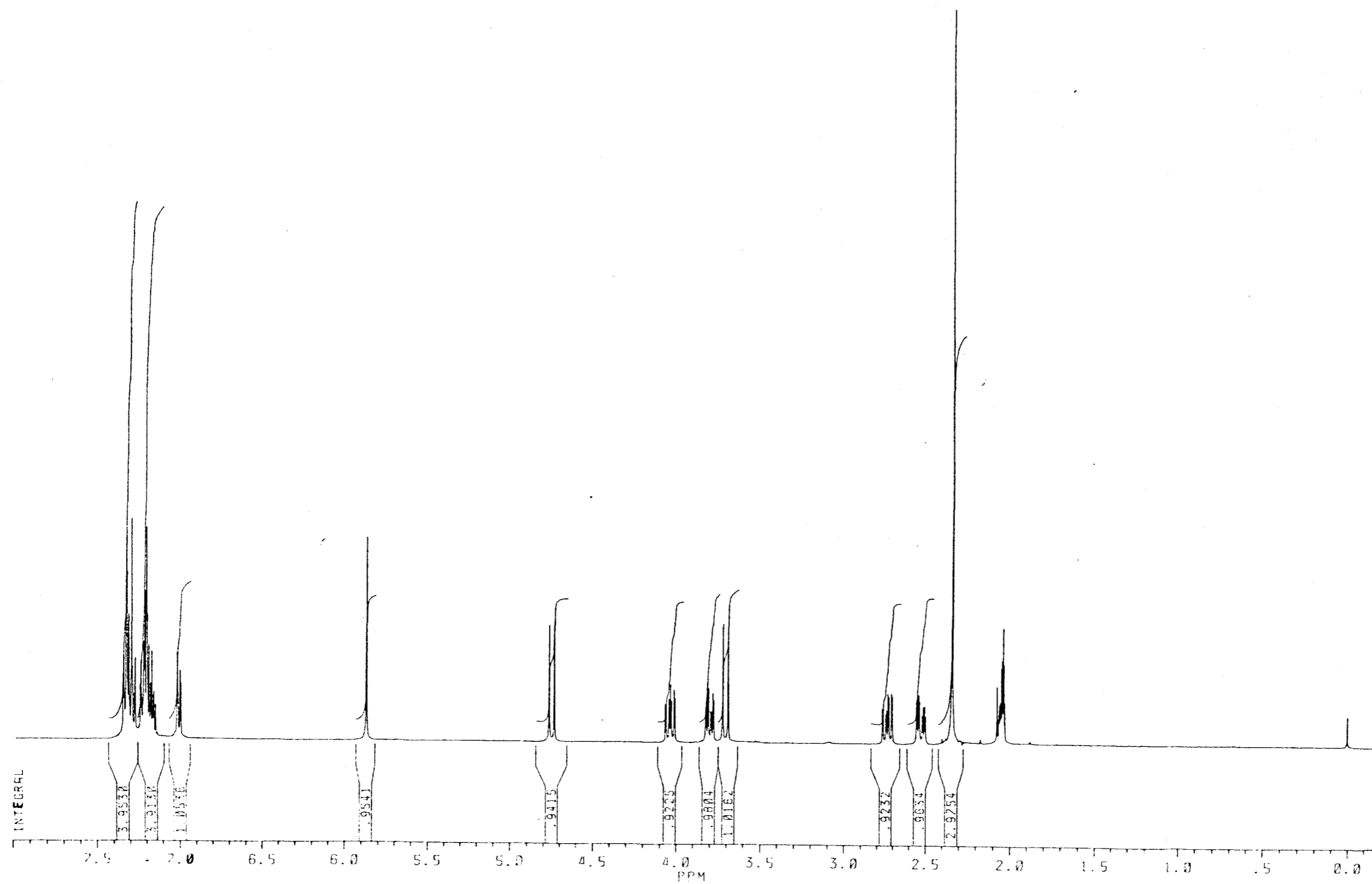


Figure V.6a Proton NMR of nefopam.

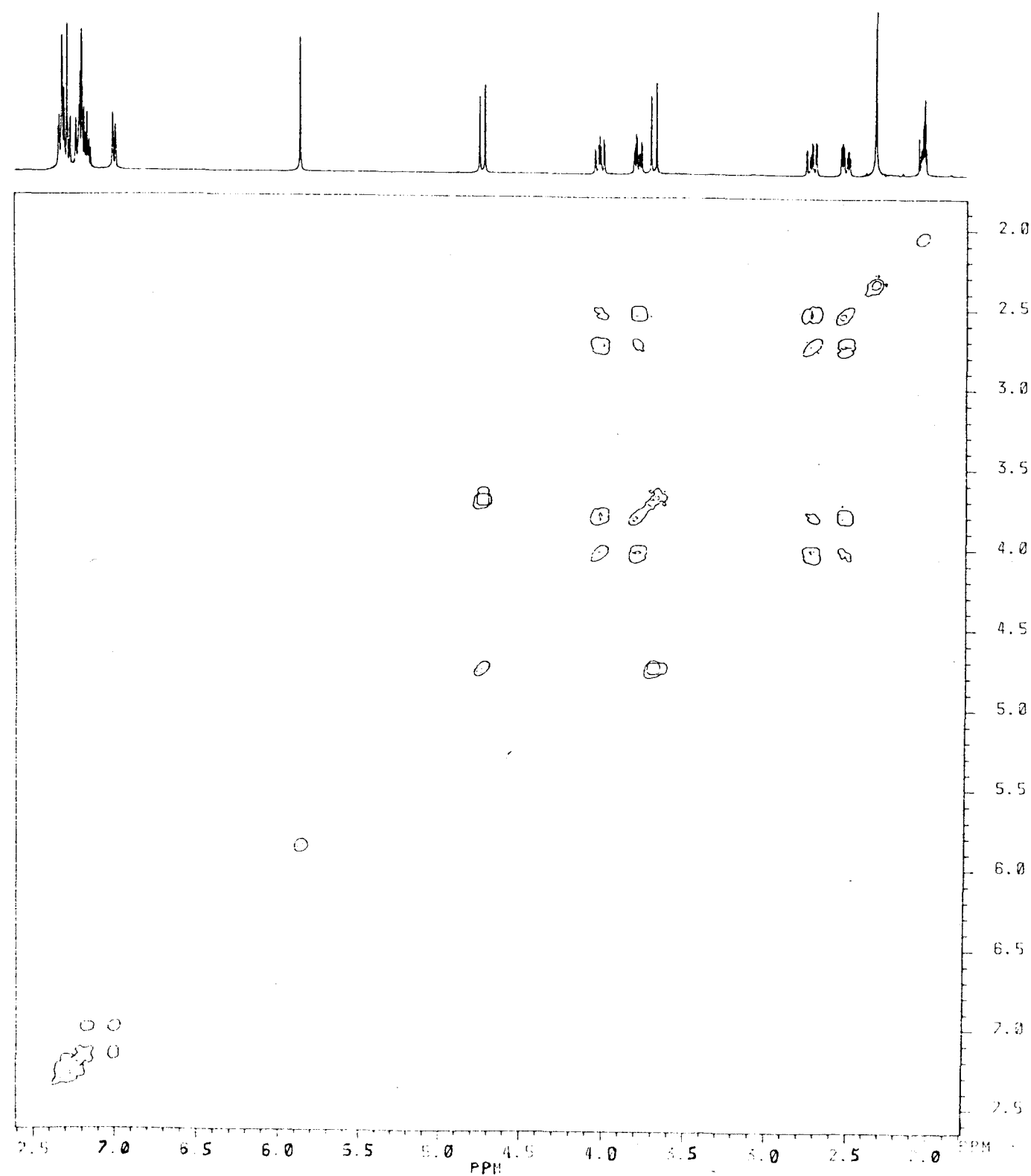


Figure V.6b COSY of nefopam.

oxygen. These electron-withdrawing groups make H₁'s signal shift strongly downfield.

The three methyl group protons (5-CH₃) are assigned to the singlet at 2.3ppm because only the area of this singlet signal corresponds to three protons. This slight downfield shift is consistent with the minor electron withdrawing power of the nitrogen attached to this methyl group.

The COSY spectrum (Fig. VI.6b), which shows the coupling relationship among protons, shows that two doublet signals at 3.7 and 4.7ppm are correlated with each other. The only fragment of nefopam which can produce these coupling signals is the isolated geminal protons on C₆. In the ¹H NMR spectrum (Fig. VI.6a), the coupling constant values for these two doublet signals are the same and in the range for geminal protons. This evidence further confirms that doublets at 3.7 and 4.7ppm are the signals of the two protons on C₆.

The COSY spectrum (Fig. VI.6b) shows four other protons in the range 2.0 to 6.0ppm that constitute a coupling system. These signals can be assigned to the protons attached to C₃ and C₄. Since C₃ is attached to an oxygen and C₄ is attached to a nitrogen, H_{3a} and H_{3b} are assigned to the two downfield multiplets at 4.05 and 3.8ppm; H_{4a} and H_{4b} are assigned to the two upfield multiplets at 2.55 and 2.75ppm. NOE was used to further confirm the above assignments. In NOE, a proton is

irradiated, and this will, in turn, change the signal intensities of the protons which are close, in space, to the irradiated proton. In the NOE experiment, the methyl group (5-CH₃) protons (at 2.3ppm) were irradiated and the signal enhancements at 2.55 and 2.75ppm were observed. Therefore, the protons which correspond to the signals at 2.55 and 2.75ppm are close to the irradiated methyl group, and therefore correspond to H_{4a} and H_{4b}.

Nine aromatic proton signals are located in the aromatic proton chemical shift range (6.9 to 7.5ppm), as expected from the nine aromatic protons from the two aromatic rings on the nefopam structure (see Fig. VI.1).

In the ¹³C NMR spectrum (Fig. VI.7), five signals are located in the non-aromatic chemical shift range and correspond to five non-aromatic carbons in the nefopam structure. Because there are two pairs of symmetric aromatic carbons, each of which produces one signal, ten signals, which are located in the aromatic chemical shift range, correspond to the twelve aromatic carbons

M1 Structure Elucidation

MS Spectra Analysis. The molecular weight of M1 was determined from the chemical ionization mass spectrum. The m/e value of the MH⁺ peak, the highest intensity peak, is 300. Therefore, the molecular weight of M1 is 299. A MC₂H₅⁺ peak at

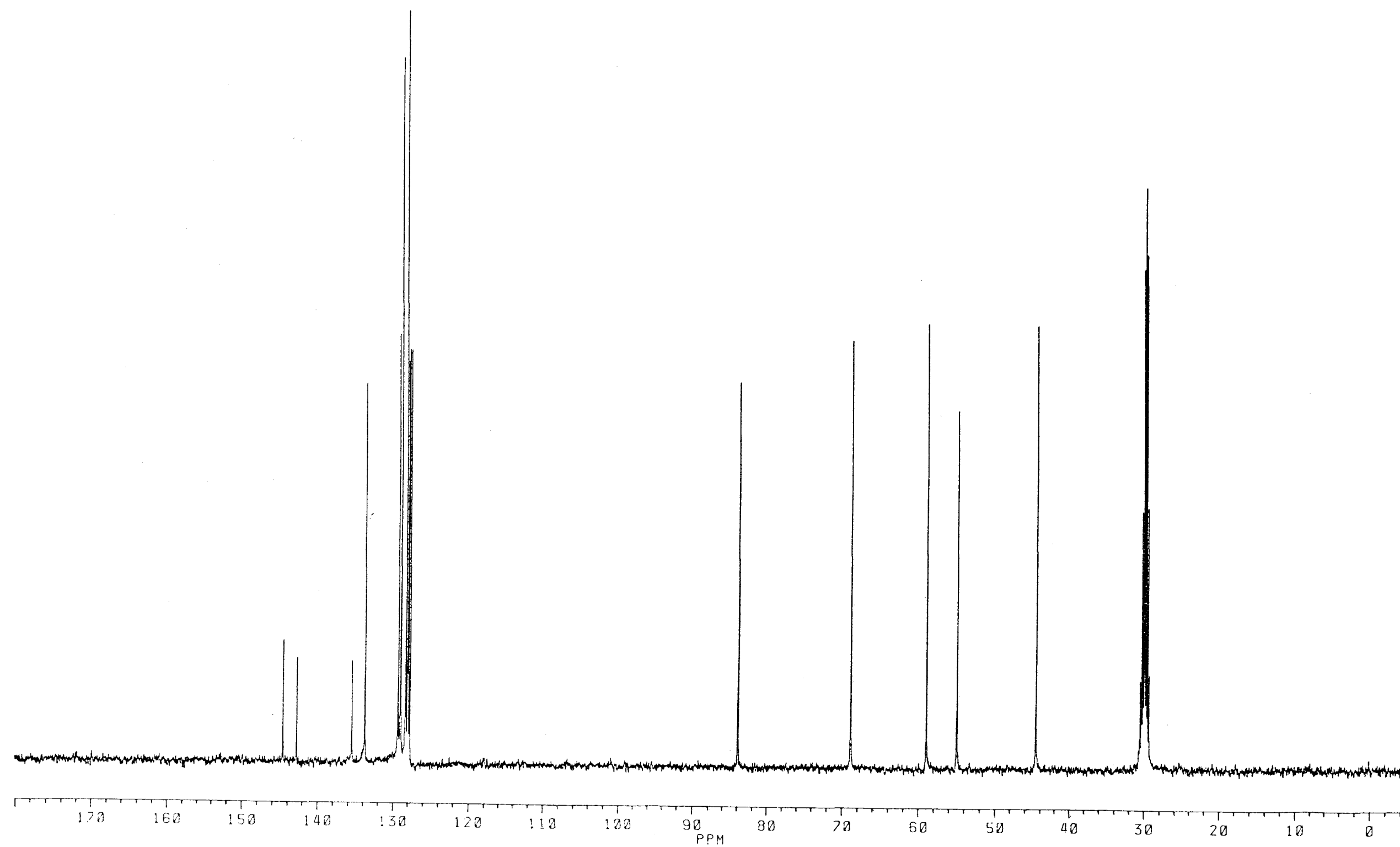


Figure V.7 Carbon NMR of nefopam.

m/e 328 and a MC_3H_5^+ peak at m/z 340 are also observed, which confirms that the m/e 300 peak is the MH^+ peak.

The molecular formula was determined from high resolution MS, which gives a molecular weight of 299.15256. This corresponds to the molecular formula $\text{C}_{18}\text{H}_{21}\text{O}_3\text{N}$ (mass deviation 1.4ppm). This result is supported by the data obtained from the ^{13}C NMR spectrum (Fig. VI.9) which shows M1 has 18 carbon atoms.

In the electron impact mass spectrum (Fig. VI.3) of M1, the molecular ion peak at m/z 299 was observed. The spectrum displayed a small fragment ion at m/z 284, which is generated by losing a methyl group. Another small fragment ion was observed at m/z 281, involving the removal of 1 H_2O . This peak indicates that the metabolite molecule has a hydroxyl group. Because the overall appearances of the nefopam⁷ and M1 spectra are similar, the structures of these two compounds may also be similar.

NMR Spectra Analysis. By comparing the NMR spectra of nefopam and M1, some information about the structure of metabolite M1 can be obtained. In the ^1H NMR (Fig. VI.8a) and ^{13}C NMR (Fig. VI.9) spectra of M1, the chemical shifts and splitting patterns of all the signals which correspond to the $-\text{CH}-\text{O}-\text{CH}_2-\text{CH}_2-\text{N}(\text{CH}_3)-\text{CH}_2-$ fragment are similar to those in the nefopam spectra, except for some slightly different chemical shift values. This means that M1 has the same 8-member ring that nefopam has.

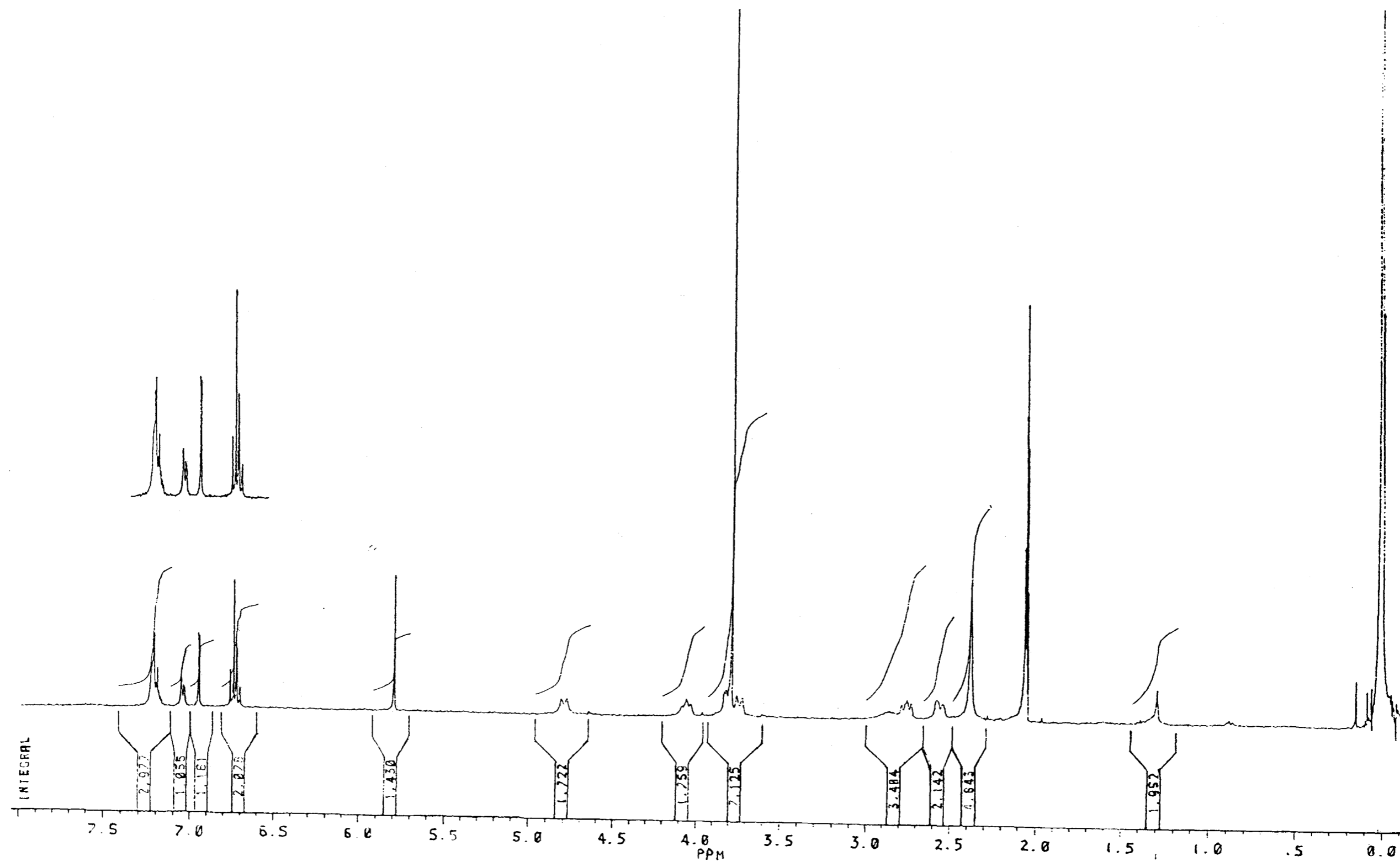


Figure V.8a Proton NMR of M1.

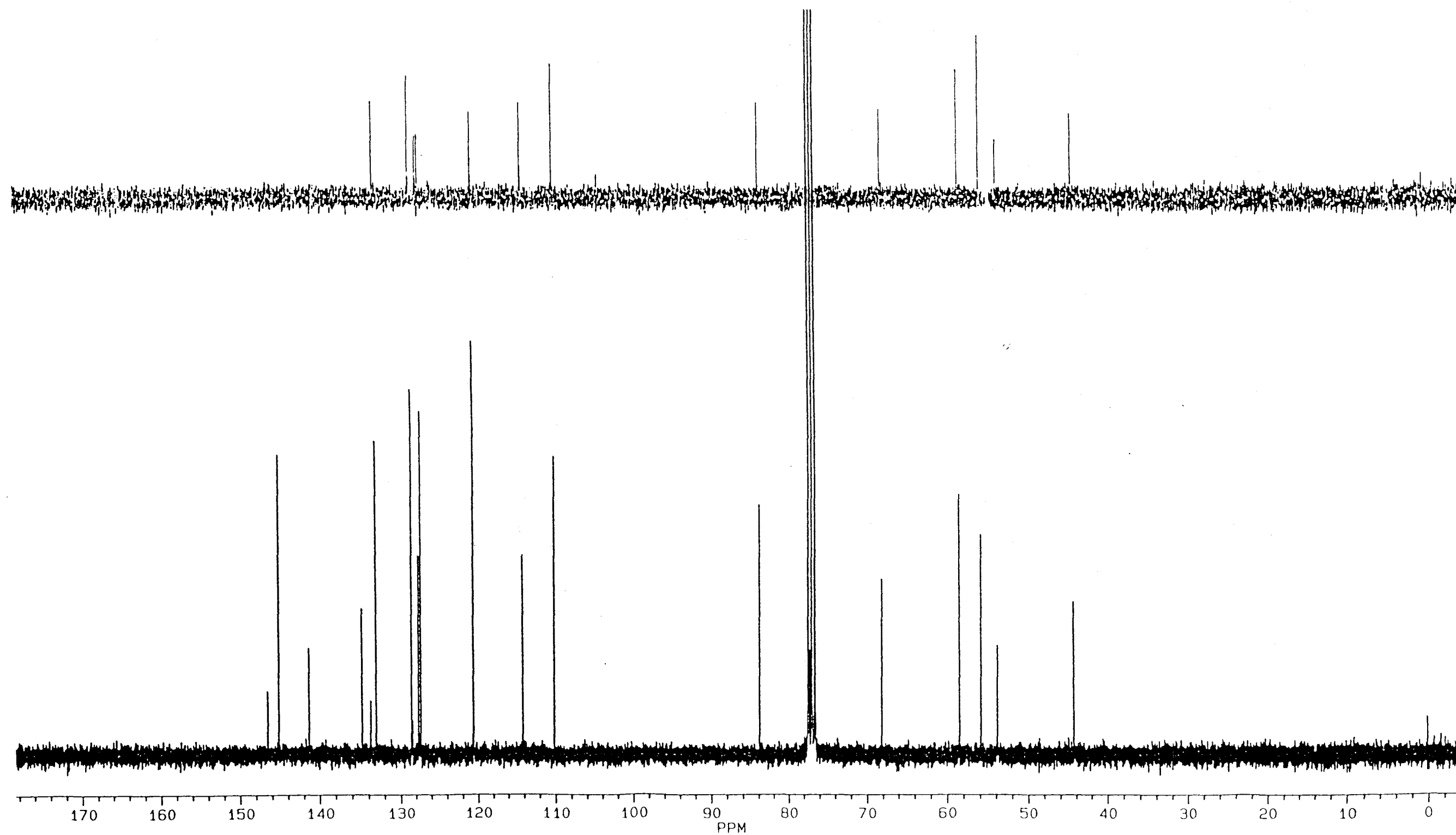


Figure V.9 Carbon NMR (lower) and DEPT 45° of M1.

In the aromatic chemical shift range, the signals of seven protons are observed for M1 in the ^1H NMR (Fig. VI.8a) instead of nine for nefopam. Twelve aromatic carbon signals are observed in the ^{13}C NMR spectrum (Fig. VI.9) for M1 (instead of ten for nefopam), and the DEPT 45 spectrum, which only shows a signal of a proton-attached carbon, shows seven aromatic carbons are attached to protons; this further confirms that there are seven protons attached to aromatic rings.

The COSY spectrum (Fig. VI.8b) shows that the seven aromatic protons constitute two coupling systems. One of them consists of three protons, the other one consists of four protons. Because protons on different aromatic rings cannot couple to each other, and this molecule has two coupling systems, therefore, this further confirms that M1 has two aromatic rings; one ring has three protons; the other ring has four protons. Because M1 has seven aromatic protons instead of nine in the nefopam structure, there are two more substituent groups attached to the aromatic rings in M1. This is the only difference between the structures of nefopam and M1.

In the ^1H NMR (Fig. VI.8a) and ^{13}C NMR (Fig. VI.9) spectra the signals corresponding to a methoxyl group (singlet 3.75ppm in ^1H -NMR; 55.8ppm in ^{13}C -NMR) are observed, hence one substituent is a methoxyl group. By subtracting all the atoms known from the M1 molecular formula $\text{C}_{18}\text{H}_{21}\text{O}_3\text{N}$, we reach the conclusion that the other substituent group is a hydroxyl group.

This conclusion is also supported by, first, the presence of the m/z 281 ($M-H_2O$) peak in the EI mass spectrum; and second, the positive response to $AgNO_3$ reagent⁹ and aqueous ferric chloride reagent¹⁰ of M1.

In order to determine the substituent positions of the methoxyl and hydroxyl groups, the first step is to use the splitting patterns of the aromatic proton signals to deduce the possible substituent positions. In the 1H NMR spectrum (Fig. VI.8a), there is only one aromatic coupling system whose splitting patterns can be observed clearly. This coupling system is called aromatic coupling system 1 (see COSY spectrum in Fig. VI.8b). The other aromatic coupling system is called aromatic coupling system 2. Aromatic coupling system 1 consists of three proton signals, One is a singlet and two are doublets. Aromatic coupling system 2 consists of four proton signals. However, the splitting patterns of most of the signals cannot be observed clearly because most of the signals are overlapped, except for one doublet. The signals whose splitting pattern can be observed clearly are used to deduce the possible substituent positions of the methoxyl and hydroxyl groups.

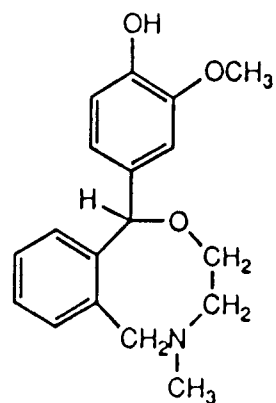
A series of NOE experiments was carried out to determine the substituent positions of the methoxyl and hydroxyl groups. In the first NOE experiment, $H_1(5.7ppm)$ was irradiated to determine if there were any protons attached to C_{10} , C_{15} and C_{19} . In this experiment, three proton signals were enhanced. This result

means that C₁₀, C₁₅ and C₁₉ are attached to protons. Because two proton signals of aromatic coupling system 1 were enhanced, the protons on ring 1 correspond to the signals of aromatic coupling system 1. We conclude that there are three protons on ring1 and the methoxyl and hydroxyl groups are on ring 1 as well. Since protons are connected with C₁₅ and C₁₉, and one of these two proton signals is a doublet, the only possible positions for the hydroxyl and methoxyl groups are C₁₇ and C₁₆ (or C₁₈). The second NOE experiment was carried out by irradiating the methoxyl protons (3.85ppm) to determine the methoxyl group's position on the aromatic ring 1. The singlet of aromatic coupling system 1 was enhanced. This result means that the hydroxyl group is connected to C₁₇, and the methoxyl group is connected to the carbon adjacent to C₁₇. Therefore, structure M1 in Fig. VI.4 is the structure of metabolite M1.

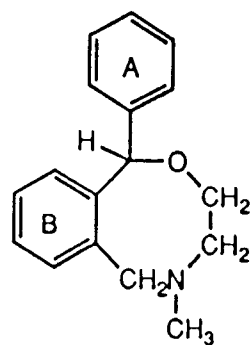
Structure Elucidation of M2. The molecular weight of M2 was determined from the chemical ionization mass spectrum. The m/z value of the MH⁺ peak is 330. Thus, the molecular weight of M2 is 329. A MC₂H₅⁺ peak at m/z 358 is also observed. This is a further evidence that the molecular weight is 329. In the EI mass spectrum (Fig. VI.3) the molecular ion peak at m/z 329 peak is observed. The spectrum also displays a small fragment ion peak at m/z 311. In addition, M2 shows the positive results for silver nitrate reagent and aqueous ferric chloride reagent. These indicate that the metabolite has a hydroxyl group.

In the m/z range 200, the spectrum of M2 is highly similar to that of M1. This suggests that the main structure of M1 and M2 are similar. The high resolution MS of the molecular peak of M2 shows a molecular weight of 329.16270 (deviation 0ppm). This corresponds the molecular formular $C_{19}H_{23}O_4N$. Therefore, it appears that M2 has one more methoxyl group than M1.

In the EI spectrum of M1, the major peaks at m/z 195, 211, 225 and 240 contain two aromatic rings with a hydroxyl group and a methoxyl group attaching to one of these two rings. If the structures of M1 and M2 are similar, presumably, the same fragmentation reactions will occur in M2. As a result, in the spectrum of M2, the m/z values of the corresponding peaks will be greater by 30 because of the second methoxyl group. That is, peaks at m/z 225, 241, 255 and 270 should be observer in the spectrum of M2. All these peaks are observed in the spectrum of M2. Therefore, the structure of M2 is the structure of nefopam with one hydroxyl group and two methoxyl groups attaching to the aromatic rings (Fig. VI.10).



M1



M2

The methoxyl groups and one hydroxyl group are attached to either A or B aromatic rings of M2.

Fig. V.10 Structures of M1 and M2.

Discussion

In our study, four metabolites have been found in greyhound urine at the therapeutic dose, 2 mg/kg. Within these four metabolites, nor-nefopam and nefopam-N-oxide have been found in humans⁷. The other two, M1 and M2, have not been reported elsewhere.

The proposed metabolic pathways of nefopam in humans and greyhounds are summarized in Fig. VI.11. In greyhounds, the results of this study show that nefopam undergoes several different metabolic pathways. For forming M1 and M2, nefopam undergoes aromatic hydroxylation first. Then the intermediates are further metabolized by O-methylation. For the major metabolite, M1, the aromatic hydroxylation reaction happens at sites B and C. For the minor metabolite, M2, hydroxylation happens at three different positions on the aromatic rings, but the exact positions are still unknown. In greyhounds, nefopam also undergoes N-demethylation and N-oxidation. The products of these two reactions, nor-nefopam and nefopam-N-oxide have been found in human urine by Ebel et al⁷. Ebel et al. also identified four phenolic metabolites by using of the Folin-Ciocalteu reagent. However, the exact structures of these four metabolites are still unknown. Therefore, we do not know whether the two phenolic metabolites we found are produced in humans. So, in the diagram, the pathways of the two greyhound's

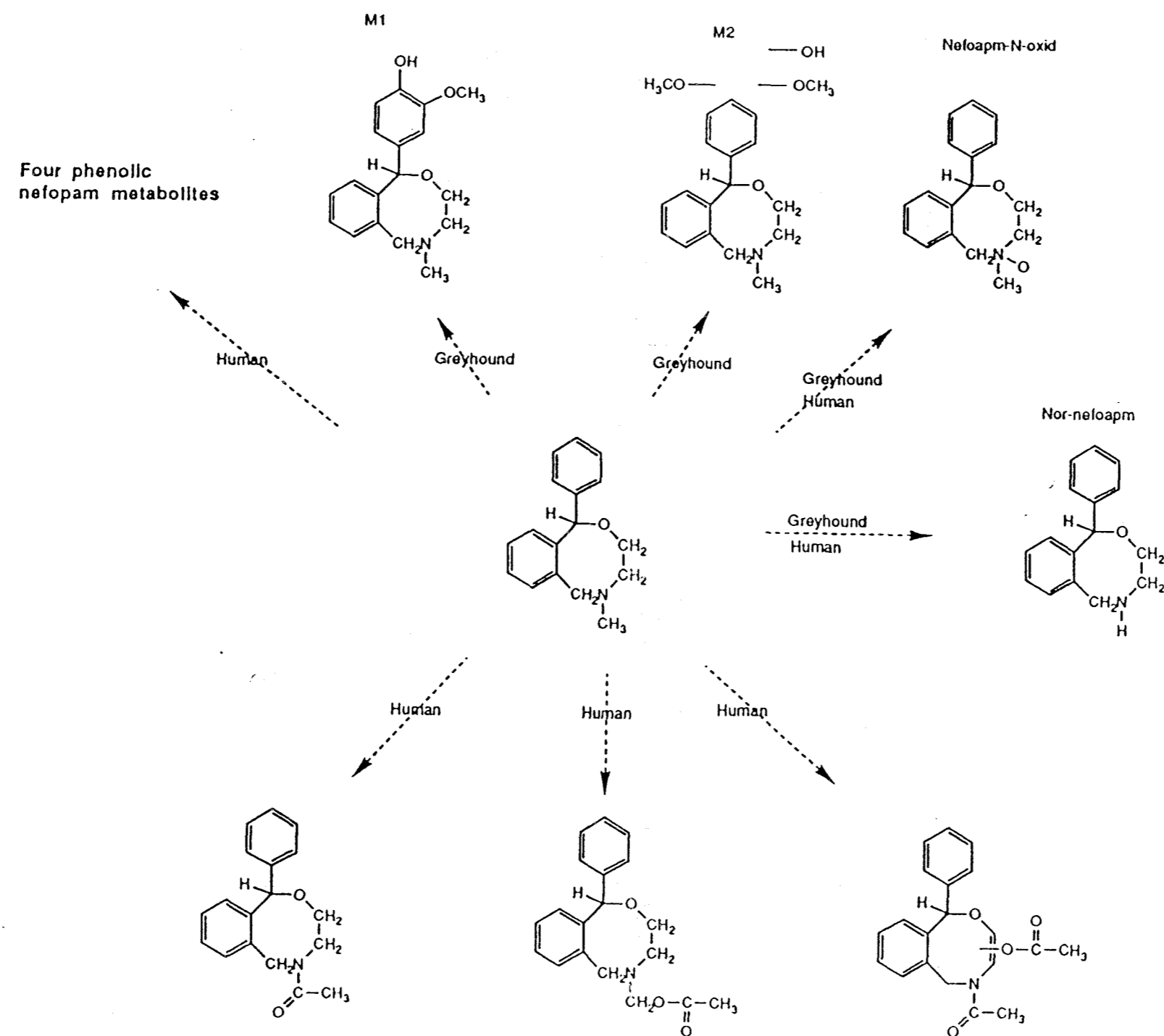


Figure V.11 Proposed metabolic pathways of mefopam in greyhounds and humans.

phenolic metabolites are not shared with humans. Maurer et al.⁷ have found another five demethylated metabolites in human urine. In humans, metabolic reactions happen extensively, and several different metabolic mechanisms are involved. However, site A is the only position which is involved in all the metabolic reactions at the non-aromatic ring. In humans, these metabolic reactions which happen at site A include N-demethylation and N-oxidation. For the phenolic metabolites, we only know that the reaction sites are at aromatic rings. However the actual positions are not clear. Since these four phenolic metabolites were found in the enzyme hydrolyzed urine, it is most likely that the aromatic hydroxylations are followed by a phase II reaction: glucuronide conjugation.

M1 and M2 were only detected in the extract from the β -glucuronidase treated urine, instead of being found in both β -glucuronidase treated and untreated urine. These results suggest that M1 and M2 are probably conjugated with glucuronic acid. Another interesting phenomenon about M1 and M2 is that the corresponding pre-O-methylation mediates of these two metabolites were not found in the urine. This phenomenon suggests that the O-methylation may accelerate the glucuronidation of an adjacent phenolic hydroxyl group.

The purpose of our study is not pharmacokinetic characteristics of nefopam in greyhounds; however, the TLC results in our study have shown some clues of the

pharmacokinetic characteristics of nefopam. The TLC results show that, in greyhounds, the disposal rate of nefopam reaches its peak at about 8 hours, and then, the rate decreases gradually. At 24 hours, only a small amount of nefopam exists in the urine. This suggests that $t_{1/2}$ of nefopam may be in the range of 8 to 12. For metabolite M1, TLC results show that its disposal rate reaches a peak in the range of 6 to 10 hours, and then, the rate decreases slowly. At 24 hours, a relatively large amount of M1 is still detected by TLC. This suggests that $t_{1/2}$ of M1 is much larger than that of nefopam. For nor-nefopam, the TLC results show that its disposal rate peak is in the range of 2 to 8 hours; then, the rate decreases rapidly. At 24 hours, nor-nefopam is hardly detected by TLC.

To determine the main metabolite pathway at the therapeutic dose (2 mg/kg), the GC chromatogram peak height ratios of nor-nefopam to M1 (Fig. VI.4) are used. After the administration of nefopam, the ratio starts to increase. About ten hours later, the ratio reaches its maximum, 0.675. Then, it starts decreasing. Twenty-four hours after the administration, the ratio decreased to 0.183. In the first 24 hours after administration, the amount of M1 excreted is always larger than that of nor-nefopam, and the ratio change trend is toward being even smaller after 24 hours. This means that the amount of M1 excreted will also be larger than that of nor-nefopam after 24 hours. We suggest that the hydroxylation in the aromatic ring

followed by O-methylation is the main biotransform pathway of nefopam in greyhounds at a dose of 2 mg/kg.

At the therapeutic dose (2 mg/kg), instead of the reactions happening on the non-aromatic ring, the aromatic hydroxylation and further O-methylation is the main pathway in greyhounds. The difference of the nefopam biotransformation pathway between humans and greyhounds may be due to the species difference. However, so far only limited information is available on the metabolism of nefopam. More extensive studies to determine the biotransformation in humans and greyhounds would be interesting.

In greyhounds, the main metabolic pathway at the therapeutic dose (2 mg/kg) is different from that at the high dose (30 mg/kg). At the high dose (30 mg/kg), nor-nefopam shows a clear dark spot in the TLC test; however, the new metabolites, M1 and M2, only show a very faint spot. The GC chromatogram peak height ratios of nor-nefopam to M1 (Table VI.1) were 0.67 at a dose of 2 mg/kg and 33 at a dose of 30 mg/kg. This difference means that the main metabolic pathways at the therapeutic dose (2 mg/kg) and the high dose (30 mg/kg) are different in greyhounds. At the therapeutic dose, the main metabolic pathways are the reactions which happen at the aromatic ring: the aromatic hydroxylation followed by O-methylation. At a dose of 30 mg/kg, the main metabolic pathway is the demethylation at side A. At the high dose, the

Table V.1 The relative peak height of nefopam and its metabolite
in the GC chromatogram and peak ratios

Dose of nefopam	Relative peak height			Peak ratio	
	N	M1	M3	N/M1	M3/M1
2mg/kg	156	117	79	1.33	0.68
30mg/kg	586	1	33	586	33

N--Nefopam

M3--Nor-nefopam

hydrosylation and further O-methylation pathway might be inhibited; and the rate of nefopam and nor-nefopam excreted in urine increased.

The possible underlying cause of the change in the pharmacokinetics of nefopam between the low and high doses may be the autoinhibition of metabolism. One of cyclic analogues of nefopam is orphenadrine. It was reported that an unexpected accumulation of orphenadrine in man had been observed under the chronic dosing condition¹¹. A metabolized product of orphenadrine has been reported to be an inhibitor of microsomal cytochrome P450 enzyme and to cause the accumulation of orphenadrine¹². Leurs et al. reported that in vitro microsomal metabolism of nefopam led to the formation of a metabolic intermediate which binds irreversibly with the reduced form of cytochrome P450, and the extent of the intermediate formation depend upon the concentration of nefopam¹³. These phenomenons may be explained by a substrate inhibition. The high concentration of nefopam inhibits further biotransformation. We suggest that this reaction may happen in humans following an oral administration of a large dose of nefopam. The metabolic pathway, aromatic hydroxylation followed by O-methylation, is inhibited to a large extent.

In this work, flash chromatography was used for cleaning up and prepreparing samples for HPLC instead of using the preparative TLC or open column chromatography. Because of the

large sample capacity and fast speed of flash chromatography¹⁴, a large amount and number of samples can be processed in a short period. First, the low polarity solvent is used to wash out most of the non-metabolic components in the sample. Then, the high polarity solvent is used to preseparate the sample for HPLC. Since flash chromatography can clean up the sample effectively, back-extraction¹⁵ is not used. The residues extracted from the enzyme hydrolyzed urine by dichloromethane is directly loaded on the flash chromatography column. Then, the cleaning up and preseparation processes are accomplished by a single run. In this way, the recovery will be higher than that of using back-extraction. Moreover, the time and solvent are also saved.

In brief, in this study, four metabolites have been found in greyhound urine. Within these four metabolites, two are newly discovered. In greyhounds, at the therapeutic dose, 2mg/kg, aromatic hydroxylation followed by O-methylation is the main metabolic pathway; at the high dose, 30 mg/kg, N-demethylation is the main metabolic pathway.

References

- 1 R. C. Heel, R. N. Brodgen, G. E. Pakes, T. M. Speight and G. S. Avery: Nefopam: A Review of its Pharmacological Properties and Therapeutic Efficacy. *Drug*, **19**, 249-267(1980).
- 2 M. W. Klohs, M. D. Draper, F. J. Petracek, K. H. Ginzel and O. N. Re: Benzoxazocines: A New Chemical Class of Centrally Acting Skeletal Muscle Relaxants. *Arzneimittel-Forschung*, **22**, 132-133(1972)
- 3 D. Schuppan, C. S. Hansen and R. E. Ober: GLC Determination of Nanogram Quantities of a New Analgesic, Nefopam, in Human Plasma, *J. Pharm. Sci.*, **67**, 1720-1723(1978).
- 4 U. Bondesson: Determination of mefopam in equine plasma by gas chromatography-mass spectrometry with chemical ionization, *J. C Chromatogr.* **377**,379-383(1986).
- 5 R.C. Heel, R.N. Brogden, G.E. Pakes, T.M. Speight and G.S. Avery: Nefopam: A Review of its Pharmacological Properties and Therapeutic Efficacy, *Drugs*, **19**, 249-267(1980).
- 6 S. Ebel and H. Schutz: Isolierung und Identifizierung des Haupt-sowie Mehrerer Nebenmetabolite, *Arch. Pharm.*, **311**, 547-552(1978).
- 7 H. Maurer and K. Pfleger: Screening Procedure for the Detection of Opioids, Other Potent Analgesics and Their Metabolites in Urine Using a Computerized Gas Chromatographic-Mass Spectrometric Technique. *Fresenius Z. Anal. Chem.* **317**, 42-52(1984).

- 8 K. Hostettmen, M. Hostettmann, A. Marston: Flash Chromatography In "Preparative Chromatography Techniques", pp41-46. Springer-Verlag, New York, 1986.
- 9 W. J. Burke, A. D. Potter, R. M. Parkhurt, *Anal. Chem.*, **32**(1960)727.
- 10 H. M. Stevens: Colour test in "Clard's Isolation and Identification of Drugs" (A. C. Moffat), pp133. Pharmaceutical press, London, 1986.
- 11 J. J. M. Labout, C. T. Thijssen, G. G. J. Keijser, and W. Hespe: Difference between Single and Multiple Dose Pharmacokinetics of Orphenadrine Hydrochloride in Man. *Eur. J. Clin. Pharmacol.*, **21**, 343-350(1982).
- 12 A. Bast, F. A. A. van Kemenade, E. M. Savenije-Chapel and J. Noordhoek: Product Inhibition in Orphenadrine Metabolism as a Result of a Stable Cytochrome P-450-metabolic Intermediate Complex Formed during the Disposition of Mono-N-desmethylophenadrine (tofenacine) in the Rat, *Res. Comm. Chem Path Pharmacol.*, **40**, 391-403(1983).
- 13 R. Leurs, D. Donnell, H. Timmerman, A. Bast: Cytochrome P450 Metabolic Intermediate Complex of Nefopam. *J. Pharm. Pharmacol.*, **39**, 835-837(1987).
- 14 K. Hostettmenn, M. Hostettmann, A. Marston: Flash Chromatography In "Preparative Chromatography Techniques", pp41-46. Springer-Verlag, New York, 1986.

BIBLIOGRAPHY

- S. Ahuja, Selectivity and Detectability Optimizations Wiley, New York, 1989.
- P. E. Antle, Chromatographia, 15(1982)277.
- A. Bartha, H. A. H. Billiet and L. D. Galan, J. Chromatogr., 458(1988)371.
- A. Bast, F. A. A. van Kemenade, E. M. Savenije-ChapNoordhoek: Product Inhibition in Orphenadrine Metabolism as a Result of a Stable Cytochrome P-450-metabolic Intermediate Complex Formed during the Disposition of Mono-N-desmethylophenadrine (tofenacine) in the Rat, *Res. Comm. Chem Path Pharmacol.*, **40**, 391-403(1983).
- J. C. Berridge, Analyst(London), 109(1984)291.
- J. C. Berridge, Chromatographia, 16(1982)173.
- J. C. Berridge, J. Chromatogr., 244(1982)1.
- J. C. Berridge, Chromatographia, 16(1982)173.
- J. C. Berridge, Paper presented at Analyticon 83, London, 1983, Paper 505.
- J. C. Berridge, Proc. Anal. Div. Chem. Soc., 19(1982)472.

J. C. Berridge, *Techniques for Automated Optimization of HPLC Separations*, Wiley, New York, 1985.

J. C. Berridge and E. G. Morrissey, *J. Chromatogr.*, 316(1984)69.

G. S. G. Beveridge and R. S. Schechter, *Optimization: Theory and Practice*, McGraw-Hill, New York, 1970.

H. A. H. Billiet, J. P. J. Van Dalen, P. J. Schoenmaker and L. De Galan, *Anal. Chem.*, 55(1983)847.

R. E. Boehm and D. E. Martire, *J. Phys. Chem.*, 84(1980)3620.

U. Bondesson: Determination of mefopam in equine plasma by gas chromatography-mass spectrometry with chemical ionization, *J. C Chromatogr.* **377**,379-383(1986).

M. P. T. Bradley and D. Gillen, *Spectra-Physics Chromatogr. Rev.*,10(2)(1983)2.

W. J. Burke, A. D. Potter, R. M. Parkhurt, *Anal. Chem.*, 32(1960)727.

H. Colin, A. Krstulovic, G. Guiochon and J. P. Bounine, *Chromatographia*, 17(1983)209.

H. A. Cooper and R. J. Hurtubise, *J. Chromatogr.*, 324(1985)1.

H. A. Cooper and R. J. Hurtubise, *J. Chromatogr.*, 328(1985)81.

S. J. Costanzo, *J. Chromatogr. Sci.*, 24(1986)89-93.

G. D'agostino, F. Mitchell, L. Castagnetta, and M. J. O'hare, J. Chromatogr., 305(1984)13-26.

H. J. G. Debet, J. Liq. Chromatogr., 15(1985)2725.

S. N. Deming and M. L. H. Turoff, Anal. Chem., 50(1978)546.

M. W. Dong, R. D. Colon and A. F. Poile, Amer. Lab. Mag., May, 1988, p. 48.

A. C. J. H. drouen, H. A. H. Billiet, P. J. Schoenmakers, and L. de Galan, Chromatographia, 16(1982)48.

A. C. J. H. drouen, H. A. H. Billiet, P. J. Schoenmakers, and L. de Galan, J. Chromatogr., 352(1986)127.

D. L. Dunn and R. E. Thompson, J. Chromatogr., 264(1983)264.

S. Ebel and H. Schutz: Isolierung und Identifizierung des Haupt- sowie Mehrerer Nebenmetabolite, *Arch. Pharm.*, **311**, 547-552(1978).

R. R. Ernst, Rev Sci. Instrum., 39(1968)998.

D. M. Fast, P. H. Culbreth and E. J. Sampson, Clin. Chem., 28(1982)444.

J. L. Glajch, J. C. Gluckman, J. G. Charikofsky, J. M. Minor, and J. J. Kirkland, J. Chromatogr., 318(1985)25.

J. L. Glajch and J. J. Kirkland, Anal. Chem., 54(1982)2593.

J. L. Glajch, J. J. Kirkland, J. Chromatogr., 218(1981)299.

J. L. Glajch, J. J. Kirkland, K. M. Squire and J. M. Minor, J. Chromatogr., 199(1980)57.

J. L. Glajch, J. J. Kirkland and L. R. Snyder, J Chromatogr., 238(1982)269.

J. L. Glajch, J. J. Kirkland, K. M. Squire and J. M. Minor, J. Chromatogr., 199(1980)57.

A. P. Glodberg, E. L. Nowakowska, P. E. Antle and L. R. Snyder, J. Chromatogr., 316(1984)241.

J. W. Gorman and J. E. Hinman, Technometrics, 4(1962)463

P. R. Haddad, A. C. J. H. Drouen, H. A. H. Billiet and L. de Galan, J. Chromatogr., 281(1983)71.

S. H. Hansen and P. Helboe, J. Chromatogr., 285(1984)53.

R. C. Heel, R. N. Brodgen, G. E. Pakes, T. M. Speight and G. S. Avery: Nefopam: A Review of its Pharmacological Properties and Therapeutic Efficacy. *Drug*, **19**, 249-267(1980).

J. H. Hildetrand, J.M. Prausnitz and R.L. Scott, *Regular and Related Solutions*, Van Nostrand Reinhold Company, (1977)3-4

K. Hostettmenn, M. Hostettmann, A. Marston: Flash

Chromatography In "Preparative Chromatography Techniques", pp41-46. Springer-Verlag, New York, 1986.

A. J. Hsu, R. J. Laub and S. J. Madden, J. Liq. Chromatogr. 7(1984)615.

H. J. Issaq, 'Statistical and Graphical Methods of Isocratic Solvent Selection for Optimal Separation in Liquid Chromatography' in J. C. Giddings, E. Grushka, J. Cazes and P. R. Brown (Eds), *Advances in Chromatography*, Vol. 24, Marcel Dekker. New York, 1984, Ch3.

H. J. Issaq, G. M. Muschik and G. M. Janini, J. Liq. Chromatogr., 6(1983)259.

D. R. Jenke, Anal. Chem., 56(1984)2674.

D. R. Jenke and G. K. Pagenkopf, Anal Chem., 56(1984)85.

L. A. Jones, R. W. Beaver and T. L. Schmoeger, Anal. Chem., 54(1982)182.

P. Jones and C. A. Wellington, J. Chromatogr., 213(1981)375.

B. L. Karger, L. R. Snyder and C. Eon, J. Chromatogr., 125(1976)71.

A. S. Kester and R. E. Thompson, J. Chromatogr., 310(1984)372.

P. G. King and S. N. Deming, Anal. Chem., 46(1974)1476.

R. J. Laub, *Int. Lab.*, May/June(1981)16.

G. M. Landers and J. A. Olson, *J. Chromatogr.*, 291(1984)51.

R. J. Laub, *Int. Lab.*, May/June(1981)16.

R. J. Laub and S. J. Madden, *J. Liq. Chromatogr.*, 8(1985).

R. J. Laub, and J. H. Purnell, *Anal. Chem.* 48(1976)1720.

R. J. Laub and J. H. Purnell, *J. Chromatogr.*, 112(1975)71.

R.J. Laub and J. H. Purnell. *J. Chromatogr.*,161(1978)49.

R. J. Laub and T. Kuwana (Ed.), *Physical Methods in Modern Chemical Analysis*, Vol. 3, Academic Press, New York, 1983, Ch. 5.

R. J. Laub, and J. H. Purnell, D. M. Summers and P. S. Williams, *J. Chromatogr.*, 199(1980)57.

R. J. Laub, J. H. Purnell, and P. S. Williams, *J. Chromatogr.*,134(1977)246.

J. J. M. Labout, C. T. Thijssen, G. G. J. Keijser, and W. Hespe:
Difference between Single and Multiple Dose
Pharmacokinetics of Orphenadrine Hydrochloride in Man. *Eur. J. Clin. Pharmacol.*, **21**, 343-350(1982).

R. Leurs, D. Donnell, H. Timmerman, A. Bast: Cytochrome P450 Metabolic Intermediate Complex of Nefopam. *J. Pharm. Pharmacol.*, **39**, 835-837(1987).

D. E. Martire and R. E. Boehm, *J. Phys. Chem.*, 87(1983)1045.

D. L. Massart, A. Dijkstra and L. Kaufman, *Evaluation and Optimization of Laboratory Methods and analytical Procedure*, Elsevier, Amsterdam, 1978.

H. Maurer and K. Pflieger: Screening Procedure for the Detection of Opioids, Other Potent Analgesics and Their Metabolites in Urine Using a Computerized Gas Chromatographic-Mass Spectrometric Technique. *Fresenius Z. Anal. Chem.* **317**, 42-52(1984).

A. C. Mehta: Sample pretreatment in the Trace Determination of Grugs in Biological Fluids, *Talanta*, **39**, 67-73(1986).

J. A. Nelder and R. Mead, *Comput. J.*, 7(1965)308.

OPTIMI Chromatographic System, Spectra Physics, San Jose, California, USA, (no date).

C. M. Noyes, *J. Chromatogr.*, 266(1983)451.

M. Otto, *Z. Chem.*, 23(1983)204.

M. Otto and W. Wegscheider, *J. Chromatogr.*, 258(1983)11.

B. Patel, J. H. Purnell and C. A. Wellington. J. High Resolut. Chromatogr. Commun., 7(1984)2674.

C. F. Poole and S. A. Schuette, Contemporary Practice of Chromatography, Elsevier, New York, 1984, p.258.

PESOS: Perkin-Elmer Solvent Optimisation System, Perkin-Elmer, Norwalk, Connecticut, USA, (no date).

J. H. Nickel and S. N. Deming, Am. Lab. (Fairfield), 16(1984)69.

M. A. Quarry, R. L. Grob, L. R. Snyder, J. W. Dolan and M. P. Riggney, J. Chromatogr., 384(1987)163.

J. Rafel, J. Chromatogr., 282(1983)287.

J. Rafel and J. Lema, Afinidad, 41(1984)30; Chem. Abstr., 100(1984)21614c.

G. Sabate, A. M. Diaz, X. M. Tomas and M. M. Gassiot, J. Chromatogr. Sci., 21(1983)439.

B. Sachok, R. C. Kong and S. N. Deming, J. Chromatogr., 199(1980)317.

B. Sachok, J. Stranahan and S. N. Deming, Anal Chem., 53(1981)70.

H. Scheffe, J. Royal Stat. Soc. B, 20(1958)344.

P. J. Schoenmakers, Optimization of Chromatographic Selectivity, Elsevier, Amsterdam, 1986.

P. J. Schoenmakers, H. A. H. Billiet and L. de Galan, J. Chromatogr., 185(1979)179.

P.J. Schoenmakers, H.A.H. Billiet and L. de Galan, Chromatographia, 15(1982)205.

P. J. Schoenmakers and T. Blaffert, J. Chromatogr., 384(1987)117.

P. J. Schoenmakers, A. C. J. H. Drouen, H. A. H. Billiet and L. de Galan, Chromatographia, 15(1982)48.

D. Schuppan, C. S. Hansen and R. E. Ober: GLC Determination of Nanogram Quantities of a New Analgesic, Nefopam, in Human Plasma, *J. Pharm. Sci.*, **67**, 1720-1723(1978).

R. P. W. Scott, *Techniques of Chemistry, Vol. XI, Contemporary Liquid Chromatography*, Wiley, New York, 1976, p.25.

R. Smits, C. Vanroelen and D. L. Massart, Fresenius Z. Anal. Chem., 273(1975)1.

R. D. Snee, Chemtech, 9(1979)702.

L. R. Snyder, Anal. Chem., 46(1974)1384.

L. R. Snyder, J. Chromatogr. Sci., 16(1978)223.

L. R. Snyder, Practical HPLC method Development, Wiley, New York, 1988.

L. R. Snyder, J. W. Dolan and J. R. Gant, J. Chromatogr., 165(1979)3.

L. R. Snyder, J. W. Dolan and M. P. Rigney, LC-GC, 4(1986)921.

L. R. Snyder, J. W. Dolan and M. A. Quarry, TrAC Trends Anal.Chem.(Pers. Ed.), 6(1987)106.

L. R. Snyder, J. L. Glajch, and J. J. Kirkland, J. Chromatogr., 218(1981)299.

L. R. Snyder, J. J. Kirkland, Introduction to Modern Liquid Chromatography, 2nd., Wiley, New York, 1979, p.36.

L. R. Snyder, J. L. Glajch and J. J. Kirkland, Practical HPLC Method Development, Wiley, New York, 1988.

L. R. Snyder, M. A. Quarry and J. L. Glajch, Chromatographia, 24(1987)33.

W. Spendley, G. R. Hext and F. R. Hinsworth, Technometrics, 4(1962)441.

SUMMIT Chromatographic System, Bruker Spectrospin, Coventry, UK, (no date).

V. Svoboda, J. Chromatogr., 201(1980)241.

TAMED Chromatographic System, LDC Milton Roy, Stone, UK,
(no date).

J. P. Thomas, A. Brun and J. P. Bounine, J. Chromatogr.,
72(1979)107.

T. Tsuneyoshi, A. Kawamoto and J. Koezuka, Clin. Chem.,
30(1984)1889.

F. V. Warren and B. A. Bidlingmeyer, Paper presented at 188th
Acs Meeting, Philadelphia, 1984, Paper 108.

M. W. Watson and P. W. Carr, Anal. Chem., 51(1979)1835.

J. W. Weyland, C. H. P. Bruins and D. A. Doornbos, J.
Chromatogr. Sci., 22(1984)31.

D.J. White. Operational Research, Wiley, New York, 1985,
p.85.

A. G. Wright, A. F. Fell and J. C. Berridge, J. Chromatogr.,
458(1988)335.